BIOTECH STUDIES

VOL 33 ISSUE 1 JUNE 2024 ISSN 2687-3761 E-ISSN 2757-5233

Published by Field Crops Central Research Institute, Ankara, TURKEY

TAGEM JOURNALS

Aims and Scope

"Biotech Studies" is the successor to the "Journal of Field Crops Central Research Institute" which has been published since 1992. The journal publishes articles on agro-biotechnology, plant biotechnology, biotechnology for biodiversity, food biotechnology, animal biotechnology, microbial biotechnology, environmental biotechnology, industrial biotechnology and bioprocess engineering, applied biotechnology, omics technologies, system biology, synthetic biology, nanobiotechnology and bioinformatics.

The journal of Biotech Studies has been published twice a year (June & December). Original research papers, critical review articles, short communications and scientific research of the journal are published in English. It is an international refereed journal.

The journal is aimed for researchers and academicians who work in or are interested in the topics of research in biotechnology.

Biotech Studies is indexed in Scopus, ULAKBIM TR Index, Scientific Indexing Services, and CrossRef.

Further information for "***Biotech Studies***" is accessible on the address below indicated:

http://www.biotechstudies.org/

You can reach table of contents, abstracts, full text and instructions for authors from this home page.

Corresponding Address

Address : Field Crops Central Research Institute, (Tarla Bitkileri Merkez Araştırma Enstitüsü)
Şehit Cem Ersever Cad. No:9/11
Yenimahalle, Ankara, Türkiye
Web : www.biotechstudies.org
E-mail : info@biotechstudies.org
Phone : + 90 312 327 09 01-2222
Fax : + 90 312 327 28 93

BIOTECH STUDIES

UN SDG Publishers Compact

As a Publisher, Biotech Studies is pleased to declare its commitment to the United Nations Sustainable Development Goals (UN SDGs) Publishers Compact. The purpose of this Compact is to accelerate progress to achieve SDGs by 2030. Signatories aspire to develop sustainable practices and act as champions of the SDGs during the Decade of Action (2020-2030), publishing books and journals that will help inform, develop, and inspire action in that direction. Furthermore, as a signatory of SDG Publishers Compact, Biotech Studies commit to:

1. **Committing to the SDGs**: Stating sustainability policies and targets on our website, including adherence to this Compact; incorporating SDGs and their targets as appropriate.
2. **Actively promoting and acquiring content** that advocates for themes represented by the SDGs, such as equality, sustainability, justice and safeguarding and strengthening the environment.
3. **Annually reporting on progress towards achieving SDGs**, sharing data and contribute to benchmarking activities, helping to share best practices and identify gaps that still need to be addressed.
4. **Nominating a person who will promote SDG progress,** acting as a point of contact and coordinating the SDG themes throughout the organization.
5. **Raising awareness and promoting the SDGs among staff** to increase awareness of SDG-related policies and goals and encouraging projects that will help achieve the SDGs by 2030.
6. **Raising awareness and promoting the SDGs among suppliers,** to advocate for SDGs and to collaborate on areas that need innovative actions and solutions.
7. **Becoming an advocate to customers and stakeholders** by promoting and actively communicating about the SDG agenda through marketing, websites, promotions, and projects.
8. **Collaborating across cities, countries, and continents** with other signatories and organizations to develop, localize and scale projects that will advance progress on the SDGs individually or through their Publishing Association.
9. **Dedicating budget and other resources towards accelerating progress** for SDG-dedicated projects and promoting SDG principles.
10. **Taking action on at least one SDG goal**, either as an individual publisher or through your national publishing association and sharing progress annually.

Besides these 10 action points, Biotech Studies endorses the SDGs, and explicitly concentrate on eight of 17 goals:

BIOTECH STUDIES

Editorial Information

BIOTECH STUDIES

Editorial Information

Technical Editors

BIOTECH STUDIES

Volume 33 Issue 1 JUNE 2024

CONTENTS

1-12 **Evaluation of anticancerogenic effect of flavonoid rich *Verbascum gypsicola* Vural & Aydoğdu methanolic extract against SH-SY5Y cell line**

Seda Şirin

13-22 **Research advances of deciphering Shalgam microbiota profile and dynamics**

Mustafa Yavuz, Halil Rıza Avcı

23-32 **Barley preferentially activates strategy-II iron uptake mechanism under iron deficiency**

Emre Aksoy

33-42 **Juglans kernel powder and jacobinia leaf powder supplementation influenced growth, meat, brain, immune system and DNA biomarker of broiler chickens fed Aflatoxin-B1 contaminated diets**

Olugbenga David Oloruntola

43-51 **Response surface methodology-based optimization studies about bioethanol production by *Candida boidinii* from pumpkin residues**

Ekin Demiray, Sevgi Ertuğrul Karatay, Gönül Dönmez

52-66 **Recent *in vitro* models and tissue engineering strategies to study glioblastoma**

Melike Karakaya, Pınar Obakan Yerlikaya

67-73 **Rhein inhibits cell proliferation of glioblastoma multiforme cells by regulating the TGF-ß and apoptotic signaling pathways**

Sümeyra Çetinkaya

Biotech Studies 33(1), 1-12
http://doi.org/10.38042/biotechstudies.1383424

BIOTECH STUDIES

RESEARCH PAPER

Evaluation of anticancerogenic effect of flavonoid rich *Verbascum gypsicola* Vural & Aydoğdu methanolic extract against SH-SY5Y cell line

Seda Şirin

Department of Biology, Faculty of Science, Gazi University, 06500, Ankara, Türkiye.

How to cite:
Şirin, S. (2023). Evaluation of anticancerogenic effect of flavonoid rich *Verbascum gypsicola* Vural & Aydoğdu methanolic extract against SH-SY5Y cell line. *Biotech Studies*, *33*(1),1-12. https://doi.org/10.38042/biotechstudies.1383424

Article History
Received 05 Semptember 2023
Accepted 30 October 2023
First Online 30 October 2023

Corresponding Author
Tel.: +90 536 616 10 98
E-mail: sdasirin@hotmail.com

Keywords
Apoptosis
Flavonoid
Mitochondrial membrane potential
Reactive oxygen species

Abstract

Neuroblastoma (NB) is an embryonal neoplasm affecting the autonomic branch of the nervous system; it is the most commonly detected cancer type in children. NBs affecting children mostly present with metastatic disease that is hardly treatable with intensive multimodal therapy and portends a poor prognosis. Therefore, the likelihood of children with high-risk NB relapse remains extremely high, which calls for urgent action to discover novel treatment options to improve survival. Assessing the anti-cancer properties of known natural compounds may offer novel therapeutic options against NB. In this study we aimed to investigate the anti-cancer properties of the *Verbacum gypsicola* methanol extract (VGME) rich in flavonoids on SH-SY5Y cell line. For this purpose, we used LC-MS analysis to investigate the flavonoid composition of VGME, MTT analysis to investigate its effect on cell viability, and flow cytometry and qRT-PCR analyses to investigate its effect on apoptosis. VGME had a high flavonoid content. Its IC_{50} dose was 50 µg/mL at 48 hours. It significantly increased intracellular ROS level, apoptotic cells' percentage, and mitochondrial disruption. The capacity of VGME to block cancer growth via an intrinsic apoptotic route implies that it might be a classic option for anticancer drug creation.

Introduction

Neuroblastoma (NB) is a prevalent malignancy that originates from the neural crest in children and represents a substantial challenge in pediatric oncology, as highlighted by Anoushirvani et al. (2023). This aggressive cancer is responsible for a significant proportion of childhood cancer-related mortality, with roughly 15% of pediatric cancer-related deaths attributed to NB. What's particularly concerning is that a substantial portion of new NB cases, close to 40%, present with high-risk criteria, and many of these cases have already metastasized at the time of diagnosis, as reported by Jacobson et al. (2023). The inherent aggressive nature and advanced disease stage at diagnosis pose significant hurdles in effectively managing this condition. The current therapeutic arsenal for NB includes a combination of treatments such as surgical removal, chemotherapy, stem cell transplantation, radiotherapy, and immunotherapy. Despite these intensive multimodal therapeutic approaches, the relapse risk in NB remains notably high. Distressingly, when the disease does recur, it often exhibits poor responsiveness to subsequent therapeutic interventions, as highlighted by Gao et al. (2023). It is noteworthy that over two-fifths of NB cases with high-risk characteristics experience relapse, underscoring the pressing need for the discovery of novel therapeutic targets and the exploration of natural therapeutic compounds, especially those derived from herbal sources, as emphasized by Hagemann et al. (2013). Additionally, in NB, imbalances in the gene and protein levels of *BAX* (BCL2 associated X), *BCL2* (B-cell CLL/lymphoma 2), *CASP3* (caspase-3), *CASP7* (caspase-7), *CASP8* (caspase-8), *CASP9* (caspase-9), and *CYCS* (cytochrome C), which are involved in the intrinsic apoptotic pathway, can lead to a predisposition of cells favoring survival over programmed cell death. This

contributes to the growth of the tumor and its resistance to treatments. Understanding how the intrinsic apoptotic pathway is impacted in NB treatment is crucial for the development of herbal treatment methods. Specifically, targeting these genes and proteins in the pathway could be a potential strategy to eradicate tumor cells (Ataur Rahman et al., 2012; Chen et al., 2014a; Rahman et al., 2013). The pursuit of innovative treatment options and the investigation of herbal compounds hold promise for improving the outlook for NB patients and addressing the unique challenges posed by this complex pediatric cancer.

The *Verbascum* genus, belonging to the Scrophulariaceae family, encompasses a rich diversity of approximately 360 species worldwide. However, it's in Turkey where *Verbascum* truly flourishes, with a remarkable 239 species and 107 hybrids, and notably, a staggering 200 of them are exclusive to this region, as highlighted by Keser et al. (2023). These plants have found a prominent place in traditional remedies and have been attributed with a wide range of medicinal properties. *Verbascum* species have been historically harnessed for their medicinal potential, serving as remedies for a plethora of health concerns. They have been valued for their anticancer, cytotoxic, immunomodulatory, antiulcerogenic, antihepatotoxic, antihyperlipidemic, antitussive, antiviral, antimicrobial, antimalarial, antioxidant, antiinflammatory, antinociceptive, antitumor, and antigermination properties, as documented by Alkowni et al. (2023) and Tatlı and Akdemir (2006). This extensive range of uses attests to the rich pharmacological potential inherent in *Verbascum* species. Furthermore, *Verbascum* species are a reservoir of diverse chemical compounds, including flavonoids, phenolics, tannins, coumarins, cardiac glycosides, quinones, and flavanones as indicated by Amiri et al. (2023), Aydın et al. (2020), Gose and Hacioglu Dogru (2021), Pourmoslemi et al. (2023), Tatlı et al. (2008). This diverse chemical profile contributes to their multifaceted therapeutic properties. Previous research, such as the work by Taşkaya et al. (2023), has unveiled the significant anticancer potential of *Verbascum napifolium*, particularly in relation to cell viability in CaCo-2 and L929 cell lines. Similarly, Demirci et al. (2023) delved into the anticancer activities of the methanol extract of *V. speciosum*, which is rich in iridoid glucosides and phenyl ethanoids. Research on the leaves of *V. sinaiticum* has led to the discovery of two flavolignans: hydrocarpin and the new compound sinaiticin. Additionally, two flavones, chrysoeriol and luteolin, were identified. All these compounds demonstrated dose-dependent cytotoxic effects on cultured P388 cells, as reported by Afifi et al. (1993). Fifty-one extracts from various parts of 14 different plants were analyzed for their cytotoxic properties using the MTT assay. Among them, the ethanol extract from the flowers of *V. sinaiticum* demonstrated cytotoxic effects against the Vero cell line, as reported by Talib and Mahasned (2010a). The *in vitro* antiproliferative effects of *V. sinaiticum* were studied against Hep-2 and MCF-7 cell lines. The ethanol extract of *V. sinaiticum* showed strong antiproliferative capabilities against these cell lines. Notably, the extract from the flowers of *V. sinaiticum* was more potent than that from its aerial parts, as documented by Talib and Mahasneh (2010b). Luteolin and 3-O-fucopyranosylsaikogenin F, extracted from *V. thapus*, have been identified to exhibit potent antiproliferative properties. Specifically, they induced apoptosis in A549 lung cancer cells, as documented by Zhao et al. (2011). Notably, the study at hand is pioneering in its investigation of the anticancer activity of *V. gypsicola* species on the SH-SY5Y cell line. The choice of SH-SY5Y cells as the experimental model is well-justified for several compelling reasons: First, it's closely associated with NB, a cancer type commonly found in children that originates from nerve cells. Hence, using SH-SY5Y cells provides a logical choice to assess the potential effects against this specific cancer type, as outlined by Kovalevich and Langford (2013). Second, these cells are of human origin, which aligns well with clinical applications for treating NB. Third, SH-SY5Y cells have a strong basis in prior research and are a widely recognized model in the fields of NB and cancer research, as evidenced by the considerable body of literature that has utilized this cell line, as underscored by Mellado et al. (2018), Pk et al. (2023), Richeux et al. (1999), and Tai et al. (2011) and Vetter et al. (2012). Lastly, SH-SY5Y cells may share similar characteristics with NB cells, thus providing a more specific model for understanding the underlying mechanisms related to NB, a feature underscored by Ataur Rahman et al. (2012). By choosing SH-SY5Y cells for this study, it not only opens the door to exploring the potential anticancer properties of *V. gypsicola* but also allows for a more nuanced understanding of the mechanisms underpinning its effects, thereby offering promising avenues for the advancement of NB research and treatment strategies.

The primary objective of the current study was to assess the potential anti-cancer properties of the flavonoid compounds present within the chemical composition of *V. gypsicola* methanolic extract (VGME). To achieve this, LC-MS/MS analysis was employed to precisely identify the specific flavonoids residing within VGME. Subsequently, VGME was evaluated for its cytotoxic effects against human neuroblastoma cancer cells (SH-SY5Y). In an effort to unravel whether VGME's cytotoxicity could be attributed to the flavonoids it contains, this study delved further into a comprehensive investigation that encompassed, for the first time, the examination of several crucial aspects. These included the assessment of intracellular ROS levels, the quantification of apoptotic cells, the determination of disrupted mitochondria, and an exploration of the influence on gene expression levels related to the apoptosis pathway. This holistic approach allowed us to not only identify the presence of flavonoids within

VGME but also to dissect the precise mechanisms through which VGME exerts its cytotoxic effects on cancer cells, shedding light on potential therapeutic avenues in the quest to combat cancer.

Materials and Methods

Plant material

Verbascum gypsicola Vural & Aydoğdu, a distinctive plant species, is known for its natural habitat within an area rich in saline salts, nestled in the scenic region of Beypazarı, located in Ankara, Turkey. This remarkable plant was thoughtfully sampled during the month of August in the year 2011, precisely when it was in full bloom, showcasing its vibrant and characteristic flowers. The precise identification and authentication of this plant specimen were expertly conducted under the discerning eye of Prof. Dr. Zeki AYTAÇ, a distinguished authority in botanical studies affiliated with Gazi University. This rigorous verification process ensured the accurate classification and taxonomy of *Verbascum gypsicola*. To further validate its identity and as a testament to its existence, a voucher specimen was meticulously preserved within the Herbarium of Gazi University. This voucher specimen bears the distinctive identifier "ZA-10440" and serves as a tangible record of *Verbascum gypsicola*'s presence in this unique ecological niche. This diligent documentation and verification process not only contribute to our understanding of this plant species but also provide valuable insights into the biodiversity and botanical richness of the Beypazarı region in Ankara, Turkey.

Preparation of the methanolic extract

The preparation of the *V. gypsicola* methanolic extract (VGME) was carried out with precision and attention to detail. Initially, 30 grams of dried and powdered *V. gypsicola* were carefully used for the extraction process. The extraction was performed at a controlled temperature of 60 °C, and it extended over a period of four h. To facilitate this process, a specialized Soxhlet apparatus was thoughtfully employed. Following the extraction, the VGME was meticulously filtered and concentrated under vacuum conditions at 80 °C using a rotary evaporator from Heidolph (Schwabach, Germany). This step ensured the removal of excess solvent and the concentration of the extract, resulting in a more potent and manageable form. Subsequently, a crucial freeze-drying process was carried out, further enhancing the stability and preservation of the extract. The extract was then carefully stored at a controlled temperature of 4 °C for a maximum period of one week, during which it remained in optimal condition and ready for chemical analyses. This methodical procedure ensured the integrity and quality of the VGME, making it well-suited for the subsequent chemical analyses required for the study's objectives.

Determination of flavonoid composition

The quantification of VGME's flavonoid contents was meticulously achieved through a precise and sophisticated analytical approach. To carry out this task, an Agilent 6460 Triple Quad LC/MS (California, USA) was expertly coupled with the Agilent 1200 series high-performance liquid chromatography (HPLC) system (California, USA). This cutting-edge instrumentation allowed for the accurate determination of the concentrations of specific flavonoids present in VGME. To do so, calibration curves correlating concentration with peak area were thoughtfully generated for each individual flavonoid of interest. By skillfully comparing the peak areas of the flavonoids in VGME to the established calibration curves, the respective concentrations of these compounds within VGME were quantified. This methodical and data-driven approach ensures the precision and reliability of the obtained results regarding VGME's flavonoid content, providing invaluable insights for the study's objectives.

Determination of cell viability

In this study, human neuroblastoma cells (SH-SY5Y, ATCC CRL-2266) were thoughtfully procured from the Foot and Mouth Institute located in Ankara, Turkey. These cells were cultivated using Dulbecco's modified Eagle's medium (DMEM) sourced from Gibco (Massachusetts, USA). The growth medium was enriched with 10% fetal bovine serum (FBS) from Gibco (Massachusetts, USA) along with 1% penicillin/streptomycin and 1% L-glutamine, both also from Gibco (Massachusetts, USA). The cell culture was meticulously maintained in a humidified environment with a 5% CO_2 and 95% air mixture at a stable temperature of 37 °C. To ensure healthy cell growth, the medium was replenished three times weekly when the cells approached confluence. This careful maintenance of cell cultures helps to guarantee their vitality and reliability in subsequent experiments. The impact of VGME on cell viability was systematically assessed by cultivating SH-SY5Y cells in 96-well plates, with an initial seeding density of 10,000 cells per well. The cells were then incubated in a controlled environment with 5% CO_2 at 37 °C. Subsequently, VGME was introduced to the wells at varying concentrations (ranging from 0 to 1000 µg/mL) and for different durations of 24, 48, and 72 h. Following the designated incubation periods, VGME was carefully removed from the wells, and the cells were thoroughly washed with phosphate-buffered saline (PBS) sourced from Merck (Pennsylvania, USA). Fresh media were then added to the wells. To assess cell viability, the widely-used MTT (3-(4,5-dimethylthiazol-2-yl)-2,5-diphenyltetrazolium bromide) assay was employed. Specifically, 20 µL of a 0.5% MTT solution from Sigma-Aldrich (Massachusetts, USA), prepared in PBS, was added to each well. After a subsequent four h incubation and removal of the medium, 200 µL of dimethyl sulfoxide (DMSO) from Sigma-Aldrich (Massachusetts, USA), was applied to dissolve the

formazan crystals that had formed. The absorbance levels were then accurately measured at 570 nm using an ELISA microplate reader from BioTek (Vermont, USA). To derive the cell viability values, the absorbance of the untreated control cells was divided by that of the treated cells. The results were expressed as percentages, providing a comprehensive view of how VGME affected the viability of SH-SY5Y cells. This rigorous experimental procedure ensured the reliability and validity of the findings in the assessment of cell viability.

Flow cytometric detection of reactive oxygen species (ROS)

In the investigation of cellular reactive oxygen species (ROS) levels, a meticulous protocol was meticulously adhered to. To assess ROS levels, the cells were deliberately treated with DCFDA (20 µM), a fluorescent probe supplied by Cayman Chemical (Michigan, USA). This step enabled the specific detection of ROS within the cellular environment. Following the introduction of DCFDA, the treated cells were subjected to a controlled incubation period at 37 °C for a duration of 30 min. During this incubation, the cells were allowed to interact with DCFDA, which is capable of detecting changes in ROS levels. After this incubation period, the cells were carefully pipetted and made ready for detailed analysis through the utilization of the ACEA NovoCyte flow cytometer (California, USA). This advanced flow cytometry system was instrumental in the systematic examination of the cells, providing a comprehensive view of ROS levels and their fluctuations. For each sample, an impressive 10^4 cells were analyzed, ensuring a statistically robust dataset. The ACEA NovoExpress software (California, USA), a powerful tool for flow cytometry data analysis, was then employed to process and record the data. The software allowed for the precise determination of the mean change in ROS levels within the cell population, shedding light on how the experimental conditions influenced the cellular oxidative stress. This information is crucial in understanding the impact of the study variables on cellular responses and oxidative processes. The careful execution of this procedure, coupled with the use of advanced equipment and software, guaranteed that the results were reliable and informative. This, in turn, greatly contributed to the comprehensive understanding of the dynamics of ROS levels in the context of the study.

Flow cytometric detection of apoptotic cells

In the meticulous evaluation of cell apoptosis, a well-thought-out procedure was meticulously followed. Specifically, a total of 5 µL of annexin V-FITC and an additional 5 µL of propidium iodide (PI), both sourced from Abcam (Cambridge, UK), were thoughtfully introduced into each 100 µL of the cell suspension, encompassing approximately 1×10^6 cells. These vital fluorescent probes were instrumental in distinguishing and quantifying different cell populations based on their membrane integrity and apoptotic status. Following the addition of annexin V-FITC and PI, the cells were subjected to a controlled incubation period in the dark, carried out at room temperature, for a duration of 15 min. This incubation allowed for the binding of annexin V-FITC and PI to the cells, enabling their distinct identification in terms of apoptotic features. After the incubation, 400 µL of 1x annexin-binding buffer was meticulously added to the cell suspension. This step served to stabilize and prepare the cells for precise analysis. The cell analysis was conducted using the advanced ACEA NovoCyte flow cytometry system (California, USA). This state-of-the-art equipment enabled the systematic examination of the stained cells, providing detailed insights into their apoptotic status and membrane integrity. For each sample, an extensive dataset was generated by analyzing a representative sample size of 10,000 cells, ensuring that the results were both comprehensive and statistically sound. Subsequently, the ACEA NovoExpress software (California, USA), designed for flow cytometry data analysis, was employed to record and process the data. The recorded data allowed for the precise determination of the percentages of live, early apoptotic, late apoptotic, and necrotic cells within the cell population. This comprehensive analysis shed light on the dynamic processes associated with cell apoptosis and provided valuable information regarding the experimental conditions' impact on cellular responses. The rigor and attention to detail in this procedure ensured that the results were robust, reliable, and informative, contributing significantly to the understanding of cell apoptosis in the context of the study.

Flow cytometric detection of mitochondrial membrane potential ($\Delta\psi_m$)

In the assessment of mitochondrial integrity, tetraethylbenzimidazolylcarbocyanine iodide (JC-1), a fluorescent probe provided by Cayman Chemical (Michigan, USA), was skillfully incorporated into the experimental setup. Specifically, 100 µL of JC-1 was meticulously added to a cell population comprising approximately 1×10^6 cells. This critical step ensured the staining of the mitochondria within the cells. The cells were then subjected to a controlled cell culture environment maintained at 37 °C for a duration of 30 min. This incubation period was crucial for allowing JC-1 to interact with the mitochondria within the cells, revealing crucial information about their integrity. Subsequently, the cells were systematically harvested and carefully pipetted for removal, followed by a thorough washing with PBS, performed twice. This rigorous washing process was essential to remove any excess JC-1 and to prepare the cells for precise analysis. To carry out the analysis, an ACEA NovoCyte flow cytometer (California, USA) was skillfully employed, a powerful instrument for conducting flow cytometry.

This high-tech equipment facilitated the assessment of mitochondrial integrity by capturing and analyzing data from the stained cells. A substantial dataset was generated by analyzing 10,000 cells per sample, ensuring a comprehensive and representative assessment. The ACEA NovoExpress software (California, USA), a sophisticated tool designed for flow cytometry data analysis, was then utilized to process the data. Through the application of this software, the percentages of intact and disrupted mitochondria were meticulously determined. This analysis provided valuable insights into the state of the mitochondria within the cell population, shedding light on their structural integrity and any alterations induced by the experimental conditions. This meticulous procedure not only offers precise quantitative data but also ensures the reliability and validity of the results in the context of mitochondrial integrity assessment, contributing to a deeper understanding of cellular responses.

qRT-PCR

In the pursuit of investigating the molecular alterations induced by VGME, a meticulously designed series of laboratory techniques was employed. Initially, total RNA extraction from SH-SY5Y cells was carried out with the highly regarded RNeasy mini kit from Qiagen (Hilden, Germany), ensuring the efficient isolation of RNA. Subsequently, the quantitect reverse transcription kit, also from Qiagen (Hilden, Germany), was conscientiously utilized to perform reverse transcription following the manufacturer's recommended protocols. This step allowed for the conversion of RNA into complementary DNA (cDNA), a pivotal transformation in molecular biology research. To delve into the VGME-mediated changes in gene expression, a quantitative real-time polymerase chain reaction (qRT-PCR) technique was executed. For this purpose, carefully selected primers tailored to each specific gene of interest, including *BAX*, *BCL2*, *CASP3*, *CASP7*, *CASP8*, *CASP9*, and *CYCS*, were thoughtfully employed. These primers facilitated the precise quantification of gene expression levels. To ensure accurate comparisons and normalize the data, *β-actin* was chosen as a reference gene, which served as a stable point of reference for the analysis. This normalization step is essential to mitigate variations in the experimental process. The qRT-PCR protocol was executed with the following settings: a preliminary 5-min denaturation step at 95 °C, followed by 40 cycles comprising 10 sec of denaturation at 95 °C, 30 sec of annealing at 60 °C, and 30 sec of extension at 72 °C. This meticulously designed protocol allowed for the precise amplification and quantification of the target genes. To determine the relative changes in gene expression levels, the $2^{-\Delta\Delta CT}$ method was meticulously employed, a widely accepted approach in qRT-PCR analysis. This method provides a robust means of calculating fold regulation and enables a clear interpretation of the alterations in gene expression induced by VGME. Finally, the results were thoughtfully presented as fold regulations, offering a comprehensive and understandable depiction of the changes in gene expression levels attributed to VGME treatment. This methodical approach ensures the reliability and validity of the molecular insights gained in this research.

Data analysis

Each experiment was thoughtfully conducted in triplicate, ensuring rigorous and reliable data for subsequent statistical analyses. The resulting data for all variables were thoughtfully presented as mean values accompanied by their corresponding standard deviations (SD), a commonly accepted practice to convey the consistency and dispersion of the measurements. For the purpose of data analysis, all statistical procedures were meticulously carried out using SPSS version 11.0 (New York, USA), a widely used and respected statistical software tool. To assess the significance of differences between the study groups in terms of means, a one-way ANOVA test, a robust statistical method, was thoughtfully employed. This test provided a comprehensive assessment of any variations among the experimental groups. It's important to note that a threshold of statistical significance was defined as a *P*-value of less than 0.05. In accordance with this criterion, any observed results with a *P*-value below 0.05 were regarded as statistically significant, underscoring the reliability and validity of the findings in the study. This rigorous approach to experimental design and data analysis ensures that the conclusions drawn from this research are both credible and meaningful.

Results and Discussion

As a preliminary study, total phenolic (15.42 ± 0.92 mg/g), total flavonoid (117.13 ± 0.78 mg/g), ascorbic acid (2.12 ± 0.93 mg/g), β-carotene (1.89 ± 0.65 mg/g), lycopene (0.63 ± 0.23 mg/g), and total alkaloid (0.45 ± 0.11 mg/g) contents of VGME were determined. Since the total flavonoid content was the main component found in VGME, the study focused on flavonoids. In a study conducted by Selseleh et al. (2020), the total flavonoid content of 10 distinct *Verbascum* species gathered from Iran was found to range from 12 to 22 mg/g. In a study conducted by Kızıltaş et al. (2022), the total flavonoid content in *V. speciosum* Schrad extracts was measured to be in the range of 5-16 µg/mL. Similarly, Luca et al. (2019) revealed that the total flavonoid content of *V. ovalifolium* Donn ex Sims extracts, prepared using various solvents, fluctuated between 17-107 mg/g. Additionally, research by Mihalovic et al. (2016) showed that extracts from *V. nigrum*, *V. phlomoides*, and *V. thapsus* had total flavonoid contents varying from 10-53 mg/g. Our results are confirming the high total flavonoid content in VGME. Our study found a higher total flavonoid content in VGME compared to the studies conducted by Kızıltaş et al. (2022), Luca et al. (2019), Mihalovic et al. (2016), and Selseleh et al. (2020).

Extensive prior phytochemical studies, as exemplified by Gökmen et al. (2021), have previously uncovered the presence of flavonoids within the chemical composition of the *Verbascum* genus. Flavonoids, regarded as a vital category of bioactive compounds in plants, have been reported to be distributed across various plant components, a fact highlighted by Amini et al. (2021). In light of these findings, our study sought to elucidate the flavonoid composition of VGME (*Verbascum gypsicola* methanolic extract) through the employment of LC-MS/MS techniques. The outcomes of our investigation revealed the presence of seven distinct flavonoids within VGME. Notably, the analysis disclosed that apigenin exhibited the highest concentration of flavonoids within VGME, while amentoflavone was found to be the least abundant, as outlined in **Table 1.** Drawing from the research conducted by Amini et al. (2021), it is evident that certain *Verbascum* species, particularly *V. saccatum* and *V. songaricum*, are distinguished by their high overall flavonoid content, featuring compounds such as apigenin, quercetin, and rutin. Further corroborating our findings, a study by Klimek et al. (2020) demonstrated that flower samples of *V. phlomoides* are notably rich in diosmin and tamarixetin, while *V. densiflorum* predominantly contains verbascoside and luteolin. Moreover, Mahmoud et al. (2007) successfully isolated and identified luteolin and chrysoeriol within *V. sinaiticum*. In the case of *V. thapsu*s, a species within the *Verbascum* genus, research by Alipieva et al. (2014) has revealed the presence of a unique bisflavonoid known as amentoflavone. Consistent with the wealth of knowledge within the existing literature, our study underscores the significant flavonoid content in *V. gypsicola*, reinforcing the potential for this plant species to serve as a valuable source of flavonoids, a feature that aligns with the established characteristics of certain other *Verbascum* species recognized for their flavonoid richness. These findings collectively emphasize the substantial value and relevance of VGME within the context of flavonoid research and its potential applications.

Table 1. Flavonoid composition and quantity of VGME

Flavonoid composition	Control (µg/g)	VGME (µg/g)
Apigenin	0.00 ± 0.00	0.47 ± 0.02*
Luteolin	0.00 ± 0.00	0.43 ± 0.03*
Quercetin	0.00 ± 0.00	0.39 ± 0.01*
Diosmin	0.00 ± 0.00	0.13 ± 0.00*
Chrysoeriol	0.00 ± 0.00	0.08 ± 0.02*
Tamarixetin	0.00 ± 0.00	0.07 ± 0.04*
Amentoflavone	0.00 ± 0.00	0.05 ± 0.04*

*P <0.05, compared with the control group

Numerous studies have delved into the pharmacological effects of plant extracts enriched with flavonoids, underscoring the increasing significance attributed to these flavonoid-rich plant sources, as noted by Shakeri et al. (2015) and emphasized by Kızıltaş et al. (2022). Consequently, the exploration of VGME's impact on cellular viability, particularly in the context of SH-SY5Y cells, becomes a critical focal point in this research. The assessment of SH-SY5Y cell viability through MTT analysis revealed a compelling and dose-dependent response to varying concentrations of VGME (ranging from 0 to 1000 µg/mL) over different time intervals (24, 48, and 72 h). Notably, an inverse relationship was observed between VGME concentrations and treatment duration, leading to a statistically significant inhibition of SH-SY5Y cell viability (P< 0.05). The calculated IC_{50} doses for VGME were found to be 96 µg/mL for 24 h, 50 µg/mL for 48 h, and 10 µg/mL for 72 h, ultimately leading to the selection of the IC_{50} dose of 50 µg/mL for 48 h as the optimal condition for subsequent investigations, as depicted in **Figure 1.** In a parallel context, Dinani et al. (2020) explored the cytotoxic properties of various saponin- and flavonoid-rich fractions derived from *V. alceoides*, a member of the *Verbascum* genus. Their study involved in vitro assessments using the MTT assay on HeLa and HUVEC cells, revealing a significant and dose-dependent inhibitory effect on cell proliferation, with components D, E, and A exhibiting IC_{50} values of 30, 39.8, and 188.6 µg/mL, respectively. Additionally, Garcia-Oliveira et al. (2022) examined the cytotoxic effects of ethanolic and infusion extracts *from V. sinuatum*, one of the traditional medicinal herbs, against four distinct cancer cell lines: MCF-7, NCI-H640, HeLa, and HepG2. Their findings demonstrated the pronounced impact of *V. sinuatum* on these cancer cell lines, with GI_{50} values ranging between 101.1 and 172.2 µg/mL for the ethanolic extract and 59.1 and 92.1 µg/mL for the infusion extract. In light of these studies, our findings are consistent with the existing literature, illustrating VGME's cytotoxic activity against SH-SY5Y cells. It is our belief that the potent cytotoxicity of VGME against SH-SY5Y cells can be primarily attributed to its abundant flavonoid content. Nevertheless, further research (to investigate the direct effect of flavanoids in VGME, it is necessary to isolate and purify these compounds from VGME) is imperative to validate and expand upon this hypothesis, shedding more light on the precise mechanisms underlying VGME's cytotoxic effects and its potential applications in the field of cytotoxicity and cancer research.

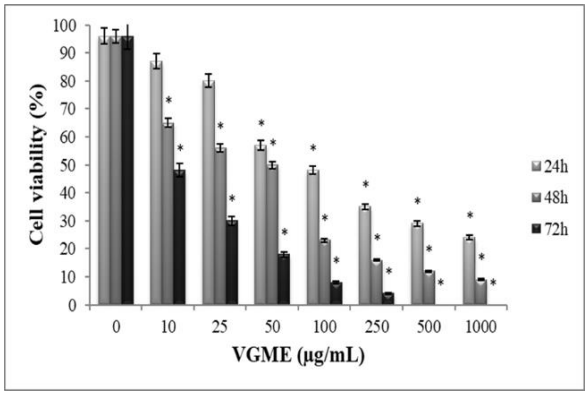

Figure 1. Effect of different VGME concentrations (0-1000 µg/mL) on cell viability for 24, 48, and 72 h in SH-SY5Y cells. *P <0.05, compared with the control group.

In specific contexts, flavonoids have been found to exhibit a paradoxical propensity towards oxidation, a phenomenon well-documented in scientific studies. This dual nature of flavonoids, which can act as both antioxidants and prooxidants, has been linked to their ability to induce oxidative stress within cells, particularly in the context of neoplastic conditions. As highlighted by Slika et al. (2022), certain flavonoids have the remarkable capacity to stimulate the accumulation of reactive oxygen species (ROS) within cells, a process that can trigger apoptosis and contribute to the reduction of tumor mass. In the context of our study, flow cytometry analysis was conducted to investigate the impact of VGME on intracellular ROS levels in SH-SY5Y cells. Our results revealed a significant reduction in ROS levels in the VGME-treated SH-SY5Y cells compared to the control cells that were not exposed to VGME ($P< 0.05$), as depicted in **Figure 2** and **Table 2.** Previous research by Shi et al. (2015) and Hu et al. (2015) has suggested that the prooxidative activity of apigenin arises from mechanisms such as partial glutathione depletion and inhibition of superoxide dismutase. Similarly, studies by Jeong et al. (2009), Gibellini et al. (2010), and Lu et al. (2006) have linked quercetin's prooxidative effects to the generation of free radicals through participation in intracellular redox reactions, as well as partial glutathione depletion and the inhibition of thioredoxin reductase. Additionally, research by Ferino et al. (2020) and Zhou et al. (2017) has demonstrated that luteolin can induce prooxidative activity by activating PI3K through oxidative stress-induced pathways, subsequently engaging the Akt/mTOR/p70S6K pathway, inhibiting Nrf2 and the prosurvival protein Snail, and activating the proapoptotic Raf kinase inhibitor protein. In consonance with the existing body of literature, our findings align well with the prooxidative activity of VGME, particularly in its ability to elevate ROS levels within SH-SY5Y cells. We posit that this prooxidative impact of VGME on SH-SY5Y cells can be attributed to its substantial flavonoid content. Nevertheless, it is crucial to emphasize that additional research (to investigate the direct effect of flavanoids in VGME, it is necessary to isolate and purify these compounds from VGME) is required to validate and expand upon this hypothesis, delving deeper into the specific mechanisms through which VGME exerts its prooxidative influence and its potential implications for applications in the context of oxidative stress and cancer research.

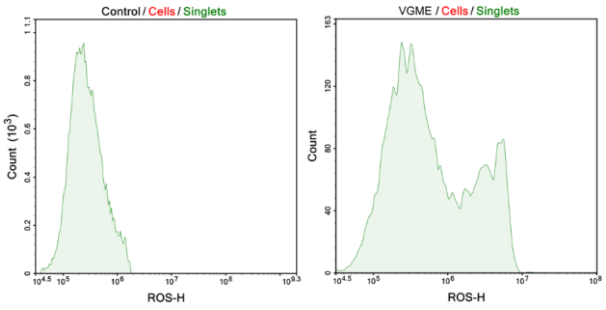

Figure 2. Effect of 50 µg/mL VGME (48 h) on intracellular ROS levels in SH-SY5Y cells.

Table 2. Effect of VGME on mean intracellular ROS levels in SH-SY5Y cells using flow cytometry

	Control	VGME
Mean ROS	192 ± 24	1360 ± 38*

*P <0.05, compared with the control group

The intrinsic apoptotic pathway, also known as the mitochondrial pathway, is one of the primary mechanisms of programmed cell death (Singh and Lim, 2022). This pathway is activated in response to intracellular stress signals such as DNA damage, lack of growth factors, or oxidative stress (Morana et al., 2022). At the heart of the intrinsic apoptotic pathway are the mitochondria. Under intracellular stress conditions, pro-apoptotic proteins like BAX and BAK permeabilize the mitochondrial outer membrane (Green, 2022a). This leads to the release of pro-apoptotic factors from the mitochondria, such as cytochrome c, into the cytosol (Lossi, 2022). Once released, cytochrome c interacts with apoptotic protease activating factor-1 (APAF-1), resulting in the formation of the apoptosome complex that activates caspase-9 (Green, 2022b). The activated caspase-9 subsequently activates caspase-3 and caspase-7, leading to controlled cell death (Gourisankar et al., 2023). On the other hand, anti-apoptotic proteins like BCL2 inhibit apoptosis by preventing the permeabilization of the mitochondrial membrane (Cetraro et al., 2022). This balance plays a critical role in determining whether a cell lives or dies and is a critical factor in many diseases, especially in cancer (Wan et al., 2022). Therefore, understanding and modulating the intrinsic apoptotic pathway forms the foundation of many therapeutic strategies (Singh et al., 2022).

Flavonoids have emerged as potent inhibitors of numerous signal transduction pathways critical to the development of cancer, exerting their influence by disrupting cell viability, angiogenesis, inhibiting distant tumor spread, and promoting apoptosis, as established by Abotaleb et al. (2018). In this context, our study focused on investigating the impact of VGME on the percentages of viable cells, cells in the early and late stages of apoptosis, as well as necrotic cells within the SH-SY5Y cell line, employing flow cytometry. The results from our study revealed a significant increase in the percentage of cells in the early and late stages of apoptosis, as well as necrotic cells when treated with VGME in comparison to the control cells that were not subjected to VGME treatment ($P< 0.05$), as illustrated in **Figure 3** and **Table 3**. Building upon these findings, Srivastava et al. (2016) conducted research on quercetin, showing that the treatment of cells led to an increase in early apoptotic cells at 6 and 12 h, while treatments over longer durations (18, 24, and 48 h) resulted in a higher percentage of late apoptotic cells. This observation strongly suggests a promotion of apoptotic pathways. Cai et al. (2011) reported a proapoptotic effect of luteolin on A549 cells, as evidenced by Hoechst 33258 and annexin V-FITC/PI staining. Flow cytometry analysis revealed a significant population of apoptotic cells and an increased number

of cells in the G2 phase. Furthermore, Souza et al. (2017) investigated the effects of apigenin and found that this compound displayed a selective cytotoxic effect, mediating apoptosis in Annexin V-marked HeLa, SiHa, CaSki, and C33A cells, while not affecting the HaCaT control cells. In accordance with the established literature, our study aligns with these findings, demonstrating that VGME has a proapoptotic impact on SH-SY5Y cells. It is our belief that VGME's proapoptotic effect against SH-SY5Y cells can be attributed to its substantial flavonoid content. However, to provide conclusive evidence, further research (to investigate the direct effect of flavanoids in VGME, it is necessary to isolate and purify these compounds from VGME) is essential to delve deeper into the precise molecular mechanisms through which VGME induces apoptosis and to explore its potential applications in cancer research and therapy.

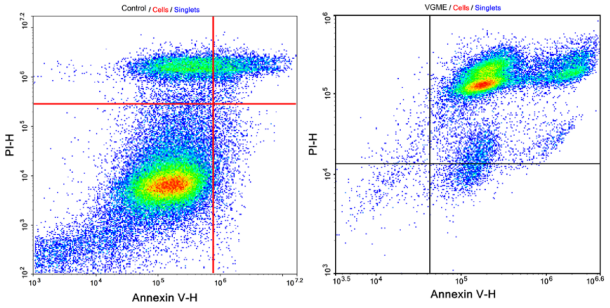

Figure 3. Effect of 50 µg/mL VGME (48 h) on live, apoptotic, and necrotic cells in SH-SY5Y cells.

Table 3. Effect of VGME on live, apoptotic, and necrotic cells (%) in SH-SY5Y cells using flow cytometry

Type of Cells	Control (%)	VGME (%)
Live	83.43 ± 5.43	3.13 ± 0.75*
Early apoptotic	2.35 ± 0.96	6.35 ± 3.23*
Late apoptotic	5.68 ± 1.23	89.78 ± 7.65*
Necrotic	8.54 ± 3.54	0.74 ± 0.50*

*P <0.05, compared with the control group

Flavonoids have been recognized for their ability to promote apoptosis in cancer cells, and this effect is often associated with their capacity to increase the generation of mitochondrial reactive oxygen species (ROS), including superoxide and hydrogen peroxide. This increase in ROS production is typically followed by the creation of mitochondrial permeability transition pores and the subsequent release of cytochrome c (*CYCS*), a pivotal event in the apoptosis process, as noted by Kachadourian and Day (2006). In light of this knowledge, our study employed flow cytometry analysis to evaluate VGME's impact on the percentage of intact and disrupted mitochondria within SH-SY5Y cells. Notably, VGME led to a substantial increase in the percentage of disrupted mitochondria in SH-SY5Y cells when compared to control cells that did not receive VGME treatment (P< 0.05), as visualized in **Figure 4** and outlined in **Table 4.** Reinforcing our findings, Chen et al. (2014b) reported that apigenin has the ability to reduce the mitochondrial membrane potential of gastric carcinoma cells, as demonstrated through JC-1 staining. Similarly, in an event reliant on mitochondrial membrane potential, Shen et al. (2016) revealed that quercetin triggered apoptosis in cells. Moreover, Chen et al. (2017) observed that luteolin induced a reduction in mitochondrial membrane potential, indicating intrinsic apoptosis mediated by JC-1. Our study aligns with the existing literature by demonstrating that VGME induces mitochondrial depolarization in SH-SY5Y cells. It is our perspective that VGME exerts its activity by causing mitochondrial depolarization in SH-SY5Y cells, likely attributed to its enriched flavonoid content. Nevertheless, further in-depth investigation (to investigate the direct effect of flavanoids in VGME, it is necessary to isolate and purify these compounds from VGME) is essential to validate and expand upon this hypothesis, unraveling the precise mechanisms through which VGME induces mitochondrial depolarization and exploring its potential implications for cancer research and therapeutic development.

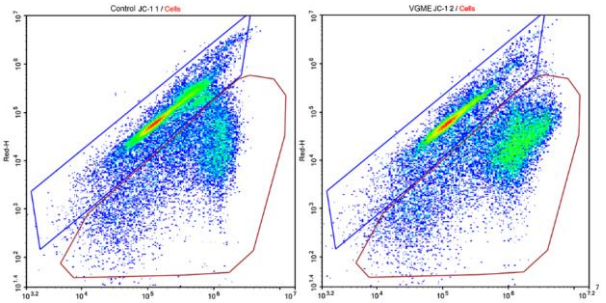

Figure 4. Effect of 50 µg/mL VGME (48 h) on intact and disrupted mitochondria in SH-SY5Y cells.

Table 4. Effect of VGME intact and distrupted mitochondria (%) in SH-SY5Y cells using flow cytometry

Types of mitochondria	Control (%)	VGME (%)
Intact	84.76 ± 5.67	57.57 ± 3.45*
Distrupted	14.97 ± 4.43	42.25 ± 2.12*

*P <0.05, compared with the control group

Flavonoids have been identified as influential agents capable of initiating events that lead to cell death by modulating the apoptotic signaling cascade, as established by Kopustinskiene et al. (2020). Our study aimed to elucidate the impact of VGME on SH-SY5Y cells by assessing its effect on genes involved in the intrinsic apoptosis pathway through quantitative real-time polymerase chain reaction (qRT-PCR). The results were striking, indicating that VGME significantly increased the expression levels of key apoptotic genes, including *BAX*, *CASP3*, *CASP7*, *CASP8*, *CASP9*, and *CYCS*, while simultaneously reducing the expression of the anti-apoptotic gene *BCL2* in SH-SY5Y cells when compared to control cells that were not exposed to VGME (P< 0.05), as depicted in **Figure 5**. Expanding upon these findings, it's worth noting that luteolin, as reported by Lin et al. (2008), has been shown to induce DNA damage and activate p53, thereby promoting the intrinsic apoptosis

pathway. This is achieved through its ability to impede the proper functioning of DNA topoisomerases. Similarly, in a study conducted by Teekaraman et al. (2019), quercetin was found to promote apoptosis in the PA-1 cell line by upregulating the expression of key apoptotic genes, including *CYCS*, *CASP9*, and *CASP3*. This suggests the activation of caspase-9 and caspase-3 via the release of cytochrome c from mitochondria, a process that may be mediated by the intrinsic pathway due to a reduction in ROS levels and the ensuing apoptosis. Moreover, apigenin, as reported by Wang and Zhao (2017), has been shown to enhance apoptosis by triggering increased intracellular ROS production, calcium release, mitochondrial membrane damage, and upregulation of gene expression related to various apoptotic factors. This cascade of events ultimately leads to cell apoptosis. In accordance with the wealth of data within the existing literature, our study demonstrates that VGME exhibits a pronounced proapoptotic effect on SH-SY5Y cells. We believe that VGME's proapoptotic activity on SH-SY5Y cells can be attributed to its rich flavonoid content. However, it is imperative to emphasize the necessity for further research (to investigate the direct effect of flavanoids in VGME, it is necessary to isolate and purify these compounds from VGME) to validate and expand upon this hypothesis, gaining a deeper understanding of the specific molecular mechanisms through which VGME induces apoptosis and exploring its potential applications in the context of cancer research and therapeutic development. While studies involving plant extracts provide valuable insights into potential health benefits or medicinal properties, it's essential to acknowledge the limitations and complexities associated with such studies. Researchers often utilize these initial findings as a springboard for more targeted investigations to identify and comprehend the specific compounds responsible for the observed effects.

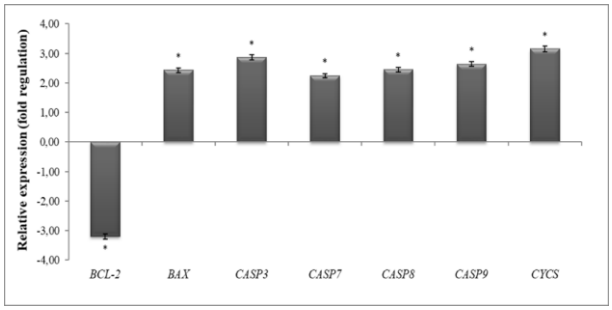

Figure 5. Effect of VGME on relative expression levels of genes involved in the intrinsic apoptosis pathway on SH-SY5Y cells. **P* <0.05, compared with the control group.

Conclusion

In summary, this comprehensive study has provided compelling evidence that VGME, rich in flavonoids, plays a pivotal role in the generation of a significant quantity of reactive oxygen species (ROS). This surge in ROS levels triggers a cascade of events within SH-SY5Y cells, including the disruption of mitochondrial membrane potential (ΔΨM) and activation of the intrinsic apoptotic pathway. Consequently, these cellular changes culminate in a noteworthy reduction in the longevity of SH-SY5Y cells. The remarkable ability of VGME to use the intrinsic apoptotic pathway as a mechanism to inhibit cancer growth has been demonstrated for the first time in this study, demonstrating its potential as a promising candidate in the development of new anticancer drugs. This research underscores the significance of exploring VGME and its flavonoid content as a potential therapeutic avenue for combating cancer, further emphasizing the need for continued investigation and development in this exciting field of study.

Acknowledgements

I would like to thank Prof. Dr. Belma Aslım for providing *Verbascum gypsicola* Vural & Aydoğdu methanolic extract.

References

Abotaleb, M., Samuel, S. M., Varghese, E., Varghese, S., Kubatka, P., Liskova, A., Büsselberg, D. (2018). Flavonoids in cancer and apoptosis. *Cancers*, *11*(1), 28. https://doi.org/10.3390/cancers11010028.

Afifi, M. S., Ahmed, M. M., Pezzuto, J. M., Kinghornt, A. D. (1993). Cytotoxic flavonolignans and flavones from Verbascum sinaiticum leaves. *Phytochemistry*, *34*(3), 839-841. https://doi.org/10.1016/0031-9422(93)85369-3.

Alipieva, K. I., Orhan, I. E., Cankaya, I. I. T., Kostadinova, E. P., Georgiev, M. I. (2014). Treasure from garden: Chemical profiling, pharmacology and biotechnology of mulleins. *Phytochemistry Reviews*, 13, 417-444. https://doi.org/10.1007/s11101-014-9361-5.

Alkowni, R., Jaradat, N., Fares, S. (2023). Total phenol, flavonoids, and tannin contents, antimicrobial, antioxidant, vital digestion enzymes inhibitory and cytotoxic activities of Verbascum fruticulosum. *European Journal of Integrative Medicine*, 60, 102256. https://doi.org/10.1016/j.eujim.2023.102256.

Amini, S., Hassani, A., Alirezalu, A., Maleki, R. (2022). Phenolic and flavonoid compounds and antioxidant activity in flowers of nine endemic Verbascum species from Iran. *Journal of the Science of Food and Agriculture*, *102*(8), 3250-3258. https://doi.org/10.1002/jsfa.11667.

Amiri, M. M., Garnida, Y., Almulla, A. F., Abduljabbar, A. S., Jalil, A. T., Mazaheri, Y., Ebrahimi, Y., Shariatifar, N. (2023). Herbal therapy for hemorrhoids: An overview of medicinal plants affecting hemorrhoids. *Advancements in Life Sciences*, *10*(1), 22-28. https://doi.org/10.1003/s101-017-2228-5.

Anoushirvani, A. A., Jafarian Yazdi, A., Amirabadi, S., Asouri, S. A., Shafabakhsh, R., Sheida, A., Khabr, M. S. H., Jafari, A., Zadeh, S. S. T., Hamblin, M. R., Kalantari, L., Zavareh, S. A. T., Mirzaei, H. (2023). Role of non-coding RNAs in neuroblastoma. *Cancer Gene Therapy*, 1-19. https://doi.org/10.1038/s41417-023-00623-0.

Ataur Rahman, M., Kim, N. H., Yang, H., Huh, S. O. (2012). Angelicin induces apoptosis through intrinsic caspase-

dependent pathway in human SH-SY5Y neuroblastoma cells. *Molecular and Cellular Biochemistry*, 369, 95-104. https://doi.org/10.1007/s11010-012-1372-1.

Aydin, Ç., Rakhimzhanova, A., Kilinçarslan, Ö., Mammadov, R. (2020). Antioxidant and phenolic characterization with HPLC of various extract of Verbascum glomeratum Linneus. *Journal of The Chemical Society of Pakistan, 42*(2), 222-227. https://doi.org/10.52568/000639/JCSP/42.02.2020.

Cai, X., Ye, T., Liu, C., Lu, W., Lu, M., Zhang, J., Wang, M., Cao, P. (2011). Luteolin induced G2 phase cell cycle arrest and apoptosis on non-small cell lung cancer cells. *Toxicology in Vitro*, *25*(7), 1385-1391. https://doi.org/10.1016/j.tiv.2011.05.009.

Cetraro, P., Plaza-Diaz, J., MacKenzie, A., Abadía-Molina, F. (2022). A review of the current impact of inhibitors of apoptosis proteins and their repression in cancer. *Cancers*, *14*(7), 1671. https://doi.org/10.3390/cancers14071671.

Chen, J., Chen, J., Li, Z., Liu, C., Yin, L. (2014b). The apoptotic effect of apigenin on human gastric carcinoma cells through mitochondrial signal pathway. *Tumor Biology*, *35*, 7719-7726. https://doi.org/10.1007/s13277-014-2014-x.

Chen, P., Zhang, J. Y., Sha, B. B., Ma, Y. E., Hu, T., Ma, Y. C., Sun, H., Shi, J.X., Dong, Z. M., Li, P. (2017). Luteolin inhibits cell proliferation and induces cell apoptosis via down-regulation of mitochondrial membrane potential in esophageal carcinoma cells EC1 and KYSE450. *Oncotarget*, *8*(16), 27471. https://doi.org/10.18632/oncotarget.15832.

Chen, J., Sun, M., Wang, X., Lu, J., Wei, Y., Tan, Y., Liu, Y., Götz, J., He, R., Hua, Q. (2014a). The herbal compound geniposide rescues formaldehyde-induced apoptosis in N2a neuroblastoma cells. *Science China Life Sciences*, *57*, 412-421. https://doi.org/10.1007/s11427-014-4643-0.

Demirci, S., Alp, C., Akşit, H., Ulutaş, Y., Altay, A., Yeniçeri, E., Köksal, E., Yaylı, N. (2023). Isolation, characterization and anticancer activity of secondary metabolites from Verbascum speciosum. *Chemical Biology & Drug Design*, *101*(6), 1273-1282. https://doi.org/10.1111/cbdd.14211.

Dinani, M. S., Malakooti, S., Akbari, V. (2020). In vitro cytotoxic activity of Verbascum alceoides against cervix carcinoma cells. *Journal of Reports in Pharmaceutical Sciences*, *9*(1), 19. https://doi.org/10.4103/jrptps.JRPTPS_65_19.

Ferino, A., Rapozzi, V., Xodo, L. E. (2020). The ROS-KRAS-Nrf2 axis in the control of the redox homeostasis and the intersection with survival-apoptosis pathways: Implications for photodynamic therapy. *Journal of Photochemistry and Photobiology B: Biology*, 202, 111672. https://doi.org/10.1016/j.jphotobiol.2019.111672.

Gao, J., Fosbrook, C., Gibson, J., Underwood, T., Gray, J., Walters, Z. (2023). Targeting EZH2 in neuroblastoma. *Cancer Treatment Reviews*, 119, 102600. https://doi.org/10.1016/10.1016/j.ctrv.2023.102600.

Garcia-Oliveira, P., Carreira-Casais, A., Pereira, E., Dias, M. I., Pereira, C., Calhelha, R. C., Stojkovic, D., Sokovic, M., Simal-Gandara, J., Prieto, M. A., Caleja, C. Barros, L. (2022). From tradition to health: Chemical and bioactive characterization of five traditional plants. *Molecules*, *27*(19), 6495. https://doi.org/10.3390/molecules27196495.

Gibellini, L., Pinti, M., Nasi, M., De Biasi, S., Roat, E., Bertoncelli, L., Cossarizza, A. (2010). Interfering with ROS metabolism in cancer cells: the potential role of quercetin. *Cancers, 2*(2), 1288–1311. https://doi.org/10.3390/cancers2021288.

Gourisankar, S., Krokhotin, A., Ji, W., Liu, X., Chang, C. Y., Kim, S. H., Li, Z., Wenderski, W., Simanauskaite, J. M., Yang, H., Vogel, H., Zhang, T., Green, M. R., Gray, N. S., Crabtree, G. R. (2023). Rewiring cancer drivers to activate apoptosis. *Nature*, *620*(7973), 417-425. https://doi.org/10.1038/s41586-023-06348-2.

Gökmen, A., Kúsz, N., Karaca, N., Demirci, F., Hohmann, J., Kırmızıbekmez, H. (2021). Secondary metabolites from Verbascum bugulifolium Lam. and their bioactivities. *Natural Product Research*, *35*(23), 5294-5298. https://doi.org/10.1080/14786419.2020.1753052.

Göse, M., Hacıoğlu, N. (2021). Bioactive compounds, antimicrobial and antibiofilm activity of two Verbascum species. *Kahramanmaraş Sütçü İmam Üniversitesi Tarım ve Doğa Dergisi*, *24*(3), 479-487. https://doi.org/10.18016/ksutarimdoga.v24i60916.750034.

Green, D. R. (2022a). The mitochondrial pathway of apoptosis Part I: MOMP and beyond. *Cold Spring Harbor Perspectives in Biology*, *14*(5), a041038. https://doi.org/10.1101/cshperspect.a041038.

Green, D. R. (2022b). The mitochondrial pathway of apoptosis Part II: The BCL-2 protein family. *Cold Spring Harbor Perspectives in Biology*, *14*(6), a041046. https://doi.org/10.1101/cshperspect.a041046.

Hagemann, S., Misiak, D., Bell, J. L., Fuchs, T., Lederer, M. I., Bley, N., Hammerle, M., Ghazy, E., Sippl, W., Schulte, J. H., Hüttelmaier, S. (2023). IGF2BP1 induces neuroblastoma via a druggable feedforward loop with MYCN promoting 17q oncogene expression. *Molecular Cancer*, *22*(1), 1-23. https://doi.org/10.1186/s12943-023-01792-0.

Hu, X. Y., Liang, J. Y., Guo, X. J., Liu, L., Guo, Y. B. (2015). 5-Fluorouracil combined with apigenin enhances anticancer activity through mitochondrial membrane potential (DeltaPsim)-mediated apoptosis in hepatocellular carcinoma. *Clinical and Experimental Pharmacology and Physiology*, *42*(2), 146–153. https://doi.org/10.1111/1440-1681.12333.

Jacobson, J. C., Clark, R. A., Chung, D. H. (2023). High-risk neuroblastoma: A surgical perspective. *Children*, *10*(2), 388. https://doi.org/10.3390/children10020388.

Jeong, J. H., An, J. Y., Kwon, Y. T., Rhee, J. G., Lee, Y. J. (2009). Effects of low dose quercetin: cancer cell-specific inhibition of cell cycle progression. *Journal of Cellular Biochemistry*, *106*(1), 73–82. https://doi.org/10.1002/jcb.21977.

Kachadourian, R., Day, B. J. (2006). Flavonoid-induced glutathione depletion: Potential implications for cancer treatment. *Free Radical Biology and Medicine*, *41*(1), 65-76. https://doi.org/10.1016/j.freeradbiomed.2006.03.002.

Keser, A. M., Yaprak, A. E. (2023). The assessment of genetic diversity and population structure of Verbascum

gypsicola by ISSR markers for conservation purposes. *Nordic Journal of Botany*, *2023*(2), e03660. https://doi.org/10.1111/njb.03660.

Kızıltaş, H., Bingöl, Z., Gören, A. C., Alwasel, S. H., Gülçin, İ. (2022). Analysis of phenolic compounds by LC-HRMS and determination of antioxidant and enzyme inhibitory properties of Verbascum speciousum Schrad. *Records of Natural Products*, *17*(3), 485-500. http://doi.org/10.25135/rnp.370.2210.2598.

Klimek, B., Olszewska, M. A., Tokar, M. (2010). Simultaneous determination of flavonoids and phenylethanoids in the flowers of Verbascum densiflorum and V. phlomoides by high-performance liquid chromatography. *Phytochemical Analysis: An International Journal of Plant Chemical and Biochemical Techniques*, *21*(2), 150-156. http://doi.org/10.1002/pca.1171.

Kopustinskiene, D. M., Jakstas, V., Savickas, A., Bernatoniene, J. (2020). Flavonoids as anticancer agents. *Nutrients*, *12*(2), 457. http://doi.org/10.3390/nu12020457.

Kovalevich, J., Langford, D. (2013). Considerations for the use of SH-SY5Y neuroblastoma cells in neurobiology. *Neuronal Cell Culture: Methods and Protocols*, 1078, 9-21. http://doi.org/10.1007/978-1-62703-640-5_2.

Lin, Y., Shi, R., Wang, X., Shen, H. M. (2008). Luteolin, a flavonoid with potential for cancer prevention and therapy. *Current Cancer Drug Targets*, *8*(7), 634-646. http://doi.org/10.2174/156800908786241050.

Lossi, L. (2022). The concept of intrinsic versus extrinsic apoptosis. *Biochemical Journal*, *479*(3), 357-384. https://doi.org/10.1042/BCJ20210854.

Lu, J., Papp, L. V., Fang, J., Rodriguez-Nieto, S., Zhivotovsky, B., Holmgren, A. (2006). Inhibition of mammalian thioredoxin reductase by some flavonoids: Implications for myricetin and quercetin anticancer activity. *Cancer Research 66*(8), 4410–4418. http://doi.org/10.2174/10.1158/0008-5472.CAN-05-3310.

Luca, S. V., Miron, A., Aprotosoaie, A. C., Mihai, C. T., Vochita, G., Gherghel, D., Ciocarlan, N., Skalicka-Woźniak, K. (2019). HPLC-DAD-ESI-Q-TOF-MS/MS profiling of Verbascum ovalifolium Donn ex Sims and evaluation of its antioxidant and cytogenotoxic activities. *Phytochemical Analysis*, *30*(1), 34-45. https://doi.org/10.1002/pca.2788.

Mahmoud, S. M., Abdel-Azim, N. S., Shahat, A. A., Ismail, S. I., Hammouda, F. M. (2007). Phytochemical and biological studies on Verbascum sinaiticum growing in Egypt. *Natural Product Sciences*, *13*(3), 186-189. https://doi.org/10.1001/s13003-133-186-89.

Mellado, M., Madrid, A., Reyna, M., Weinstein-Oppenheimer, C., Mella, J., Salas, C. O., Sanchez, E., Cuellar, M. (2018). Synthesis of chalcones with antiproliferative activity on the SH-SY5Y neuroblastoma cell line: Quantitative structure–activity relationship models. *Medicinal Chemistry Research*, 27, 2414-2425. http://doi.org/10.1007/s00044-018-2245-2.

Mihailović, V., Kreft, S., Benković, E. T., Ivanović, N., Stanković, M. S. (2016). Chemical profile, antioxidant activity and stability in stimulated gastrointestinal tract model system of three Verbascum species. *Industrial Crops and Products*, 89, 141-151. https://doi.org/10.1016/j.indcrop.2016.04.075.

Morana, O., Wood, W., Gregory, C. D. (2022). The apoptosis paradox in cancer. *International Journal of Molecular Sciences*, *23*(3), 1328. https://doi.org/10.3390/ijms23031328.

Pk, N., Rajan, R. K., Nanchappan, V., Karuppaiah, A., Chandrasekaran, J., Jayaraman, S., Gunasekaran, V. (2023). C–Glucosyl Xanthone derivative Mangiferin downregulates the JNK3 mediated caspase activation in Almal induced neurotoxicity in differentiated SHSY-5Y neuroblastoma cells. *Toxicology Mechanisms and Methods*, *33*(9), 707-718 https://doi.org/10.1080/15376516.2023.2237106.

Pourmoslemi, S., Larki-Harchegani, A., Daneshyar, S., Dastan, D., Nili-Ahmadabadi, A., Jazaeri, M. (2023). Antibacterial and anti-glucosyltransferase activity of Verbascum speciosum against cariogenic streptococci. *Journal of Pharmacopuncture*, *26*(2), 139. http://doi.org/10.3831/KPI.2023.26.2.139.

Rahman, M. A., Yang, H., Lim, S. S., Huh, S. O. (2013). Apoptotic effects of Melandryum firmum root extracts in human SH-SY5Y neuroblastoma cells. *Experimental Neurobiology*, *22*(3), 208. http://doi.org/10.3831/10.5607/en.2013.22.3.208.

Richeux, F., Cascante, M., Ennamany, R., Saboureau, D., Creppy, E. E. (1999). Cytotoxicity and genotoxicity of capsaicin in human neuroblastoma cells SHSY-5Y. *Archives of Toxicology*, 73, 403-409. http://doi.org/10.1007/s002040050680.

Selseleh, M., Ebrahimi, S. N., Aliahmadi, A., Sonboli, A., Mirjalili, M. H. (2020). Metabolic profiling, antioxidant, and antibacterial activity of some Iranian Verbascum L. species. *Industrial Crops and Products*, 153, 112609. https://doi.org/10.1016/j.indcrop.2020.112609.

Shakeri, A. R., Farokh, A. (2015). Phytochemical evaluation and antioxidant activity of Verbascum sublobatum Murb. leaves. *Research Journal of Pharmacognosy*, *2*(3), 43-47. https://doi.org/10.1002/s20003-203-43-47.

Shen, X., Si, Y., Wang, Z., Wang, J., Guo, Y., Zhang, X. (2016). Quercetin inhibits the growth of human gastric cancer stem cells by inducing mitochondrial-dependent apoptosis through the inhibition of PI3K/Akt signaling. *International Journal of Molecular Medicine*, *38*(2), 619-626. http://doi.org/10.3892/ijmm.2016.2625.

Shi, M. D., Shiao, C. K., Lee, Y. C., Shih, Y. W. (2015). Apigenin, a dietary flavonoid, inhibits proliferation of human bladder cancer T-24 cells via blocking cell cycle progression and inducing apoptosis. *Cancer Cell ınternational*, 15, 33. http://doi.org/10.1186/s12935-015-0186-0.

Singh, P., Lim, B. (2022). Targeting apoptosis in cancer. *Current Oncology Reports*, *24*(3), 273-284. http://doi.org/10.1007/s11912-022-01199-y.

Singh, V., Khurana, A., Navik, U., Allawadhi, P., Bharani, K. K., Weiskirchen, R. (2022). Apoptosis and pharmacological therapies for targeting thereof for cancer therapeutics. *Sci*, *4*(2), 15. https://doi.org/10.3390/sci4020015.

Wan, Y., Yang, L., Jiang, S., Qian, D., Duan, J. (2022). Excessive apoptosis in ulcerative colitis: crosstalk between apoptosis, ROS, ER stress, and intestinal homeostasis. *Inflammatory bowel diseases*, *28*(4), 639-648. https://doi.org/10.1093/ibd/izab277.

Slika, H., Mansour, H., Wehbe, N., Nasser, S. A., Iratni, R., Nasrallah, G., Shaito, A., Ghaddar, T., Koneissy, F., Eid, A.

H. (2022). Therapeutic potential of flavonoids in cancer: ROS-mediated mechanisms. *Biomedicine & Pharmacotherapy*, 146, 112442. http://doi.org/10.1016/j.biopha.2021.112442.

Souza, R. P., Bonfim-Mendonça, P. D. S., Gimenes, F., Ratti, B. A., Kaplum, V., Bruschi, M. L., Nakamura, C. V., Silva, S. O., Maria-Engler, S. S., Consolaro, M. E. (2017). Oxidative stress triggered by apigenin induces apoptosis in a comprehensive panel of human cervical cancer-derived cell lines. *Oxidative Medicine and Cellular Longevity*, 2017, 152745. http://doi.org/10.1155/2017/1512745.

Srivastava, S., Somasagara, R. R., Hegde, M., Nishana, M., Tadi, S. K., Srivastava, M., Choudhary, B., Raghavan, S. C. (2016). Quercetin, a natural flavonoid interacts with DNA, arrests cell cycle and causes tumor regression by activating mitochondrial pathway of apoptosis. *Scientific Reports*, *6*(1), 1-13. http://doi.org/10.1038/srep24049.

Tai, K. K., Pham, L., & Truong, D. D. (2011). Idebenone induces apoptotic cell death in the human dopaminergic neuroblastoma SHSY-5Y cells. *Neurotoxicity Research*, 20, 321-328. http://doi.org/10.1007/s12640-011-9245-z.

Talib, W. H., & Mahasneh, A. M. (2010a). Antiproliferative activity of plant extracts used against cancer in traditional medicine. *Scientia Pharmaceutica*, *78*(1), 33-46. http://doi.org/10.3797/scipharm.0912-11.

Talib, W. H., & Mahasneh, A. M. (2010b). Antimicrobial, cytotoxicity and phytochemical screening of Jordanian plants used in traditional medicine. *Molecules*, *15*(3), 1811-1824. http://doi.org/10.3390/molecules15031811.

Taşkaya, A., Şahin, B., Güvensen, N. C., Mammadov, R. (2023). A preliminary dtudy on anticancer and antimicrobial potential of methanolic extracts of Verbascum napifolium. *ISPEC Journal of Agricultural Sciences*, *7*(1), 135-145. https://doi.org/10.5281/zenodo.7749361.

Tatli, I. I., Akdemir, Z. F. (2006). Traditional uses and biological activities of Verbascum species. *FABAD Journal of Pharmaceutical Sciences*, *31*(2), 85-96. https://doi.org/10.1003/s31002-312-185-96.

Tatli, I. I., Akdemir, Z. S., Yesilada, E., & Küpeli, E. (2008). Anti-inflammatory and antinociceptive potential of major phenolics from Verbascum salviifolium Boiss. *Zeitschrift für Naturforschung C*, *63*(3-4), 196-202. https://doi.org/10.1515/znc-2008-3-406.

Teekaraman, D., Elayapillai, S. P., Viswanathan, M. P., Jagadeesan, A. (2019). Quercetin inhibits human metastatic ovarian cancer cell growth and modulates components of the intrinsic apoptotic pathway in PA-1 cell line. *Chemico-Biological Interactions*, 300, 91-100. https://doi.org/10.1016/j.cbi.2019.01.008.

Vetter, I., Mozar, C. A., Durek, T., Wingerd, J. S., Alewood, P. F., Christie, M. J., Lewis, R. J. (2012). Characterisation of Nav types endogenously expressed in human SH-SY5Y neuroblastoma cells. *Biochemical Pharmacology*, *83*(11), 1562-1571. https://doi.org/10.1016/j.bcp.2012.02.022.

Wang, B., Zhao, X. H. (2017). Apigenin induces both intrinsic and extrinsic pathways of apoptosis in human colon carcinoma HCT-116 cells. *Oncology Reports*, *37*(2), 1132-1140. https://doi.org/10.3892/or.2016.5303.

Zhao, Y. L., Wang, S. F., Li, Y., He, Q. X., Liu, K. C., Yang, Y. P., & Li, X. L. (2011). Isolation of chemical constituents from the aerial parts of Verbascum thapsus and their antiangiogenic and antiproliferative activities. *Archives of Pharmacal Research*, 34, 703-707. https://doi.org/10.1007/s12272-011-0501-9.

Zhou, M., Shen, S., Zhao, X., Gong, X. (2017). Luteoloside induces G0/G1 arrest and prodeath autophagy through the ROS-mediated AKT/mTOR/p70S6K signalling pathway in human non-small cell lung cancer cell lines. *Biochemical and Biophysical Research Communications*, *94*(1–2), 263–269. https://doi.org/10.1016/j.bbrc.2017.10.042.

Biotech Studies 33(1), 13-22
http://doi.org/10.38042/biotechstudies.1422918

BIOTECH STUDIES

REVIEW

Research advances of deciphering Shalgam microbiota profile and dynamics

Mustafa Yavuz[1]*, Halil Rıza Avcı[1]

[1]Central Research Institute of Food and Feed Control, Republic of Türkiye Ministry of Agriculture and Forestry, 16160, Osmangazi, Bursa, Türkiye.

How to Cite

Yavuz, M. & Avcı, H. R. (2024). Research advances of deciphering Shalgam microbiota profile and dynamics. *Biotech Studies, 33(*1), 13-22. https://doi.org/10.38042/biotechstudies.1422918

Article History
Received 17 April 2023
Accepted 30 October 2023
First Online 06 November 2023

Corresponding Author
Tel.: +90 224 246 47 20
E-mail: mustafa-yavuz@tarimorman.gov.tr

Keywords
Shalgam microbiota
Culture-independent
Culture-dependent methods
Lactic acid bacteria
Yeast

Abstract

The relationship between the microbiota and their functions in the quality and characteristic flavors of the fermented foods that provide them autochthonous attributes has been remained elusive, so far. With the demand in elucidating the microbiota of the autochthonous fermented foods, the characterization of the shalgam microbiota via culture-dependent and culture-independent methods has been carried out. To shed light on shalgam microbiota harboring Lactic acid bacteria (LAB) and yeasts, microorganisms isolated from shalgam have been identified by culture-dependent methods including 16S rRNA and ITS (Internal Transcribed Spacer) gene regions sequencing, RAPD-PCR, Rep-PCR, and API CHL50. Culture-independent characterization methods such as 16S rRNA and ITS meta-barcoding sequencing were performed to pinpoint the microbial diversity within shalgam. More recently, bioinformatics and *in vitro* analysis of bacteria and yeast isolated from shalgam to find prospective probiotics and elucidate shalgam microbiota dynamics due to the types of salts used in shalgam production have been reported. In this review, we intend to collate the data on microorganisms identified via culture-dependent and culture-independent methods. Taken together, we presented a broad perspective on the shalgam microbiota and how future endeavors in shalgam microbiota research can move forward.

Introduction

Obtained through the fermentation of black carrot and/or turnip, a member of radish family vegetables, shalgam has been an autochthonous and unique fermented beverage for Turkey. According to the regulatory definition of the shalgam, it contains fermented black carrot, turnip, salt, sourdough extract, bulgur flour, and water. Even though shalgam resembles an Indian fermented drink kanji, the production methods and microbiota of both beverages differ from each other (Coşkun, 2017; Lamba et al., 2019; Özdemir & Güldemir, 2021; Tangüler et al., 2020).

With black carrot fermentation of LAB and yeast, shalgam has been manufactured through two different methods that are classified as traditional and direct production methods (Altay et al., 2013; Coşkun, 2017; Tangüler et al., 2022). Traditional shalgam production has been carried out within two consecutive fermentation steps, in which both steps simply have been connected via the use of the water extract from the first dough fermentation, as a starter culture for the second fermentation. At the first step of the traditional fermentation; yeast, bulgur flour, water, and salt are kneaded to form a dough, and subsequently the dough fermentation continued for three days. Having completed the dough fermentation, the extraction to obtain a water-based liquid that is enriched with yeast

and LAB is performed by washing the dough three to five times with water. Chopped black carrot, tap water, and salt are treated with the water extract from the first fermentation, and then the second fermentation commences. The second fermentation lasts for three-ten days till the final fermented shalgam reaches to its characteristic flavor and structure (Tangüler et al., 2017, 2022). Considering the long fermentation time and uncontrolled nature of traditional shalgam production, the direct production of shalgam was applied. Two different direct production methods have been utilized so far: adding 15% of previous batch production to a new shalgam fermentation batch and the inoculating baker`s yeast as a starter culture into a mix containing black carrot, turnip, salt, bulgur flour, and water (Canbaş & Fenercioğlu, 1984; Tangüler & Erten, 2012a). Shalgam production methods were shown in **Figure 1**. Shalgam has been deemed a functional food since it contains anthocyanin and phenolic compounds that provide health benefits to humans (Dereli et al., 2015; Ekinci et al., 2016; Kelebek et al., 2018; Kırca et al., 2007; Tazehkand & Valipour, 2019; Türker et al., 2004; Türkyılmaz et al., 2012). It was reported that the type of shalgam production methods affected anthocyanin quantity and profile in shalgam (Tangüler et al., 2021). Tanrıseven et al. (2020) tested the effects of production methods on shalgam, resulting in the determination of seven different anthocyanins in shalgam. 235.76 mg/L anthocyanin in shalgam was produced by the direct production methods, and 185.26 mg/L was produced by the traditional production methods (Tanrıseven et al., 2020). Phenolic compounds and anthocyanins were affected by newly proposed shalgam process steps such as pasteurization and depectinization for the clarification of fermented black carrot juice to obtain a clear visual of the final product of shalgam fermentation (Dereli et al., 2015). In traditionally produced shalgam samples that contained 16 different phenolic compounds, the amount of phenolic compounds was higher at the end of the second fermentation as compared to the first stage of shalgam fermentation (Toktaş et al., 2018). It was reported that the phenolic compounds and anthocyanins of the shalgam fermentation was affected not only by production methods, but also the materials used in shalgam altered the content of bioactive compounds in shalgam (Bayram et al., 2014). The source of phenolic compounds could be black carrots used in the shalgam production (Bayram et al., 2014). That was statistically confirmed by the correlation between increasing phenolic compounds with adding more black carrot into shalgam fermentation (Bayram et al., 2014). In parallel with that, the size of chopped black carrot affected quantities of anthocyanin and phenolic composition that were produced during shalgam fermentation (Tangüler et al., 2014). Grape pomace was added to shalgam fermentation to increase polyphenolic content and reveal to what extent grape pomace increased the ethanol content in shalgam. Up to 50% of grape pomace-added shalgam`s ethanol did abide by the legislatively authorized limit of ethanol content in shalgam, which is 0.5% ethanol (Akbulut & Çoklar, 2020).

With respect to the shalgam production process, anthocyanin and phenolic compound-rich shalgam might have problems during and after production (Erten et al., 2008; Karaoğlan, 2013; Tangüler et al., 2015); (iii) the lack of widely-used starter culture for traditional shalgam production; (iv) the absence of optimum process conditions aiming quality improvement and/or shelf life extension (Demir et al., 2006; Erten et al., 2008; Özdemir-Alper & Acar, 1996). Apart from those problems, manufacturing standard fermented food products is an issue to overcome for transitioning from the traditional production of autochthonous fermented foods to their industrial production (Materia et al., 2021). Although the standardization problem for shalgam production has not been reported in previous studies, traditional and direct production pose risks for industrial shalgam production as they are not optimized in terms of process inputs and conditions. Process conditions, microbiota, and shalgam ingredients have been considered to impact the end product of shalgam fermentation (Erten et al., 2008). Shalgam microbiota contributes to shalgam quality and flavors by assimilating and metabolizing available carbon sources such as sucrose, glucose, and fructose during the fermentation. In exchange of carbon source by the resident microbes in shalgam, the microbiota generates not only aroma compounds but also organic acids

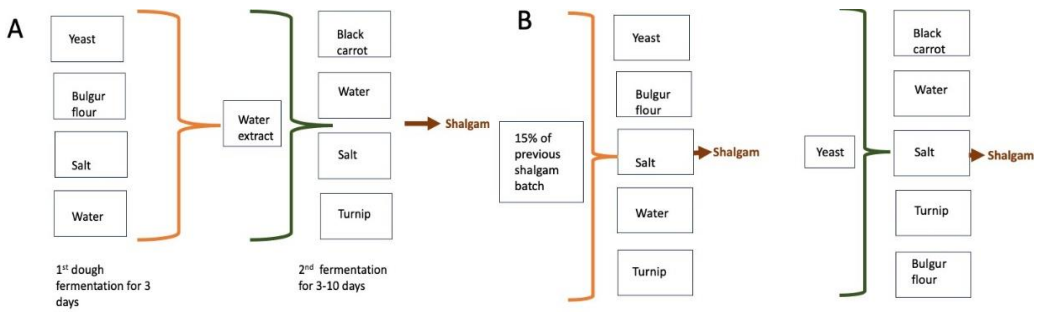

Figure 1. Process methods of the shalgam production methods. A) traditional shalgam production and B) direct shalgam production.

including lactic acid, acetic acid, citric acid, propionic acid, and succinic acid. The overall microbial community in shalgam entails ethanologenic yeast and LAB, resulting in main fermentation products as lactic acid and the trace amount of ethanol (Ekinci et al., 2016; Ulucan, 2019). Despite the presence of yeasts in shalgam, LAB-dominance in the shalgam microbiota has been reported (Ağırman & Erten, 2018; Demir et al., 2006; Erginkaya & Turhan, 2016; Özer & Çoksöyler, 2015; Tangüler & Erten, 2012a). It was indicated that the microbial load of LAB in shalgam microbiota has been influenced by pH, fermentation temperature, salt type and quantity, and black carrot size and quantity (Okçu et al., 2016: Tangüler & Erten, 2013). It was also reported that altering shalgam content by adding ayran, which is a water-added yogurt drink, increased the number of *Streptococcus* colonies after 7 days of storage at 4 ˚C as compared to the non-added shalgams (Uzay et al., 2021).

Shalgam's characteristic flavors and aroma compounds could be attributed to the contingency of shalgam microbiota, urging researchers to elucidate the microbial diversity of shalgam through microbial characterization methods. Hitherto, culture-dependent (RAPD-PCR, Rep-PCR, API CHL50, ITS gene sequencing, and 16S rRNA gene sequencing) and culture-independent (16S and ITS metabarcoding) microbial characterization methods have been deployed in **Figure 2**. This review was intended to provide insights gained from the shalgam microbiota research for deeper understanding of the microbial diversity in shalgam.

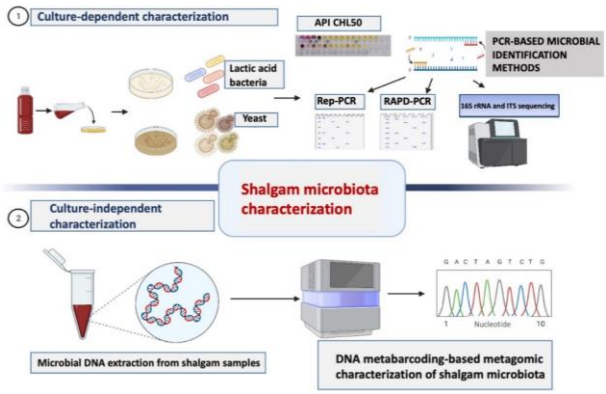

Figure 2. Schematic representation of shalgam microbiota characterizations.

Culture-dependent microbial characterization of shalgam microbiota

The studies on elucidating the microbial community of sourdough revealed that LAB has more diversity than yeasts in sourdough. As a result of that, LAB outperformed yeast in terms of the contribution to generating aroma compounds and improving shelf life stability (Gobbetti et al., 2016; Minervini et al., 2019). Thus, LAB diversity is of great importance for shalgam due to the use of the LAB-rich water extract that is obtained from the dough fermentation at the beginning of traditional shalgam production (Erten et al., 2008). In the culture-dependent characterization of shalgam microbiota, resident, and intact microorganisms in shalgam can be reproduced under the metabolic and physiological requirements provided in the culture medium. Up to now, for the microbial identification of LAB isolated from shalgam microbiota, the culture-dependent characterization methods such as API 50 CHL test, 16S rRNA gene sequencing, Randomly Amplified Polymorphic DNA-Polymerase Chain Reaction (RAPD-PCR), and Repetitive element sequence-based Polymerase Chain Reaction (Rep-PCR) were utilized (Ağırman et al., 2021; Arıcı, 2004; Baser et al., 2012; Erginkaya & Hammes, 1992; Kafkaskıray, 2020; Mete et al., 2017; Tangüler & Erten, 2012a, b ; Tangüler et al., 2014).

API 50 CHL was used to identify LAB and related genera. Incubated in Man Rogosa Sharpe (MRS) medium, isolated microorganisms were put into API 50 CH test kits that harbor 49 carbohydrates. In microbial fermentation of carbohydrates located in API 50 CH test kits, acids produced after microbial fermentation would change the pH of strips so that the color in strips shifts to indicate the occurrence of microbial fermentation. The color pattern created by microbial fermentation helps identify isolated microorganisms at the species level (Schilinger & Lücke, 1987). The first microbial isolation from shalgam was carried out in traditionally produced shalgam samples, identifying *Lactiplantibacillus plantarum*, *Levilactobacillus brevis*, and *Limosilactobacillus fermentum* as isolated LAB. The identification was initially performed by inspection of the color of colonies, cellular morphologies, and finally by performing the API 50 CH test (Erginkaya & Hammes 1992). In another microbial isolation effort, Arıcı (2004) found that *Lacticaseibacillus paracasei* subsp. *paracasei*, and *L. plantarum* were dominant microorganisms in shalgam.

11 LAB species from 135 microorganisms isolated from commercial shalgam samples were identified via API CHL 50 test. Except for one shalgam sample, among isolated LAB species *L. plantarum*, *L. brevis,* and *Leuconostoc mesenteroides* subsp. *mesenteroides/dextranicum* were always present (Tangüler & Erten, 2012c). Accordingly, the same group showed that *L. plantarum* was the dominant LAB species in shalgam (Tangüler & Erten, 2012b, 2012c). To ascertain the shalgam microbiota alterations during traditional production, microbial isolation was performed for two stages of fermentation. It was found that although *Lactobacillus delbrueckii* subsp. *delbrueckii*, *Leuconostoc mesenteroides* subsp. *cremoris*, *Leuconostoc mesenteroides* subsp. *mesenteroides,* and *Pediococcus pentosaceus* were isolated at the first stage of the traditional production, they vanished at the end of the second fermentation (Tangüler & Erten, 2012b). Aiming to choose the appropriate starter cultures for shalgam production, commercial and lab-made shalgam samples were subjected to culturing and 447 candidate strains for starter cultures were obtained. Having evaluated the strains in the face of hurdles that might

occur during shalgam production, 18 strains identified via API 50 CHL test were potential starter cultures. *L. plantarum, L. paracasei* subsp. *paracasei*, *P. pentosaceus, L. delbrueckii* subsp. *delbrueckii, L. mesenteroides* subsp. *mesenteroides/dextranicum, Limosilactobacillus fermentum, Lactococcus lactis, L. penthosus,* and *Lentilactobacillus buchneri* were identified species among 18 strains (Tangüler & Erten, 2013). Previously, Tangüler & Erten (2013) isolated three LAB species (*L. plantarum, L. paracasei* subsp. *paracasei,* and *L. fermentum*). They were separately utilized as a starter culture for shalgam production. When *L. plantarum* was used for the shalgam production as a starter culture, the highest amount of volatile organic compounds was generated in shalgam samples (Tangüler et al., 2017). From 42 commercial shalgam samples, 21 LAB with phenolic acid decarboxylase activity were identified via API 50 CHL test. *L. mesenteroides* subsp. *mesenteroides/dextranicum*, *L. plantarum*, *P. pentasaceus*, *L. acidophilus,* and *L. helveticus* were identified LAB species, *L. plantarum* was the most isolated and identified LAB at about 28.57% of all isolates among isolated strains (Okçu et al., 2016). Traditionally produced shalgams were kept for five days at 25 ˚C after the second fermentation to trace the source of biogenic amines found in shalgams. In the study, LAB isolation was performed during the second fermentation. API 50 CHL test-based characterization of traditionally produced shalgam samples demonstrated *Lactobacillus subsp*. (51 strains), *Lactococcus* subsp. (three strains), *Streptococcus* subsp. (one strain), and *Leuconostoc* subsp. (one strain) that can generate biogenic amine putrescine during the fermentation (Mete et al., 2017). Erginkaya and Turhan (2016) isolated ten bacteria and ten yeasts from two stages of traditional shalgam fermentation. The result of the identification of isolated bacteria that was applied onto API 50 CHL test strips indicated *L. plantarum* and *L. pentosus* as isolated LAB; *Saccharomyces cerevisiae* and *Candida krusei* as isolated yeasts in shalgam samples.

16S rRNA gene sequence-based identification of bacteria has been widely used as the gold standard. 16S rRNA gene of bacteria contains different vector regions that has different gene sequence. The variation within these vector regions that can be different from bacteria to bacteria makes 16S rRNA gene sequencing a nascent identification method for stratification (Weinroth et al., 2022). The very first culture-dependent characterization of shalgam based on 16S rRNA gene sequencing was reported *L. casei*, *L. plantarum*, *L. plantarum* subsp. *argentoratensis*, *L. acidophilus*, *L. brevis*, *L. helveticus*, *L. paracasei* subsp. *paracasei*, *L. paracasei* subsp. *tolerans*, *L. parabrevis*, *L. reuteri*, *L. delbrueckii* subsp. *lactis*, *L. delbrueckii* subsp. *delbrueckii*, *L. delbrueckii* subsp. *indicus*, *L. gasseri,* and *L. sharpeae* as LAB from shalgam (Baser et al., 2012). The effects of production methods and using starter cultures (*L. plantarum*, *L. fermentum,* and *L. paracasei* subsp. *paracasei*) on shalgam microbiota were sought in another study (Tangüler et al., 2015). The microbial isolation was carried out for laboratory-made shalgams, and samples were collected at the beginning and the end of the fermentation. of 38 isolated LAB, nine species including *L. mesenteroides* subsp. *mesenteroides*, *L. plantarum*, *P. pentosaceus*, *L. casei*, *Lactobacillus sp*., *L. buchneri*, *Ln. parabuchneri*, *L. brevis*, and *L. pentosus* were found in the study. Regardless of the production methods used in the study, it was interesting to note that even though *P. pentosaceus* and *L. mesenteroides* subsp. *mesenteroides* were present at the beginning of the fermentation, those strains were not found at the end of the fermentation (Tangüler et al., 2015). 21 LAB strains isolated from commercial shalgams were characterized through species-specific PCR, and then their stratifications were further confirmed by 16S rRNA gene sequencing. *L. plantarum*, *L. plantarum* subsp. *argentoratensis*, *L. casei*, *L. paracasei* subsp. *paracasei*, *L. sharpeae*, *L. brevis*, *L. parabrevis*, *L. reuteri*, *L. delbrueckii* subsp. *lactis*, *L. delbrueckii* subsp. *delbrueckii*, *L. delbrueckii* subsp. *indicus*, *L. helveticus*, *L. gasseri*, and *L. acidophilus* were reported in commercial shalgam samples (Ekinci et al., 2016).

60 isolated bacteria from shalgam and gilaburu were initially characterized by Fourier Transform Infrared (FTIR) to determine whether the isolates did belong to LAB or not. Having determined that 41 out of 60 isolated bacteria did belong to the *Lactobacillus* genera, 16S rRNA gene sequencing was performed for LAB isolated from shalgams and gilaburu. *L. plantarum, L. fermentum*, and *L. pentosus* were the three main strains identified in shalgams (Akman et al., 2021).

Yeasts, a part of the shalgam microbiota, have been isolated from shalgam samples as well. A study was conducted to identify yeasts and bacteria during the shalgam fermentation. Two-stage identification process was geared towards identifying 110 bacteria and 36 yeast isolated from traditionally produced shalgams. Initially, Rep-PCR with $(GTG)_5$ primers facilitated the identification of isolated microorganisms. Then, 16S rRNA and 26S gene sequencing were carried out for the identification of bacteria and yeast species, respectively. As indicated in the study, *L. plantarum* and *S. cerevisiae* were the only isolated strains at the end of the dough fermentation of traditionally produced shalgams. *L. plantarum*, *L. brevis, L. lactis*, *Bacillus circulans*, *Pantoea agglomerans*, *Staphylacoccus pasteuri*, *L. mesenteroides*, *Paenibacillus cucumis*, *Micrococcus yunnanensis*, and *Staphylococcus hominis* as bacteria; *S. cerevisiae* and *Pichia kudriavzevii* as yeasts were identified in shalgams (Kafkaskıray, 2020).

Kahve et al. (2022) performed yeast isolation and identified yeasts through Inter-priming binding sites (iPBS) retrotransposon marker system and ITS gene sequencing. iPBS retrotransposon marker system has been proposed to characterize yeasts, previously (Aydın et al., 2020;İbrahim et al., 2022). In this system, transposons, which are mobile and short DNA

fragments, are in different regions of the organisms` genome for adaptation to the environment and resistance to stressors. Transposons cause alterations in the genome, supporting organisms` phenotypical adaptation to any stressors in the living environment. Retrotransposons, a class of transposons, has been inserted a DNA fragment into the genome, in which the insertion is mediated by RNA. Therefore, the way of genomic DNA insertions (retrotransposons) would help organisms uphold a higher copy number of insertion DNA in the genome, enabling genetic diversity within yeasts (Boeke & Devine, 1998). By PCR-based amplification of inter-priming binding sites (iPBS) retrotransposons in the yeast genome, the identification of isolated yeasts has been carried out by Aydın et al. (2020). Similar to the 16S gene region, ITS (Internal Transcribed Spacer) gene sequencing has been carried out to identify isolated yeasts. With the help of iPBS system and confirmation by ITS gene sequencing, 172 yeasts isolated from shalgam samples were stratified. The sampling for shalgam characterization was performed at four different fermentation time periods (0,7,14, and 21 days) of four different commercial shalgams produced using traditional and direct methods. *Pichia kudriavzevii*, *Saccharomyces cerevisiae*, *Pichia fermentans*, *Candida oleophila*, *Kazachstania bulderi*, and *Geotrichum candidum* as yeasts were identified via iPBS. In the study, *Pichia* yeast was reported to be the most isolated yeasts at 77.9% of 172 isolated yeasts (Kahve et al., 2022).

Culture-independent microbial characterization of shalgam microbiota

Culturing the microbiota of fermented food might not be enough to reproduce the full spectrum of microbial diversity. The microbiota consists of a variety of cell types and states, such as intact, viable, non-viable, autolyzed cells, and cell lysates. In culture-independent characterization, it is likely to identify those cells within the microbial community of a fermented food (Carraro et al., 2011). Ekici et al. (2022) conducted the very first and the only culture-independent characterization of traditionally fermented shalgam microbiota. Towards that end, the microbial diversity in shalgam that is traditionally produced was investigated by taking samples from six time points (3, 7, 10, 13, 17, and 20 days) during 20 days of the second fermentation. The bacterial identification without microbial isolation was performed via DNA extraction and PCR amplification of 16S rRNA V4-V5 vectors. For yeast identification in shalgam samples, the ITS2 gene from extracted DNA extracts was amplified via PCR. After PCR-amplified DNA samples were sequenced, *Candida boidinii,* and *Saccharomyces cerevisiae*, *L. mesenteroides* and *L. lactis* were reported as dominant yeast and bacteria species, respectively (Ekici et al., 2022). On the contrary to the culture-independent characterization of shalgam samples, in the culture-dependent characterization of shalgam, Arici (2004) pointed out *L. plantarum* and *L. paracasei* subsp. *paracasei* as dominant LAB species. To the best of our knowledge, never have 13 LAB species and 15 yeasts found in this study been reported in shalgam, previously. It is also interesting to note that even though *Weisella* species have never been reported in culture-dependent characterization of shalgam, the culture-independent characterization of shalgam demonstrated *Weisella* presence in shalgam microbiota for the first time. As compared to the culture-dependent characterization of shalgam microbiota, *Pichia* and *Lacticasei* group bacteria including *L. paracasei, L.casei* were not found in the metabarcoding analysis (Ekici et al., 2022). Through the metagenomic analysis of shalgam samples, 35 bacteria and seven yeasts were found at the end of shalgam fermentation. With the help of culture-independent characterization of shalgam samples, it was found that the bacterial diversity in shalgam fluctuated dynamically during the fermentation while yeast diversity in the microbiota remained less fluctuated as compared to bacterial species (Ekici et al., 2022). At **Table 1**, the identified LAB and yeast species were collated and classified as culture-dependent and culture-independent characterizations of shalgam samples microbiota so that it can be inferred that characterization methods might lead to the identification of different microorganisms in shalgam.

Bioinformatic analysis of whole genome sequenced LAB isolated from shalgam

Having resilience in dealing with harsh conditions of gastrointestinal transit and the capability to bind intestinal mucosa, probiotics confer health benefits (Gumustop & Ortakci, 2022). Isolated microorganisms from shalgam might carry probiotic traits and be robust under the gastrointestinal conditions. *In vitro* assays of isolated *Pichia kudriavzevii* (Gumustop & Ortakci, 2022), *L. plantarum* subsp. *plantarum* W2, *L. fermentum* Akhavan E3, and *L. Pentosus* XL963 (Akman et al., 2021) were carried out to vet the probiotic traits of isolated microorganisms. Recently, three isolated LAB strains` (*L. plantarum* DY46, *Liquorilactobacillus nagelii* AGA58, and *L. fermentum* AGA52) genomes were sequenced and genomic data were evaluated *in silico* (Yetiman et al., 2022, 2023; Yetiman & Ortakçı, 2023). For *L. fermentum* AGA52 isolated from shalgam, *in silico* analysis of the probiotic traits, carbohydrate utilization capacity, bacteriophage resistance, antioxidant capacity, and *in vitro* analysis of the ability of cholesterol degradation, and gamma amino butyric acid (GABA) producing capability were appraised.

On the basis of the results obtained from *in silico* and *in vitro* assays, the ability to utilize cholesterol and produce GABA corroborated that *L. fermentum* AGA52 had probiotic attributes (Yetiman et al., 2023). In line with that, as a result of bioinformatic analysis of *L. plantarum* DY46 genome isolated from shalgam, antibiotic resistance genes were present in its genome. Moreover, its genome consisted of a plantaricin-

Table 1. The list of LAB and yeasts identified based on culture-dependent and culture-independent microbial characterization methods

Culture-dependent microbial identification	
LAB	*Lactiplantibacillus plantarum, Limosilactobacillus fermentum*, Lacticaseibacillus paracasei subsp. paracasei*, Lacticaseibacillus casei*, Lacticaseibacillus paracasei subsp.tolerans*, Levilactobacillus brevis, Lactiplantibacillus plantarum subsp. agentoratensis*, Lentilactobacillus buchneri*, Lentilactobacillus parabuchneri*, Pediococcus pentosaceus*, Leuconostoc mesenteroides, Lactococcus lactis, Lactobacillus coryniformis*, Lactobacillus delbrueckii subsp. delbrueckii*, Leuconostoc mesenteroides subsp. jonggajibkimchii*, Lactiplantibacillus paraplantarum*, Liquorilactobacillus nagelii** and *Lactiplantibacillus pentosus**
Yeasts	*Saccharomyces cerevisiae, Candida krusei, Pichia kudriavzevii*, Pichia fermentans*, Candida oleophila*, Kazachstania bulderi** and *Geotrichum candidum**
Culture-independent microbial identification	
LAB based on Meta-barcoding metagenomics analysis	*Leuconostoc mesenteroides, Lactococcus lactis, Leuconostoc pseudomesenteroides*, Leuconostoc inhae*, Weissella confusa*, Lactococcus raffinolactis*, Leuconostoc kimchii*, Leuconostoc lactis*, Lactiplantibacillus plantarum, Lactococcus piscium*, Weissella soli*, Levilactobacillus brevis, Lactobacillus curvatus*, Lactococcus garvieae*, Leuconostoc fallax*, Liquorilactobacillus nagelii, Lactobacillus paracollinoides** and *Lactobacillus paracollinoides**
Yeasts based on Meta-barcoding metagenomics analysis	*Saccharomyces cerevisiae, Candida Bodinii*, Wickerhamomyces anomalus*, Rhodotorula mucilaginosa*, Barnettozyma californica*, Trichosporon coremiiforme*, Typhula ishikariensis*, Naganishia albida*, Rhodotorula glutinis*, Meyerozyma guilliermondii*, Trebouxia sp. *, Acremonium antarcticum*, Sporidiobolus salmonicolor*, Candida humilis*, Malassezia restricta** and *Rhodotorula diobovata**

Strains with asterisk **(*)** indicate that the isolated species were only found in the characterization methods used in the table.

producing gene cluster, except for the gene that can produce Pln J peptide (Yetiman et al., 2022). The same group reported that they managed to isolate *Liquorilactobacillus nagelii* from shalgam. The *Liquorilactobacillus nagelii* AGA58 genome and probiotic traits have been evaluated *in silico* and *in vitro*. As a result of bioinformatic analysis on the *Liquorilactobacillus nagelii* AGA58 genome, *Liquorilactobacillus nagelii* AGA58 carried an A2 lantipeptide producing gene (Yetiman & Ortakçı, 2023). In the light of *in vitro* and *in silico* analysis of shalgam-originated LAB that might confer probiotic traits, it can be purported that shalgam might be considered as a probiotic beverage.

The effect of different salts on the shalgam microbiota

The mineral content of shalgam determined by Inductively Cold Plasma (ICP) analysis has been reported in the published literature (Ağırman et al., 2021; Demir et al., 2004; Özdemir-Alper & Acar, 1996; Yılmaz-Ersan & Turan, 2012). Minor and major elements in shalgam have been found via ICP-OES (Inductively Cold Plasma-Optical Emission Spectrometry) analysis. In terms of abundance and detectability in shalgam samples, Na, K, Ca, Mg, and P were considered as major elements while minor elements were indicated as Fe, Cu, Zn, Ni, Mn, Pb, and Sn (Yılmaz-Ersan & Turan, 2012). When Aspergillus aculeatus Pectinex Ultra SP-L enzyme and citric acid were added into the shalgam fermentation, ICP analysis demonstrated shalgam samples treated with the enzyme and citric acid contained Na, K, Ca, Mg, and Fe elements. Also, the highest Mg levels in shalgam samples were archived when Pectinex Ultra SP-L enzyme and citric acid were present during the fermentation (Demir et al., 2004).

To lower the sodium chloride (NaCl) concentration in shalgam, when 1.5% NaCl was used, shalgam was prepared with black carrot juice concentrate and whey was the most appealing in the sensorial evaluation of shalgams (Güven et al., 2019). In the face of the health hazards of excessive salt consumption, it has been targeted to reduce salt content and/or substitute table salts with other salts used in shalgam production (Ağırman & Erten, 2018, Ağırman et al., 2021; Güven et al., 2019). Such actions to overcome health concerns related to NaCl reduction might lead to alterations in the aroma profile of fermented food as exemplified in cheese (Brandsma et al., 2022). The sodium salts used in the fermentation of shalgam were replaced with calcium and potassium salts and following that the effect of the salts on the microbiota of shalgam was investigated through culture-dependent characterization of shalgam samples. The highest amount of LAB was found when NaCl and potassium chloride (KCl) were used together in shalgam production. It has also been observed that different salts did not have any effect on the number of LAB colonies in the dough fermentation of shalgam. However, a decrease of 2 log CFU/mL in the total number of mesophilic aerobic bacteria was observed in all salts during shalgam fermentation (Ağırman & Erten, 2018). In the following study of the same group, shalgam samples totally containing 1.5% chloride salts prepared with KCl+$CaCl_2$ (50%+50%) and KCl+$CaCl_2$+NaCl (33.3%+33.3%+33.3%) salt mixes were culture-dependently characterized. The stratifications in the

study were first performed by RAPD-PCR to sort out LAB among isolates and followed by 16S rRNA gene sequencing. L. paracasei was found in the water extract from the first fermentation and eight-day fermented shalgams prepared with NaCl+KCl (50%+50%), $NaCl+CaCl_2$ (50%+50%), and $NaCl+KCl+CaCl_2$ (33.3%+33.3%+33.3%) salt mixtures, indicating that L. paracasei was the most persistent strain found through shalgam production. L. paracasei was identified throughout the fermentation in the presence of $CaCl_2$ and KCl while the shalgam fermentation with NaCl salt did not help L. paracasei remain in the second and the fourth day of shalgam fermentation. Throughout the shalgam fermentation prepared with $KCl+CaCl_2$ (50%+50%) and $NaCl+KCl+CaCl_2$ (33.3%+33.3%+33.3%) salt mixtures, L. lactis isolated from shalgams was the most persistent strain. It was interesting that L. pentosus and L. coryniformis were isolated when only NaCl (100%) salt was used in the shalgam fermentation (Ağırman et al., 2021).

Even though the types of salts` effects on shalgam microbiota were elucidated through culture-dependent characterization of shalgams made with different salts and salts mixtures, little did we know how other mineral contents of shalgam would alter shalgam microbiota throughout the fermentation.

Conclusion

In culture-based characterization of shalgam, the isolation of LAB has been the focal point. With the help of ever-growing state-of-art technologies such as next-generation sequencing Nanopore and PacBio, and MALDI-TOF-MS as a phenotype-based identification method, more comprehensive microbiota characterization of shalgam can be applied in the future. The structure-function relationship in a fermented food, which shows the contribution of microorganisms to the production of compounds generated during fermentation, has not yet been fully exploited in shalgam. Recently, research on unraveling which microorganisms can produce which aromatic compounds has been carried out through co-occurrence and network analysis in fermented foods (Wang et al., 2019; Wu et al., 2022). Also, finding the core microbiota of autochthonous fermented foods has accelerated the development of autochthonous starter cultures (Wu et al., 2022). Also, experimental studies intertwining the production of aroma components and the microbiota in shalgam have not been conducted yet. By conducting metagenomic analysis and *in silico* analysis of the metagenomic data, it will be possible to reveal which microorganisms in shalgam can produce anthocyanins, aroma components, phenolic compounds.

References

Ağırman, B., & Erten, H. (2018). The Influence of Various Chloride Salts to Reduce Sodium Content on the Quality Parameters of Şalgam (Shalgam): A Traditional Turkish Beverage Based on Black Carrot. *Journal of Food Quality*, *11*. https://doi.org/10.1155/2018/3292185

Ağırman, B., Settanni, L., & Erten, H. (2021). Effect of different mineral salt mixtures and dough extraction procedure on the physical, chemical and microbiological composition of Shalgam: A black carrot fermented beverage Dough (dough fermentation) Sorting-Grading. *Food Chemistry*, *344*. https://doi: 10.1016/j.foodchem.2020.128618

Akbulut, M., & Çoklar, H. (2020). Utilization of Black Grape Pomace in the Production of Shalgam Juice: Effect on the Ethyl Alcohol Levels. *Journal of Halal Life Style*, *2*(2), 109–115.

Akman, K. P., Özülkü, G., Tornuk, F., & Yetim, H. (2021). Potential probiotic lactic acid bacteria isolated from fermented gilaburu and shalgam beverages. *LWT*, *149*(May), 111705. https://doi.org/10.1016/j.lwt.2021.111705

Altay, F., Karbancioğlu-Güler, F., Daşkaya-Dikmen, C., & Heperkan, D. (2013). A review on traditional Turkish fermented non-alcoholic beverages: Microbiota, fermentation process and quality characteristics. *International Journal of Food Microbiology*, *167*(1), 44–56. https://doi.org/10.1016/j.ijfoodmicro.2013.06.016

Arıcı, M. (2004). Microbiological and chemical properties of a drink called shalgam. (Mikrobiologische und chemische eigenschaften von Shalgam), Ernahrungs-Umschau., 51 (1), 10.

Aydın, F., Özer, G., Alkan, M., & Çakır, İ. (2020). The utility of iPBS retrotransposons markers to analyze genetic variation in yeast. *International Journal of Food Microbiology*, *325*. https://doi: 10.1016/j.ijfoodmicro.2020.108647.

Baser, M., Sofu, A., Özcan, E., Korachi, M., & Ekinci, F. Y. (2012). Characterization of dominant microbial populations in shalgam juice using 16S rRNA. *New Biotechnology*, *29* (September),118. https://doi.org/10.1016/j.nbt.2012.08.331

Bayram, M., Erdoğan, S., Esin, Y., Saraçoğlu, O., & Kaya, C. (2014). Farklı siyah havuç miktarlarının şalgam suyunun bileşimine ve duyusal özellikleri üzerine etkisi. *Akademik Gıda*, *12*(1), 29–34 (In Turkish)

Boeke, J. D., & Devine, S. E. (1998). Yeast retrotransposons: finding a nice quiet neighborhood. *Cell*, *93*(7), 1087-1089. https://doi.org/10.1016/S0092-8674(00)81450-6

Brandsma, J. B., Rustandi, N., Brinkman, J., Wolkers-Rooijackers, J. C., Zwietering, M. H., & Smid, E. J. (2022). Pivotal role of cheese salting method for the production of 3-methylbutanal by *Lactococcus lactis*. *International Journal of Dairy Technology*, *75*(2), 421-430. https://doi.org/10.1111/1471-0307.12839

Canbaş, A.; Fenercioglu, H. (1984). Şalgam suyu uzerine bir arastirma. *Gıda (Food)*., *9*(5), 279–286 (In Turkish)

Carraro, L., Maifreni, M., Bartolomeoli, I., Martino, M. E., Novelli, E., Frigo, F., Marino M. & Cardazzo, B. (2011). Comparison of culture-dependent and-independent methods for bacterial community monitoring during Montasio cheese manufacturing. *Research in Microbiology, 162*(3), 231-239. https://doi.org/10.1016/j.resmic.2011.01.002

Coşkun, F. (2017). A traditional Turkish fermented non-alcoholic beverage, shalgam. *Beverages*, *3*(4). https://doi.org/10.3390/beverages3040049

Demir, N., Acar, J., & Bahçeci, K. S. (2004). Effects of storage on quality of carrot juices produced with lactofermentation and acidification. *European Food Research and Technology*, *218*(5), 465–468. https://doi.org/10.1007/s00217-004-0883-8

Demir, N., Bahçeci, K. S., & Acar, J. (2006). The effects of different initial *Lactobacillus plantarum* concentrations on some properties of fermented carrot juice. *Journal of Food Processing and Preservation*, *30*(3), 352–363. https://doi.org/10.1111/j.1745-4549.2006.00070.x

Dereli, U., Türkyilmaz, M., Yemiş, O., & Özkan, M. (2015). Effects of Clarification and Pasteurization on the Phenolics, Antioxidant Capacity, Color Density and Polymeric Color of Black Carrot (*Daucus Carota* L.) Juice. *Journal of Food Biochemistry*, *39*(5), 528–537. https://doi.org/10.1111/jfbc.12155

Ekici H., Kadiroğlu P., & Ilgaz C. (2022). Next-generation sequencing of shalgam flavor influencing microflora. *Journal of Food Processing and Preservation*, 1–12. https://doi.org/10.1111/jfpp.15982

Ekinci, F. Y., Baser, G. M., Özcan, E., Üstündağ, Ö. G., Korachi, M., Sofu, A., Blumberg, J. B., & Chen, C. Y. O. (2016). Characterization of chemical, biological, and antiproliferative properties of fermented black carrot juice, shalgam. *European Food Research and Technology*, *242*(8), 1355–1368. https://doi.org/10.1007/s00217-016-2639-7

Erginkaya, Z., & Hammes, W. P. (1992). Şalgam suyu fermentasyonu sırasında mikroorganizmaların gelişimi ve izole edilen laktik asit bakterilerinin tanımlanmaları üzerine bir araştırma. *Gıda 17*(5), 311–314 (In Turkish)

Erginkaya, Z., & Turhan, E. Ü. (2016). Enumeration and Identification of Dominant Microflora during the Fermentation of Shalgam. *Akademik Gıda*, *14*(2), 92–97.

Erten, H., Tanguler, H., & Canbaş, A. (2008). A traditional Turkish lactic acid fermented beverage: Shalgam (Şalgam). *Food Reviews International*, *24*(3), 352–359. https://doi.org/10.1080/87559120802089324

Gobbetti, M., Minervini, F., Pontonio, E., Di Cagno, R. & De Angelis, M. (2016). Drivers for the establishment and composition of the sourdough lactic acid bacteria biota. *Int. J. Food Microbiol.* 239, 3–18. https://doi.org/10.1016/j.ijfoodmicro.2016.05.022

Gümüştop, İ. & Ortakçı, F. (2022). Evaluating the microbial growth kinetics and artificial gastric digestion survival of a novel *Pichia kudriavzevii* FOL-04. *Biotech Studies. 31*(1), 28-35. http://doi.org/10.38042/biotechstudies.1103767

Güven, N., Yetim, H., & Cankurt, H. (2019). Physicochemical and Sensory Properties of low salt turnip juıce produced by using black carrot juıce and whey. *Avrupa Bilim ve Teknoloji Dergisi Sayı*, *15*, 599–610 https://doi.org/10.31590/ejosat.539492 (In Turkish)

İbrahim, H., Akbulut, M., & Coklar, H. (2022). Identification and technological characterization of endogenous yeast isolated from fermented black carrot juice, shalgam. *LWT*, *154*, 112823. https://doi.org/10.1016/j.lwt.2021.112823

Kahve, H. I., Akbulut, M., & Coklar, H. (2022). Identification and technological characterization of endogenous yeast isolated from fermented black carrot juice, shalgam. *LWT*, *154*, 112823. https://doi.org/10.1016/j.lwt.2021.112823

Kafkaskıray, E. S. (2020). Şalgam suyu fermantasyon sürecinin mikrobiyal profilinin moleküler yöntemlerle belirlenmesi. Yüksek Lisans Tezi. İstanbul Sabahattin Zaim Üniversitesi (In Turkish)

Karaoğlan A. (2013). Şalgam suyunda bozulma yapan mayaların atımlı UV ışık ile inaktivasyonu. Yüksek Lisans Tezi. Cumhuriyet Üniversitesi (In Turkish)

Kelebek, H., Kadiroğlu, P., Sönmezdağ, A. S., Güçlü, G., Kola, O., Selli, S. (2018). Characterization of bioactive compounds and antioxidant potential of fermented beverage: Shalgam, International Conference on Raw Materials to Processed Foods, 11–13 April, http://rpfoods2018.org/.

Kırca, A., Özkan, M., & Cemeroğlu, B. (2007). Effects of temperature, solid content and pH on the stability of black carrot anthocyanins. *Food Chemistry*, *101*(1), 212–218. https://doi.org/10.1016/j.foodchem.2006.01.019.

Lamba, J., Goomer, S., & Saxena, S. K. (2019). International Journal of Gastronomy and Food Science Study the lactic acid bacteria content in traditional fermented Indian drink: Kanji. *International Journal of Gastronomy and Food Science*, *16*(May 2018), 100143. https://doi.org/10.1016/j.ijgfs.2019.100143

Materia, V. C., Linnemann, A. R., Smid, E. J., & Schoustra, S. E. (2021). Contribution of traditional fermented foods to food systems transformation: value addition and inclusive entrepreneurship*. Food Security, 13*(5), 1163-1177. https://doi.org/10.1007/s12571-021-01185-5

Mete, A., Coşansu, S., Demirkol, O., & Ayhan, K. (2017). Amino acid decarboxylase activities and biogenic amine formation abilities of lactic acid bacteria isolated from shalgam. *International Journal of Food Properties*, *20*(1), 171–178. https://doi.org/10.1080/10942912.2016.1152479

Minervini, F., Dinardo, F. R., Angelis, M. De, & Gobbetti, M. (2019). Tap water is one of the drivers that establish and assembly the lactic acid bacterium biota during sourdough preparation. *Scientific Reports*, *July 2018*, 1–12. https://doi.org/10.1038/s41598-018-36786-2

Okçu, G., Ayhan, K., Güneş Altuntaş, E., Vural, N., & Poyrazoğlu, E. S. (2016). Determination of phenolic acid decarboxylase produced by lactic acid bacteria isolated from shalgam (şalgam) juice using green analytical chemistry method. *Lwt*, *66*, 615–621. https://doi.org/10.1016/j.lwt.2015.10.072

Özdemir-Alper N., Acar, J. (1996) Flüssiges Obst 63:521–523 (In Turkish)

Özdemir S.S.& Güldemir O. Şalgam Ve Kanji: Kültürlerarasi Bir Ürün Olarak Fermente Siyah Havuç İçecekleri. (2021). *Motif Akademi Halkbilimi Dergisi*, *14*(35), 0–3 (In Turkish). https://doi.org/10.12981/mahder.935537

Özer, N. & Çoksöyler, F. N. (2015). Şalgam Suyunun Bazi Kimyasal Mikrobiyoloji Özellikleri. *Gıda*, *40*, 31–38. https://doi.org/10.15237/gida.GD14068

Schillinger, U., & Lücke, F. K. (1987). Identification of lactobacilli from meat and meat products. *Food Microbiology*, *4*(3), 199–208. https://doi.org/10.1016/0740-0020(87)90002-5

Tangüler, H. (2021). The Effect of Using Different Size Purple Carrots and Lactobacillus Plantarum on the Properties of Fermented Shalgam (Şalgam). *Turkish Journal of Agriculture-Food Science and Technology*, *9*(10), 1759–1766.

https://doi.org/10.24925/turjaf.v9i10.1759-1766.4246

Tangüler, H., Dinç, S. Ö., & Beylikci, S. C. (2020). Suggestions and Last Trends Related to Şalgam Beverage which is Traditional Product of Turkey. *Turkish Journal of Agriculture-Food Science and Technology*, *8*(6), 1266–1271. https://doi.org/10.24925/turjaf.v8i6.1266-1271.3266

Tangüler, H., Dinç, S. Ö., Ekenel, G., Aytekin, D. A., Şimşek, C., & Ataklı, H. (2022). Effect of Production Method and Temperature on Quality Characteristics of Shalgam Beverages during Storage. *Akademik Gida*, *20*(1), 20–29. https://doi.org/10.24323/akademik-gida.1097814

Tangüler, H. & Erten, H. (2012a). Şalgam Suyu Üretiminde Gerçekleştirilen Hamur Fermantasyonu Sırasında. *Akademik Gıda*, *10*(2), 48–54. (In Turkish)

Tangüler, H., & Erten, H. (2012b). Occurrence and growth of lactic acid bacteria species during the fermentation of shalgam (şalgam), a traditional Turkish fermented beverage. *Lwt*, *46*(1), 36–41. https://doi.org/10.1016/j.lwt.2011.10.026

Tangüler, H., & Erten, H. (2012c). Chemical and Microbiological Characteristics of Shalgam (Şalgam): A Traditional Turkish Lactic Acid Fermented Beverage. *Journal of Food Quality*, *35*(4), 298–306. https://doi.org/10.1111/j.1745-4557.2012.00447.x

Tangüler, H., & Erten, H. (2013). Selection of potential autochthonous starter cultures from shalgam, a traditional Turkish lactic acid-fermented beverage. *Turkish Journal of Agriculture and Forestry*, *37*(2), 212–220. https://doi.org/10.3906/tar-1205-37

Tangüler, H., Erten, H., Bozdogan, A., Aksay, S., & Kelebek, H. (2021). Comparison of anthocyanin profiles in şalgams (shalgams) produced with different production procedures. *Journal of Food Processing and Preservation*, 1–11. https://doi.org/10.1111/jfpp.14770

Tangüler, H., Saris, P. E. J., & Erten, H. (2015). Microbial, chemical and sensory properties of shalgams made using different production methods. *Journal of the Science of Food and Agriculture*, *95*(5), 1008–1015. https://doi.org/10.1002/jsfa.6781

Tangüler, H., Selli, S., Sen, K., Cabaroglu, T., & Erten, H. (2017). Aroma composition of shalgam: a traditional Turkish lactic acid fermented beverage. *Journal of Food Science and Technology*, *54*(7), 2011–2019. https://doi.org/10.1007/s13197-017-2637-1

Tangüler, H., Utus, D., & Erten, H. (2014). Effect of black carrot size usage on the quality of shalgam (şalgam): A traditional Turkish lactic acid fermented beverage. *Indian Journal of Traditional Knowledge*, *13*(4), 647–653.

Tanrıseven, D., Selli, S., & Kelebek, H. (2020). LC-DAD-ESI-MS / MS-assisted elucidation of the phenolic compounds in shalgams: Comparison of traditional and direct methods. *Food Chemistry*, *305*(March 2019). https://doi.org/10.1016/j.foodchem.2019.125505

Tazehkand, M. N., & Valipour, E. (2019). Cytotoxic , antimicrobial and DNA breaking activity of Şalgam. *Indian Journal of Biochemistry & Biophysics*, *56*, 169–174.

Toktaş, B., Bildik, F., & Özçelik, B. (2018). Effect Of Fermentation On Anthocyanin Stability And *In Vitro* Bioaccessibility During Shalgam (Şalgam) Beverage Production. *Journal of the Science of Food and Agriculture*, *98*(8), 3066–3075. https://doi.org/10.1002/jsfa.8806

Türker, N., Aksay, S., & Ekiz, H. I. (2004). Effect of storage temperature on the stability of anthocyanins of a fermented black carrot (*Daucus carota* var. L.) beverage: Shalgam. *Journal of Agricultural and Food Chemistry*, *52*(12), 3807–3813. https://doi.org/10.1021/jf049863s

Türker, N., Aksay, S., Istanbullu, O., & Artuvan, E. (2007). A study on the relation between anthocyanin content and product quality: shalgam as a model beverage. *Journal of food quality, 30*(6), 953-969. https://doi.org/10.1021/jf049863s

Türkyılmaz, M., Yemi, O., & Özkan, M. (2012). Clarification and pasteurisation effects on monomeric anthocyanins and percent polymeric colour of black carrot (*Daucus carota* L.) juice. *Food Chemistry*, *134*(2), 1052–1058. https://doi.org/10.1016/j.foodchem.2012.03.013

Ulucan, E. (2019). Fermentasyon Sonrasi Ultrason Uygulamasinin Şalgam Sularinin Bazi Fizikokimyasal ve Mikrobiyolojik Ozelligi Uzerine Etkisi. Yüksek Lisans Tezi. Selçuk Üniversitesi. (In Turkish)

Uzay, M., Öztürk, H. İ., Buzrul, S., & Maskan, M. (2021). A study on rheological properties, sensory evaluation and shelf life of ayran–shalgam mixtures. *Journal of Food Science and Technology, 58*(7), 2479-2486. https://doi: 10.1007/s13197-020-04754-2

Wang, S., Wu, Q., Nie, Y., Wu, J., & Xu, Y. (2019). Construction of synthetic microbiota for reproducible flavor compound metabolism in Chinese light-aroma-type liquor produced by solid-state fermentation. *Applied and Environmental Microbiology*, *85*(10), 1–14. https://doi.org/10.1128/AEM.03090-18

Weinroth M. D., Belk A. D., Dean C., Noyes N., Dittoe D. K., Rothrock, M. J., Ricke S. C., Myer P. R., Henniger M. T., Ramírez G. A., Oakley B. B., Summers K. L., Miles A. M., Ault-Seay T. B., Yu Z., Metcalf J. L., Wells J. E. (2022) Considerations and best practices in animal science 16S ribosomal RNA gene sequencing microbiome studies, *Journal of Animal Science*, *100*(2), https://doi.org/10.1093/jas/skab346

Wu, W., Wang, Z., Xu, B., Cai, J., Cheng, J., Mu, D., Wu, X., & Li, X. (2022). Exploring Core Microbiota Based on Characteristic Flavor Compounds in Different Fermentation Phases of Sufu. *Molecules*, *27*(15). https://doi.org/10.3390/molecules27154933

Yavuz, M., Kasavi, C., & Öner, E. T. (2021). Developments in effective use of volatile organic compound analysis to assess flavour formation during cheese ripening. *Journal of Dairy Research, 88*(4), 461-467. https://doi: 10.1017/S0022029921000790

Yetiman, A. E., Keskin, A., Darendeli, B. N., Kotil, S. E., Ortakci, F., & Dogan, M. (2022). Characterization of genomic, physiological, and probiotic features *Lactiplantibacillus plantarum* DY46 strain isolated from traditional lactic acid fermented shalgam beverage*. Food Bioscience, 46.* https://doi.org/10.1016/j.fbio.2021.101499

Yetiman, A. E., & Ortakci, F. (2023). Genomic, probiotic, and metabolic potentials of *Liquorilactobacillus nagelii* AGA58, a novel bacteriocinogenic motile strain isolated from lactic acid-fermented shalgam. *Journal of Bioscience and Bioengineering, 135*(1), 34-43. https://doi.org/10.1016/j.jbiosc.2022.10.008

Yetiman, A., Horzum, M., Bahar, D., & Akbulut, M. (2023). Assessment of Genomic and Metabolic Characteristics of Cholesterol-Reducing and GABA Producer

imosilactobacillus fermentum AGA52 Isolated from Lactic Acid Fermented Shalgam Based on “In Silico” and “In Vitro” Approaches. *Probiotics and Antimicrobial Proteins*, 1-18. https://doi.org/10.1007/s12602-022-10038-2

Yılmaz-Ersan, L., & Turan, M. A. (2012). Major and minor element concentrations in fermented shalgam beverage. *International Journal of Food Properties*, *15*(4), 903–911. https://doi.org/10.1080/10942912.2010.506621

Biotech Studies 33(1), 23-32
http://doi.org/10.38042/biotechstudies.1442001

BIOTECH STUDIES

RESEARCH PAPER

Barley preferentially activates strategy-II iron uptake mechanism under iron deficiency

Emre Aksoy*

Biological Sciences, Middle East Technical University, 06800 Ankara, Türkiye.

How to cite:
Aksoy, E. (2024). Barley preferentially activates strategy-II iron uptake mechanism under iron deficiency. *Biotech Studies*, *33*(1),23-32. http://doi.org/10.38042/biotechstudies.1442001

Article History
Received 13 September 2023
Accepted 29 December 2023
First Online 08 February 2024

Corresponding Author
Tel.: +90 312 210 64 64
E-mail: emreaks@metu.edu.tr

Keywords
Ferric chelate reductase activity
Gene expression
Iron deficiency
Phytosiderophore secretion
Rhizosphere acidification

Abstract

Plants utilize two main strategies for iron (Fe) uptake from the rhizosphere. Strategy-I is based on the reduction of ferric (Fe^{3+}) to ferrous (Fe^{2+}) iron by ferric chelate reductase (FCR) and is mainly observed in dicots. Strategy-II utilizes the complexation of Fe^{3+} with phytosiderophores secreted from the plant roots and mainly evolved in Gramineous species, including barley (*Hordeum vulgare*). Recent studies suggest that some species use a combination of both strategies for more efficient Fe uptake. However, the preference of barley for these strategies is not well understood. This study investigated the physiological and biochemical responses of barley under iron deficiency and examined the expression levels of the genes involved in Strategy-I and Strategy-II mechanisms in the roots. Fe deficiency led to decreased root and shoot lengths, fresh and dry weights, and Fe accumulation in the roots. Parallel to the chlorosis observed in the leaves, FCR activity and rhizosphere acidification were also significantly reduced in the roots, while the release of phytosiderophores increased. Furthermore, Strategy-II genes expressed higher than the Strategy-I genes in the roots under Fe deficiency. These findings demonstrate that Strategy-II is more activated than Strategy-I for Fe uptake in barley roots under Fe-deficient conditions.

Introduction

Iron (Fe) is an important nutrient for plant growth and development because it functions as a cofactor for enzymes involved in important biochemical pathways such as DNA and chlorophyll biosynthesis. Fe deficiency leads to interveinal leaf chlorosis, a decrease in leaf and root biomasses, and yield losses (Nikolic & Pavlovic, 2018). Although iron is sufficiently found in the soil, plants cannot easily absorb it from the rhizosphere in the bioavailable form since it makes a complex with chelates easily in the soil (Lindsay & Schwab, 1982). This is a big problem, especially for crops grown in alkaline soils because the increase in soil pH decreases the solubility of iron.

Two different mechanisms are evolved in plants for the uptake of iron into the roots (Aksoy *et al.*, 2018). Dicots such as *Arabidopsis thaliana* mainly use a mechanism based on the reduction of ferric iron (Fe^{3+}) to ferrous iron (Fe^{2+}) (Strategy-I). In this mechanism, local acidification is performed by first releasing protons into the rhizosphere by H^+-ATPase (AHA) transporters located in the root epidermis (Santi & Schmidt, 2009). Subsequently, Fe^{3+} is reduced to soluble Fe^{2+} by an oxidoreductase named ferric chelate reductase (FCR/FRO) (Jeong & Connolly, 2009). Finally, Fe^{2+} ions are taken into the root epidermis via a metal transporter called IRON-REGULATED TRANSPORTER1 (IRT1) (Connolly *et al.*, 2002). The genes involved in Strategy I are upregulated under iron deficiency (Kobayashi & Nishizawa, 2012). In addition to Fe^{2+}, IRT1 can transport

other divalent metals, including zinc (Zn^{2+}) and manganese (Mn^{2+}), and their concentrations increase dramatically in roots and shoots when plants are exposed to Fe deficiency (Vert *et al.*, 2002).

Gramineous plants such as barley (*Hordeum vulgare*) mainly use a chelation-based mechanism (Strategy-II) (Martín-Barranco *et al.*, 2021). Within this mechanism, plants produce various phytosiderophores (PS) through the sulfur assimilation pathway. In PS production, firstly S-adenosyl-L-methionine (SAM) is converted to nicotianamine (NA) by NICOTIANAMINE SYNTHASE (NAS), then NA is converted to 3'-keto acid by NICOTIANAMINE AMINOTRANSPHERESE (NAAT), and finally, 3'-keto acid is converted to 2'-deoxymugineic acid (DMA) by DEOXYMUGINEIC ACID SYNTHASE (DMAS). DMA is converted to mugineic acid (MA) by IRON DEFICIENCY SPECIFIC CLONE3 (IDS3), which functions as a dioxygenase in barley roots (Kobayashi *et al.*, 2001). Nine MAs have been identified so far in rye and barley (Bandyopadhyay & Prasad, 2021). They are released from plant roots to the rhizosphere as PS via TRANSPORTER OF MA1 (TOM1) (Nozoye *et al.*, 2011), forming a complex with insoluble Fe^{3+} in the soil, and then they are taken up into the root epidermis by specific oligopeptide transporters such as YELLOW STRIPE1 (YS1) in *Zea mays* and YELLOW STRIPE-LIKE15 (YSL15) in *Oryza sativa* (Aksoy *et al.*, 2018; Rai *et al.*, 2021). Similar to IRT1 in nongraminaceous plants, *Z. mays* YS1 serves as a major entry point for metals, utilizing the PS precursor NA to transport both beneficial (Fe^{2+}) and potentially hazardous (Fe^{3+}, Zn^{2+}, Mn^{2+}) ions into the plant (Murata *et al.*, 2006).

Previous studies showed that *O. sativa IRT1* and *IRT2* were induced in the roots under Fe deficiency (Ishimaru *et al.*, 2006; Walker & Connolly, 2008). Similar results were also shown in *Z. mays*, where *IRT1* and *IRT2* were upregulated by Fe deficiency in the roots (Li *et al.*, 2013; Li *et al.*, 2022), and *Triticum aestivum*, where *FRO2-2A* and *IRT1a-4A* were highly upregulated under Fe deficiency (Hua *et al.*, 2022). Opposite to these results, the expression of *ZmIRT1, Sorghum bicolor IRT1* and *Triticum polonicum IRT1A,* and *IRT1B* were not altered by Fe deficiency in maize (Wairich *et al.*, 2019), sorghum (Wairich *et al.*, 2019) and wheat (Jiang *et al.*, 2021), respectively. The inconsistent upregulation of *IRT* transporters across Gramineae suggests a fundamental ambiguity: is Strategy-I truly ubiquitous within this clade, or does its deployment remain an enigmatic, species-dependent phenomenon? To unravel this ambiguity in barley (*Hordeum vulgare* L.), a comprehensive approach was employed, examining the physiological, biochemical, and molecular aspects of barley under Fe deficiency, focusing specifically on transporter expression levels. This study was designed to elucidate whether barley utilizes both Strategy-I and Strategy-II, or exhibits a species-specific reliance on one strategy over the other.

Materials and Methods

Plant material

Seeds of the Turkish barley cultivar Tarm-92 were obtained from the Bahri Dağdaş International Agricultural Research Institute, Turkey. Developed in 1992 by the Field Crops Central Research Institute, Tarm-92 is a medium-early barley cultivar with high tillering capacity, resistance to lodging, drought, salinity, and high temperature (Benlioğlu & Özkan, 2015; Doğru *et al.*, 2020). While sensitive to lead and selenium (Doğru, 2019; Çakır, 2007), it exhibits tolerance to boron toxicity (Torun *et al.*, 2002; Öz, 2012; Çatav *et al.*, 2023) and Zn deficiency (Erenoglu *et al.*, 2000). Despite sensitivity to Fe deficiency (Erenoglu *et al.*, 2000), Tarm-92's molecular responses under this stress were unstudied, leaving its preferred Fe uptake strategy from the rhizosphere unknown.

Plant growth and stress application

For surface sterilization, barley seeds were shaken in a solution containing 3% sodium hypochlorite (Sigma) and 0.05% Tween-20 (Sigma) for 20 minutes and were washed five times with sterile distilled water. For germination, the seeds were placed in plastic Petri dishes containing sterile filter papers moistened with 3 mL of half-strength (1/2) Hoagland's nutrient solution (Hoagland & Arnon, 1950) at 22 ± 2 °C in a growth chamber for 2 days in the dark under 70% relative humidity. While preserving root integrity, the pre-germinated seedlings were meticulously positioned through a cheesecloth membrane atop 150 mL plastic containers (diameter: 10 cm) containing 1/2 Hoagland's nutrient solution (pH 5.8) supplemented with 50 µM Fe^{3+}-EDTA (Sigma) sufficient for barley growth. The plants were grown in a growth chamber at 22 ± 2 °C for 7 days under 70% relative humidity, on a 16-hour light (300 µmol m^{-2} s^{-1}) and 8-hour dark cycle. The nutrient solution was regularly renewed every 24 hours to maintain consistent nutrient availability and prevent oxygen depletion. The experiment was carried out in 6 repetitions (plastic containers) according to the randomized block design, where 5 plants were grown in each container. Container positions were randomized daily using a random number generator to minimize environmental effects and maintain consistent growth conditions.

Stress treatment was carried out 7 days after the plants were transferred to the containers. For iron deficiency, Fe^{3+}-EDTA was not added to the nutrient solution; instead, a Fe chelator, 300 µM FerroZine (3-(2-Pyridyl)-5,6-diphenyl-1,2,4-triazine-p,p'-disulfonic acid monosodium salt hydrate - Sigma), was added to remove all potential iron from the nutrient solution (Aksoy *et al.*, 2013). Control groups were grown in fresh nutrient solution containing 50 µM Fe^{3+}-EDTA. On the fifth day following the stress application, relevant physiological, biochemical, and molecular analyses were performed on barley seedlings.

Physiological measurements

Following the stress application, the root and shoot lengths of the plants were measured with the help of a ruler and recorded. Measurements were made with a total of thirty plants in six containers for each of the Fe-sufficient (control) and Fe-deficient (stress) media. Chlorophyll index was determined by the Soil Plant Analysis Development (SPAD) measurements (SPAD-502 Plus, Konica Minolta, Japan) from the first fully developed leaves. Next, the roots and shoots of the plants were separated, their length was measured with a ruler and their fresh weights were recorded. Then, the tissues were dried in an oven at 65 °C for 24 hours and their dry weights were recorded. All physiological and biochemical analyses were made with 15 plants in three containers for each Fe-sufficient and Fe-deficient media except for the length measurements, which were taken from 30 plants, and divalent metal concentrations, which were taken from 3 randomly selected plants.

Total chlorophyll content

Total chlorophyll content was determined from 100 mg of first fully developed leaves following extraction in 2 mL of 80% acetone using a plastic pestle in microcentrifuge tubes (Aksoy *et al.*, 2013). Samples were incubated in the extraction buffer for 24 hours in the dark at 4 °C for complete extraction. The absorbance readings of the extracts were determined at 470, 646.8, and 663.2 nm as compared to 80% acetone and the total chlorophyll content was calculated according to Lichtenthaler & Wellburn (1983).

FCR enzyme activity

For the measurement of FCR activity, first the root fresh weights were recorded after brief drying with tissue paper. Then, the root samples were incubated in a 20 mL of solution of 0.1 mM Fe (III)-EDTA (Sigma) and 0.3 mM ferrozine (Sigma) for 24 hours in the dark at room temperature (Aksoy & Koiwa, 2013). Then, the absorbance of the solution was read at 562 nm against the blank without roots. The enzyme activity was calculated with a molar extinction coefficient of 28.6 mM^{-1} cm^{-1}.

Phytosiderophore release

Phytosiderophore release was quantified according to Reichman & Parker (2007). Briefly, two hours after the lights are turned on, plant roots were washed with distilled water three times and transferred into 20 mL of 200 µM $CaCl_2$ to collect the exudates by incubating them in the growth chamber for 6 hours. Microbial degradation of the PS was inhibited by addition of 50 µg/L Micropur into the extraction solution. At the end of the incubation, exudates were filtered through a 0.45 µm filter and quantified by Fe-binding assay. 0.5 mL of 0.2 mM FeCl3 was added onto 10 mL filtered exudate solution and mixed for 15 minutes on a rotary shaker. Then, 1 mL of 1 M sodium acetate (pH 7.0) buffer is added into the mixture and it was shaken for another 10 minutes. The mixture was filtered into 0.25 mL of 6 M HCl via a coarse filter paper to reduce Fe^{3+} to Fe^{2+} and 0.5 mL of 80 g/L hydroxylamine hydrochloride was added on top. Finally, the solution was incubated at 55°C for 30 minutes to complete the reduction process. When the solution was cooled down to room temperature, 0.25 mL of 2.5 g/L ferrozine and 1 mL of 2 M sodium acetate (pH 4.7) buffer were added to start the Fe-binding reaction. Immediately, the mixture was briefly mixed by hand and the absorbance was measured at 562 nm against the blank without plants. PS concentration was calculated according to standard curve generated by $FeCl_3$ series.

Divalent metal concentrations

For the measurement of root and leaf Fe, Zn, and Mn concentrations, the samples were incubated in 2 mM $CaSO_4$ and 10 mM EDTA for 10 minutes followed by washing twice with distilled water to eliminate any metal particles attached to the sample surface. Then, the samples were divided into 3 technical repeats of 100 mg and dried in test tubes for 24 hours at 65 °C (Aksoy *et al.*, 2013). Then, the samples were digested in 4 mL of 98.8% HNO_3 (Sigma) and 1 mL of concentrated HCl (Sigma) at 100 °C for 1 hour, 150 °C for 1 hour, 180 °C for 1.5 hours, and lastly at 210 °C until no liquid is left in the test tubes by using a furnace (Vasconcelos *et al.*, 2006). Finally, the samples were re-dissolved with 10 mL of 2% HNO_3, and the metal contents were determined in Inductively Coupled Plasma Mass Spectrometry (ICP-MS) (Bruker Aurora M90) in the pulse detector mode.

Rhizosphere acidification

The protons released from the roots were measured according to Pizzio *et al.* (2015) with minor modifications. Briefly, after the stress application, all plant roots were immersed in 20 mL of acidification solution (1/2 Hoagland's solution, 2 mM MES buffer, pH 5.8) and allowed to grow in the growth cabinet for an additional 48 hours. At the end of the incubation, the pH of the solution was measured with a pH meter (pH1000L, VWR) against the solution without plants. Then, the fresh weights of the plant roots were recorded. The pH = - log $[H^+]$ formula was used to calculate the proton release, according to the change in pH between the first and last reading.

Gene expression analyses by real-time PCR (RT-qPCR)

Total RNA was isolated from barley roots by RNeasy Plant Mini Kit (Qiagen). Genomic DNA contamination in the samples was removed using the RapidOut DNA Cleaning Kit (ThermoFisher). 1st strand cDNA synthesis from 2 µg of total RNA samples was performed using the RevertAid First Strand cDNA Synthesis Kit (ThermoFisher). 200 ng cDNA sample was amplified on a Rotorgene (Qiagen) with LightCycler 480 SYBR Green I Master Mix (Roche) in a total volume of 20 µL using 0.8 µM specific primers (Table 1). *HvACT* was used as a housekeeping gene in the normalization of

gene expression (Gines *et al.* 2018). Gene expression analyses were performed two times (technical replicates) for each of the 3 biological replicates.

Statistical analyses

Differences between control and stress treatments were analyzed using the Minitab 19 package program according to Student's t-test (P<0.05).

Results and Discussion

Barley roots and shoots are adversely affected by Fe deficiency

Five days of Fe deficiency significantly impacted barley, highlighting its sensitivity to this nutrient limitation (**Figure 1**). Strikingly, root and shoot lengths plummeted significantly (P<0.05) by 40% and 20%, respectively (**Figure 2a, b**). This stunted growth extended to biomass, with 58.7% and 56.2% reductions in root and shoot fresh weights (**Figure 2c, d**) and 57.9% and 50.0% declines in dry weights (**Figure 2e, f**). Notably, Fe deficiency triggered visible chlorosis in leaves (**Figure 3a**), leading to a staggering 60.6% drop in total chlorophyll content compared to controls (**Figure 3b**). Chlorophyll index measurements confirmed this trend, revealing a 33.8% decrease under Fe deficiency (**Figure 3c**). This validates both measurements as reliable indicators of Fe deficiency-induced chlorophyll degradation in barley (Jiang *et al.*, 2017). Although a previous study reported more severe phenotypes under longer Fe deprivation (Erenoglu *et al.*, 2000), results of this current study demonstrate that just five days were sufficient to elicit clear deficiency symptoms in barley leaves. This aligns with research indicating a direct correlation between treatment duration and chlorosis severity in Fe-sensitive cultivars (Bandyopadhyay & Prasad, 2021; Martín-Barranco *et al.*, 2021). Thus, Tarm-92 emerges as highly sensitive to Fe deficiency, exhibiting significant impairments even after a short-term deprivation.

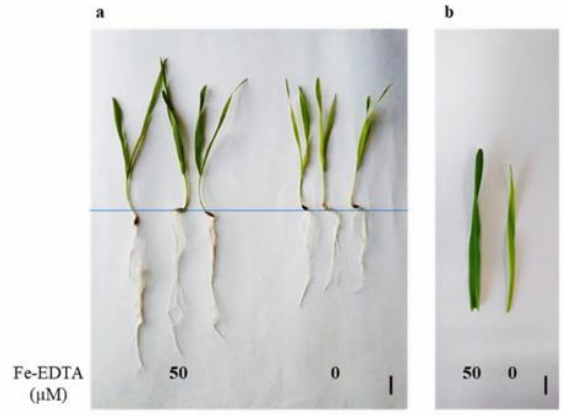

Figure 1. Overall look of the barley plants after iron deficiency treatment. Tarm-92 variety of barley was exposed to the Fe deficiency for 5 days after grown on ½ Hoagland medium for 9 days. a. Root and shoots of plants after stress application. b. Leaf chlorosis after stress application. Bar: 1 cm.

Fe accumulation in the roots and shoots of barley show opposite trends under Fe deficiency

Despite five days of Fe deficiency, shoot Fe concentrations remained remarkably stable (**Figure 4**). However, root Fe levels dropped by a significant 40.9% compared to controls (P<0.05). This selective decrease contradicts observations from longer-term studies where shoot Fe content fell substantially after comparable or even shorter Fe deprivations (Nikolic *et al.*, 2019; Mikami *et al.*, 2011; Erenoglu *et al.*, 2000). This divergence suggests two possibilities: either barley exhibits exceptional resilience in maintaining shoot Fe content even during short-term deficiency, or the five-day treatment window simply was not sufficient for significant depletion in shoots.

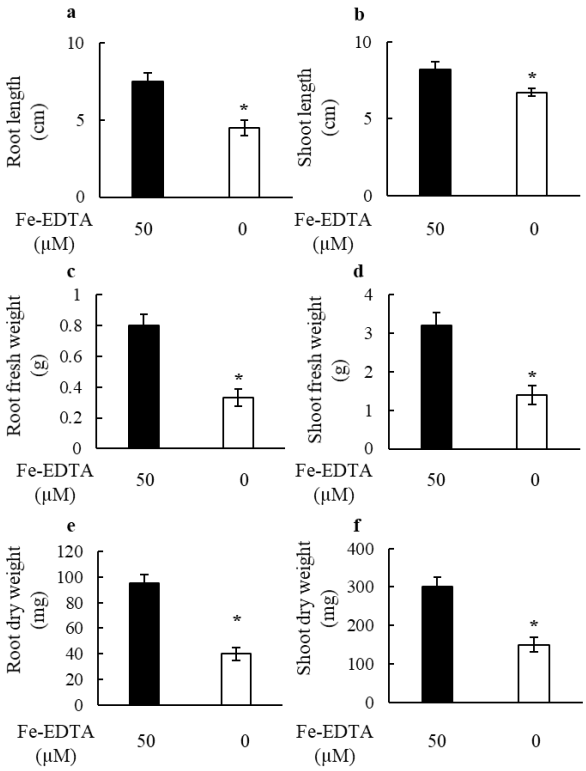

Figure 2. Physiological changes after Fe deficiency treatment. a. Root length. b. Shoot length. c. Root fresh weight. d. Shoot fresh weight. e. Root dry weight. f. Shoot dry weight. Values indicate the means ± SEM (n = 30 for an and b; n = 15 for c-f). * indicates a significant difference between the treatments according to Student's *t*-test (P<0.05).

Intriguingly, the unchanged shoot Fe content did not prevent Fe deficiency responses. Both biomass and chlorophyll levels were markedly decreased (**Figures 2 and 3**), showcasing the plant's sensitivity despite seemingly adequate shoot Fe reserves. This raises the intriguing possibility that root Fe concentrations, despite their decline, trigger downstream signaling pathways in the leaves, activating deficiency responses even before impacting shoot iron stores. This hypothesis finds support in previous studies identifying root and leaf-derived signals under Fe deficiency (Hindt & Guerinot, 2012; Tabata, 2023). Alternatively, root Fe

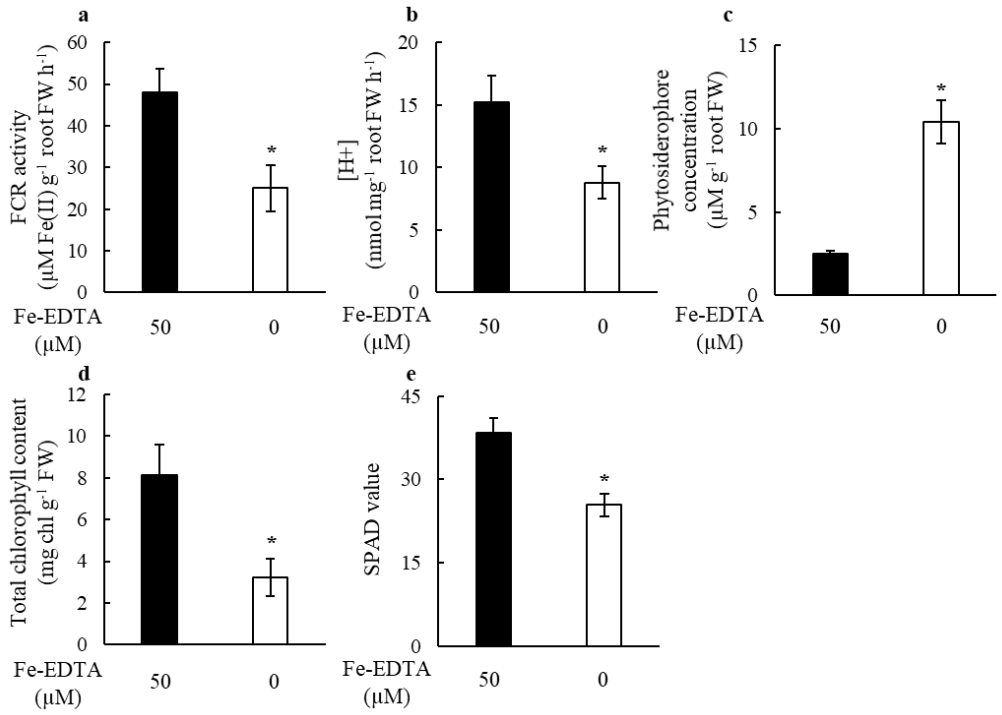

Figure 3. Biochemical changes after Fe deficiency treatment. a. FCR activity at the roots. b. Rhizosphere acidification. c. Phytosiderophore concentration. d. Total chlorophyll content. e. SPAD value. Values indicate the means ± SEM (n = 15). * indicates a significant difference between the treatments according to Student's *t*-test (P<0.05).

deprivation might trigger the overaccumulation of other divalent metals in leaves, reaching toxic levels and inducing chlorosis, as observed in some studies (Blasco *et al.*, 2018).

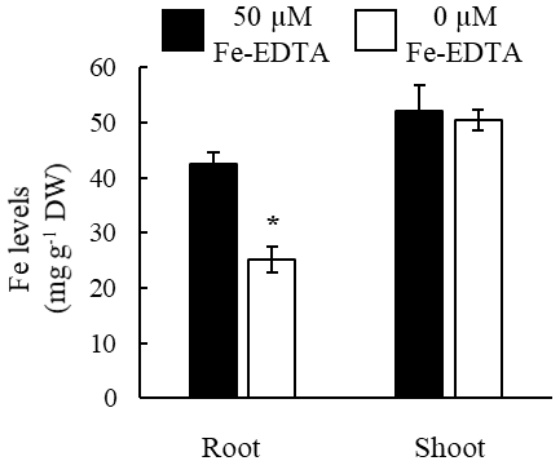

Figure 4. Fe levels in the roots and shoots after iron deficiency. Values indicate the means ± SEM (n = 3). * indicates a significant difference between the treatments according to Student's *t*-test (P<0.05).

Fe deficiency causes overaccumulation of zinc and manganese in the roots and shoots of barley

Fe deficiency triggers the accumulation of other divalent metals, like Zn^{2+} and Mn^{2+}, which can be co-transported into the root epidermis by IRT1 (Connolly *et al.*, 2002) and YS1 (Murata *et al.*, 2006). As expected, barley plants exhibited significantly higher levels of these metals in both roots and shoots under Fe deficiency (**Figure 5**). Notably, Zn^{2+} concentrations in roots and shoots climbed a staggering 65.7% and 45.1%, respectively, while Mn^{2+} surged by a remarkable 209.1% and 43.7%. This striking overaccumulation suggests that IRT1 and/or YS1 overworks under Fe deficiency, inadvertently ushering in an influx of detrimental metals. Corroborating these findings, studies on tobacco (Kobayashi *et al.*, 2003) and maize (Mozafar, 1997; Kanai *et al.*, 2009) demonstrated similar Zn^{2+} and Mn^{2+} overaccumulation in roots and leaves under Fe deficiency, leading to impaired photosynthesis and biomass. Interestingly, other divalent metals, such as copper (Cu^{2+}) and cobalt (Co^{2+}) did not overaccumulate under Fe deficiency in tobacco (Kobayashi *et al.*, 2003) whereas Cu^{2+} concentration was increased in Arabidopsis leaves and roots (Vert *et al.*, 2002) and barley xylem (Alam *et al.*, 2001) under Fe deficiency. These data paint a concerning picture, where barley's observed chlorosis under Fe deficiency (significantly decreased chlorophyll content) might be driven not just by Fe scarcity, but also by a cascade of toxicity resulting from excessive Zn^{2+} and Mn^{2+} accumulation facilitated by IRT1 and/or YS1 (Panda *et al.*, 2012). Indeed, some studies provided evidence for the accumulation of reactive oxygen species (ROS) under Fe deficiency due to excessive Zn^{2+} and Mn^{2+} accumulation, preventing chlorophyll biosynthesis and active photosynthesis (Blasco *et al.*, 2018; Fan *et al.*, 2021). Without neglecting the direct effects of Fe deficiency on ROS production (Santos *et al.*, 2019), this highlights the intricate

interplay between nutrient deficiencies and metal uptake pathways, urging further investigation into the specific mechanisms behind such collateral damage caused by Fe deficiency.

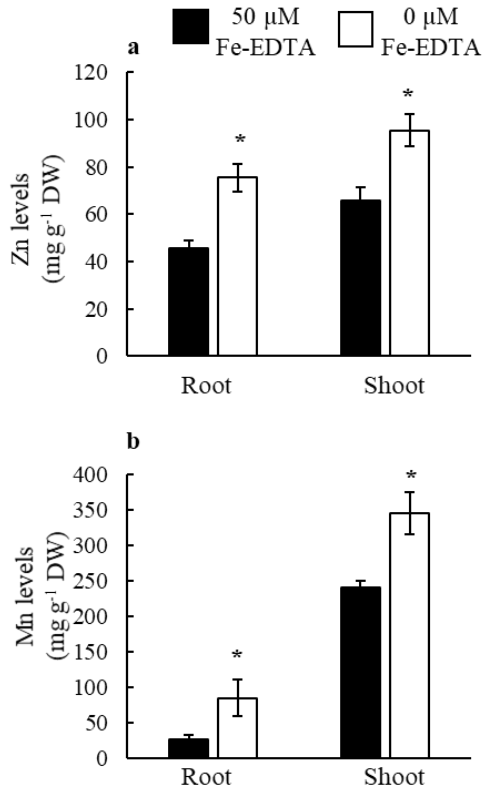

Figure 5. Zinc and manganese levels in the roots and shoots after iron deficiency. a. Zn levels. b. Mn levels. Values indicate the means ± SEM (n = 3). * indicates a significant difference between the treatments according to Student's *t*-test (*P*<0.05).

Strategy-I and Strategy-II are affected at the biochemical level in barley under Fe deficiency

To elucidate whether barley prioritizes the chelation-based Strategy-II or the reduction-based Strategy-I for Fe acquisition during deficiency, key biochemical parameters in the roots of barley were investigated under Fe-limited conditions (**Figure 6**). Firstly, Strategy-II utilization was confirmed by quantifying the release of phytosiderophores (PS). As expected, barley unveiled its arsenal, raising PS levels a remarkable 4.2-fold under Fe deficiency compared to Fe sufficient condition (**Figure 6a**). This robust response aligns with previous reports highlighting a positive correlation between PS release rate, Fe deficiency tolerance, and treatment duration in barley (Erenoglu *et al.*, 2000; Rai *et al.*, 2021). Thus, barley appears to adhere to the canonical tenets of Strategy-II Fe acquisition. However, a striking incongruity emerged. Despite significantly elevated PS released from the roots, barley displayed pronounced symptoms of Fe deficiency, exemplified by higher chlorosis and reduced root Fe content. This dissociation between robust PS production and impaired Fe uptake suggests the possibility of an alternative, strategy employed by barley to compensate for the reduced efficiency of its Strategy-II system within the roots. Following confirmation of Strategy-II utilization through elevated PS release, barley's Fe acquisition repertoire was further explored by examining the potential contribution of a complementary Strategy-I pathway. Intriguingly, we observed a significant reduction of traits associated with this pathway. FCR activity exhibited a substantial reduction of 47.9% under Fe deficiency (**Figure 6b**), while rhizosphere acidification, characterized by H^+ release, declined by 42.1% (**Figure 6c**). This deviation from the classic Strategy-I response, characterized by increased FCR activity and proton release (Aksoy *et al.*, 2018), suggests that barley does not readily engage this pathway to compensate for its apparent limitation in Strategy-II efficiency. While the observed reduction of Strategy-I in barley deviates from typical responses documented in non-Gramineae species, it highlights the intricate nature of plant Fe acquisition and the potential for species-specific adaptations. Some studies report enhanced FCR activity and rhizosphere acidification in Fe-tolerant non-Gramineae (Vasconcelos & Grusak, 2014), showcasing the diverse array of responses across plant lineages. Further complicating the picture, differences in timing and magnitude of these responses are apparent in diverse species. For instance, while FCR peaks in cucumber after five days of Fe deficiency (Pavlovic *et al.*, 2013) and Arabidopsis after 72 hours (Aksoy *et al.*, 2013), our barley model exhibited a significant decline in both FCR activity and rhizosphere acidification. Yet, interestingly, Mikami *et al.* (2011) reported a similar non-significant decrease in FCR activity in barley after seven days, suggesting potential intraspecific diversity in strategy utilization. Taken together, these data suggest that barley does not solely depend on Strategy-I to support the Strategy-II to uptake Fe from the rhizosphere, which means that it can utilize another alternative strategy to uptake Fe efficiently. Recently, an alternative Fe acquisition strategy was identified in non-Gramineae species (Robe *et al.*, 2021). In this strategy, plants secrete secondary metabolites like coumarins into the rhizosphere, which complexes with Fe^{3+}. Although, in silico evidence suggest that this strategy was not evolved in barley (Clemens & Weber, 2016), coumarin accumulation was shown in the vacuoles of barley leaf mesophyll cells (Werner & Matile, 1985).

This intricate tapestry of response patterns underscores the need for comparative studies across diverse plant models employing different Fe uptake strategies. By investigating a broader range of species and treatment timeframes, we can begin to elucidate the spectrum of adaptive plasticity in Fe acquisition and unravel the factors influencing specific pathway preferences. Such comprehensive research promises to advance our understanding of plant resilience and adaptability in the face of nutrient limitations.

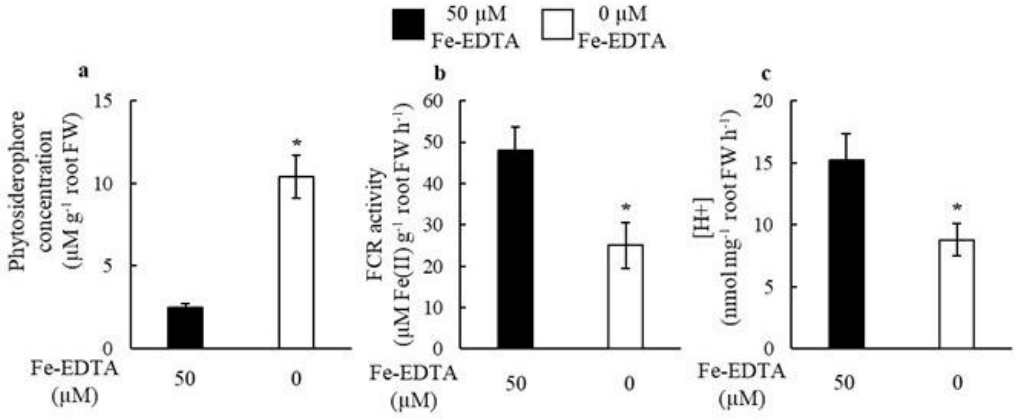

Figure 6. Biochemical changes in the roots after Fe deficiency. a. Phytosiderophore concentration. b. FCR activity at the roots. c. Rhizosphere acidification. Values indicate the means ± SEM (n = 15). * indicates a significant difference between the treatments according to Student's *t*-test (P<0.05).

The expression levels of genes responsible for Fe uptake are altered significantly in the roots of barley under Fe deficiency

The effect of short-term Fe deficiency on decreased root Fe levels but stable shoot Fe levels implies that the stress signaling was not sufficiently affected and the Fe translocation has not yet been altered in the early days of stress treatment in barley. To evaluate how stress signaling was affected in barley cultivar, the expression levels of the genes involved in both strategies were determined in the roots (Figure 7). Accordingly, the expression levels of *HvIRT1, HvIRT2, HvFRO1, HvFRO2,* and *HvAHA2* functioning in Strategy-I and *HvNAS1, HvIDS2, HvIDS3, HvYS1, HvTOM1* and *HvDMAS1* working in Strategy-II were increased significantly under Fe deficiency (Figure 7a). Similar to our results, the expression levels of the genes coding for IRT transporters (*IRT1* and *IRT2*), FCRs (*FRO1* and *FRO2*) and proton pump (*AHA2*) increases under Fe deficiency in non-Gramineous species (Hindt & Guerinot, 2012). Similarly, *HvIRT1* also increases in the roots of barley under Fe deficiency (Pedas *et al.*, 2008). The observed difference between FCR activity and rhizosphere acidification (**Figure 6b and c**) in relation to the expression levels of *HvFRO1, HvFRO2*, and *HvAHA2* suggests that, while the genes were activated after five days of iron deficiency, the corresponding enzymes may not have become fully functional. This aligns with the possibility that Strategy-II, as evidenced by PS release, is activated earlier for initial Fe acquisition, while Strategy-I may require a longer exposure to Fe deficiency to fully engage and support sufficient Fe uptake for tolerance. Further research investigating enzyme activity across longer timeframes may shed light on the activation dynamics of different Fe acquisition strategies in barley.

Among Strategy-II genes, *HvTOM1* and *HvIDS2* expressions increased by 10 folds while *HvNAS1* expression increased by 8.9 folds (Figure 7b). In a previous study, the expression levels of *HvDMAS1* and *HvNAS1* increased by four folds and the level of *HvTOM1* increased by three folds in barley roots under 7 days of Fe deficiency (Nikolic *et al.*, 2019). In the same study, *HvYS1* expression increased approximately 1.8 times in a 2-day stress application. In our study, genotypic and developmental stage differences may be among the reasons for the higher increases in the expression levels of the same genes in barley roots exposed to 5 days of Fe deficiency. Among Strategy-I genes, the top two genes with the highest expression levels were *HvAHA2* and *HvIRT1*, with 5.7 and 5.0-fold increases, respectively. Therefore, it is noteworthy that among the increases in gene expressions, the expression levels of genes involved in Strategy-II were higher than those in Strategy-I. These results are in with PS release rates (Figure 6a), suggesting that Strategy-II is the main Fe acquisition mechanism in barley roots.

Even though two Fe uptake strategies, namely Strategy-I and Strategy-II, were evolved in different plant groups, a combined strategy was proposed only for the cultivated rice to absorb Fe from the rhizosphere since it is adapted to live in paddies (Sperotto *et al.*, 2012), where Fe^{2+} is the more abundant form compared to Fe^{3+} in submerged conditions (Ishimaru *et al.*, 2006). Recently, this combined strategy was also shown in *Oryza* genus (Wairich *et al.*, 2019) and other Gramineous species, suggesting that plants have evolved alternative mechanisms to adapt to changing environmental conditions, such as flooding, to continue absorbing Fe from the rhizosphere. However, depending on the species, either one or both of the Fe uptake strategies may have been selectively employed for efficient Fe acquisition (Grillet, & Schmidt, 2019). Results presented in this study suggest that, while barley primarily relies on Strategy-II for Fe uptake evidenced by the substantial increase in PS levels (Figure 6a), this reliance should not mask the potential contribution of other mechanisms. The observed downregulation of

Strategy-I components, like FCR activity and rhizosphere acidification, hints at potential limitations in solely relying on Strategy-II. Therefore, while Strategy-II appears to be the main player, alternative Fe uptake pathways, including components of Strategy-I, likely play a complementary role in supporting Fe acquisition in barley roots.

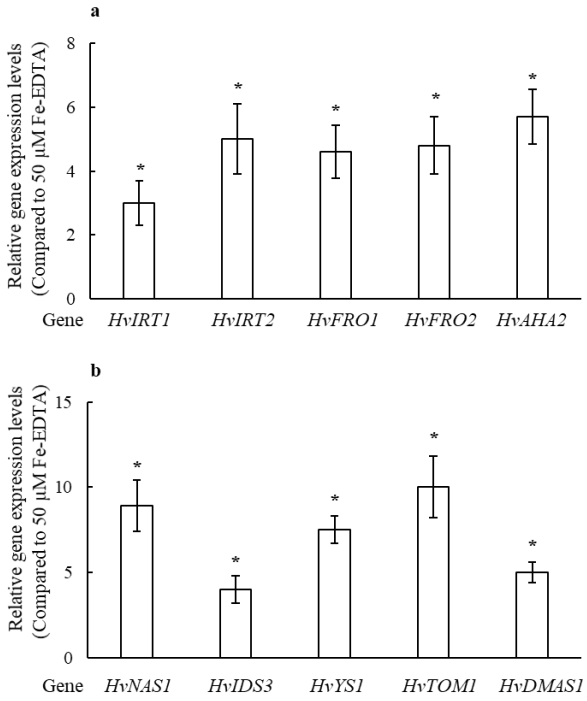

Figure 7. Relative expression of the genes in the roots of barley plants after Fe deficiency treatment. a. Genes involved in Strategy-I. b. Genes involved in Strategy-II. The expression level of each gene was compared to the expression level of the same gene in iron sufficient medium. Values indicate the means ± SEM (n = 3). * indicates a significant difference between the treatments according to Student's *t*-test (P<0.05).

Conclusion

This study showed that the FCR activity and rhizosphere acidification, which take part in Strategy-I, decreased significantly in barley roots under iron deficiency. The decrease in both activities led to a reduction in the Fe accumulation in the roots. On the other hand, although no significant change was observed in the shoot Fe levels, the severity of the chlorosis in the leaves increased, which might be attributed to the over-accumulation of Zn and Mn. Plants secreted more phytosiderophores to the rhizosphere as a response to the Fe deficiency. The expression levels of genes involved in both Strategy-I and Strategy-II increased in the roots of barley exposed to iron deficiency, but this increase was more significant in Strategy-II genes. Taken together, the results of this study prove that the Tarm-92 is sensitive to Fe deficiency and it activates Strategy-II stronger than Strategy-I under Fe deficiency.

Funding Information

This study was supported by the Niğde Ömer Halisdemir University Research Projects Unit (project number GTB 2017/01-BAGEP) and the COST Association (grant CA19116 "PLANTMETALS").

References

Aksoy, E., Jeong, I. S., & Koiwa, H. (2013). Loss of function of Arabidopsis C-terminal domain phosphatase-like1 activates iron deficiency responses at the transcriptional level. *Plant Physiology*, *161*(1), 330-345. https://doi.org/10.1104/pp.112.207043

Aksoy, E., & Koiwa, H. (2013). Determination of ferric chelate reductase activity in the *Arabidopsis thaliana* root. *Bio-protocol*, *3*(15), e843-e843. https://doi.org/10.21769/BioProtoc.843

Aksoy, E., Yerlikaya, B. A., Ayten, S., & Abudureyimu, B. (2018). Iron uptake mechanisms from the rhizosphere in plants. *Turkish Journal of Agriculture-Food Science and Technology*, *6*(12), 1673-1683. https://doi.org/10.24925/turjaf.v6i12.1673-1683.1326

Alam, S., Kamei, S., & Kawai, S. (2001). Effect of iron deficiency on the chemical composition of the xylem sap of barley. *Soil Science and Plant Nutrition*, *47*(3), 643-649. https://doi.org/10.1080/00380768.2001.10408428

Bandyopadhyay, T., & Prasad, M. (2021). IRONing out stress problems in crops: a homeostatic perspective. *Physiologia Plantarum*, *171*(4), 559-577. https://doi.org/10.1111/ppl.13184

Benlioğlu, B., & Özkan, U. (2015). Bazı arpa çeşitlerinin (*Hordeum vulgare* L.) çimlenme dönemlerinde farklı dozlardaki tuz stresine tepkilerinin belirlenmesi. *Tarla Bitkileri Merkez Araştırma Enstitüsü Dergisi*, *24*(2), 109-114. https://doi.org/10.21566/tbmaed.07412

Blasco, B., Navarro-León, E., & Ruiz, J.M. (2018). Oxidative stress in relation with micronutrient deficiency or toxicity. In M. A. Hossain, T. Kamiya, D.J. Burritt, L-S. P. Tran, & T. Fujiwara (Eds.), *Plant micronutrient use efficiency* (pp. 181-194). Academic Press. https://doi.org/10.1016/B978-0-12-812104-7.00011-3

Clemens, S., & Weber, M. (2016). The essential role of coumarin secretion for Fe acquisition from alkaline soil. *Plant Signaling and Behavior, 11*(2), e1114197. https://doi.org/10.1080/15592324.2015.1114197

Connolly, E. L., Fett, J. P., & Guerinot, M. L. (2002). Expression of the *IRT1* metal transporter is controlled by metals at the levels of transcript and protein accumulation. *The Plant Cell*, *14*(6), 1347-1357. https://doi.org/10.1105/tpc.001263

Çakır S. (2007). Selenyum Toksisitesinin İki Arpa (*Hordeum vulgare* L.) Çeşitinde (TARM 92, BÜLBÜL 89) Antioksidan Enzim Aktivitesine Etkisi, Yüksek Lisans Tezi, Fen Bilimleri Enstitüsü, Erciyes Üniversitesi, Kayseri.

Çatav, Ş.S., Çetin, E., Vural, E., & Bürün, B. (2023). Boron toxicity tolerance in barley may be related to intrinsically higher levels of reactive oxygen species in the shoots. *Botanica Serbica*, *47*(1), 113-124. https://doi.org/10.2298/BOTSERB2301113C

Doğru, A. (2019). Bazi arpa genotiplerinde kurşun toleransinin klorofil a floresansi ile değerlendirilmesi. *Bartın University International Journal of Natural and Applied Sciences*, *2*(2), 228-238.

Doğru, A., 2020. Evaluation of Heat Shock-Induced Stress Tolerance to Some Abiotic Factors in Barley Seedlings by Chlorophyll a Fluorescence Technique. *Sinop Üniversitesi Fen Bilimleri Dergisi*, *5*(2), 112-124. https://doi.org/10.33484/sinopfbd.630690

Erenoglu, B., Eker, S., Cakmak, I., Derici, R., & Römheld, V. (2000). Effect of iron and zinc deficiency on release of phytosiderophores in barley cultivars differing in zinc efficiency. *Journal of Plant Nutrition*, *23*(11-12), 1645-1656. https://doi.org/10.1080/01904160009382130

Fan, X., Zhou, X., Chen, H., Tang, M., & Xie, X. (2021). Cross-talks between macro-and micronutrient uptake and signaling in plants. *Frontiers in Plant Science*, *12*, 663477. https://doi.org/10.3389/fpls.2021.663477

Gines, M., Baldwin, T., Rashid, A., Bregitzer, P., Maughan, P. J., Jellen, E. N., & Klos, K. E. (2018). Selection of expression reference genes with demonstrated stability in barley among a diverse set of tissues and cultivars. *Crop Science*, *58*(1), 332-341. https://doi.org/10.2135/cropsci2017.07.0443

Grillet, L., & Schmidt, W. (2019). Iron acquisition strategies in land plants: not so different after all. *New Phytologist, 224*(1), 11-18. https://doi.org/10.1111/nph.16005

Hindt, M.N., & Guerinot, M.L. (2012). Getting a sense for signals: regulation of the plant iron deficiency response. *Biochimica et Biophysica Acta (BBA)-Molecular Cell Research*, *1823*(9), 1521-1530. https://doi.org/10.1016/j.bbamcr.2012.03.010

Hoagland, D. R., & Arnon, D. I. (1950). The water-culture method for growing plants without soil. *California Agricultural Experiment Station Circular*, *347*(2), 32.

Hua, Y. P., Wang, Y., Zhou, T., Huang, J. Y., & Yue, C. P. (2022). Combined morpho-physiological, ionomic and transcriptomic analyses reveal adaptive responses of allohexaploid wheat (*Triticum aestivum* L.) to iron deficiency. *BMC Plant Biology, 22*(1), 234. https://doi.org/10.1186/s12870-022-03627-4

Ishimaru, Y., Suzuki, M., Tsukamoto, T., Suzuki, K., Nakazono, M., Kobayashi, T., Wada, Y., Watanabe, S., Matsuhashi, S., Takahashi, M., & Nishizawa, N. K. (2006). Rice plants take up iron as an Fe^{3+}-phytosiderophore and as Fe^{2+}. *The Plant Journal, 45*(3), 335-346. https://doi.org/10.1111/j.1365-313X.2005.02624.x

Jiang, Y., Chen, X., Chai, S., Sheng, H., Sha, L., Fan, X., Zeng, J., Kang, H., Zhang, H., Xiao, X., & Zhou, Y. (2021). *TpIRT1* from Polish wheat (*Triticum polonicum* L.) enhances the accumulation of Fe, Mn, Co, and Cd in Arabidopsis. *Plant Science, 312,* 111058. https://doi.org/10.1016/j.plantsci.2021.111058

Jiang, C., Johkan, M., Hohjo, M., Tsukagoshi, S., & Maruo, T. (2017). A correlation analysis on chlorophyll content and SPAD value in tomato leaves. *HortResearch, 71*(71), 37-42.

Jeong, J., & Connolly, E. L. (2009). Iron uptake mechanisms in plants: functions of the FRO family of ferric reductases. *Plant science*, *176*(6), 709-714. https://doi.org/10.1016/j.plantsci.2009.02.011

Kanai, M., Hirai, M., Yoshiba, M., Tadano, T., & Higuchi, K. (2009). Iron deficiency causes zinc excess in *Zea mays*. *Soil Science and Plant Nutrition, 55*(2), 271-276. https://doi.org/10.1111/j.1747-0765.2008.00350.x

Kobayashi, T., & Nishizawa, N. K. (2012). Iron uptake, translocation, and regulation in higher plants. *Annual Review of Plant Biology*, *63*, 131-152. https://doi.org/10.1146/annurev-arplant-042811-105522

Kobayashi, T., Nakanishi, H., Takahashi, M., Kawasaki, S., Nishizawa, N.K., & Mori, S. (2001). In vivo evidence that *Ids3* from *Hordeum vulgare* encodes a dioxygenase that converts 2'-deoxymugineic acid to mugineic acid in transgenic rice. *Planta*, *212*, 864-871. https://doi.org/10.1007/s004250000453

Kobayashi, T., Yoshihara, T., Jiang, T., Goto, F., Nakanishi, H., Mori, S., & Nishizawa, N.K. (2003). Combined deficiency of iron and other divalent cations mitigates the symptoms of iron deficiency in tobacco plants. *Physiologia Plantarum, 119*(3), 400-408. https://doi.org/10.1034/j.1399-3054.2003.00126.x

Li, S., Song, Z., Liu, X., Zhou, X., Yang, W., Chen, J., & Chen, R. (2022). Mediation of zinc and iron accumulation in maize by ZmIRT2, a novel iron-regulated transporter. *Plant and Cell Physiology, 63*(4), 521-534. https://doi.org/10.1093/pcp/pcab177

Li, S., Zhou, X., Huang, Y., Zhu, L., Zhang, S., Zhao, Y., Guo, J., Chen, J., & Chen, R. (2013). Identification and characterization of the zinc-regulated transporters, iron-regulated transporter-like protein (ZIP) gene family in maize. *BMC Plant Biology, 13*(1), 1-14. https://doi.org/10.1186/1471-2229-13-114

Lichtenthaler, H. K., & Wellburn, A. R. (1983). Determinations of total carotenoids and chlorophylls a and b of leaf extracts in different solvents. *Biochemical Society Transactions, 11(5)*, 591–592. https://doi.org/10.1042/bst0110591

Lindsay, W. L., & Schwab, A. P. (1982). The chemistry of iron in soils and its availability to plants. *Journal of Plant Nutrition*, *5*(4-7), 821-840. https://doi.org/10.1080/01904168209363012

Martín-Barranco, A., Thomine, S., Vert, G., & Zelazny, E. (2021). A quick journey into the diversity of iron uptake strategies in photosynthetic organisms. *Plant Signaling and Behavior*, *16*(11), 1975088. https://doi.org/10.1080/15592324.2021.1975088

Mikami, Y., Saito, A., Miwa, E., & Higuchi, K. (2011). Allocation of Fe and ferric chelate reductase activities in mesophyll cells of barley and sorghum under Fe-deficient conditions. *Plant Physiology and Biochemistry*, *49*(5), 513-519. https://doi.org/10.1016/j.plaphy.2011.01.009

Mozafar, A. (1997). Distribution of nutrient elements along the maize leaf: Alteration by iron deficiency. *Journal of Plant Nutrition, 20*(7-8), 999-1005. https://doi.org/10.1080/01904169709365312

Murata, Y., Ma, J.F., Yamaji, N., Ueno, D., Nomoto, K., & Iwashita, T. (2006). A specific transporter for iron (III)–phytosiderophore in barley roots. *The Plant Journal, 46*(4), 563-572. https://doi.org/10.1111/j.1365-313X.2006.02714.x

Nikolic, D.B., Nesic, S., Bosnic, D., Kostic, L., Nikolic, M. & Samardzic, J.T. (2019). Silicon alleviates iron deficiency in barley by enhancing expression of strategy II genes and metal redistribution. *Frontiers in Plant Science, 10*, 416. https://doi.org/10.3389/fpls.2019.00416

Nikolic, M. & Pavlovic, J. (2018). Plant responses to iron deficiency and toxicity and iron use efficiency in plants. Oxidative stress in relation with micronutrient deficiency or toxicity. In M. A. Hossain, T. Kamiya, D.J. Burritt, L-S. P. Tran, & T. Fujiwara (Eds.), *Plant micronutrient use efficiency* (pp. 55-69). Academic Press. https://doi.org/10.1016/B978-0-12-812104-7.00004-6

Nozoye, T., Nagasaka, S., Kobayashi, T., Takahashi, M., Sato, Y., Sato, Y., Uozumi, N., Nakanishi, H. & Nishizawa, N.K. (2011). Phytosiderophore efflux transporters are crucial for iron acquisition in graminaceous plants. *Journal of Biological Chemistry*, *286*(7), 5446-5454. https://doi.org/10.1074/jbc.M110.180026

Öz M. T. (2012). Microarray based expression profiling of barley under boron stress and cloning of 3H boron tolerance gene. PhD Thesis, Middle East Technical University, Ankara, Türkiye.

Panda, B. B., Sharma, S. G., Mohapatra, P. K., & Das, A. (2012). Iron stress induces primary and secondary micronutrient stresses in high yielding tropical rice. *Journal of Plant Nutrition*, *35*(9), 1359-1373. https://doi.org/10.1080/01904167.2012.684128

Pavlovic, J., Samardzic, J., Maksimović, V., Timotijevic, G., Stevic, N., Laursen, K.H., Hansen, T.H., Husted, S., Schjoerring, J.K., Liang, Y., & Nikolic, M. (2013). Silicon alleviates iron deficiency in cucumber by promoting mobilization of iron in the root apoplast. *New Phytologist*, *198*(4), 1096-1107. https://doi.org/10.1111/nph.12213

Pedas, P., Ytting, C.K., Fuglsang, A.T., Jahn, T.P., Schjoerring, J.K., & Husted, S. (2008). Manganese efficiency in barley: identification and characterization of the metal ion transporter HvIRT1. *Plant Physiology, 148*(1), 455-466. https://doi.org/10.1104/pp.108.118851

Pizzio, G. A., Regmi, K., & Gaxiola, R. (2015). Rhizosphere acidification assay. *Bio-protocol*, *5*(23), e1676-e1676. https://doi.org/10.21769/BioProtoc.1676

Rai, S., Singh, P.K., Mankotia, S., Swain, J., & Satbhai, S.B. (2021). Iron homeostasis in plants and its crosstalk with copper, zinc, and manganese. *Plant Stress, 1*, 100008. https://doi.org/10.1016/j.stress.2021.100008

Reichman, S. M., & Parker, D. R. (2007). Critical evaluation of three indirect assays for quantifying phytosiderophores released by the roots of Poaceae. *European Journal of Soil Science*, *58*(3), 844-853. https://doi.org/10.1111/j.1365-2389.2006.00874.x

Robe, K., Izquierdo, E., Vignols, F., Rouached, H., & Dubos, C. (2021). The coumarins: secondary metabolites playing a primary role in plant nutrition and health. *Trends in Plant Science, 26*(3), 248-259. https://doi.org/10.1016/j.tplants.2020.10.008

Santi, S., & Schmidt, W. (2009). Dissecting iron deficiency-induced proton extrusion in Arabidopsis roots. *New Phytologist*, *183*(4), 1072-1084. https://doi.org/10.1111/j.1469-8137.2009.02908.x

Santos, C.S., Ozgur, R., Uzilday, B., Turkan, I., Roriz, M., Rangel, A.O., Carvalho, S.M., & Vasconcelos, M.W. (2019). Understanding the role of the antioxidant system and the tetrapyrrole cycle in iron deficiency chlorosis. *Plants, 8*(9), 348. https://doi.org/10.3390/plants8090348

Sperotto, R. A., Ricachenevsky, F. K., de Abreu Waldow, V., & Fett, J. P. (2012). Iron biofortification in rice: it's a long way to the top. *Plant Science, 190*, 24-39. https://doi.org/10.1016/j.plantsci.2012.03.004

Tabata, R. (2023). Regulation of the iron-deficiency response by IMA/FEP peptide. *Frontiers in Plant Science, 14*, 1107405. https://doi.org/10.3389/fpls.2023.1107405

Torun, B., Kalayci, M., Ozturk, L., Torun, A., Aydin, M., & Cakmak, I. (2002). Differences in Shoot Boron Concentrations, Leaf Symptoms, and Yield of Turkish Barley Cultivars Grown on Boron-Toxic Soil in Field. *Journal of Plant Nutrition*, *26*(9), 1735-1747. https://doi.org/10.1081/PLN-120023279

Vasconcelos, M. W., & Grusak, M. A. (2014). Morpho-physiological parameters affecting iron deficiency chlorosis in soybean (*Glycine max* L.). *Plant and soil*, *374*, 161-172. https://doi.org/10.1007/s11104-013-1842-6

Vasconcelos, M., Eckert, H., Arahana, V., Graef, G., Grusak, M.A., & Clemente, T. (2006). Molecular and phenotypic characterization of transgenic soybean expressing the Arabidopsis ferric chelate reductase gene, *FRO2*. *Planta, 224*, 1116-1128. https://doi.org/10.1007/s00425-006-0293-1

Vert, G., Grotz, N., Dédaldéchamp, F., Gaymard, F., Guerinot, M.L., Briat, J.F., & Curie, C. (2002). IRT1, an Arabidopsis transporter essential for iron uptake from the soil and for plant growth. *The Plant Cell*, *14*(6), 1223-1233. https://doi.org/10.1105/tpc.001388

Wairich, A., de Oliveira, B. H. N., Arend, E. B., Duarte, G. L., Ponte, L. R., Sperotto, R. A., Ricachenevsky, F.K., & Fett, J. P. (2019). The combined strategy for iron uptake is not exclusive to domesticated rice (*Oryza sativa*). *Scientific Reports, 9*(1), 16144. https://doi.org/10.1038/s41598-019-52502-0

Walker, E. L., & Connolly, E. L. (2008). Time to pump iron: iron-deficiency-signaling mechanisms of higher plants. *Current Opinion in Plant Biology, 11*(5), 530-535. https://doi.org/10.1016/j.pbi.2008.06.013

Werner, C., & Matile, P. (1985). Accumulation of coumarylglucosides in vacuoles of barley mesophyll protoplasts. *Journal of Plant Physiology, 118*(3), 237-249. https://doi.org/10.1016/S0176-1617(85)80225-X

Biotech Studies 33(1), 33-42
http://doi.org/10.38042/biotechstudies.1442037

BIOTECH STUDIES

RESEARCH PAPER

Juglans kernel powder and jacobinia leaf powder supplementation influenced growth, meat, brain, immune system and DNA biomarker of broiler chickens fed Aflatoxin-B1 contaminated diets

Olugbenga David Oloruntola

Department of Animal Science, Adekunle Ajasin University, Akungba Akoko, Nigeria.

How to cite:
Oloruntola, O. D. (2024). Juglans kernel powder and jacobinia leaf powder supplementation influenced growth, meat, brain, immune system and DNA biomarker of broiler chickens fed Aflatoxin-B1 contaminated diets. *Biotech Studies*, *33*(1), 33-42. http://doi.org/10.38042/biotechstudies.1442037

Article History
Received 18 May 2023
Accepted 09 January 2024
First Online 08 February 2024

Corresponding Author
Tel.: +234 803 584 16 26
E-mail:
olugbenga.oloruntola@aaua.edu.ng

Keywords
Antioxidants
Immune response
Phytosupplement
Mycotoxins
Poultry

Abstract

This study investigates the impact of Juglans kernel powder (JKP) and Jacobinia leaf powder (JLP) supplementation on Aflatoxin-B1 (AF) exposed broiler chickens. 200 Cobb-500 broiler chicks were grouped to four treatments: CONT: No supplement; AFNS: 0.5 mg/kg AF; AFJK: 0.5 mg/kg AF+ 350 mg/kg JKP; AFJL: 0.5 mg/kg AF+350 mg/kg JLP. On day 42, the broiler chicken's relative growth rate, and dressed percentage were lowest in AFNS compared to the rest treatments. Meat cholesterol was lower in AFNS, AFJK, and AFJL, compared to CONT. Meat catalase in AFNS was lower than those in CONT, AFJK, and AFJL. Meat glutathione peroxidase levels of birds in AFNS are similar to AFJL but were lower than those in CONT, and AFJK. Lipid oxidation, and protein oxidation activities of broiler chickens in AFNS were higher than those in the rest of the treatments. Brain catalase, acetylcholinesterase, and glutathione peroxidase activities of birds in AFNS were lower than CONT, AFJK, and AFJL. Expressions of proinflammatory cytokines, and 8-hydroxy-2'-deoxyguanosine in AFNS were higher compared to other treatments. The immunoglobulins A, E and G of broiler chickens in AFNS were lower than CONT, AFJK, and AFJL. 350 mg/kg JKP or JLP ameliorate the effects of AF contamination on broiler chickens.

Introduction

Commercial broiler chicken production is one of the profitable ventures that bring back profits on capital investment in a relatively short period because broiler chickens are fast and can reach a market weight of about 2 kg in less than 7 weeks of age (Kpomasse et al., 2021; Tallentire et al., 2016).

Feed quality has been identified as a significant challenge, exerting a negative impact on the performance and health of broiler chickens (Houndonougbo et al., 2012). According to Udomkun et al. (2017), one of the main causes of food insecurity is feed contamination by mycotoxins, which harm 25% of the world's crops (Pankaj et al., 2018). Aflatoxins (AFs), a class of very hazardous mycotoxins are known to infect a wide range of foods, including grains like maize and groundnuts (Iqbal et al., 2015; Mahato et al., 2019). Since ingestion of AF-contaminated diets by animals or humans produces serious health complications, strict regulations for AFs in feed and food are implemented to maintain public health (Juan et al., 2012; Mahato et al., 2019).

Several hazardous secondary metabolites, including aflatoxins B1, B2, G1, and G2, are frequently produced in response to the growth of *Aspergillus flavus* or *Aspergillus parasiticus* in poultry feeds (Fouad et al., 2019). Aflatoxin B1 is the most harmful and prevalent

mycotoxin among these metabolites (Pitt & Miller, 2017). It is known to be hepatotoxic, cancer-causing, and mutagenic (De Ruyck et al., 2015), and the risks associated with aflatoxin B1 in chickens include low productivity and a high propensity for disease (Fouad et al., 2019). Additionally, it has been hypothesized that Aflatoxin B1 can cause cells to produce intracellular Reactive Oxygen Species (ROS) like superoxide anion, hydroxyl radical, and hydrogen peroxide (An et al., 2017; Towner et al., 2003). Consequently DNA, lipids, and proteins are damaged by oxidation, which causes serious cellular dysfunctions (Forni et al., 2019).

Since the increase in ROS and subsequent oxidative stress and inflammation are closely related to the pathophysiological processes of aflatoxicosis, the use of phytosupplements with well-known antioxidant and anti-inflammatory effects is presently gaining attention (Forni et al., 2019). For example, it is well known that ROS act as physiologic activators of transcription factors like Nuclear Factor B and Activator Protein-1 that, in turn, can modulate the transcription of proinflammatory cytokines like Tumor Necrosis Factor, Interleukin 6, 8, and 1 (Nordberg & Arnér, 2001). Therefore, a fascinating approach for potential clinical applications is the utilisation of phytosupplements with antioxidant and anti-inflammatory action (Forni et al., 2019).

Recently, JKP and JLP were reported as potential phytogenic supplements that possess antioxidant and anti-inflammatory properties and other nutraceutical properties that could be explored to mitigate the negative effects of Aflatoxin dietary contamination (Oloruntola, 2022a; Oloruntola et al., 2022a). Therefore, the objectives of this work are to study the effects of Juglans kernel powder and Jacobina leaf powder supplementation on the growth, carcass, immune system, and DNA biomarkers of broiler chickens fed Aflatoxin B1 contaminated diets.

Materials and Methods

Ethical approval, juglans kernel and jacobinia leaf powder, aflatoxin B1, and experimental diets

The animal care and use procedure was approved by the Animal Care and Use Committee of the Department of Animal Science at Adekunle Ajasin University in Akungba Akoko, Nigeria. The JKP and JLP were produced as described by Oloruntola (2022a) and Oloruntola et al. (2022a), respectively. The pure culture of *Aspergillus flavus* (NRRL 3251), which was grown on potato dextrose agar, produced aflatoxin. The autoclavable polypropylene bags containing 500 g of corn grits were heated to 121 °C and then exposed to a pressure of 120 kPa for 60 min. After being inoculated with an *A. flavus* spore suspension, the autoclaved grit maize was cultivated for seven days at a temperature of 28 °C. Once the fungus had grown, the grit maize was dried in a 70°C oven and ground into powder. Aflatoxin B1 (AF) levels were measured in triplicate using thin-layer chromatography in maize (AOAC, 2010).

A baseline diet (**Table 1**) was prepared, divided into four halves, and given the designations for the starter and finisher stages:

CONT: No aflatoxin AF contamination and no supplementation.

AFNS: No phytosupplement was added to 0.5 mg/kg of AF-contaminated baseline diet.

AFJK: 350 mg/kg of JKP was added to the 0.5 mg/kg of AF-contaminated baseline diet.

AFJL: 350 mg/kg of JLP was added to the 0.5 mg/kg of AF-contaminated baseline diet.

The 0.5 mg/kg AF/kg dietary contamination utilized in this study is 25 times higher than the dietary concentration for chicken authorized by the National Agency for Food and Drug Administration and Control (NAFDAC) and the European Union (EU) (Burel *et al.*, 2009).

Table 1. Composition of the experimental diets

Ingredients (%)	Starter phase	Finisher phase
Maize	50.36	58.36
Rice bran	0.00	3.02
Maize bran	3.00	0.00
Soy oil	1.00	1.00
Soybean meal	38.00	30.00
Fish meal	3.00	3.00
Bone meal	3.00	3.00
Premix	0.31	0.31
Limestone	0.49	0.47
Salt	0.31	0.31
Methionine	0.29	0.29
Lysine	0.24	0.24
Nutrient composition		
Metabolizable energy (Kcal/kg)	3018.10	3108.20
Crude protein (%)	22.17	20.04

Birds used in experiments and experimental design

At one day of age, 200 Cobb 500 broiler chickens were randomly assigned to four diets, each of which contained five replicas of 10 chicks. Water and feed were continuously accessible during the six-week feeding trial period.

Blood collection and analysis

On day 42, four randomly chosen birds per replication were marked or tagged, and blood samples of roughly 10 ml were taken using a syringe and needle from the brachial vein. For the measurement of pro-inflammatory cytokines and immunoglobulins into plain sample vials. The samples from plain bottles were centrifuged, and their serum was split into a different set of plain bottles and refrigerated at 20°C before being used. The Nuclear Factor Kappa B (NFK B) was determined using a Rat NFKB-p65 ELISA kit (Elabscience Biotechnology Inc. USA); the Tumor Necrosis Factor Alpha (TNF α) was determined with an ELISA kit (Elabscience Biotechnology Inc. USA) while the Interleukin 6 (IL 6) was determined using a Rat IL-6 ELISA kit (Elabscience Biotechnology Inc. USA). The

immunoglobulins A (IgA), E (IgE), G (IgG) and M (IgM) were determined using ELISA kits (Fortress Diagnostics Limited, United Kingdom). The 8-hydroxy-2'-deoxyguanosine (8-OHdG) was determined as described by Zhang et al. (2013).

Relative growth rate and carcass traits

Broiler chickens that were used in the experiment were weighed before the feeding experiment began (day 1) and when the experiment was over (day 42). The relative growth rate (RGR) was estimated (Adebayo et al., 2020) by using the formula:

RGR=[(wt2-wt1)/((w1+w2))/2]*100.

wt1= the broiler chickens' initial weight before the experiment, and wt2= the broiler chicks' weight on the final day of the experiment.

On the 42nd day of the experiment, 14 birds were arbitrarily chosen from each treatment group (two birds/replica), weighed, and slaughtered in accordance with the EU regulation on animal protection during slaughter and killing (Osowe et al., 2022; Uijttenboogaart, 1999). Afterwards, the carcasses were spray-washed and cooled for 30 min at 2 °C. The ratio of the carcass weight to the final body weight was used to estimate the dressing percentage. Also, the relative weights of the heart, liver, lung, pancreas, gizzard, and spleen (percentage of final weight) were computed (Osowe et al., 2022).

Meat and brain analysis

After being slaughtered, a total of five birds (one bird per replication) were chosen from each treatment group to be tested for the level of the enzymes catalase, glutathione peroxidase, lipid peroxidation, and protein oxidation, as well as meat cholesterol. Catalase, acetylcholinesterase (AChE), glutathione peroxidase, and ferric ion-reducing antioxidant power (FRAP) in the brain were also examined. A portion of the breast meat from the carcasses was removed, wrapped aerobically in an oxygen-permeable bag, and frozen for 20 days at -18 °C.

The concentration of meat cholesterol was measured spectrophotometrically using commercial kits (Asan Pharm. Co., Ltd., Seoul). The catalase and glutathione peroxidase activities were determined as reported by Muhlisin et al. (2016) and Cichoski et al., (2012), respectively. The thiobarbituric acid (TBA) assay method was used to determine the degree of lipid oxidation in the meat (Tokur et al., 2006). The meat protein oxidation was determined as described by Souza et al. (2013).

Using a high-speed homogenizer, the entire brains of broiler chickens were removed and homogenized in cold saline at 0.9% in a ratio of 1:10 (w/v). The homogenate samples were divided into 1.0 ml aliquots and stored at -18 °C until use after being centrifuged at 2000 rpm for 20 min. The brain catalase (Khan et al. 2012), FRAP (Benzie and Strain, 1996; Sadeghi et al., 2019), and glutathione peroxidase (Khan et al. 2012) activities were determined. The brain AChE activity was determined spectrophotometrically using a modified Ellman's method (Freitas et al., 2016; Silva et al., 2004).

Statistical data analysis

The data were subjected to an analysis of variance (ANOVA) using SPSS v.20, and the Duncan multiple range test of the same program was used to see whether the treatment means differed (Oloruntola et al., 2018).

Results

The comprehensive examination of broiler chickens subjected to AF contamination, coupled with JKP and JLP dietary supplementation, reveals multifaceted impacts on various physiological parameters and meat properties. **Figure 1** shows that the relative growth rate (RGR) was lowest in AFNS compared to the rest of the treatments. In addition, the RGR of birds in AFJK and AFJL were similar but significantly higher than the CONT and AFNS.

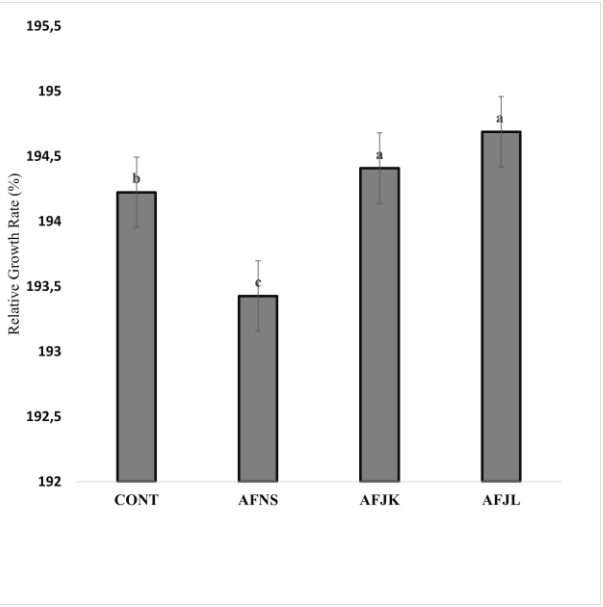

Figure 1. Effects of Justicia kernel powder and Jabobinia leaf powder on the Relative growth rate of broiler chickens fed aflatoxin B1 contaminated diets. CONT: No contamination/supplementation; AFNS: 0.5 mg/kg AF; AFJK: 0.5 mg/kg AF +350 mg/kg JK; AFJL: 0.5 mg/kg AF+350 mg/kg JL.

Table 2 shows the effects of JKP and JLP supplementation on the carcass and internal organs weight (% slaughter weight) of broiler chickens fed an AF-contaminated diet. The dressed percentage of the birds in AFNS was significantly lower than that in CONT and the rest treatments (AFJK and AFJL). There was significant inflammation of the liver, and pancreas of birds in AFNS compared to those in CONT and the rest of the treatments. The enlargement of the spleen recorded in AFNS is similar to AFJK but was significantly higher than those in CONT and AFJL.

Table 2. Effects of Juglans kernel powder and Jacobinia leaf powder supplementation on the carcass and internal organs weight (% slaughter weight) of broiler chickens fed Aflatoxin B1-contaminated diet

Parameters	CONT	AFNS	AFJK	AFJL	SEM	P value
Dressed percentage	75.92^{a}	68.59^{b}	76.22^{a}	74.49^{a}	0.78	0.01
Heart	0.48	0.44	0.43	0.53	0.01	0.05
Liver	2.76^{b}	3.56^{a}	2.34^{bc}	2.82^{b}	0.01	0.01
Lung	0.53	0.54	0.52	0.47	0.-02	0.50
Pancrease	0.24^{c}	0.36^{a}	0.30^{b}	0.24^{c}	0.01	0.01
Gizzard	2.23	1.92	1.97	2.31	0.07	0.22
Spleen	0.19^{bc}	0.26^{a}	0.24^{ab}	0.16^{c}	0.01	0.01

$^{a-c}$Means within a row with different letters are significantly different (P<0.05); AF: Aflatoxin B1; CONT: No contamination/supplementation; AFNS: 0.5 mg/kg AF; AFJK: 0.5 mg/kg AF +350 mg/kg JK; AFJL: 0.5 mg/kg AF+350 mg/kg JL; SEM: Standard error of means.

Table 3. Effects of Juglans kernel powder and Jacobinia leaf powder supplementation on the meat properties of broiler chickens fed Aflatoxin B1-contaminated diet

Parameters	CONT	AFNS	AFJK	AFJL	SEM	P value
Cholesterol (mmol/l)	5.38^{a}	4.84^{b}	4.00^{c}	4.25^{c}	0.12	0.01
Catalase (kU/ml)	48.65^{a}	32.35^{c}	42.41^{b}	42.46^{b}	1.32	0.01
Glutathione peroxidase (µmole)	208.34^{a}	168.62^{b}	202.05^{a}	178.43 ^{ab}	4.19	0.01
Lipid oxidation (mgMDA/g)	1.21^{b}	1.78^{a}	1.16^{b}	1.28^{b}	0.06	0.01
Protein oxidation (nmol/mg)	99.57^{b}	141.65^{a}	107.04^{b}	105.33^{b}	3.72	0.01

$^{a-c}$Means within a row with different letters are significantly different (P<0.05); AF: Aflatoxin B1; CONT: No contamination/supplementation; AFNS: 0.5 mg/kg AF; AFJK: 0.5 mg/kg AF +350 mg/kg JK; AFJL: 0.5 mg/kg AF+350 mg/kg JL; SEM: Standard error of means.

The AF dietary contamination, and phytosupplementation have significant effects on the meat properties in the broiler chickens (Table 3). The meat cholesterol concentration was significantly lower in AFNS, AFJK and AFJL, compared to those in CONT. The meat catalase of birds in AFNS was significantly lower than that in CONT, AFJK, and AFJL. The meat glutathione peroxidase levels of birds in AFNS are similar to AFJL but were lower than those in CONT and AFJK although the glutathione peroxidase of broiler chicken's meat in AFJL was comparable to CONT and AFNS. The lipid oxidation and protein oxidation activities of broiler chickens in AFNS were significantly higher than those in CONT, AFJK, and AFJL.

The effects of JKP and JLP supplementation on the brains of broiler chickens fed AF-contaminated diet are shown in Table 4. The brain catalase, AChE, and glutathione peroxidase activities of birds in AFNS were significantly lower than CONT, AFJK, and AFJL. The brain FRAP of birds in AFNS was lower than those in CONT, AFJK, and AFJL although the FRAP in AFJK and AFJL were lower than CONT.

The NFKB, TNF-α, and IL-6 expressions in AFNS were significantly lower than in CONT, AFJK, and AFJL (Table 5).

Effects of JKP and JLP supplementation on the immunoglobulins of broiler chickens fed AF-contaminated diet are shown in Table 6. The immunoglobulins A, E, and G of broiler chickens in AFNS were lower in AFNS, compared to CONT, AFJK, and AFJL while the immunoglobin M of broiler chickens in AFNS was similar to AFJK but was lower than CONT and AFJL.

Table 4. Effects of Juglans kernel powder and Jacobinia leaf powder supplementation on the brain of broiler chickens fed Aflatoxin B1-contaminated diet

Parameters	CONT	AFNS	AFJK	AFJL	SEM	P value
Catalase (u/mg protein)	7.51^{a}	5.10^{b}	6.68^{a}	6.54^{a}	0.24	0.01
Acetylcholinesterase (u/ml)	0.23^{a}	0.11^{b}	0.21^{a}	0.20^{a}	0.01	0.01
Glutathione peroxidase (U/L)	57.94^{a}	49.13^{b}	56.19^{a}	56.24^{a}	0.99	0.03
FRAP (µM(Fe(II))	74.37^{a}	58.13^{c}	69.06^{b}	69.57^{b}	1.42	0.01

$^{a-c}$Means within a row with different letters are significantly different (P<0.05); AF: Aflatoxin B1; CONT: No contamination/supplementation; AFNS: 0.5 mg/kg AF; AFJK: 0.5 mg/kg AF +350 mg/kg JK; AFJL: 0.5 mg/kg AF+350 mg/kg JL; FRAP: Ferric ion Reducing Antioxidant Power; SEM: Standard error of means.

Table 5. Effects of Juglans kernel powder and Jacobinia leaf powder supplementation on the proinflammatory cytokines of broiler chickens fed Aflatoxin B1-contaminated diet

Parameters	CONT	AFNS	AFJK	AFJL	SEM	P value
NFKB (pg/ml)	26.57^{b}	38.17^{a}	27.99^{b}	26.71^{b}	1.14	0.01
TNF ALFA (pg/ml)	34.47^{b}	63.78^{a}	42.05^{b}	43.57^{b}	3.09	0.01
IL6 (pg/ml)	14.31^{c}	39.53^{a}	22.71^{b}	24.42^{b}	2.18	0.01

$^{a-c}$Means within a row with different letters are significantly different (P<0.05); AF: Aflatoxin B1; CONT: No contamination/supplementation; AFNS: 0.5 mg/kg AF; AFJK: 0.5 mg/kg AF +350 mg/kg JK; AFJL: 0.5 mg/kg AF+350 mg/kg JL; SEM: Standard error of means.

Table 6. Effects of Juglans kernel powder and Jacobinia leaf powder supplementation on the immunoglobulins of broiler chickens fed Aflatoxin B1-contaminated diet

Parameters	CONT	AFNS	AFJK	AFJL	SEM	P value
Immunoglobulin A (mg/dl)	219.54[a]	171.43[b]	243.99[a]	230.67[a]	8.34	0.01
Immunoglobulin E (IU/ml)	1073.83[a]	931.01[b]	1068.58[a]	1105.87[a]	15.66	0.01
Immunoglobulin G (mg/dl)	316.48[a]	210.78[b]	317.17[a]	329.87[a]	11.26	0.02
Immunoglobulin M (mg/dl)	373.64[b]	330.21[c]	348.35[bc]	410.25[a]	7.80	0.01

[a-c]Means within a row with different letters are significantly different (P<0.05); AF: Aflatoxin B1; CONT: No contamination/supplementation; AFNS: 0.5 mg/kg AF; AFJK: 0.5 mg/kg AF +350 mg/kg JK; AFJL: 0.5 mg/kg AF+350 mg/kg JL; SEM: Standard error of means.

However, the immunoglobulin M level was higher in AFKL, compare to the rest diets.

The effects of JKP and JLP on the serum 8-OHdG of broiler chickens fed AF-contaminated diets were depicted in **Figure 2**. The expression of 8-OHdG in AFNS was significantly higher than CONT, AFJK, and AFJL. The 8-OHdG in AFJK and AFJL were similar to CONT.

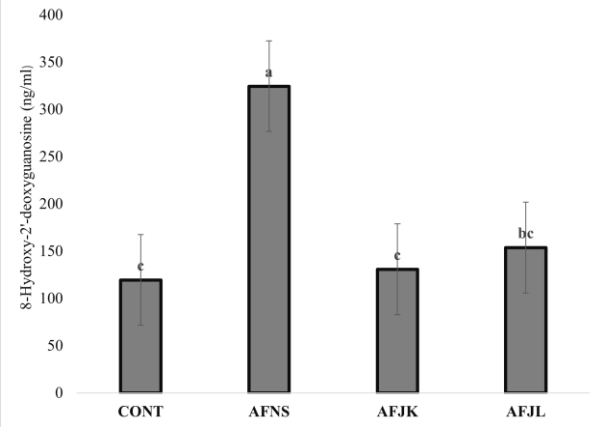

Figure 2. Effects of Justicia kernel powder and Jabobinia leaf powder on the serum 8-Hydroxy-2'-deoxyguanosine of broiler chickens fed aflatoxin B1 contaminated diets. CONT: No contamination/supplementation; AFNS: 0.5 mg/kg AF; AFJK: 0.5 mg/kg AF +350 mg/kgJK; AFJL: 0.5 mg/kg AF+350 mg/kg JL.

Discussion

Examining JKP and JLP supplementation in broiler chickens exposed to Aflatoxin-B1, this discussion explores comprehensive effects on growth, meat, brain, immune system, and DNA biomarkers. The observed lower relative growth rate in this study's experimental birds fed 0.5 mg/kg of AF was comparable to the reduced body weight gain in broiler chickens documented in response to AF dietary contamination by Nazarizadeh et al. (2019). Aflatoxicosis resulted in stunted growth and may have been caused by gastrointestinal dysfunction, which is typically accompanied by reduced feed efficiency (Sarma et al., 2017). The improved relative growth rate observed in the experimental birds fed AF-contaminated diets supplemented with JKP and JLP (AFJK and AFJL) in this study, however, indicates the potential of these phytosupplements to counteract growth-suppressing effects of dietary AF contamination in broiler chickens by improving the nutrient digestion and absorption (Hashemi & Davoodi, 2010; Valenzuela-Grijalva et al., 2017). Previous studies have indicated phytosupplements as growth promoters in animals and particularly broiler chickens (Olarotimi et al., 2022; Oloruntola 2022b; Valenzuela-Grijalva et al., 2017). According to this study, JKP and JLP supplements boosted growth performance in broiler birds fed diets contaminated with AF. Specifically, broiler chicks fed diets contaminated with AF showed enhanced body weight gain as a result of JKP and JLP supplementation. This improvement may be attributed to a variety of biological activities, including the antioxidant, antibacterial, and flavor-enhancing effects of phytogenic supplements (Valenzuela-Grijalva et al., 2017).

The observed reduced dress percentage recorded in AFNS in this study could also be due to the same factor that affected their relative growth rate. Furthermore, the animals' relative internal organ weights may have increased abnormally, which could be a sign that their internal organs are reacting to a toxin in their diet (Ayodele et al., 2016). As recorded in this study, the increased liver, pancreas, and spleen relative weights of the experimental birds due to aflatoxicosis were linked to the carcinogenic, mutagenic, immunosuppressive, and teratogenic activities of AF causing significant interference with the normal protein synthesis and inhibition of myriad metabolic systems, and consequently, causing pathological processes in various organs such as the heart, kidney, and liver (Mohammed & Metwally, 2009). The pancreas (El-Haleem et al., 2011) and spleen (Li et al., 2019) are also among the common organs affected by aflatoxicosis.

There is currently an increased global preference for low-cholesterol chicken meat by consumers and more dietary modifications are being adopted to decrease the fat and cholesterol contents of poultry meat (Ponte et al., 2004). By implication, the observed reduced meat cholesterol concentration of birds in AFNS, AFJK, and, AFJL in this study is of benefit. The reduced meat cholesterol concentration in broiler chickens fed aflatoxin-contaminated feed could be due to gastrointestinal dysfunction resulting in reduced nutrients e.g., fat utilization and consequently low concentration of fat and cholesterol in their meat (Sarma et al., 2017). Additionally, the phytogenic supplements in AFJK and AFJL may contain bioactive substances like tannin and saponins that prevent the absorption of fat and an excessive buildup of lipids in the meat (Oloruntola et al., 2022b; Thinh et al., 2018).

Catalase, glutathione peroxidase, and superoxide dismutase are antioxidant enzymes that are active in meat's enzymatic defense systems (Min et al., 2008). The decreased catalase, and glutathione peroxidase activities in the meat of the birds fed a diet contaminated with AF were consistent with earlier studies that explained that aflatoxicosis caused the antioxidant enzymes superoxide dismutase, glutathione peroxidase, and catalase to be downregulated, increasing the byproducts of lipid peroxidation (Da Silva et al., 2018). Previous reports show that JKP and JLP have antioxidant activities and nutraceutical values (Oloruntola, 2022a; Oloruntola et al., 2022a). This may explain the improved meat catalase and glutathione peroxidase activities in AFJK and AFJL birds' meat when compared to AFNS. Recent studies suggest that several phytosupplements have advantageous antioxidant properties and may significantly contribute as natural substitutes for synthetic antioxidant feed additives in enhancing the meat's antioxidant status (Abbas et al., 2015; Lee et al., 2017).

The elevated birds' meat lipid oxidation and protein oxidation activities in AFNS agreed with Da Silva et al. (2018) while similar lipid oxidation and protein oxidation activities found in the meat of broiler chickens fed AF-contaminated diets being supplemented with JKP and JLP and those fed the control diet in this study point to the presence of antioxidants and the potency of these phytosupplements (JKP and JLP) in stabilizing or delaying the lipid and protein oxidation processes in the meat of broiler chickens. According to earlier research, using dietary antioxidants can delay the oxidation process. (Cortinas et al., 2005; Smet et al., 2008). For instance, Cortinas et al. (2005) found positive oxidative stability after dietary supplementation with tocopheryl acetate. Additionally, polyphenols and flavonoids regulate oxidation by stopping or restricting chain reactions after radicals are created (Keppler et al., 2020).

AF induces neurotoxicity by causing DNA damage, apoptosis, and an interruption of the S-phase cell cycle (Huang et al., 2020). This may help to an extent explain why broiler chickens fed AFNS had reduced catalase, acetylcholinesterase, glutathione peroxidase, and ferric ion-reducing antioxidant power. Increased lipid peroxidation, increased oxidative pathways, and lower levels of antioxidant enzymes have all been associated with AF (Gugliandolo et al., 2020). However, the stable catalase, acetylcholinesterase, glutathione peroxidase, and ferric ion-reducing antioxidant power in AFJK and AFJL, when compared to CONT, further support the antioxidant and nutraceutical activities of JKP and JLP and their neuroprotective potentials (Kumar & Khanum, 2012; Oloruntola, 2022a; Oloruntola et al., 2022a).

By affecting the function of receptors for the main inhibitory neurotransmitters, phytosupplements from medicinal plants play a crucial part in preserving the chemical balance of the brain (Kumar & Khanum, 2012). Some phytosupplements have been demonstrated to have antioxidant and/or anti-inflammatory properties in a range of peripheral systems. Anti-inflammatory herbal medicine and its contents are now being demonstrated to be an effective neuroprotector against many brain disorders, as increasing data suggest that neuroglia-derived chronic inflammatory responses play a pathogenic function in the central nervous system (Kumar & Khanum, 2012; Pueyo & Calvo, 2009).

The observed amplified serum NFKB, TNF-α, and IL-6 in birds AFNS could be the expression of the mycotoxins' ability to cause or worsen inflammation through a variety of molecular processes, including the activation of inflammasomes and the generation of reactive oxygen species (Brown et al., 2021; Zhen & Zhang, 2019). It has also been demonstrated that food contamination with AF raises the levels of pro-inflammatory cytokines (Kraft et al., 2021). In addition, the stabilized serum NFKB, TNF-α, and IL-6 of birds in AFJK and AFJL could be due to the anti-inflammatory activities and other nutraceutical properties of JKP and JLP, the phytosupplement used in this study (Oloruntola, 2022a; Oloruntola et al., 2022a). A number of compounds originating from plants have lately been theorized to act as anti-inflammatory agents by controlling the production of proinflammatory microRNAs (Saleh et al., 2021). When consumed, bioactive substances originating from plants, such as phenolic compounds, which include flavonoids and tannins, glucosinolates, alkaloids, and terpenoids, get involved in a variety of biological processes in the body, including redox reactions, cell signaling, and inflammation (Perez-Gregorio & Simal-Gandara, 2017). As a result, natural products are increasingly showing promise in the treatment of a variety of inflammatory disorders arising from aflatoxicosis and related cases (Gautam & Jachak, 2009; Mahoney & Molyneux, 2004).

The depressed immunoglobulins A, E, G, and M of birds in AFNS agreed with Soltani et al. (2019), who recorded lower immunoglobulins G and M in broiler chickens fed AF-contaminated diet, compared to those fed the control diet. The inhibition of protein synthesis, which lowers the production of immunoglobulin as a result of aflatoxicosis, could be the cause of the decreased immunological responses of broiler chickens in AFNS (Soltanin et al., 2019; Sur & Celik, 2003). Furthermore, the stable immunoglobulins A, E, G, and M of broiler chickens in AFJK and AFJL, when compared to those in CONT in this study, further unveils the immunomodulatory properties of phytosupplements (Oloruntola et al., 2016). It has been demonstrated that phenolic compounds also have an impact on humoral immunity by promoting the release of certain immunoglobulins (Allam et al., 2016). Previous studies shows that serum immunoglobulins M and G levels are significantly enhanced by the phenolic compounds in phytosupplements (Allam et al., 2016; Maheshwari et al., 2022).

The best non-invasive indicator of DNA oxidative damage is 8-OHdG, which is the most representative product of oxidative alterations in DNA (Valavanidis et

al., 2009; Guo et al., 2016). The amplified expression of serum 8-OHdG of broiler birds in AFNS indicates the possibility of DNA oxidative damage being precipitated by AF exposure. As is popularly known, AF is mostly metabolized by cytochrome P450 enzymes producing the genotoxic metabolite 8,9-epoxide-AFB1 (AFBO) (Guengerich et al., 1998; Feng et al., 2016). AF-DNA adducts can be formed when AFBO binds to DNA. Consequently, AF-DNA adducts may obstruct regular transcription and replication, leading to damage in double-stranded DNA (Feng et al., 2016). The levels of 8-OHdG found in the serum of broiler chickens in AFJK and AFJL are comparable to those in CONT, suggesting that JKP and JLP, taken as dietary supplements, have antioxidant and other nutraceutical properties that support the delay of reactive oxygen species' detrimental effects on DNA integrity and prevent DNA damage (Ye et al., 2023). In addition, it has been demonstrated that a number of phytosupplements prevent tumor onset and growth by causing DNA damage (Ye et al., 2023). For instance, dietary polyphenols can shield the organism from reactive oxygen species' negative effects on DNA integrity (Azqueta & Collins, 2016).

Conclusion

The 0.5 mg/kg AF dietary contamination produced a retarded relative growth rate, depressed dress percentage and inflammation of the liver and pancreas, which were ameliorated by 350 mg/kg JKP and JLP supplementations while the 0.5 mg/kg AF dietary contamination with or without JKP or JLP supplementation caused a reduced meat cholesterol level. The reduced meat catalase, glutathione peroxidase and increasing lipid peroxidation and protein peroxidation activities being caused by AF dietary contamination are prevented by both JKP and JLP dietary supplementations. In addition, the brain AChE and glutathione peroxidase activities and the serum IgA, IgE, IgG, NFKB, TNF-α and IL-6 were reduced as a result of 0.5 mg/kg AF exposure while the expression of 8-OHdG was also depleted by AF dietary contamination. Therefore, 350 mg/kg JKP or JLP supplementations are recommended to improve the growth, meat oxidative status, immune system, and health status of broiler chickens when exposed to AF dietary contaminated diets.

Ethical Statement

The animal care and use procedure was approved by the Animal Care and Use Committee of the Department of Animal Science at Adekunle Ajasin University in Akungba Akoko, Nigeria.

Acknowledgements

The author extends heartfelt gratitude to Dr. S.A. Adeyeye, Head of the Department of Animal Health and Production Technology, and Dr. A. Fadiyimu, Provost of The Federal College of Agriculture, Akure, Nigeria, for graciously allowing the execution of this research within the College's facilities.

References

Abbas, Z. K., Saggu, S., Sakeran, M. I., Zidan, N., Rehman, H., & Ansari, A. A. (2015). Phytochemical, antioxidant and mineral composition of hydroalcoholic extract of chicory (*Cichorium intybus* L.) leaves. *Saudi Journal of Biological Sciences*, *22*(3), 322–326. https://doi.org/10.1016/j.sjbs.2014.11.015

Adebayo, F. B., Adu, O. A., Chineke, C. A., Oloruntola, O. D., Omoleye, O. S., Adeyeye, S. A., & Ayodele, S. O. (2020). The performance and heamatological indices of broiler chickens fed Chromium Picolinate and vitamin C supplemented diets. *Asian Journal of Research in Animal and Veterinary Sciences*, *6*(4), 54-61.

Allam, G., Abuelsaad, A. S. A., Alblihed, M. A., & Alsulaimani, A. A. (2016). Ellagic acid reduces murine *Schistosomiasis mansoni* immunopathology via up-regulation of IL-10 and down-modulation of pro-inflammatory cytokines production. *Immunopharmacology and Immunotoxicology*, *38*(4), 286-297. https://doi.org/10.1080/08923973.2016.1189561

An, Y., Shi, X., Tang, X., Wang, Y., Shen, F., Zhang, Q., Wang, C., Jiang, M., Liu, M., & Yu, L. (2017). Aflatoxin B1 Induces Reactive Oxygen Species-Mediated Autophagy and Extracellular Trap Formation in Macrophages. *Frontiers in Cellular and Infection Microbiology*, 7, 53. https://doi.org/10.3389/fcimb.2017.00053

AOAC. (2010). Official method of analysis, 18th edition. Association of Official Analytical Chemists, Washington D.C.

Ayodele, S. O., Oloruntola, O. D., & Agbede, J. O. (2016). Effect of diet containing *Alchornea cordifolia* leaf meal and enzyme supplementation on performance and digestibility of Weaner rabbits. *World Rabbit Science*, 24, 201-206. https://doi.org/10.4995/wrs.2016.3933

Azqueta, A., & Collins, A. (2016). Polyphenols and DNA Damage: A Mixed Blessing. *Nutrients*, 8(12), 785. https://dx.doi.org/10.3390/nu8120785

Benzie, I. F., & Strain, J. J. (1996). The ferric reducing ability of plasma (FRAP) as a measure of "antioxidant power": The FRAP assay. *Analytical Biochemistry*, 239(1), 70-6. https://doi.org/10.1006/abio.1996.0292

Brown, R., Priest, E., Naglik, J. R., & Richardson, J. P. (2021). Fungal Toxins and Host Immune Responses. *Frontier Microbiology*, 12, 643639. https://doi.org/10.3389/fmicb.2021.643639

Burel, S. D., Favrot, M. C., Fremy, J. M., Massimi, C., Prigent, P., Debongnie, L. P., & Morgavi, D. (2009). Review of mycotoxin-detoxifying agents used as feed additives: mode of action, efficacy and feed/food safety. EFSA-Q-pp.2009-00839, EFSA J, Dec 82012; 2012:564367. https://doi.org/10.2903/sp.efsa.2009.EN-22

Cichoski, A.J., Rotta, R.B., Scheuermann, G., Junior, A.C., & Barin, J.S. (2012). Investigation of glutathione peroxidase

activity in chicken meat under different experimental conditions. *Food Science and Technology*, 32(4), 661-667. https://doi.org/10.1590/S0101-20612012005000107

Cortinas, L., Barroeta, A., Villaverde, C., Galobart, J., Guardiola, F., & Baucells, D. (2005). Influence of the dietary polyunsaturation level on chicken meat quality: Lipid oxidation. *Poultry Science*, 84, 48-55. https://doi.org/10.1093/ps/84.1.48

Da Silva, E. O., Bracarense, A. P. F. L., & Oswald, I. P. (2018). Mycotoxins and oxidative stress: Where are we? *World Mycotoxin Journal*, 11, 113–134. https://doi.org/10.3920/WMJ2017.2267

De Ruyck, K., De Boevre, M., Huybrechts, I., & De Saeger, S. (2015). Dietary mycotoxins, co-exposure, and carcinogenesis in humans: Short review. Mutation Research. *Review in Mutatation Research*, 766, 32–41. https://doi.org/10.1016/j.mrrev.2015.07.003

El-Haleem, A., Reda, M., & Mohamed, D. A. (2011). The effects of experimental aflatoxicosis on the pancreas of adult male albino rats and the role of ginger supplementation a histological and biochemical study. *The Egyptian Journal of Histology*, 34(3), 423-435. *https://doi.org/*10.1097/EHX.0000398847.67845.55

Feng, W. H., Xue, K. S., Tang, L., Williams, P. L., & Wang, J. S. (2016). Aflatoxin B_1-Induced Developmental and DNA Damage in *Caenorhabditis elegans*. *Toxins*, 9(1), 9. https://doi.org/10.3390/toxins9010009.

Forni, C., Facchiano, F., Bartoli, M., Pieretti, S., Facchiano, A., D'Arcangelo, D., Norelli, S., Valle, G., Nisini, R., Beninati, S., Tabolacci, C., & Jadeja, R. N. (2019). Beneficial Role of Phytochemicals on Oxidative Stress and Age-Related Diseases. *BioMed Research International*, 2019, 8748253. https://doi.org/10.1155/2019/8748253

Fouad, A. M., Ruan, D., El-Senousey, H. K., Chen, W., Jiang, S., & Zheng, C. (2019). Harmful Effects and Control Strategies of Aflatoxin B_1 Produced by *Aspergillus flavus* and *Aspergillus parasiticus* Strains on Poultry: Review. *Toxins*, 11(3), 176. https://doi.org/10.3390/toxins11030176

Freitas, A. P., Santos, C. R., Sarcinelli, P. N., Silva Filho, M. V., Hauser-Davis, R. A., & Lopes, R. M. (2016). Evaluation of a Brain Acetylcholinesterase Extraction Method and Kinetic Constants after Methyl-Paraoxon Inhibition in Three Brazilian Fish Species. *PloS One*, 11(9), e0163317. https://doi.org/10.1371/journal.pone.0163317

Gautam, R., & Jachak, S. M. (2009). Recent developments in anti-inflammatory natural products. *Medicinal Research Reviews*, 29(5), 767–820. 10.1002/med.20156.

Guengerich, F. P., Johnson, W. W., Shimada, T., Ueng, Y. F., Yamazaki, H., & Langouet, S. (1998). Activation and detoxication of Aflatoxin B1. *Mutatation Research*, 402:121–128. https://doi/10.1016/S0027-5107(97)00289-3

Gugliandolo, E., Peritore, A. F., D'Amico, R., Licata, P., & Crupi, R. (2020). Evaluation of Neuroprotective Effects of Quercetin against Aflatoxin B1-Intoxicated Mice. *Animals: An Open Access Journal from MDPI*, 10(5), 898. https://doi.org/10.3390/ani10050898

Guo, C., Li, X., Wang, R., Yu J., Ye, M., Mao, L., Zhang, S., & Zheng, S. (2016). Association between Oxidative DNA Damage and Risk of Colorectal Cancer: Sensitive Determination of Urinary 8-Hydroxy-2'-deoxyguanosine by UPLC-MS/MS Analysis. *Scientific Reports*, 6, 32581 (2016). https://doi.org/10.1038/srep32581

Hashemi, S. R., & Davoodi, H. (2010). Phytogenics as new class of feed additive in poultry industry. *Journal of Animal and Veterinary Advances*, 9, 2295–2304.

Houndonougbo, M. F., Chwalibog, A., & Chrysostome, C. A. A. M. (2012). Effect of processing on feed quality and bio-economic performances of broiler chickens in Benin. *International Journal of Applied Poultry Research*, 1(2), 47–54.

Huang, B., Chen, Q., Wang, L., Gao, X., Zhu, W., Mu, P., & Deng, Y. (2020). Aflatoxin B1 Induces Neurotoxicity through Reactive Oxygen Species Generation, DNA Damage, Apoptosis, and S-Phase Cell Cycle Arrest. *International Journal of Molecular Sciences*, 21(18), 6517. https://doi.org/10.3390/ijms21186517

Iqbal, S. Z., Jinap, S., Pirouz, A. A., & Faizal, A. A. (2015). Aflatoxin M1 in milk and dairy products, occurrence and recent challenges: A review. *Trends in Food Science & Technology*, *46*(1), 110-119. https://doi.org/10.1016/j.tifs.2015.08.005

Juan, C., Ritieni, A., and Mañes, J. (2012). Determination of trichothecenes and zearalenones in grain cereal, flour and bread by liquid chromatography tandem mass spectrometry. *Food Chemistry*, 134, 2389–2397. https://doi.org/10.1016/j.foodchem.2012.04.051

Keppler, J. K., Schwarz, K., & van der Goot, A. J. (2020). Covalent modification of food proteins by plant-based ingredients (polyphenols and organosulphur compounds): A commonplace reaction with novel utilization potential. *Trends in Food Science and Technology*, 101 (2020), 38-49. https://doi.org/10.1016/j.tifs.2020.04.023

Khan, R. A., Khan, M. R., & Sahreen, S. (2012). Brain antioxidant markers, cognitive performance and acetylcholinesterase activity of rats: efficiency of Sonchus asper. *Behavioral and Brain Functions*, 8, 21. https://doi.org/10.1186/1744-9081-8-21

Kpomasse, C. C., Oke, O. E., Houndonougbo, F. M., & Tona, K. (2021). Broiler production challenges in the tropics: A review. *Veterinary Medicine and Science*, 7(3), 831–842. https://doi.org/10.1002/vms3.435

Kraft, S., Buchenauer, L., & Polte, T. (2021). Mold, Mycotoxins and a Dysregulated Immune System: A Combination of Concern. *International Journal of Molecular Sciences*, 22(22), 12269. https://doi.org/10.3390/ijms222212269

Kumar, G. P., & Khanum, F. (2012). Neuroprotective potential of phytochemicals. *Pharmacognosy Reviews,* 6(12), 81–90. https://doi.org/10.4103/0973-7847.99898

Lee, M. T., Lin, W. C., Yu, B., & Lee, T. T. (2017). Antioxidant capacity of phytochemicals and their potential effects on oxidative status in animals - A review. *Asian-Australasian Journal of Animal Sciences*, 30(3), 299–308. https://doi.org/10.5713/ajas.16.0438

Li, H., Guan, K., Zuo, Z., Wang, F., Peng, X., Fang, J., Cui, H., Zhou, Y., Ouyang, P., Su, G., & Chen, Z. (2019). Effects of aflatoxin B1 on the cell cycle distribution of splenocytes in chickens. *Journal of Toxicologic Pathology*, 32(1), 27–36. https://doi.org/10.1293/tox.2018-0015

Mahato, D. K., Lee, K. E., Kamle, M., Devi, S., Dewangan, K. N., Kumar, P., & Kang, S.G. (2019). Aflatoxins in Food and

Feed: An Overview on Prevalence, Detection and Control Strategies. *Frontier in Microbiology*, 10, 2266. https://doi.org/10.3389/fmicb.2019.02266

Maheshwari, S., Kumar, V., Bhadauria, G., & Mishra, A. (2022). Immunomodulatory potential of phytochemicals and other bioactive compounds of fruits: A review. *Food Frontiers*. 3 (2), 221-238. https://doi.org/10.1002/fft2.129

Mahoney, N., & Molyneux, R. J. (2004). Phytochemical Inhibition of Aflatoxigenicity in Aspergillus flavus by Constituents of Walnut (*Juglans regia*). *Journal of Agricultural and Food Chemistry*, 52 (7), 1882–1889. https://doi.org/10.1021/jf030812p

Min, B., Nam, K. C., Cordray, J., & Ahn, D. U. (2008). Endogenous factors affecting oxidative stability of beef loin, pork loin, and chicken breast and thigh meats. *Journal of Food Science*, 73, 439–446. https://doi.org/10.1111/j.1750-3841.2008.00805.x

Mohammed, A. M. & Metwally, N. S. (2009). Antiaflatoxicogenic activities of some aqeous plant extracts against AFB1 induced Renal and Cardiac damage. *Journal of Pharmacology and Toxicology,* 4 (1), 1-16. https://doi.org/10.3923/jpt.2009.1.16

Muhlisin, M., Utama, D.T., Lee, J.H., Choi, J.H., & Lee, S.K. (2016). Antioxidant enzyme activity, iron content and lipid oxidation of raw cooked meat of Korean native chickens and other poultry. *Asian-Australasian Journal of Animal Sciences*, 29(5), 695–701. https://doi.org/10.5713/ajas.15.0256

Nazarizadeh, H., Mohammad Hosseini, S., & Pourreza, J. (2019). 'Effect of plant extracts derived from thyme and chamomile on the growth performance, gut morphology and immune system of broilers fed aflatoxin B1 and ochratoxin A contaminated diets', *Italian Journal of Animal Science*, 18, 1073-1081. https://doi.org/10.1080/1828051X.2019.1615851

Nordberg, J., & Arnér, E. S. J. (2001). Reactive oxygen species, antioxidants, and the mammalian thioredoxin system. *Free Radical Biology and Medicine*, 31(11), 1287–1312. https://doi.org/10.1016/S0891-5849(01)00724-9

Olarotimi, O. J., Gbore, F. A., Adu, O. A., Oloruntola, O. D., & Falowo, A. B. (2022). Effects of ginger meal supplementation on performance and meat antioxidative enzymes of broilers fed monosodium glutamate. *Acta Fytotechn Zootechn*, 25, *2022*(3), 174–184. https://doi.org/10.15414/afz.2022.25.03.174-184

Oloruntola, O. D. (2022a). *Juglans regia* kernel meal; A prospective nutraceutical feed supplement. *Biotech Studies*, 31(2), 87-94. https://doi.org/10.38042/biotechstudies.1222785

Oloruntola, O. D. (2022b). Utilization of processed kola nut husk meal in poultry: Effects on the performance, carcass, biochemical indicators and antioxidant enzymes of broiler chickens. *Waste and Biomass Valorization*, 13(3). https://doi.org/10.1007/s12649-022-01730-z

Oloruntola, O. D., Ayodele, S. O., Adeyeye, S. A., Fasuhami, O. S., Osowe C. O., & Ganiyu, T. O. (2022a). Proximate composition, phytochemical profile, antioxidant, antidiabetic and anti-inflammatory properties of *Justicia carnea* leaf powder. *Black Sea Journal of Agriculture*, 5(4), 415-423. https://doi.org/10.47115/bsagriculture.1145262

Oloruntola, O. D., Ayodele, S. O., Agbede, J. O., Oloruntola, D..A., Ogunsipe, M. H., & Omoniyi, I. S. (2016). Effect of *Alchornea cordifolia* leaf meal and enzyme supplementation on growth, haematological, immunostimulatory and serum biochemical response of rabbits. *Asian Journal of Biological and Life Sciences*, 5(2), 190-195.

Oloruntola, O. D., Ayodele, S. O., Omoniyi, I. S., Adeyeye, S. A., & Adegbeye, M. J. (2022b). The effect of dietary supplementation of Mucuna leaf meal on the growth performance, blood parameters, and carcass quality of broilers. *Acta Scientiarum*, V44, e55362. https://doi.org/10.4025/actascianimsci.v44i1.55362

Oloruntola, O. D., Agbede, J. O., Onibi, G. E., Igbasan, F. A., Ayodele, S. O. Arogunjo, M. A & Ogunjo, S. T (2018). Rabbits fed fermented cassava starch residue I: Effect on performance and health status. *Archivos de Zootecnia*, *67*(260), 578-586.

Osowe, C. O., Adu, O. A., Oloruntola, O. D., Chineke, C. A., Atansuyi, A. J. & Olateju, I. S. (2022). The impact of breed, *Ficus exasperata* leaf powder and vitamin C on carcass traits, brain and meat oxidative enzymes of broiler chickens raised under the tropical condition. *Tropical Animal Health and Production*, *54*(6), 404. https://doi.org/10.1007/s11250-022-03386-2

Pankaj, S. K., Shi, H., & Keener, K. M. (2018). A review of novel physical and chemical decontamination technologies for aflatoxin in food. *Trends Food Science and Technology*, 71, 73–83. https://doi.org/10.1016/j.tifs.2017.11.007

Perez-Gregorio, R., & Simal-Gandara, J. (2017). A critical review of bioactive food components, and of their functional mechanisms, biological effects and health outcomes. *Current Pharmaceutical Design*, *23*(19), 2731–41. https://doi.org/10.2174/1381612823666170317122913

Pitt, J. I., & Miller, J. D. (2017). A concise history of mycotoxin research. *Journal of Agriculture and Food Chemistry*, 65, 7021–7033. https://doi.org/10.1021/acs.jafc.6b04494

Ponte, P. I. P., Mendes, I., Quaresma, M., Aguiar, M. N. M., Lemos, J. P. C., Ferreira, L. M. A., Soares, M. A. C., Alfaia, C. M., Prates, J. A. M., & Fontes, C. M. G. A. (2004). Cholesterol Levels and Sensory Characteristics of Meat from Broilers Consuming Moderate to High Levels of Alfalfa. *Poultry Science,* 83, 810–814. https://doi.org/10.1093/ps/83.5.810

Pueyo, I. U., & Calvo, M. I. (2009). Phytochemical Study and Evaluation of Antioxidant, Neuroprotective and Acetylcholinesterase Inhibitor Activities of *Galeopsis ladanum* L. extracts. *Pharmacognosy Magazine*, 5, 287–290. https://dx.doi.org/10.4103/0973-1296.58146

Sadeghi, A., Ghahari, L., & Yousefpour, M. (2019). Vitamin E Supplementation Reduces Oxidative Stress in the Male Wistar Rats' Brain Against Polyvinyl Chloride Products. *Annals of Military and Health Sciences Research*, 17(2):e92768. https://doi.org/10.5812/amh.92768

Saleh, H. A., Yousef, M. H., & Abdelnaser, A. (2021). The Anti-Inflammatory Properties of Phytochemicals and Their Effects on Epigenetic Mechanisms Involved in TLR4/NF-κB-Mediated Inflammation. *Frontiers in Immunology*, 12, 606069. https://doi.org/10.3389/fimmu.2021.606069

Sarma, U. P., Bhetaria, P. J., Devi, P., & Varma, A. (2017). Aflatoxins: Implications on Health. *Indian Journal of Clinical Biochemistry*, 32(2), 124–133. https://doi.org/10.1007/s12291-017-0649-2

Silva, Filho, M. V., Oliveira, M. M., Salles, J. B., Bastos, V. L., Cassano, V. P., & Bastos, J. C. (2004). Methyl-paraoxon comparative inhibition kinetics for acetylcholinesterases from brain of neotropical fishes. *Toxicology Letters*, 153(2), 247–254. https://doi.org/10.1016/j.toxlet.2004.04.026

Smet, K., Raes, K., Huyghebaert, G., Haak, L., Arnouts, S., & De Smet, S. (2008). Lipid and Protein Oxidation of Broiler Meat as Influenced by Dietary Natural Antioxidant Supplementation, *Poultry Science*, 87 (8), 1682-1688. https://doi.org/10.3382/ps.2007-00384

Soltani, D. M., Shahryar H.A., Hosseini, S. A., Ebrahimnezhad, Y., & Aghashahi, A. (2019). Effects of dietary inclusion of commercial toxin binders and prebiotics on performance and immune responses of broiler chicks fed aflatoxin-contaminated diets. *South African Journal of Animal Science*, 49(2), 322-331. https://dx.doi.org/10.4314/sajas.v49i2.12

Souza, M. A. A., Visentainer, J. V., Carcalho, R. H., Garcia, F., Ida, E. I & Shimokomaki, M. (2013). Lipid and protein oxidation in charqui meat and jerked beef. *Brazilian Archives of Biology and Technology*, 56(1), 107-112. https://doi.org/10.1590/S1516-89132013000100014

Sur, E. & Celik, I. (2003). Effect of aflatoxin B1 on the development of the bursa of Fabricius and blood lymphocyte acid phosphatase of the chicken. *British Poultry Science*, 44, 558-566. https://doi.org/10.1080/00071660310001618352

Tallentire, C. W., Leinonen, I., & Kyriazakis, I. (2016). Breeding for efficiency in the broiler chicken: A review. *Agronomy for Sustainable Development*, 36, 66. https://doi.org/10.1007/s13593-016-0398-2

Thinh, N. H., Vinh, N. T., Linh, N. V., Giang, N. T. P., Doan, B. H., & Dang, P. K. (2018). Effect of dietary supplementation with green tea powder on performance characteristic, meat organoleptic quality and cholesterol content of broilers. *Livestock Research for Rural Development*, *30*(9). http://www.lrrd.org/lrrd30/9/nhti30160.html

Tokur, B., Korkmaz, K., & Ayas, D. (2006). Comparison of two Thiobarbituric Acid (TBA) Method for monitoring lipid oxidation in fish. *EU Journal of Fisheries and Aquatic Science*, 23(3 4), 331–334.

Towner, R. A., Qian, S. Y., Kadiiska, M. B., & Mason, R. P. (2003). In vivo identification of aflatoxin-induced free radicals in rat bile. *Free Radical Biology and Medicine,* 35, 1330–1340. https://doi.org/10.1016/j.freeradbiomed.2003.08.002

Udomkun, P., Wiredu, A. N., Nagle, M., Müller, J., Vanlauwe, B., & Bandyopadhyay, R. (2017). Innovative technologies to manage aflatoxins in foods and feeds and the profitability of application–A review. *Food Control*, 76, 127–138. https://doi.org/10.1016/j.foodcont.2017.01.008

Uijttenboogaart, T.G., (1999). European perspective on poultry slaughter technology. *Poultry Science*, 78, 295-297. https://doi.org/10.1093/ps/78.2.295

Valavanidis, A., Vlachogianni, T., & Fiotakis, C. (2009). 8-hydroxy-2' -deoxyguanosine (8-OHdG): A critical biomarker of oxidative stress and carcinogenesis. Journal of environmental science and health. Part C. *Environmental Carcinogenesis and Ecotoxicology Reviews*, 27(2), 120–139. https://doi.org/10.1080/10590500902885684

Valenzuela-Grijalva, N. V., Pinelli-Saavedra, A., Muhlia-Almazan, A., Domínguez-Díaz, D., & González-Ríos, H. (2017). Dietary inclusion effects of phytochemicals as growth promoters in animal production. *Journal of Animal Science and Technology*, 59, 8. https://doi.org/10.1186/s40781-017-0133-9

Ye, Y., Ma, Y., Kong, M., Wang, Z., Sun, K., & Li, F. (2023). Effects of Dietary Phytochemicals on DNA Damage in Cancer Cells. *Nutrition and Cancer*, 75(3), 761–775. https://doi.org/10.1080/01635581.2022.2157024

Zhang, C., Nestorova, G., Rissman R. A., & Feng, J. (2013).Detection and quantification of 8-hydroxy-2'-deoxyguanosine in Alzheimer's transgenic mouse urine using capillary electrophoresis. *Electrophoresis*, 34(15), 2268-74. https://doi.org/10.1002/elps.201300036

Zhen, Y., & Zhang H. (2019). NLRP3 Inflammasome and Inflammatory Bowel Disease. *Frontiers in Immunology*, 10, 276. https://doi.org/10.3389/fimmu.2019.00276

Biotech Studies 33(1), 43-51
http://doi.org/10.38042/biotechstudies.1442102

BIOTECH STUDIES

RESEARCH PAPER

Response surface methodology-based optimization studies about bioethanol production by *Candida boidinii* from pumpkin residues

Ekin Demiray[1]*, Sevgi Ertuğrul Karatay[2], Gönül Dönmez[2]

[1]Medical Laboratory Techniques Department, Vocational Health School, Ankara Yıldırım Beyazıt University, 06760, Çubuk, Ankara, Türkiye
[2]Biology Department, Science Faculty, Ankara University, 06100, Beşevler, Ankara, Türkiye

How to cite:
Demiray, E., Karatay, S. E., & Dönmez, G. (2024). Response surface methodology-based optimization studies about bioethanol production by *Candida boidinii* from pumpkin residues. *Biotech Studies*, *33*(*1*),43-51. http://doi.org/10.38042/biotechstudies.1442102

Article History
Received 23 April 2023
Accepted 15 January 2024
First Online 08 February 2024

Corresponding Author
Tel.: +90 312 906 18 74
E-mail: edemiray@ankara.edu.tr

Keywords
Candida boidinii
Saccharomyces cerevisiae
Pumpkin residues
Bioethanol
Response surface
Methodology

Abstract

For sustainable bioethanol production, the investigation of novel fermentative microorganisms and feedstocks is crucial. In this context, the goals of the current study are suggesting pumpkin residues as new raw material for bioethanol production and investigating the fermentative capacity of the *Candida boidinii*, which is a newly isolated yeast from sugar factory wastes. Response surface methodology was used to determine the effect of enzyme (cellulase and hemicellulase) concentration and enzymatic hydrolysis time. The maximum bioethanol concentration was 29.19 g/L when fermentation parameters were optimized. However, it is revealed that enzymatic hydrolysis and hydrolysis duration (48-72 h) have significant effects on reducing sugar concentration. The highest reducing sugar was 108.86 g/L when the 20% initial pumpkin residue was hydrolyzed at 37.5 FPU/g substrate cellulase and 37.5 U/mL hemicellulase at the end of 72 h. Under these optimized conditions, the bioethanol production of *C. boidinii* increased by 22.91% and reached 35.88 g/L. This study shows pumpkin residues are promising feedstocks and *C. boidinii* is a suitable microorganism for efficient bioethanol production.

Introduction

Biofuels are sustainable, eco-friendly, and cheap alternatives to fossil fuels. Among them, bioethanol attracts attention because of its renewable and eco-friendly features (Nowicka et al., 2020). Furthermore, another usage area of bioethanol is the production of hand sanitizers or disinfectants which are very useful agents against pathogen microorganisms. Moreover, the COVID-19 outbreak caused a massive demand for alcohol-based disinfectants and ethanol shortage (Itiki & Chowdhury, 2020). For this reason, ethanol prices increased and ethanol production gained importance for public health. Therefore, the studies about bioethanol production gained importance in the literature (Mahlia et al., 2019; Palupi et al., 2020; Song et al., 2020).

Bioethanol is derived from biomass and this substance can be classified into different generations according to the type of raw materials used. The first-generation bioethanol is produced by sugar-containing feedstocks such as starch, maize, wheat, sugarcane, or sugar beet. Raw materials from the first generation have high productivity rates; however, they have a negative impact on food prices. On the other hand, the source of the second-generation bioethanol is lignocellulosic

feedstock which is one of the most abundant and cheap materials on earth (Adıgüzel, 2013). Third-generation bioethanol is obtained from photosynthetic microorganisms and genetically modified microorganisms are used for fourth-generation ethanol production.

Lignocellulose is the most abundant and under-utilized feedstock on Earth. Thus, it does not compete with edible sources for energy production and, does not affect the food production chain (Kumar et al., 2016; Naik et al., 2010). However, lignocellulosic bioethanol production is still problematic because of the recalcitrance of the raw materials (Paul & Dutta, 2018). Moreover, by-products that are generated from the pre-treatment of lignocellulose can reduce the activity of the enzymes or inhibit microbial growth (Aytaş et al., 2023). Therefore, the determination of the efficient bioethanol producer organisms or available feedstocks can contribute to more effective bioethanol production processes.

Efficient ethanol production from all sugars present in lignocellulosic raw material is crucial for more economical bioethanol production. Xylose is the second most abundant fermentable sugar in lignocellulose after glucose. Therefore, the utilization of xylose is of great importance for efficient fermentation. However, commercially available yeasts such as *Saccharomyces cerevisiae* cannot ferment xylose into ethanol (Zhao et al. 2016). For these reasons, it is vital to identify novel yeast strains which are able to ferment a broad range of sugars into ethanol. In this context, *C. boidinii* can be a good alternative to conventional ethanol producers such as *S. cerevisiae* because of its high acid tolerance and broad range of sugar utilization capacity (Osawa et al., 2009; Santana et al., 2018). However, despite its potential, studies on the bioethanol production from *C. boidiini* in the literature are very limited. For these reasons, in the current study, the bioethanol production of *C. boidinii* was compared to that of *S. cerevisiae* that is the most commonly used ethanol-producing microorganism for bioethanol production.

Investigation of food by-products which contain lignocellulosic biomass is an important step for environmental protection and bioethanol production (Schieber et al., 2001). Pumpkin residues (PR) are rich in carbohydrate, β-carotene, as well as cellulose and hemicelluose. For these reasons, the main objective of the current study is the evaluation of PR as a raw material for bioethanol production.

Response Surface Methodology (RSM), one of the statistical methods, is useful for making predictions that are more accurate and require less experimental datasets. When conventional methods are unable to identify the combined impacts of all the variables, the method also enables researchers to examine how different variables interact (Yolmeh & Jafari, 2017; Pereira et al., 2021). Due to its advantages, RSM is commonly used in lignocellulosic pre-treatment and bioethanol production research (Chen et al., 2020; Manmai et al., 2021). Therefore, we used the same trend and used RSM in the current study (Yolmeh & Jafari, 2017; Pereira et al., 2021). Due to its advantages, RSM is commonly used in lignocellulosic pre-treatment and bioethanol production research (Chen et al., 2020; Manmai et al., 2021). Therefore, we used the same trend and used RSM in the current study (Yolmeh & Jafari, 2017; Pereira et al; 2021). For the mentioned reasons, during lignocellulosic pre-treatment and bioethanol production studies RSM is widely applied (Chen et al, 2020; Manmai et al. 2021). Because of the mentioned reasons RSM was used for bioethanol production optimization in the current study.

In the first part of the study, bioethanol production, glucose and xylose assimilation capacities of the different yeasts were tested. After that step, fermentation conditions were optimized by RSM. During the experiments, enzymatic hydrolysis rate were increased with optimization and bioethanol production of the yeasts were monitored. According to the results, the novel isolate of *C. boidinii* produced more bioethanol than model microorganism *S. cerevisiae.* This isolate was also able to assimilate xylose as well as glucose. To the best of our knowledge, this is the first report about bioethanol production from pumpkin residues used by *C. boidinii*.

Materials and Methods

Isolation, PCR and sequencing of yeast cells

The samples were collected from sugar factory waste and were used for isolation studies. These samples were centrifuged and spread (0.1 mL) on Petri plates containing Potato Dextrose Agar (PDA/Merck-Germany) media. PDA media was supplemented with 600.000 IU penicillin, and were incubated at 30 °C. Cells from microcolonies on these plates were isolated and purified by streaking the cells repeatedly on the PDA plates. The pure cultures were kept at +4 °C and were transferred to fresh PDA media periodically. Purified colonies were screened for their bioethanol production capacities. The cell that showed the most promising ethanol production capacity was identified. Sugar beet molasses medium was used for screening. For this purpose, 300 g/L sugar beet molasses was pre-treated with 1.5% H_2SO_4 (Merck-Germany), and autoclaved at 121 °C for 15 minutes (min). This stock medium was diluted to 8% (v/v) with sterile distilled water. pH was adjusted to 5 with 10 N NaOH (Merck-Germany). 1.0 g/L $(NH_4)_2SO_4$ (Merck-Germany) and 0.5 g/L KH_2PO_4 (Merck-Germany) were added to molasses medium and 1 g/L cells were inoculated to molasses medium. Incubation time was set to 30 °C.

ITS regions were amplified with ITS1 and ITS4 primers (Glass & Donaldson, 1995). DNA extraction was carried out with EurX GeneMATRIX Bacterial & Yeast DNA kit (Poland). Thermo Scientific Nanodrop 2000 (Massachusetts/USA) was used for calculations of DNA purity and concentration. PCR was conducted by initial

denaturation at 94 °C for 1 min followed by 40 cycles of denaturation at 95 °C for 45 seconds (s). Annealing was performed at 57 °C for 45 s, and extension was carried out at 72 °C for 60 s. MAGBIO "HighPrep™ PCR Clean-up System" (AC-60005) were used for the PCR product was purification. ABI 3730XL (Applied Biosystems, Foster City, CA) with BigDye Terminator v3.1 Cycle (Applied Biosystems, Foster City, CA) sequencing kit was used for DNA was sequencing. Identification was performed by an external laboratory (Refgen, Ankara, Turkey).

Pre-treatment of PR

PR was collected from the local market in Ankara/Turkey. These PR were dried in an oven overnight at 70 °C (Nuve/Turkey), and the dried residues were grounded in laboratory type mill with a 0.1 cm mesh size screen, and kept in a screw cap bottle until used in the experiments.

1% H_2SO_4 (Merck-Germany) was used for pre-treatment experiments. PR was autoclaved in 121 °C (ALP/CL-40M/Germany) for 15 min immediately after acid pre-treatment. For the fermentation assays, this slurry was filtered through Whatman No.1 paper and used for fermentation experiments.

Enzymatic hydrolysis

Commercial cellulase CelliCTec2 (d: 1.15 g/mL, 121 FPU/mL, Sigma-Aldrich) and hemicellulase from *Aspergillus niger* (0.3-3.0 U/ mg solid, Sigma-Aldrich) were used for enzymatic hydrolysis. Cellulase concentration was adjusted to 15 FPU/g cellulose and hemicellulase loading was set to 15 U/mL. Enzymatic hydrolysis was carried out at 50 °C and pH 4.8 in the presence of 50 mM citrate buffer for 72 hours (h). Agitation speed was adjusted to 100 rpm (Chen et al., 2012).

Response surface methodology

To evaluate the effects of independent variables on the bioethanol production of the new isolate, The Design Expert Software program (StatEase®) was used for RSM (6 center points, 20 total run) was used. Total 20 runs were generated for RSM. Cellulase loading (15-60 FPU/g cellulose), hemicellulase loading (15-60 U/mL), and enzymatic hydrolysis time (24-72 h) were selected as independent factors for RSM experiments. 1% H_2SO_4 (v/v) pre-treatment was performed for all RSM experiments because of its low cost and effectiveness (Loow et al. 2016).

Fermentation experiments

The fermentation experiments were performed at 100 mL Erlenmeyer flasks with a working volume of 50 mL PR media. Incubation temperature was set to 30 °C for 96 h at 100 rpm agitation speed. PR media was supplemented with peptone (Merck-Germany/0.5 g/L), yeast extract ((Merck-Germany/3.0 g/L), $MgSO_4.7H_2O$ (Merck-Germany/0.5 g/L), KH_2PO_4 (Merck-Germany/1.0 g/L), $CaCl_2$ (Merck-Germany/0.1 g/L), and $ZnSO_4$ (Merck-Germany/0.05 g/L).

Analytical methods

Ethanol content was measured with gas chromatography (GC), (GC2010/Shimadzu/Japan). Before GC analysis, 1.5 mL of samples were centrifuged at 10000 rpm for 10 min (Hettich/320R/Germany). The supernatant was filtered through 0.22 µm membrane filter, and 1 µL of sample was injected through the SPL unit. The Restek Rtx-Wax column (60 m length, 0.25 mm ID.) and flame ionization detector (FID) were used for ethanol detection. The temperature of the injection port, and detector were set at 140 ºC and 160 ºC, respectively. The initial column temperature was 50 ºC, and the column temperature was increased to 150 ºC within 19 min. Column flow was 1.86 mL/min, and nitrogen was used as a carrier gas (Wistara et al., 2016).

The HPLC (Shimadzu/Japan) system with Coregel 87H3 (Transgenomic/USA) column and refractive index detector (RID10A) were used for the detection of the sugars, 5-hydroxymethylfurfural (HMF), acetic acid and formic acid present in PR. Before the analysis, 1.5 mL of samples were centrifuged at 10000 rpm for 10 min. The supernatant was filtered through 0.22 µM membrane filter. The column oven temperature was held at 70 ºC, and the total flow was set at 0.5 mL/min. 5 mM H_2SO_4 was used as a mobile phase. Samples were analysed for 25 min (Motoda et al., 2019).

Total reducing sugar was determined by the DNS method (Miller, 1959). Filter paperase unit (FPU) of the enzyme was determined according to Adney and Baker (2008). Theoretical ethanol yields were calculated according to Eq. (1) which was presented below (Kim & Lee, 2007).

Eq.(1):

$$Theoretical\ ethanol\ yield\ (\%) = \frac{ethanol\ (gL^{-1})}{initial\ sugar\ (gL^{-1}) \times 0.511} \times 100$$

Volumetric ethanol productivity (Qp) was calculated according to Eq. (2), as described as describe in the research published by (Roca & Olsson, 2003).

Eq. (2):

$$Q_p(g/Lh) = \frac{ethanol\ (gL^{-1})}{h_{\text{maximum}\ ethanol}}$$

Ethanol yields ($Y_{P/S}$) were determined according to Eq. (3) (Günan Yücel & Aksu, 2015):

Eq. (3):

$$Y_{P/S}\ (g/g) = \frac{maximum\ ethanol\ (gL^{-1})}{consumed\ sugar\ (gL^{-1})}$$

The cellulose concentration of raw PR was determined according to the standard ISO protocol (ISO 5498-1981). Cellulose determination was performed by an external laboratory, namely Düzen Norwest/Ankara.

Results and Discussion

Identification of yeast and effect of biomass loading and inhibitory compounds on bioethanol production

Table 1. Effect of increased PR loading on reducing sugar, inhibitory compounds and ethanol concentrations of *C. boidinii* and *S. cerevisiae* (Pre-treatment conditions: 1% H_2SO_4 at 121 °C for 15 min, pH: 5, fermentation time: 48 h)

		Biomass loading (%, w/v)		
		10%	**20%**	**30%**
Reducing sugar (g/L)		43.65±4.67	59.80±4.21	78.32±0.64
Acetic acid (g/L)		0.37±0.07	0.47±0.04	0.81±0.13
Formic acid (g/L)		0.14±0.00	0.20±0.01	0.38±0.06
HMF (g/L)		0.027±0.002	0.063±0.01	0.10±0.03
Ethanol (g/L)	***C. boidinii***	8.55±0.32	21.00±1.31	26.57±3.06
	S. cerevisiae	8.17±0.4	20.67±1.32	24.58±1.00

For sustainability, it is crucial to find and identify novel bioethanol-producer microorganisms which can grow in lignocellulosic feedstocks. In this context, the isolation stage has vital importance. Therefore, the yeast which showed the highest growth in PR medium was selected and sequenced for identification.

Morphologically, yeast that used in the current study are approximately 0.05 mm, smooth, and form white colonies. Density of the cell is opaque and form of the colonies is circular. Microscopically, the cell shape was ellipsoidal budding. Whole cells from the exponentially growing culture of the isolate were used for internal transcribed spacers (ITS's). According to the sequencing results, the isolate showed 100% similarity with one *C. boidinii* strain (ON409985.1) and has more than 98% similarity with many other *C. boidinii* strains, such as UCDFST:09-399, CBS:6202 or CBS7299.

Initial biomass loading is an important parameter for the fermentation process. Moreover, higher initial biomass loadings are desirable since they result in higher sugar yields and lower production costs (Dutra et al., 2018). For these reasons, three different initial biomass loadings (10%, 20%, and 30% w/v) were tested in order to determine their effects on reducing sugar and ethanol concentrations. Results are presented in Table 1. It was observed that increased biomass loading caused higher sugar concentrations. The maximum sugar concentration was obtained from a 30% initial biomass loading at 78.32 g/L. On the other hand, 43.65 g/L and 59.80 g/L reducing sugar were found in 10% and 20% initial biomass loadings, respectively. These values are similar to those reported by Mithra and Padmaja (2017a), who obtained 40.56 g/L reducing sugar from 15% pumpkin peel when the biomass was pre-treated with 1% H_2SO_4 at 121 °C for 60 min.

During the experiments conducted with initial biomass loading, the ethanol concentrations of *C. boidinii* and *S. cerevisiae* were determined. Similar to reducing sugar concentrations, increased initial biomass loading resulted in increased ethanol production in both tested yeasts. There was no significant difference between the ethanol production of yeasts which are 21.00 g/L and 20.67 g/L respectively, at the end of 48 h fermentation time. Furthermore, ethanol concentration of *C. boidinii* increased to 26.57 g/L when the 30% initial biomass was used. At the same conditions, 24.58 g/L of ethanol was observed by *S. cerevisiae* (**Table 1**).

According to the results, the ethanol production capacity of *C. boidinii* was slightly higher than obtained from *S. cerevisiae,* which is the primary microorganism for commercial ethanol production. These results clearly indicate that *C. boidinii* is a promising agent for ethanol production. Therefore, *C. boidinii* was selected for further experiments in the current study.

Inhibitory compounds such as HMF, acetic acid, or formic acid have a negative effect on microbial growth and ethanol fermentation (Palmqvist & HahnHägerdal, 2000). For these reasons, inhibitor concentrations of PR were also identified in this part of the study. The results in **Table 1** demonstrate that higher biomass loading caused increasing in inhibitor concentrations. The highest acetic acid, and formic acid concentrations were detected as 0.81 g/L and 0.38 g/L, respectively, in the presence of 30% initial biomass loading. Nevertheless, these inhibitor concentrations are low in comparison with the literature (Parajó et al., 1998). Furthermore, much lower HMF concentrations were detected in comparison with acetic and formic acids. At 10% initial PR loading, 0.027 g/L HMF was obtained, and this value increased to 0.10 g/L when the initial PR loading adjusted to 30%. According to the report of Santana et al. (2018), *C. boidinii* metabolized more than 99% of the HMF present in the hemicellulolytic hydrolysate of non-detoxified cocoa pod husks. By this context, in the current study, mild pre-treatment conditions, low inhibitor concentrations of PR, and inhibitory tolerance of *C. boidinii* may have caused the higher bioethanol concentrations observed even in the presence of high PR loading.

Although the highest sugar and ethanol concentrations were observed in the presence of 30% (w/v) initial PR loading, due to the mass transfer limitations and water holding capacity of PR, further studies were carried out in the presence of 20% (w/v) initial PR loading.

Effects of enzymatic hydrolysis

Before enzymatic hydrolysis, 20% PR was pretreated with 1% H_2SO_4 for 15 min at 121 °C. The data in **Figure 1** depicts that enzymatic hydrolysis of 20% PR loading caused higher sugar concentrations than 30% initial PR loading without enzymatic hydrolysis. 81.58 g/L the reducing sugar was obtained from 20% enzymatically hydrolyzed PR. A previous report in the literature showed that dilute acid pre-treatment and enzymatic hydrolysis of 10% PR resulted in 52.47 g/L reducing sugar (Mithra & Padmaja, 2017b).

In the current study, *C. boidinii* and *S. cerevisiae* produced similar ethanol concentrations from PR. However, the highest ethanol concentration was found to be 29.19 g/L from *C. boidinii* at the end of the 48 h fermentation time. *S. cerevisiae* produced 26.92 g/L ethanol (**Figure 1**). These values are higher than the report of Gonçalves et al. (2013), who used *C. boidinii* UFMG14 and found 12 g/L ethanol at the end of the same fermentation period from the hemicellulosic hydrolysate of macauba presscake. Furthermore, in the current study, after 48 h of fermentation, the ethanol concentrations of *C. boidinii* and *S. cerevisiae* declined to 24.43 g/L and 18.70 g/L, respectively. This decline may be related to assimilating of accumulated ethanol. Similar assimilation patterns were also reported previously from *C. boidinii* (Vandeska et al., 1995) and *Pichia stipitis* (Huang et al., 2009). Moreover, a significant ethanol production difference was observed between two yeasts in the early stages of fermentation. For instance, *C. boidinii* and *S. cerevisiae* produced 8.17 g/L and 21.44 g/L of ethanol in 18 hours and 11.09 g/L and 24.24 g/L of ethanol in 24 hours, respectively (**Figure 1**). This difference can be explained by the Crabtree effect. In Crabtree-positive yeasts such as *S. cerevisiae*, alcoholic fermentation can be initiated when aerobic and sugar-limited cultures are exposed to sugar excess. On the other hand, this instantaneous response is not observed in Crabtree-negative yeasts, such as *C. boidinii* (Osawa et al., 2009). Therefore, prolonged bioethanol production period can be attributed to Crabtree-negative nature of *C. boidinii*.

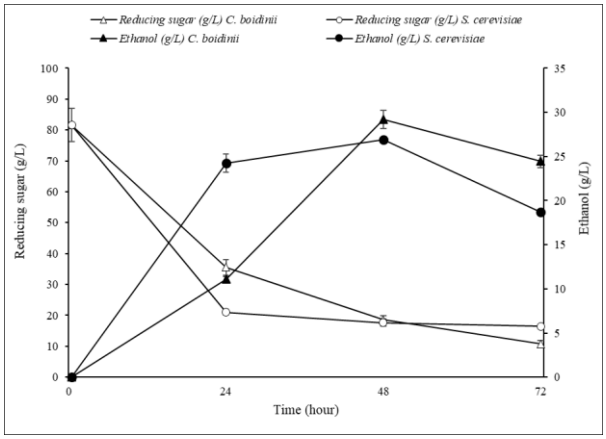

Figure 1. Bioethanol production of *C. boidinii* and *S. cerevisiae* in the presence of dilute acid pre-treated and enzymatically hydrolyzed PR during the fermentation (Pre-treatment conditions: 1% H_2SO_4 at 121 °C for 15 min, pH: 4.8, cellulase loading: 15 FPU/g cellulose, hemicellulase loading: 15 U/mL, initial PR loading: 20% w/v).

Kinetic parameters for bioethanol production belonging to both yeasts were given in **Table 2**, and kinetic parameters of *C. boidinii* were higher than those of *S. cerevisiae*. The highest theoretical ethanol yield from *C. boidinii* was 70.0%. On the other hand, *S. cerevisiae* reached 64.5% of the theoretical ethanol yields. At the end of the 48-hour fermentation period, *C. boidinii* and *S. cerevisiae* generated 0.60 and 0.56 g/L.h. of ethanol, respectively. The respective ethanol yields of these yeasts were 0.46 and 0.42 g/g. These values are higher than when NaOH and ammonia conditioned rice straw was used in the literature (Lin et al., 2012). The reason of higher yields may be the efficient recovery of the xylose after dilute acid pretreatment.

Table 2. Kinetic parameters of *C. boidinii* and *S. cerevisiae* (Pre-treatment conditions: 1% 447 H_2SO_4 at 121 °C for 15 min, pH: 4.8, cellulase loading: 15 FPU/g cellulose, hemicellulase 448 loading: 15 U/mL, fermentation time: 48 h, initial biomass loading: 20% w/v)

	Initial reducing sugar (g/L)	Ethanol (g/L)	Theoretical ethanol yield (%)	Q*p* (g/L.h)	Y*P/S* (g/g)
C. boidinii	81.58±5.44	29.19±0.69	70.0	0.60	0.46
S.cerevisiae		26.92±0.31	64.5	0.56	0.42

Response surface methodology

Descriptive table of the independent variables and response belong to the RSM are shown in **Table 3**. The results of experimental runs with three independent variables (cellulase loading, hemicellulase loading, and hydrolysis time) and response (reducing sugar) are given in **Table 4**. All experiments were performed in triplicate.

A polynomial quadratic equation for the reducing sugar concentration is given in Eq. (4).

Final equation in terms of coded factors:

Eq (4). Reducing sugar (X) (g/L) = $92.78 + 6.46 * A + 3.01 * B + 12.53 * C - 0.6650 * AB + 1.64 * AC + 0.2425 * BC - 5.71 * A^2 - 6.07 * B^2 + 3.30 * C^2$

Where X is the reducing sugar concentration (g/L), A, B, and C are the coded values of cellulase loading (FPU/g cellulose), hemicellulase loading (U/mL), and hydrolysis time (hour), respectively.

Table 3. Types and levels of independent variables and response used in RSM for pre-treatment of pumpkin residues (Initial design: Central composite, Design model: Quadratic)

Response	Factors	Experimental values	
		Lower	Higher
Reducing sugar (g/L)	A-Cellulase loading (FPU/g cellulose)	15	60
	B- Hemicellulase loading (u/mL)	15	60
	C- Hydrolysis time (hour)	24	72

The effect of different parameters on the reducing sugar concentrations of the PR were given in **Figure 2**. In the response surface graphs, the relationship between the variables and the response was investigated. ANOVA for the model showed that the relationship between variables was high with a good R^2 which was obtained as 0.9529. The lack of fit of the model which is a vital criterion measuring the failure of the model for data representation was also found to be not significant (F value: 0.2797). A non-significant lack of fit is positive for the model and sufficient to estimate response in the presence of various variables (Yücel & Göycıncık 2015). Moreover, according to the model, all the criteria tested

Table 4. Experimental responses for reducing sugar concentrations of pumpkin residues using central composite design of RSM (Pre-treatment: 1% H_2SO_4 for 15 min 121 °C, pH: 4.8, initial biomass loading: 20% w/v)

Run No	Factor 1 A: Cellulase FPU/ g cellulose	Factor 2 B: Hemicellulase U/mL	Factor 3 C: Time (hour)	Response 1 Reducing sugar (g/L)	Predicted Reducing sugar(g/L)
1	60	37.5	48	92.50	93.52
2	15	37.5	48	83.25	80.61
3	37.5	37.5	48	93.89	92.78
4	37.5	60	48	92.56	89.72
5	37.5	37.5	48	91.46	92.78
6	37.5	37.5	48	89.53	92.78
7	60	15	24	75.51	74.48
8	15	60	72	91.21	92.64
9	37.5	37.5	48	90.10	92.78
10	37.5	37.5	72	108.86	108.60
11	60	60	24	77.9	78.69
12	37.5	37.5	48	88.19	92.78
13	60	15	72	102.82	102.33
14	37.5	37.5	24	84.91	83.55
15	60	60	72	107.8	107.51
16	37.5	37.5	48	100.24	92.78
17	37.5	15	48	82.48	83.69
18	15	60	24	69.49	70.39
19	15	15	72	85.19	84.80
20	15	15	24	62.82	63.52

were found as significant ($p<0.0001$). Furthermore, hydrolysis time was observed as the most significant parameter ($p<0.0001$) was followed by cellulase loading (p: 0.0002) and hemicellulase loading (p: 0.0214). In **Figure 2a**, 35-40 FPU/g cellulose and 35-40 U/mL enzyme loading were observed as sufficient for the sugar released from PR. Reducing sugar amounts did not change dramatically above those enzyme concentrations. This situation depicts the enzyme substrate interaction reached its saturation point (Kim et al. 2008).

On the other hand, hydrolysis time showed the greatest impact on the sugar concentrations, and it was observed that longer hydrolysis time resulted in higher sugar concentrations for both enzymes (**Figure 2b and 2c**). Similarly, Gul et al. (2018) showed that longer hydrolysis time caused higher saccharification efficiency from Kallar grass. Furthermore, Kshirsagar et al. (2015) found the optimal conditions for reducing sugar yield from rice straw as 40 FPU/g enzyme and 17.50% biomass loading for 72 h when the researchers used RSM for the experiments.

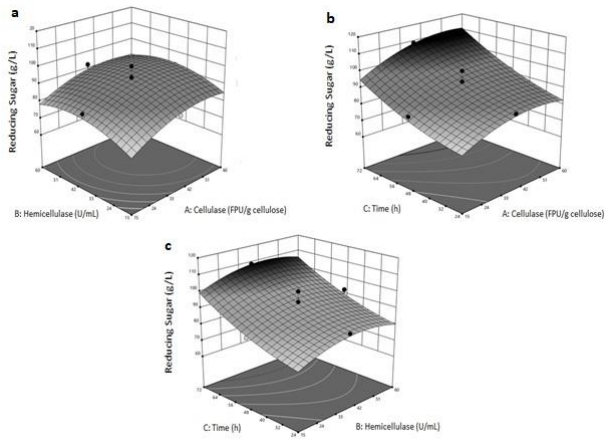

Figure 2. Effect of cellulase, hemicellulase and hydrolysis time on reducing sugar concentrations of PR (initial biomass loading: 20% (w/v), pH: 4.8, Pre-treatment: 1% H_2SO_4 for 15 min 121 °C).

According to the RSM results, the highest reducing sugar concentration was obtained as 108.86 g/L when PR was hydrolyzed with 37.5 FPU/g cellulase, and 37.5 U/mL hemicellulase for 72 h. On the other hand, increased enzyme loading did not cause higher sugar concentrations, and 107.8 g/L reducing sugar was found when the RS was hydrolyzed with 60 FPU/g cellulase, and 60 U/mL hemicellulase for 72 h. Theoretically, increased enzyme loading and extended incubation periods result in higher sugar concentrations. However, the relationship between enzyme loading and sugar concentration may not be linear under all conditions. Loss of the catalytic activity due to the product inhibition, high viscosity and osmolarity or the feedback mechanism may prevent the higher sugar concentrations from increased enzyme loading. Similarly, sugar decreasing trends with the increased enzyme loadings were also reported from sugarcane tops (Sindhu et al., 2014) or *Paspalum scrobiculatum* bran residues (Balakrishnan et al., 2018). The results can also be comparable with ethanol concentrations obtained from sweet sorghum bagasse (Wang et al., 2013) or kitchen wastes (Uncu & Cekmecelioglu, 2011).

Moreover, the maximum ethanol concentration was observed at the end of 72 h. The ethanol concentration of *C. boidinii* increased by 22% and reached to 35.88 g/L under the optimized conditions with RSM in comparison with the experiments carried out without RSM (**Figure 3**).

Conclusion

It is very important to investigate new raw materials and microorganisms for renewable energy-producing sectors for the sustainability. For these reasons, in the

present study, the bioethanol production of newly isolated *C. boidinii* was determined in the

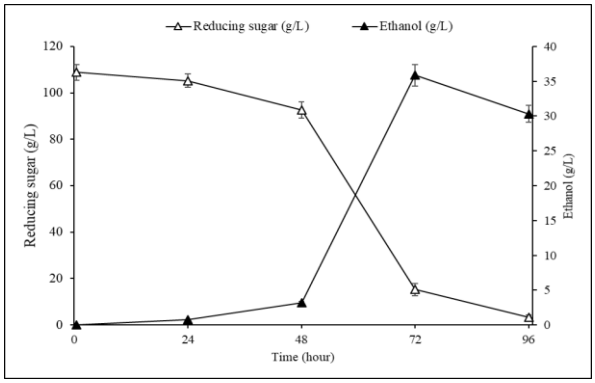

Figure 3. Bioethanol production of *C. boidinii* under optimized conditions (initial biomass loading: 20% (w/v), pH: 4.8, cellulase loading: 37.5 FPU/g cellulose, hemicellulase loading: 37.5 U/mL, enzymatic hydrolysis time: 72 h.

fermentation medium which was prepared with PR. Results of the RSM experiments revealed that sugar concentrations of PR increased from 59.80 to 108.86 g/L at the end of 72 h when 37.5 FPU/g cellulose and 37.5 U/mL enzymes were used. Moreover, under these optimized conditions, the highest bioethanol concentration was observed as 35.88 g/L. This study shows that PR is a promising raw material and *C. boidinii* is an appropriate agent for efficient bioethanol production.

Funding Information

This work was supported by Research Foundation of Ankara University (Project Number: 17L0430007).

Author Contributions

First Author: Investigation, writing-original draft; Second Author: Conceptualization, funding acquisition, resources, methodology, writing; Third Author: Review and editing.

Conflict of Interest

The author(s) declare that they have no known competing financial or non-financial, professional, or personal conflicts that could have appeared to influence the work reported in this paper.

References

Adıgüzel, A., O. (2013). Biyoetanolün Genel Özellikleri ve Üretimi İçin Gerekli Hammadde Kaynakları. *BEÜ Journal of Science,* 2(2), 204-220.

Adney, B. & Baker, J. (2008). Measurement of Cellulase Activities Laboratory Analytical Procedure (LAP) Issue Date : 08 / 12 / 1996 Measurement of Cellulase Activities Laboratory Analytical Procedure (LAP). *Renewable Energy*, *January*, 8.

Aytaş, Z. G., Tunçer, M., Kul, Ç. S., Cilmeli, S., Aydın, N., Doruk, T., & Adıgüzel, A. O. (2023). Partial characterization of β-glucosidase, β-xylosidase, and α-l-arabinofuranosidase from Jiangella alba DSM 45237 and their potential in lignocellulose-based biorefining. *Sustainable Chemistry and Pharmacy*, *31*, 100900. https://doi.org/10.1016/j.scp.2022.100900.

Balakrishnan, R., Reddy Tadi, S. R., Sivaprakasam, S. & Rajaram, S. (2018). Optimization of acid and enzymatic hydrolysis of kodo millet (Paspalum scrobiculatum) bran residue to obtain fermentable sugars for the production of optically pure D (−) lactic acid. *Industrial Crops and Products*, *111*, 731–742. https://doi.org/10.1016/j.indcrop.2017.11.041.

Chen, X., Shekiro, J., Franden, M. A., Wang, W., Zhang, M., Kuhn, E., Johnson, D. K. & Tucker, M. P. (2012). The impacts of deacetylation prior to dilute acid pretreatment on the bioethanol process. *Biotechnology for Biofuels*, *5,* 1-14. https://doi.org/10.1186/1754-6834-5-8.

Chen, L., Wei, Y., Shi, M., Li, Z., & Zhang, S. H. (2020). Statistical optimization of a cellulase from Aspergillus glaucus CCHA for hydrolyzing corn and rice straw by RSM to enhance yield of reducing sugar. *Biotechnology letters*, *42*, 583-595. https://doi.org/10.1007/s10529-020-02804-5.

Dutra, E. D., Santos, F. A., Alencar, B. R. A., Reis, A. L. S., de Souza, R. de F. R., Aquino, K. A. da S., Morais, M. A. & Menezes, R. S. C. (2018). Alkaline hydrogen peroxide pretreatment of lignocellulosic biomass: status and perspectives. *Biomass Conversion and Biorefinery*, *8*(1), 225–234. https://doi.org/10.1007/s13399-017-0277-3.

Glass, N. L. & Donaldson, G. C. (1995). Development of primer sets designed for use with the PCR to amplify conserved genes from filamentous ascomycetes. *Applied and Environmental Microbiology*, *61*(4), 1323–1330. https://doi.org/10.1128/aem.61.4.1323-1330.1995.

Gonçalves, D. B., Batista, A. F., Rodrigues, M. Q. R. B., Nogueira, K. M. V. & Santos, V. L. (2013). Ethanol production from macaúba (Acrocomia aculeata) presscake hemicellulosic hydrolysate by Candida boidinii UFMG14. *Bioresource Technology*, *146*, 261–266. https://doi.org/10.1016/j.biortech.2013.07.075.

Gul, A., Irfan, M., Nadeem, M., Syed, Q. & Haq, I. ul. (2018). Kallar grass (Leptochloa fusca L. Kunth) as a feedstock for ethanol fermentation with the aid of response surface methodology. *Environmental Progress and Sustainable Energy*, *37*(1), 569–576. https://doi.org/10.1002/ep.12701

Günan Yücel, H. & Aksu, Z. (2015). Ethanol fermentation characteristics of Pichia stipitis yeast from sugar beet pulp hydrolysate: Use of new detoxification methods. *Fuel*, *158*, 793–799. https://doi.org/10.1016/j.fuel.2015.06.016.

Huang, C. F., Lin, T. H., Guo, G. L. & Hwang, W. S. (2009). Enhanced ethanol production by fermentation of rice straw hydrolysate without detoxification using a newly adapted strain of Pichia stipitis. *Bioresource Technology*, *100*(17), 3914–3920. https://doi.org/10.1016/j.biortech.2009.02.064.

Itiki, R. & Chowdhury, R. P. (2020). Fast deployment of COVID-19 disinfectant from common ethanol of gas stations in Brazil: COVID-19 disinfectant from common ethanol. *Health Policy and Technology*, *9*(3), 384–390.

https://doi.org/10.1016/j.hlpt.2020.07.002.

Kim, T. H. & Lee, Y. Y. (2007). Pretreatment of Corn Stover by Soaking in Aqueous Ammonia at Moderate Temperatures. *Applied Biochemistry And Biotechnology*, *136*(7), 81–82. https://doi.org/10.1007/978-1-60327-181-3_8.

Kim, J. K., Oh, B. R., Shin, H. J., Eom, C. Y., & Kim, S. W. (2008). Statistical optimization of enzymatic saccharification and ethanol fermentation using food waste. Process Biochemistry, *43*(11), 1308-1312. https://doi.org/10.1016/j.procbio.2008.07.007.

Kshirsagar, S. D., Waghmare, P. R., Loni, P. C., Patil, S. A., & Govindwar, S. P. (2015). Dilute acid pretreatment of rice straw, structural characterization and optimization of enzymatic hydrolysis conditions by response surface methodology. *RSC Advances*, *5*(58), 46525-46533. https://doi.org/10.1039/C5RA04430H.

Kumar, A. K., Parikh, B. S. & Pravakar, M. (2016). Natural deep eutectic solvent mediated pretreatment of rice straw: bioanalytical characterization of lignin extract and enzymatic hydrolysis of pretreated biomass residue. *Environmental Science and Pollution Research*, *23*(10), 9265–9275. https://doi.org/10.1007/s11356-015-4780-4.

Lin, T. H., Huang, C. F., Guo, G. L., Hwang, W. S. & Huang, S. L. (2012). Pilot-scale ethanol production from rice straw hydrolysates using xylose-fermenting Pichia stipitis. *Bioresource Technology*, *116*, 314–319. https://doi.org/10.1016/j.biortech.2012.03.089.

Loow, Y. L., Wu, T. Y., Md. Jahim, J., Mohammad, A. W., & Teoh, W. H. (2016). Typical conversion of lignocellulosic biomass into reducing sugars using dilute acid hydrolysis and alkaline pretreatment. *Cellulose*, *23*, 1491-1520. https://doi.org/10.1007/s10570-016-0936-8.

Mahlia, T. M. I., Ismail, N., Hossain, N., Silitonga, A. S., & Shamsuddin, A. H. (2019). Palm oil and its wastes as bioenergy sources: a comprehensive review. *Environmental Science and Pollution Research*, *26*, 14849-14866. https://doi.org/10.1007/s11356-019-04563-x.

Manmai, N., Unpaprom, Y., & Ramaraj, R. (2021). Bioethanol production from sunflower stalk: application of chemical and biological pretreatments by response surface methodology (RSM). *Biomass Conversion and Biorefinery*, *11*, 1759-1773. https://doi.org/10.1007/s13399-020-00602-7.

Miller, G. L. (1959). Use of Dinitrosalicylic Acid Reagent for Determination of Reducing Sugar. *Analytical Chemistry*, *31*(3), 426–428. https://doi.org/10.1021/ac60147a030.

Mithra, M. G. & Padmaja, G. (2017a). Comparative Alterations in the Compositional Profile of Selected Root and Vegetable Peels Subjected to Three Pretreatments for Enhanced Saccharification. *International Journal of Environment, Agriculture and Biotechnology*, *2*(4), 1732–1744. https://doi.org/10.22161/ijeab/2.4.34.

Mithra, M. G. & Padmaja, G. (2017b). Strategies for enzyme saving during saccharification of pretreated lignocellulo-starch biomass: effect of enzyme dosage and detoxification chemicals. *Heliyon*, *3*(8), e00384. https://doi.org/10.1016/j.heliyon.2017.e00384.

Motoda, T., Yamaguchi, M., Tsuyama, T. & Kamei, I. (2019). Down-regulation of pyruvate decarboxylase gene of white-rot fungus Phlebia sp. MG-60 modify the metabolism of sugars and productivity of extracellular peroxidase activity. *Journal of Bioscience and Bioengineering*, *127*(1), 66–72. https://doi.org/10.1016/j.jbiosc.2018.06.017.

Naik, S. N., Goud, V. V., Rout, P. K. & Dalai, A. K. (2010). Production of first and second generation biofuels: A comprehensive review. *Renewable and Sustainable Energy Reviews*, *14*(2), 578–597. https://doi.org/10.1016/j.rser.2009.10.003.

Nowicka, A., Zieliński, M. & Dębowski, M. (2020). Microwave support of the alcoholic fermentation process of cyanobacteria Arthrospira platensis. *Environmental Science and Pollution Research*, *27*(1), 118–124. https://doi.org/10.1007/s11356-019-05427-0.

Osawa, F., Fujii, T., Nishida, T., Tada, N., Ohnishi, T., Kobayashi, O., Komeda, T. & Yoshida, S. (2009). Efficient production of L-lactic acid by Crabtree-negative yeast Candida boidinii. *Yeast*, *26*, 485–496. https://doi.org/10.1002/yea.1702.

Palmqvist, E., & Hahn-Hägerdal, B. (2000). Fermentation of lignocellulosic hydrolysates. I: inhibition and detoxification. Bioresource technology, 74(1), 17-24. https://doi.org/10.1016/S0960-8524(99)00160-1

Palupi, B., Fachri, B. A., Rahmawati, I., Susanti, A., Setiawan, F. A., Adinurani, P. G. & Mel, M. (2020). Bioethanol used as topical antiseptics: Pretreatment optimization of bioethanol production from tobacco industrial waste. *Annals of Tropical Medicine and Public Health*, *23*(8), 1213–1219. https://doi.org/10.36295/ASRO.2020.2384.

Parajó, J. C., Domínguez, H. & Domínguez, J. M. (1998). Biotechnological production of xylitol. Part 3: Operation in culture media made from lignocellulose hydrolysates. *Bioresource Technology*, *66*(1), 25–40. https://doi.org/10.1016/S0960-8524(98)00037-6.

Paul, S. & Dutta, A. (2018). Challenges and opportunities of lignocellulosic biomass for anaerobic digestion. *Resources, Conservation and Recycling*, *130*, 164–174. https://doi.org/10.1016/j.resconrec.2017.12.005.

Pereira, L. M. S., Milan, T. M., & Tapia-Blácido, D. R. (2021). Using Response Surface Methodology (RSM) to optimize 2G bioethanol production: A review. *Biomass and Bioenergy*, *151*, 106166. https://doi.org/10.1016/j.biombioe.2021.106166.

Roca, C. & Olsson, L. (2003). Increasing ethanol productivity during xylose fermentation by cell recycling of recombinant Saccharomyces cerevisiae. *Applied Microbiology and Biotechnology*, *60*(5), 560–563. https://doi.org/10.1007/s00253-002-1147-9.

Santana, N. B., Teixeira Dias, J. C., Rezende, R. P., Franco, M., Silva Oliveira, L. K. & Souza, L. O. (2018). Production of xylitol and bio-detoxification of cocoa pod husk hemicellulose hydrolysate by *Candida boidinii* XM02G. *PLoS ONE*, *13*(4), 1–15. https://doi.org/10.1371/journal.pone.0195206.

Schieber, A., Stintzing, F. C. & Carle, R. (2001). By-Products of Plant Food Processing as a Source of Valuable Compounds-recent developments. *Trends in Food Science and Technology*, *12*(2001), 401–413. https://doi.org/10.1016/S0924-2244(02)00012-2.

Sindhu, R., Kuttiraja, M., Binod, P., Sukumaran, R. K. & Pandey, A. (2014). Physicochemical characterization of alkali pretreated sugarcane tops and optimization of enzymatic saccharification using response surface methodology. *Renewable Energy*, *62*, 362–368.

https://doi.org/10.1016/j.renene.2013.07.041.

Song, Y., Gyo Lee, Y., Jin Cho, E. & Bae, H. J. (2020). Production of xylose, xylulose, xylitol, and bioethanol from waste bamboo using hydrogen peroxicde-acetic acid pretreatment. *Fuel*, *278*, 118247. https://doi.org/10.1016/j.fuel.2020.118247.

Uncu, O. N. & Cekmecelioglu, D. (2011). Cost-effective approach to ethanol production and optimization by response surface methodology. *Waste Management*, *31*(4), 636–643. https://doi.org/10.1016/j.wasman.2010.12.007.

Vandeska, E., Kuzmanova, S. & Jeffries, T. W. (1995). Xylitol formation and key enzyme activities in Candida boidinii under different oxygen transfer rates. *Journal of Fermentation and Bioengineering*, *80*(5), 513–516. https://doi.org/10.1016/0922-338X(96)80929-9.

Wang, L., Luo, Z. & Shahbazi, A. (2013). Optimization of simultaneous saccharification and fermentation for the production of ethanol from sweet sorghum (Sorghum bicolor) bagasse using response surface methodology. *Industrial Crops and Products*, *42*(1), 280–291. https://doi.org/10.1016/j.indcrop.2012.06.005.

Wistara, N. J., Pelawi, R. & Fatriasari, W. (2016). The Effect of Lignin Content and Freeness of Pulp on the Bioethanol Productivity of Jabon Wood. *Waste and Biomass Valorization*, *7*(5), 1141–1146. https://doi.org/10.1007/s12649-016-9510-8.

Yolmeh, M. & Jafari, S. M. (2017). Applications of Response Surface Methodology in the Food Industry Processes. *Food and Bioprocess Technology*, *10*(3), 413–433. https://doi.org/10.1007/s11947-016-1855-2.

Yücel, Y., & Göycıncık, S. (2015). Optimization and modelling of process conditions using response surface methodology (RSM) for enzymatic saccharification of spent tea waste (STW). *Waste and biomass valorization*, *6*, 1077-1084. https://doi.org/10.1007/s12649-015-9395-y.

Zhao, X., Xiong, L., Zhang, M. & Bai, F. (2016). Towards efficient bioethanol production from agricultural and forestry residues: Exploration of unique natural microorganisms in combination with advanced strain engineering. *Bioresource Technology*, *215*, 84–91. https://doi.org/10.1016/j.biortech.2016.03.158.

Biotech Studies 33(1), 52-66
http://doi.org/10.38042/biotechstudies.1463814

BIOTECH STUDIES

REVIEW

Recent *in vitro* models and tissue engineering strategies to study glioblastoma

Melike Karakaya [1], Pınar Obakan Yerlikaya [2*]

[1] Biruni University, Department of Biomedical Engineering, 340110, Istanbul, Türkiye
[2] Istanbul Medeniyet University, Department of Molecular Biology and Genetics, 34700, Istanbul, Türkiye

How to cite:
Karakaya, M. & Obakan Yerlikaya, P. (2024). Recent *in vitro* models and tissue engineering strategies to study glioblastoma. *Biotech Studies*, 33(*1*), 52-66. https://doi.org/10.38042/biotechstudies.1463814

Article History
Received 14 June 2023
Accepted 06 February 2024
First Online 29 March 2024

Corresponding Author
Tel.: +90 216 280 42 11
E-mail:
pinar.obakan@medeniyet.edu.tr

Keywords
Glioblastoma
Molecular mechanisms
Tissue engineering

Abstract

Glioblastoma is a highly malignant brain tumor classified as grade IV with a poor prognosis and approximately a year of survival rate. The molecular changes that trigger primary glioblastoma are usually epidermal growth factor receptor mutations and amplifications, *Mouse Double Minute* and *TP53* mutations, *p16* deletion, *phosphatase and tensin homolog* and *telomerase* promoter mutations. In the vast majority of glioblastomas, altered signaling pathways were identified as receptor tyrosine kinase/Ras/PI3K, p53. Isocitrate dehydrogenase 1/2 mutations have also been associated with poor prognosis in glioblastoma The treatment options are very limited and complicated because of the diverse composition and heterogeneity of the tumors and unresponsiveness to the treatments with the existence of barriers reaching the brain tissue. Despite new trials, drug candidates that appeared effective in cell culture or mouse models failed in the clinic. Recently, new sophisticated experimental systems, including the those that mimic the tumor microenvironment, have started being used by several research groups, which will allow accurate prediction of drug efficacy. Tissue engineering strategies are also being combined with innovative cancer models, including spheroids, tumorspheres, organotypic slices, explants, tumoroids, and organoids. Such 3D systems provide powerful tools for studying glioblastoma biology by representing the dynamic evolution of the disease from the early to the metastatic stages and enabling interaction with the microenvironment. In this review, we both enlighten the molecular mechanisms that lead to glioblastoma development and detailed information on the tissue engineering approaches that have been used to model glioblastoma and the tumor microenvironment with the advantages and disadvantages. We anticipate that these novel approaches could improve the reliability of preclinical data by reducing the need for animal models.

Introduction

Glioblastoma

Glioblastoma (GBM) is a rare primary fatal brain cancer type that originates from glial cells, which exist in the central nervous system (CNS) (Uddin et al., 2020). GBM, usually occurring in adults (constituting more than 60% of all brain tumors), is the most aggressive tumor of the CNS, with a low survival rate and poor prognosis even approximately 15 months after adjuvant chemotherapy following surgical resection of current therapy (Montemurro, 2020; Rock et al., 2012). There is a relationship between age and the incidence of the disease since the research show that most GBM patients are generally 65 years of age and older (Sasmita et al., 2018). The estimated prevalence among all primary brain tumors is 4-8 per 100,000 people while this prevalence is 250,000 cases globally (Nejo et al., 2020). According to statistics from 2011 to 2015, the estimated

yearly age-adjusted incidence of GBM in the United States is 3.21 per 100,000 people, with the prevalence depending on age and gender. It was determined that men are 1.58 times more likely than women to develop GBM. In respect of race or ethnicity, white people have the highest incidence. The total incidence of GBM is reported to be 9.23 cases per 100,000 population, with the prevalence in the United States (Tan et al., 2020a).

GBM has malignant tumor characteristics such as atypical cells, nuclear hyperchromasia, increased mitotic figures, angiogenesis, and necrotic areas with high vascularity. The infiltrative nature of GBM complicates treatment and reduces the effect of chemical agents. In addition, its direct effects on the neurological function of the brain, psychological health, and quality of life also cause problems in treatment (Reardon & Wen, 2006). GBM is known to be derived from glial cells; however, neural stem cells, at the stage of differentiation into glia, may also give rise to cancer development. Because of the active DNA repair and regeneration features, GBM stem cells are hard to treat (Stoyanov et al., 2018a). As of 2016, GBM tumors are classified by the WHO as 90% Isocitrate dehydrogenase (IDH)-wild type and 10% IDH 1 and 2 mutants, when compared to the wild type, mutant *IDH 1 and 2* have a better prognosis (Batash et al., 2017).

GBM tumors can be found in any region of the CNS as primary and secondary types of malignant and non-malignant tumors (Nejo et al., 2020). Those types have different genetic pathways, so their influence on patients varies as to patients' ages (Sasmita et al., 2018). Primary GBM accounts for more than 80% of GBM and arises from neural stem cell precursors, whereas secondary GBM arises from mutations of grown neural cells (Stoyanov et al., 2018a). Primary GBM has been linked to *epidermal growth factor (EGF*) overexpression, *phosphatase and tensin homolog on chromosome ten* (*PTEN)* mutation, *cyclin-dependent kinase inhibitor 2A (CDKN2A)* deletion, and, less frequently, *murine double minute 2* (*MDM2)* amplification (Ohgaki et al., 2004). The *tumor protein 53 (p53)* mutation is commonly found as a precursor in secondary GBM (Kleihues & Ohgaki, 1999). While primary GBMs are seen in older patients with an average age of 62, secondary GBMs originate from lower-grade astrocytoma or oligodendroglioma generally indicate in the frontal lobe and are seen in younger patients with an average age of 45 (Shah et al., 2021). *IDH1* and *IDH2* are found in approximately 70% of secondary GBM and low-grade glioma, although they occur in less than 10% of primary GBM (Zeng et al., 2015). The prognosis of primary GBM is not as good as that of secondary GBM. The standard care for GBM is to apply surgery following radiotherapy in combination with concomitant and up to six maintenance cycles of temozolomide chemotherapy to the majority of newly diagnosed patients (le Rhun et al., 2019) (**Figure 1**).

Glioblastoma Molecular Mechanisms

70% of IDH-wild-type GBMs carry *EGFR* amplification and *Telomerase Reverse Transcriptase (TERT)* promoter mutations (Brennan et al., 2013). *TERT* promotor mutations result in the creation of new ETS (Erythroblast Transformation Specific) transcription factor binding sites and increased TERT activity, promoting TERT transcription and, thereby, tumor cell immortalization (Horn et al., 2013). *TERT* mutations that reduce survival probability increase TERT expression and are exclusive to *ATRX* mutations found in IDH mutant astrocytic gliomas. The *TERT* promoter mutation is found in oligodendrocytic tumors with the 1p/19q deletion in IDH-mutant GBM. Eribulin, a tubulin polymerization inhibitor, has been shown to reduce TERT activity in GBM models, justifying its clinical exploration (Takahashi et al., 2019). Furthermore, in adult GBM, proto-oncogenes have impressed on the *EGFR*, *platelet-derived growth factor receptor A (PDGFRA)*, and *hepatocyte growth factor receptor (HGFR)* genes, as well as the cyclin-dependent kinase genes *CDK4* and *CDK6*, and the murine double minute genes *MDM2* and *MDM4*. Overexpression, amplification, and mutation can cause EGFR phenotypic alterations in GBM, and nearly 50% of EGFR-enhanced GBM have the potential to carry a deletion mutation. *EGFR* amplification can occur via transcription or RNA insertion and correlates with the presence of EGFR protein variants. One specific variant of EGFR, EGFRvIII, has a deletion in the N-terminal ligand binding site between amino acids 6 and 273 and leads to ligand-independent activation of EGFR and is a constitutively active potential neoantigen. The therapeutic usage of conventional tyrosine kinase inhibitors like gefitinib is

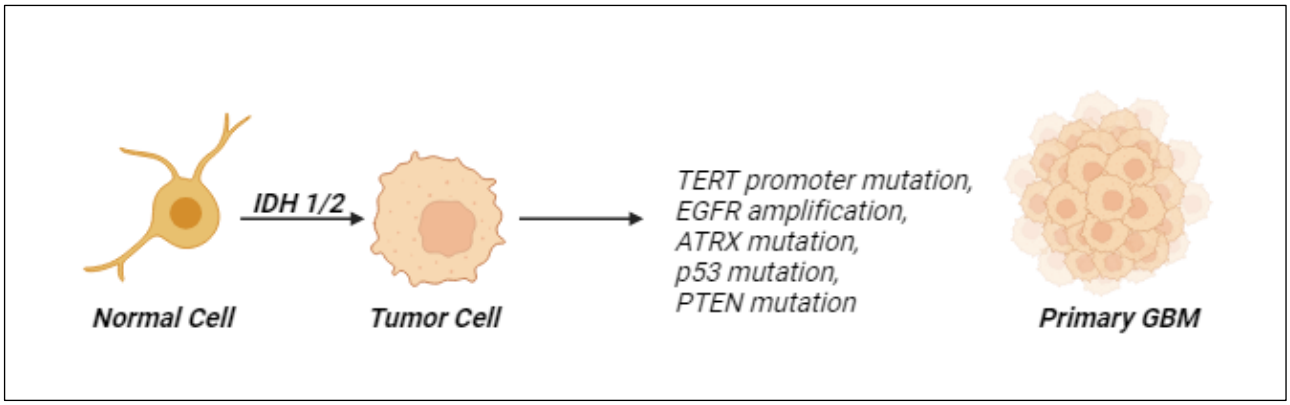

Figure 1. Mutations observed in glioblastoma.

limited due to the particular character of EGFRvIII, and it is therapeutically important that EGFRvIII has a therapeutic effect against malignancies. Protein Kinase A (PKA)-dependent phosphorylation of DOCK180, a Rac1 guanine exchange factor, is mediated by EGFRvIII. In a cell line expressing EGFRvIII, overexpression of mutant DOCK180 lacking the S1280 phosphorylation site reduced receptor-stimulated proliferation and survival. Although EGFRvIII-specific PKA phosphorylation may be a good therapeutic target if it can be inhibited by the EGFRvIII/PKA/DOCK180 interaction, EGFRvIII is not associated with overall median survival, except in cases with survivors of more than one year, which limits the therapeutic value of this target (Carlsson et al., 2014). The failure of EGFR tyrosine kinase inhibitors to show single-agent action has been reviewed in numerous publications, and it is not certain that the medications will limit the pathway's activity even if they reach the tumor site (Peralta-Arrieta et al., 2022). In another study, expression of EGFR or EGFRvIII was targeted in EGFRvIII-positive recurrent GBM within the vaccine called rindopepimut, which produces a viability signal when combined with bevacizumab, but failed in phase III in newly diagnosed patients (NCT01498328) (Weller et al., 2017). Also, when combined with temozolomide, depatuxizumab mafodotin, an antibody-drug combination consisting of an EGFR antibody ABT-806 linked to monomethyl auristatin F, was expected to be active in GBM with EGFR amplification, but it was ineffective (NCT02573324). While EGFR amplification is maintained throughout the disease, the loss of *EGFRvIII* expression observed as a result of phase III indicated that EGFRvIII expression may not be stable suggesting that chimeric antigen receptor (CAR) T cells or bispecific T-cell-binding antibodies targeting EGFRvIII may not work as well (Gedeon et al., 2018; O'Rourke et al., 2017; Van Den Bent et al., 2015).

p53 is a tumor suppressor protein and initiates apoptosis when DNA damage cannot be repaired. The *p53* mutations lead to the transition from low-grade astrocytoma to high-grade GBM. Induction of apoptosis and enhanced survival in a mouse model after normal chemotherapy have been demonstrated in recent gene therapy research with nanoparticle delivery of the *p53* gene targeting GBM and cancer stem cells. However, this has not been evaluated in human trials. The fact that *PAX3*, a member of the *PAX* gene family and acting in a *p53*-dependent manner to inhibit apoptosis, is up-regulated in many cancer types, including GBM, suggesting that it might be a potential oncogene. *PAX3*, which is an important factor in the differentiation of NSCs into astrocytes, can be considered as a diagnostic marker in GBM treatment (Zhu et al., 2018). *PTEN* mutations or deletions were discovered in more than half of the samples in primary tumors expressing mutant *p53*, indicating that GBM development is characterized by several concurrent tumor suppressor alterations (Zheng et al., 2008). Neutralization studies focused on *MDM2* or *MDM4* gene amplification are ongoing for patients with impairments in *p53* function (NCT03107780) (le Rhun et al., 2019). *PTEN* is a tumor suppressor of phosphatase that is essential for cellular homeostasis. Mutations in *PTEN* are found in 5 to 40% of GBM cases and may be a prognostic indicator in patients over the age of 45 (Srividya et al., 2011). PTEN protects the neural stem cell population by blocking cell cycle entry under normal conditions, while *PTEN* null mutants are more sensitive to growth stimuli and more prone to proliferation than wild-type neural stem cells (Groszer et al., 2006). PTEN levels are positively connected with patient survival; hence, it could be a useful diagnostic tool (Ermoian et al., 2002). The loss of *PTEN* can be seen in the IDH-wild-type of GBM tumors, resulting in excessive activation of the PI3K/AKT and mammalian target of rapamycin (mTOR) signaling. By suppressing protein metabolism, the PI3K/AKT/mTOR pathway regulates anabolic pathways in the cell and controls tumor formation. mTOR controls *PTEN* loss by phosphorylating p70S6 kinase 1 (S6K1) and eIF4E binding protein (4EBP), which are activated and inactivated, respectively. Accordingly, mutated oncogenic PI3K subunits increase. The PI3K/mTOR pathway is unavoidably changed as a result of the loss of tumor suppressor phosphatase and *PTEN* mutation. Activation of the PI3K/mTOR pathway suppresses autophagy and impairs proteasome function (Benitez et al., 2021). PI3K/AKT/mTOR pathway activates mutations in phosphatidylinositol- 4,5-bisphosphate 3-kinase catalytic subunit alpha *(PIK3CA),* which encodes the catalytic subunit p110 alpha (p110α) and in phosphoinositide- 3-kinase regulatory subunit 1 (PIK3R1), which encodes the p85α regulatory subunit. This pathway has been used with standard TMZ and chemotherapy treatment or in place of TMZ in patients with *MGMT* promoter-unmethylated GBM. As a result, no efficacy was observed, but mTOR inhibitors were slightly tolerated despite TMZ (Ma et al., 2015; Wick et al., 2016).

The *MET, FGFR,* and *AXL* genes are three independently acting receptor tyrosine kinases (RTKs) that are linked to cancer cell proliferation. *MET* gene encoding the hepatocyte growth factor receptor plays an important role in the migration and invasion of glioma cells in response to the inhibition of angiogenesis and hypoxia (Li et al., 2011). However, inhibition of MET, whose amplification has been proven in crizotinib treatment, does not affect the disease (Chi et al., 2012; Wen et al., 2011). Some IDH-wild-type GBM cases have oncogenic fusions between *fibroblast growth factor receptor (FGFR)* and *transforming, acidic, coiled-coil-containing protein (TACC)* genes, serving constitutive kinase activity. This fusion could be a target for drugs that inhibit FGFR (Perry & Wesseling, 2016).

Vascular endothelial growth factor (VEGF or VEGF-A) is an important signalling molecule of the nervous system and is responsible for GBM angiogenesis. Glioblastoma stem-like cells (GBSCs) are micrometastases that are formed after primary GBM

lesions are surgically removed. These small tumor cells have the potential to be used as therapeutic targets. GBSCs lead to tumor formation as a result of up-regulated signal pathways to protect NSC characteristics. Cellular responses are mediated by VEGF Receptor 1 (VEGFR1, Flt1) and VEGFR2 (KDR/Flk1) expressed on the surface of GBSCs. Cytokines (e.g., HGF, VEGF, PDGF, and PIGF) produced by endothelial cells can alter the biology of cancer stem cells by stimulating the survival of the adjacent cancer stem cells. Simultaneously, as GBM grows rapidly, it begins to be deprived of oxygen, resulting in hypoxia. During hypoxia, inducible transcription factors like hypoxia-inducible factors (HIFs) can stimulate VEGF secretion, and VEGF upregulation has a negative impact on therapy. An increase in VEGF has been shown to promote tumorigenesis in human GBSCs (Xu et al., 2013). Under hypoxic conditions, HIFs could be a potential upstream regulator of PAX3 in differentiated GSCs (Zhu et al., 2018). Bevacizumab, a drug approved by the Food and Drug Administration (FDA), is still being studied for its effect on tumor dynamics, despite showing good survival results. Subgroups of patients who benefited from bevacizumab's long survival were difficult to identify, and researchers were unable to develop a model in which VEGF could be targeted. Other VEGF inhibitors, such as cediranib, have also been shown in randomized clinical trials to be ineffective (Batchelor et al., 2013; le Rhun et al., 2019).

Transforming growth factor-β (TGF-β) regulates cell proliferation, differentiation, and apoptosis, and binds and activates a membrane receptor serine/threonine kinase complex that, when activated, phosphorylates several Smad family proteins, such as Smad2, which prognostically adversely affects GBM. TGF-β stimulates the expression of genes that control the cell cycle and the extracellular matrix (ECM), such as plasminogen activator inhibitor (PAI)-1 and PDGF. TGF-β also activates important tyrosine kinase receptor (TKR) effector pathways, such as PKB/AKT and ERK, independently of Smad. TGF-β is thought to be a tumor suppressor factor, and the mutations it acquires as a result of antiproliferative effects facilitate its pro-tumorigenic activity (Frei et al., 2015). TGF-β 1/2 proteins have been identified as key molecules in the immunosuppression of GBM. Although TGF-β inhibition has shown promising results in animal studies, clinical translation of TGF-β targeting using TGF-2 specific antisense oligonucleotides or tyrosine kinase inhibitors targeting TGF-β receptor II has been unsuccessful with galunisertib. The limited dose limit of TGF-β receptor inhibitors due to toxicity makes them difficult to use in clinical studies (le Rhun et al., 2019).

Human *Ras genes (Rat Sarcoma)*, such as *H-Ras, N-Ras,* and *K-Ras*, are oncogenes, and their activation and deactivation are regulated by binding to guanosine triphosphate (GTP) or guanosine diphosphate (GDP), as it is a G protein. Activation of RAF kinase by Ras regulates some signaling pathways, including mitogen-activated protein kinase (MAPK) and phosphatidylinositol 3-kinase (PI3K)/Akt pathways, and is an effective factor in the regulation of cell proliferation, signal transduction, apoptosis, and tumorigenesis. Raf is activated after growth factor signalling driven by EGFR (epithelial growth factor receptor) and PDGFR (platelet-derived growth factor receptor), and by this way it regulates Ras activity. The Ras/MAPK pathway disruption has been shown to cause aberrant cell proliferation and, ultimately, cancer. The increase in the expression levels of Ras, EGFR, PDGFR, and other receptor tyrosine kinases. Therefore, it was concluded that the Ras/MAPK pathway can be targeted for the treatment of GBM (Mao et al., 2012).

Signal transducers and activators of transcription (STAT) protein complexes, a family of Src Homology-2 (SH2)-dependent proteins involved in the function of transcription factors, activate transcription of target genes having roles in proliferation and apoptosis. STAT3, one of the STAT proteins activated by EGF, is upregulated in GBM and has an important role in the development of astrocytes. STAT3 may also function as a tumor suppressor in GBM. Numerous metalloenzymes and zinc-dependent transcription factors use zinc as a catalytic/structural component. Research has established a connection between zinc levels and the risk of cancer, and it has been observed that the zinc transporter (ZIP4) is upregulated in cases of human pancreatic cancer. Upregulation of ZIP4 in cancer cells enhances cell proliferation, and overexpression of ZIP4 increases Interleukin 6 (IL-6) transcription via cyclic adenosine monophosphate response element binding (CREB), which activates STAT3 and raises cyclin D1 production. Studies have shown that ZIP4 is overexpressed in GBM and that new therapeutic targets may emerge in the control of malignancy by targeting relevant molecular activities (Mao et al., 2012).

Secondary GBM is defined by mutations in the metabolic enzymes isocitrate dehydrogenase 1 and 2 (IDH1/2), which are also genetic markers for GBM. IDH-1 mutations are found in the active site, where somatic point mutations prohibit the enzyme from successfully converting isocitrate to alpha-ketoglutarate and can cause a drop in enzyme efficiency or an increase in enzymatic performance depending on the substrate. Furthermore, in 90% of cases, the arginine at codon 132 is replaced by a histidine (Yan et al., 2009). The R132H mutation allows IDH-1 to convert alpha-ketoglutarate to 2-hydroxyglutatate (2HG), an onco-metabolite (Jin et al., 2013). 2HG levels can be identified using magnetic resonance thus it could be a good biomarker for IDH-1 mutations. The studies about the IDH inhibitors were proven to be successful in glioma xenografts; IDH-1 is now being targeted for therapeutic usage. Drug candidate AG-120 is currently undergoing a phase II trial (clinicaltrials.gov; NCT04056910). In patients over the age of 55, IDH-R132H mutation is used to differentiate between IDH-wild-type and IDH-mutant GBMs. Sequencing is usually recommended if the result is

negative in young patients. Copy number gains on chromosome 7, monosomy of chromosome 10, mutations in the phosphatase and *PTEN* tumor suppressor gene homozygous deletion of the cyclin-dependent kinase inhibitor 2A and 2B *(CDKN2A/p14ARF and CDKN2B)* loci on 9p21, and *TERT* promoter mutations are all common in IDH wild-type tumors. A phenotype of CpG island hypermethylation may also characterize a subset of IDH-mutant glioblastomas, with promoter methylation at numerous loci. Under grade IV gliomas, the WHO 2016 classification added a new subtype: H3F3A or HIST1H3B/C K27M (H3-K27M)-mutant diffuse midline gliomas. They are most common in children and young adults and have an extremely poor prognosis. These tumors were previously classified as glioblastomas, but they are now considered a distinct entity (Tan et al., 2020a). Advances in genomic sequencing are helping to shape personalized treatment for GBM. To create integrated analysis on a shared dataset, The Cancer Genome Atlas (TCGA) has made public genomic databases of more than 20 tumors. In GBM, a *Neurotrophic Tyrosine Kinase Receptor Type 1–Neurophacin* gene fusion was discovered using TCGA RNA-Seq data. This gene fusion boosted the proliferation of 3T3 cells in vitro, implying a carcinogenic role (J. Kim et al., 2014). The utilization of huge databases like TCGA has made oncogenic gene fusion analysis a burgeoning subject. However, the TCGA GBM dataset provides potential prognostic utility in addition to oncogenesis targets (Q. Zhao et al., 2015). The histological grade is critical in determining postoperative management. Adjuvant radiotherapy and/or chemotherapy are used to treat grade III gliomas. Treatment may be postponed in patients with grade II lesions until the disease progresses. Furthermore, patients with IDH mutant astrocytic gliomas and *IDH* and *TERT* promoter mutant oligodendrogliomas had different overall survival rates (Masui et al., 2016).

Some methylated promoters in GBM cause changes in the expression of tumor suppressor genes such as *PTEN*, *pRB*, and *p53*. *O(6)-methylguanine-DNA methyltransferase (MGMT)*, which is seen in 40% of primary GBMs, is one of the important markers for GBM. Silencing of the DNA repair enzyme *MGMT* gene promoter is associated with being a marker of DNA methylation, and *MGMT* predicts a favorable outcome in patients with GBM due to its sensitivity to alkaline chemotherapy agents. The reinstatement of guanine from O-6-methylguanine, the type of genomic lesion induced by alkylating agents used for chemotherapy drugs such as temozolomide, may be explained by the sensitivity of *MGMT* to alkaline chemotherapy agents. Studies have shown that treatments with alkaline agents give more positive results. Poor survival on treatment is associated with unmethylated tumors, confirming the predictive value of *MGMT* promoter methylation for response to chemotherapy in IDH1/2 wild-type GBMs. *MGMT* promoter methylation used as a predictive marker in elderly patients determines the best therapy and inclusion of TMZ. Patients with *MGMT* methylation are divided into those who require only radiotherapy (patients with *MGMT* promoter unmethylated tumors) and those who require TMZ chemotherapy or a combination of TMZ and radiotherapy (patients with *MGMT* promoter-methylated tumors). Treatment with TMZ separately from the detecting *MGMT* methylation in non-elderly GBM patients remains controversial, and patients' pseudoprogression (PsPD) may be beneficial for their *MGMT* methylation status. PsPD appears as an increase in tumor size on radiological imaging with standard (radiotherapy and TMZ) therapy. While not triggering any symptoms, it is found in 91% of patients with a methylated *MGMT* promoter and 41% of patients with an unmethylated *MGMT* promoter (Aldape et al., 2015).

Treatment Strategies

Although there is a lot of information about the molecular mechanism of GBM, there is still no definitive and effective treatment technique due to its localization, complexity, and heterogeneity (molecular subtypes: neural, proneural, classical, and mesenchymal) (Alifieris & Trafalis, 2015b; Bruns et al., 2021). While radiation applied five times a week for six weeks and the daily oral chemotherapy drug TMZ are the most effective standard treatment options after surgical resection, targeting the pathways specified in its molecular mechanism may create better treatment options for GBM. Individualization of treatment will produce the best positive outcome, as treatment depends on several factors, such as time of diagnosis, new onset or relapse, performance status, and age of the patient. Among the chemotherapy agents used in GBM are the combination of carboplatin, irinotecan, carmustine (BCNU), etoposide and procarbazine, lomustine, and vincristine regimen (PCV). Based on the outcomes of this phase II phase of GBM therapy, it has been shown that certain combinations represent an improvement in some GBM inhibitors, such as EGFR, mTOR, and angiogenesis medicines (Alifieris & Trafalis, 2015a; Mao et al., 2012). Surgery is an essential component of standard care as it overcomes many things such as reducing tumor burden, controlling seizures, reversing neurological deficits, introducing local therapeutic agents, and improving quality of life (Kardan & Satter, 2016). Surgical resection is divided into two classes as gross total resections, which is generally recommended, and subtotal resection. Since GBM is a locally invasive tumor, it cannot be completely cured by surgical resection, and is observed that 80% of the disease recurs approximately in seven months (Scott et al., 2011). Patients with a better prognosis may be younger, have a lower tumor volume, and have acceptable functional status prior to surgery (Nam & De Groot, 2017). The effect of surgical resection depends on the location of the tumor in the brain and regions such as the cortex, brain stem or basal ganglia are not

suitable for surgical resection. Such dangerous areas have a negative impact on prognosis (Scott et al., 2011).

Radiotherapy is one of the treatment methods used to destroy the remaining tumor cells after surgical resection and has been found to correlate with the increased median survival rates, especially when GTR (gross total resection) could not be performed. In standard therapy, 60 Gy is given in 2-Gy fractions five times a week for six weeks. Hypofractionated radiotherapy is administered at a biologically equivalent dose of 40 Gy, given in fractions of 2.67 Gy for three weeks, because long-term radiation is not suitable for patients aged 70 years and older with a poor prognosis. Hypofractionated radiotherapy results in better survival when administered with an alkylating agent usually preferred in the first-line therapy, temozolomide (TMZ). In elderly patients with *MGMT* promoter methylation, radiation-free temozolomide alone is used, and re-irradiation is an option in selected situations at relapse (Tan et al., 2020b). Because EGFRvIII upregulates DNA double-strand break repair machinery, imparting cellular resistance to such treatments, EGFRvIII inhibitors may increase overall tumor susceptibility to radiation therapy, which can be an issue in GBM. Gamma knife therapy brings stereotactic high doses of radiation to the targeted GBM area, but it is considered ineffective in the treating primary tumors due to the excessively large tumor volume (Carlsson et al., 2014). Radiation therapy has some limitations and risks associated with its invasive nature, necrosis, permanent neuron damage, and radioresistance (Smith et al., 2001). Recent radiation-based therapies to be evaluated in patients with malignant gliomas include intensity-modulated radiation therapy and boron neutron capture therapy (Norden & Wen, 2006).

Various chemotherapeutic agents have been tested to improve the survival rate of GBM patients and have evolved, mostly with the approval of TMZ, an alkylating agent for newly diagnosed GBM. Apart from TMZ, active alkylating agents such as carmustine (BCNU) and lomustine (CCNU) have also been tested (Alifieris & Trafalis, 2015b). BCNU and CCNU are very cytotoxic and have many side effects. Drugs such as carboplatin, oxaliplatin, etoposide, and irinotecan are known as second-line drugs. Other chemotherapeutic drugs of GBM include anti-VEGF monoclonal antibodies (Bevacizumab), anti-FGF antibodies, monoclonal antibodies targeting EGFR (Erlotinib and Gefitinib), and tyrosine kinase inhibitors (Iacob & Dinca, 2009).

A more effective treatment could not be developed after the standard GBM treatment (TMZ + radiation therapy) was introduced in 2005. The anti-VEGF antibody bevacizumab has been approved by the FDA for recurrent GBM, but survival has not improved in phase III studies. One of the challenging aspects of establishing a treatment for GBM is the physical barrier, the blood-brain barrier (BBB). The blood-brain barrier (BBB) consists of various proteins, including claudins, occludins, and junctional adhesion molecules, which form tight junctions that connect capillary endothelial cells. The BBB only allows the passage of molecules <500 Da and <400 nm, and provides passive diffusion of lipophilic molecules. Other molecules can cross the BBB via pinocytosis, receptor or carrier proteins. BBB and its homeostatic balance are supported with ATP-binding cassette transporters (e.g., multidrug resistance-1 (MDR1), P-glycoprotein, breast cancer resistance protein, and numerous other drug resistance proteins) that are expressed on vessel walls. In high-grade neural cancers such as GBM, the BBB is heterogeneously disrupted. With heterogeneity, tumor vessels form niches with different permeability to oxygen, nutrients, and drugs. GSCs are located in the perivascular hypoxic niches of the brain and are important for cytotoxic therapies. Many drugs do not pass the BBB adequately. For example, the PI3K/AKT/mTOR pathway is one that is activated in approximately 30% of GBMs. However, a certain amount of the developed drugs can pass through the BBB, which makes the treatment unsuccessful. While clinical trials are ongoing for inhibitors of the PI3K pathway, GDC-0068, and GDC-0084 (NCT02430363 and NCT03522298), it is not yet clear whether these failed results are due to poor BBB penetration or tumor heterogeneity (Ou et al., 2021).

Temozolomide (TMZ) is the most preferred oral drug in the chemotherapy of GBM as a pro-drug capable of crossing the BBB with an alkyl group. TMZ initiates apoptosis by adding methyl groups to bases in DNA, but more than half of patients with GBM are resistant to TMZ because they have the O6-methylguanine methyltransferase (MGMT)-based repair system. In this defense mechanism, damaged alkylated guanine nucleotides are repaired by transferring the methyl at the O6 site of guanine to its cysteine residues. Thus, TMZ might fail to kill cancer cells due to elevated DNA repair. In recurring GBM, TMZ also fails as there is acquired resistance (Karachi et al., 2018). The side effects of TMZ, such as toxicity in the blood and nausea, are milder than the side effects of other tested drugs (Chua et al., 2019). TMZ is stable at acidic pH levels, while it is unstable at basic pH levels. It is easily absorbed in the circulation due to its 194 Da weight and spontaneously decomposed to generate monomethyl triazene 5-(3-methyltriazen-1-yl)-imidazole-4-carboxamide (MTIC). Activated MTIC methylates DNA in guanine-rich regions (Denny et al., 1994; Tsang et al., 1990).

In a controlled study for Lomustine (CCNU; chloroethyl cyclohexyl nitrosourea), another FDA-approved drug for the treatment of GBM, the median survival time was noted as 11.5 months. CCNU has been shown to induce apoptosis by cross-linking DNA and RNA, and is currently used for patients with recurrent GBM and patients with the unmethylated MGMT repair system. Its combination with bevacizumab did not provide an extra advantage in terms of patient survival. When the PVC (P: procarbazine, C: lomustine, V: vincristine) treatment determined by the FDA for GBM

was compared with TMZ, survival rates were found to be similar (Fisher & Adamson, 2021).

Carmustine (BCNU; bis-chloroethyl nitrosourea) is another FDA-approved alkylating agent with an average survival of 11.75 months and is used in the treatment of recurrent GBM. In addition to cross-linking of DNA and RNA, it also binds to lutathione reductase, inducing apoptosis. Among the toxicities it shows, the most common ones are pulmonary, ocular, and bone marrow toxicities. It is administered intravenously (dose ratio: 150-200 mg/m2) every 6 weeks. Like carmustine, carmustine wafer implants are FDA-approved for GBM and contain 7.7 mg of BCNU per wafer (8 doses recommended). The aim of the treatment, which is applied directly to the tumor resection cavity, is to reduce toxicity, and it has been observed to significantly improve survival. BCNU wafers are not used as standard care because of their high cost and high complication rates (Fisher & Adamson, 2021).

Bevacizumab (BVZ) received FDA approval in 2009 following favorable outcomes in Phase II trials for the treatment of recurrent GBM. VEGF produced in tumor cells regulates blood vessels and cell growth. BVZ inhibits the binding of VEGF-A to the cell *surface VEGF* receptor tyrosine kinases VEGFR1 and VEGFR2, thereby arresting GBM progression. BVZ shows anti-vascular and anti-edema effects by reducing vascularity (M. M. Kim, Umemura, and Leung 2018). When BVZ and TMZ were compared with TMZ alone, no extra benefit was seen, on the contrary, side effects were increased. In addition, cytotoxic drugs such as etoposide and carboplatin are not FDA-approved, although they show benefits for recurrent GBM when administered with BVZ. BVZ, which is still used to treat symptomatic edema and radiation necrosis, also reduces the need for steroid medications and their negative effects (Fisher and Adamson 2021).

Tissue Engineering Strategies to Study Glioblastoma

Tissue engineering (TE) aims to create new tissue or organ by combining a large number of cells together with biocompatible materials and cell transplantation fields for the treatment of damaged tissue or organ (Duvall et al., 2013a, 2013b; Enderle & Bronzino, 2011). The fields of biomaterials, three-dimensional (3D) printing technologies, nanotechnology, induced pluripotent stem cells (iPSCs), and gene editing technologies (such as clustered regularly interspaced short palindromic repeats, CRISPR) are technologies that TE benefits from and are important for modeling disease and treatment modalities. In this way, organoids and 3D tissue studies are carried out, the control and manipulation of cells in the environment are taken under control, and developments in the field of personalized therapy are experienced. Thus, serious diseases such as cancer became more understandable, and improved treatments were found for many diseases. The use of 3D models is also advantageous in terms of reducing animal experiments (Figure 2) (Chandra et al., 2020).

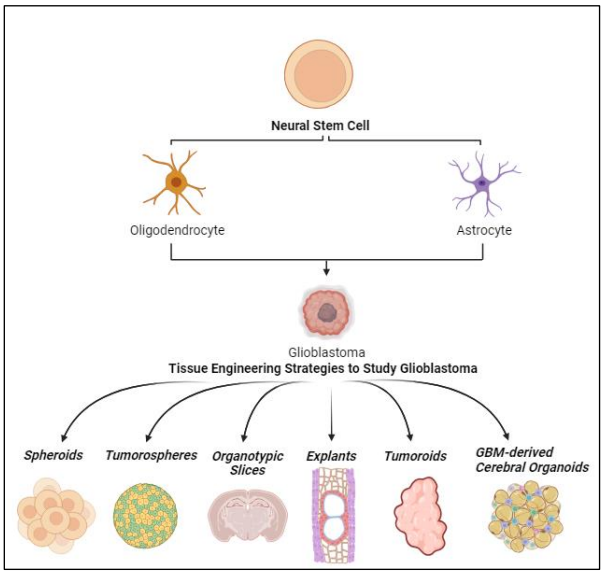

Figure 2. 3D in vitro culture strategies for glioblastoma research.

Numerous novel antineoplastic medications have been used in the realm of cancer biology. The resistance mechanisms of various cancer types have been elucidated, aided by bioinformatics profiling. Additionally, the effectiveness of anticancer drugs has been assessed in vitro using single-layer cancer cell lines. However, the monolayer does not provide a result beyond prediction as to whether the findings will be conclusive information for the clinic. The obvious reason for this is that cells are pulled out of their existing microenvironment, such as the ECM, soluble signals, 3D structure, stromal cells, and disordered microvasculature that surrounds tumor cells *in vivo*. Tumor growth in humans is complex, and the microenvironment of the tumor is better understood in animal models. However, animal models and the results of *in vitro* tests may not provide definitive solutions. In this direction, 3D *in vitro* cancer models have been developed, and the most widely used model is the human tumor spheroid (**Figure 2**). The purpose of using spheroids with features such as cell morphology and gene expression is for preclinical testing of anticancer drugs. Biological gels exhibit the microenvironment of the 3D cancer model to a greater extent than spheroids. Polymer matrices have been used recently and emerged as a technique by which the 3D cancer environment can be better adjusted as a substrate. Polymer matrices 3D development confers treatment resistance to cells in this system (Burdett et al., 2010). In conclusion, being able to mimic the GBM microenvironment is a crucial point for *in vitro* models and the generation of new treatments. The microenvironment of GBM includes astrocytes and oligodendrocytes mentioned in the previous sections, as well as ECM proteins, glucosaminoglycans, soluble signals, and extracellular vesicles that trigger ECM release and cell migration. During tumor formation, low levels of fibrous proteins (collagen, laminin, and hyaluronic acid) are upregulated.

Thus, the ECM concentration rises from 20% to 48% (Bruns et al., 2021).

There are successful 3D models for GBM that have been developed over time. Tumoroids developed in GBM tissue or cancer stem-like cells (CSLCs), organotypic slices developed with cells isolated from the brain or grafting spheroids, cerebral organoids, and tumorospheres emerging with the discovery of CSLCs are among these models (Soubéran & Tchoghandjian, 2020) (Figure 2).

Spheroids

As one of the most widely used 3D models, spheroids are more advantageous in terms of eliminating cost and ethical concerns, and they are a very important need in terms of producing more effective drugs by modeling tumor lesions *in vivo* for cancer treatment. Tumor lesions in suspension spheroids can be obtained with cell culture approaches as well as bioreactor usage. However, the characteristics of the ECM of the native tumor are not similar; however only the morphological and functional features can be mimicked. Matrix-grown spheroids are a more advantageous alternative to suspensions, as they better mimic the microenvironment and stroma and produce more cancer stem cells. Clonal expansion is one of the techniques used in tumor spheroids for drug screening and is formed by dividing a single cell into spheroids over several weeks after immobilization of the matrix (matrigel, polyethylene glycol [PEG], fibrin, etc.). An FDA-approved panel (NCI-60) of 60 cell lines representing cancer types is used in the production of the spheroids. Yet, this does not reflect well the characteristics of primary cells and tumor heterogeneity, resulting in a different cell-matrix interaction. Simple GBM spheroid models that allowed cell-matrix interaction and accurately reflected heterogeneity, as well as the physical and chemical aspects of GBM, provided a wealth of information about treatment responses (Bruns et al., 2021). As an example, U87-originated GBM spheroids multiply quicker in soft gels and their infiltration rises, whereas tumor spheroids' invasive capacity is affected by matrix thickness. In addition, drug response was examined in U87 GBM spheroids encapsulated in fibrin gels and infiltrated into the matrix, and as a result, applied atorvastatin caused decreased infiltration capacity and increased apoptosis. Besides, chitosan/PEG hydrogels have been proven to increase drug resistance more than Matrigel-formed spheroids. Studies have shown that different drug responses can be observed for different GBM subtypes and unique, varying microenvironments (Bruns et al., 2021).

Tumorospheres

Tumorospheres formed by symmetric or asymmetric division by taking advantage of the self-renewal property of stem cells grown by clonal expansion were first developed for normal neural stem cells grown as neurospheres. Surface indicators such as A2B5, L1CAM, integrin6, CD15, CD44, and CD133, which were found to increase in the population of CSLC, have been identified thanks to tumorospheres that enable a better understanding in brain tissue. Tumorospheres have been generated in many different cancer types in the following years, however, a single proven marker to identify CSLCs with sufficient sensitivity and specificity has not proposed yet (Soubéran & Tchoghandjian, 2020; Weiswald et al., 2015). Primary tumorospheres are formed by the mechanical and enzymatic degradation of GBM tissue. Besides cell culture medium, growth factors such as EGF or FGF support the proliferation and maintenance of observed gene expression traits. The various neural cells (neurons, astrocytes, or oligodendrocytes) that are formed after differentiation in the tumorospheres reflect the heterogeneity and organization of tumor cells. While tumorospheres are an important tool for studying CSLC differentiation and migration in GBM, their lack of GBM microenvironment cells is a severe drawback (Soubéran & Tchoghandjian, 2020).

Organotypic Slices

Transferring a 200-400 µm-thick slice of GBM cells or spheroids/tumoroids from a healthy rodent brain into cell culture and supplementing with cell culture media, or neurobasal media yields the organotypic slice model. Organotypic slice models, as they preserve vasculature, reflect heterogeneity better, and allow GBM to be studied in the native microenvironment without tissue thawing or culture migration. Organotypic slices bridge the gap between ex vivo and *in vivo* research, allowing researchers to manipulate tumor cells as well as the brain microenvironment. Depletion of microglia over time can also be utilized to explore the role of immune cells in tumor growth and therapeutic response (Parker et al., 2017; Soubéran & Tchoghandjian, 2020).

Explants

Explants are models created by growing small tumor parts with the logic of placement in conjunction with the cancer cells' surroundings. The quality of the selected tumor fragments is crucial to the explants' success; thus the resected sample with surgery should be cleaned and filtered with phosphate-buffered saline before being cut into pieces and covered with glass coverslips. The cells are cultured on the explant, in addition to cancer cells and CSLCs, as well as vessels, fibroblasts, and immune cells, and begin to migrate after being cultured. While explants are used to detect the proliferation, differentiation and growth of the tumor by preserving the microenvironment, the absence of healthy tissue can be considered as a limitation (Soubéran & Tchoghandjian, 2020).

Tumoroids

Tumoroid models are tumor reconstitutions from a small tumor piece in a culture medium or with

dissociated CSLCs for long-term use. To make tumoroid models, certain culturing procedures are used. Based on MRI imaging, tumors can be formed from multiple tumor areas of the parental tumor. Although their proliferation rate slows down after a few months in culture, tumors can stay stable and viable for more than a year. The success rate of this technique is between 30-90% and can be frozen for later use. Tumoroids also retain tumor features and tissue architecture, as well as glial, ECM material and immune cells such as astrocytes, oligodendrocytes, neurons, fibroblasts, striated collagen fibers, macrophages, and T cells. The tumoroid model constitutes a suitable approach for GBM research because it accurately reflects heterogeneity. The model represents a fast growth rate that allows the identification of mixed cellular responses, and may be used to create tailored assays. However, the disadvantage might be that the results are not reproducible because of the lack of heterogeneity of the microenvironment in tumoroids derived from CSLCs (Soubéran and Tchoghandjian 2020).

GBM-derived cerebral organoids

Human embryonic stem cells (hESCs) and induced pluripotent stem cells can be used to create GBM models obtained from cerebral organoids (hiPSCs) (Soubéran & Tchoghandjian, 2020). Patient-derived primary cultures, xenografts, and genetically modified glioblastomas were used to construct one of the first models to be cultivated organoids utilizing matrigel-based 3D culture methods. The cellular shape of these organoids has been shown to help monitor radiation resistance and GBM metastasis. GBM organoids can also be cryopreserved and define the histological characteristics, cellular diversity, and transcriptional profiles. Patient responses to chemotherapy and tumor development were examined by exposing GBM organoids to several treatment options. The lack of a normal brain microenvironment and vascular system, however, is one of the cons. Neoplastic cerebral organoids (neoCORs) were created to alter cerebral organoids genetically to promote GBM tumor growth. To develop tumors in iPSC-derived brain organoids, CRISPR-based genome editing techniques were applied. GBM organoids are primarily cancer cells, whereas neoCORs are tumors that are formed within cerebral organoids produced from iPSCs. As a result, neoCOR models can be used to study tumors in their early stages. Although its application is limited, CRISPR may be able to broaden its application because it effectively summarizes the heterogeneity of GBM. The glioblastoma cells used to create GLICOs (Glioblastoma Co-cultures) were cultured from patient tumor tissue under defined conditions to promote the maintenance of a stem cell phenotype. Although the GLICO model incorporates the advantages of the GBM organoids and neoCOR models, it suffers from the same flaws as other organoid-GBM models in terms of vascularization and immune cells (Zhang et al., 2020).

CSLCs became a focal point in GBM research after studies on mice revealed that they are more cancer-prone. In the 2D culture medium, primary CSLC spheroids do not properly reflect tumor invasion, microenvironment, interactions, or shape (Rybin et al., 2021). 3D organoid models were used to solve these flaws and provide a better comprehension of the cellular connections of GBM. In 3D organoid models, genetically modified transgenic mice, murine models, and patient-generated xenografts (PDX) are employed. PDX models that accurately reflect patient cancers, such as histological markers and invasiveness, are employed since transgenic models do not portray tumor complexity and heterogeneity well. PDX models using freshly resected tumors or CSLCs cultivated at different stages with a fluorescent marker protein or other genetic alteration accurately mimic 3D growth and GBM phenotyping. Despite these benefits, PDX has drawbacks such as excessive time, cost, and a lack of the microenvironment. To address these issues, some sophisticated organoid-GBM culture systems that are compatible with heterogeneity and microenvironment have been designed. Lancaster et al. were the first to try to make a cerebral organoid from hiPSCs or hESCs by producing embryoid bodies (EBs). The ectoderm germ layer is found in neural tissue, and EBs with neuroectoderm development were cultivated and placed in matrigel to achieve organoid structure. Next, the bioreactor was used to preserve and mature the organoid oxygen and nutrient absorption. Cerebral organoids differentiated over a period of 1-2 months and formed different parts of the brain. The progenitor region has been demonstrated by immunofluorescence staining using the neuron-specific class III beta-tubulin (TUJ1), which is used as a marker of neurons in the central and peripheral nervous systems from the early stage of neural differentiation, and the sex-determining region Y box 2 (SOX2), a well-known marker of neural stem and progenitor cells, and their function is self-renewal of these cells (Sun et al., 2021).

Cerebral-derived organoids can be used to examine the chronology of mutational steps, to investigate the developmental natural history of cancer ex vivo, to make more general analyses such as tumor proliferation, invasion and progression, as well as to investigate the interactions between tumor cells and non-neoplastic cells because they are cultured in the same culture dish. Due to the paucity of vascular structures and other cells in the microenvironment, these models lack histological characteristics such as microvascular growth and necrosis that are typical of GBMs (Soubéran & Tchoghandjian, 2020).

Discussion

GBM is the most common fatal brain tumor of the central nervous system, known for its poor prognosis and survival rate. GBMs, which can be pathologically primary and secondary, are derived from astrocytoma

or oligodendroglioma. This grade IV tumor is more likely to occur with age, and the average survival time is 15 months (Rock et al., 2012). GBM stem cells are difficult to treat as they enable more mutations to occur, and thus maintaining resistance to therapy and exhibit active DNA repair and regeneration properties (Stoyanov et al., 2018b). The classification by WHO as IDH-wild-type (90%) and IDH-mutant (10%) with a better prognosis was defined in 2016 (Batash et al., 2017). The typical treatment for this condition is TMZ and radiation, with MRI and CT used for diagnostic and treatment monitoring (Ali et al., 2020).

Looking at the molecular mechanism of GBM, *EGFR* amplification and *TERT* promoter mutations are found in 70% of IDH-wild-type tumors (Brennan et al., 2013). *PTEN* and *p53* mutations have also been found (Zheng et al., 2008). *PTEN* mutations are seen in 5-40% of GBMs, and they're more common in patients over 45 years old (Srividya et al., 2011). *PTEN* mutations decrease autophagic induction by activating the *PI3K/AKT/mTOR* pathway (Benitez et al., 2021). *Retinoblastoma (RB)* gene is mutated in most other cancers but only 6%–11% in GBM has been observed; therefore, therapy for *RB* mutations is not a common path. Furthermore, RTKs that enhance cancer cell aggressiveness, such as *MET, FGFR,* and *AXL*, or increased levels of growth hormones like VEGF, which promote the growth of GBSC-derived tumors, also raise the risk of GBM formation (Batchelor et al., 2013; Li et al., 2011). *TGF-β*, a tumor suppressor gene that regulates numerous biological processes and phosphorylates the prognostic Smad family protein, boosts the expression of *PDGF*, which controls the cell cycle, and ECM, which governs gene expression (Frei et al., 2015). Clinical trials, however, have failed due to the toxicity of TGF- β receptor inhibitors (le Rhun et al., 2019). Up-regulation of STAT3 protein from the STAT protein family, *IDH1* and *IDH2* mutations are also seen in the molecular mechanism of GBM. *MGMT*, which is found in 40% of GBMs and induces alterations in the expression of tumor suppressor genes like *PTEN, pRB,* and *p53*, is clearly one of the most important targets in GBM therapy (Aldape et al., 2015).

GBM is challenging to treat because of its various molecular subtypes and complexity. Although the outcome of treatment is dependent on several aspects such as the time of diagnosis and the patient's resistance, establishing a treatment is extremely challenging (Alifieris & Trafalis, 2015b). Although surgical resection is indicated in people under the age of 70, the tumor's location may influence the resection possibility (Gilard et al., 2021; Scott et al., 2011). Radiotherapy is used to eradicate residuals following surgical resection; however, it is not indicated for people over the age of 70 (Tan et al., 2020b). In addition to these treatments, various chemical compounds that might impact the GBM molecular mechanism have been explored. TMZ, CCNU, BCNU, and BVZ are FDA-approved and clinically available drugs. TMZ is the most favored chemotherapeutic drug in GBM treatment, notwithstanding its resistance to GBMs with *MGMT* activity (Karachi et al., 2018).

TE is a discipline that uses biocompatible treatments, including 3D printing biomaterials, nanotechnology, iPSCs, and gene editing approaches, to better understand and treat the disease. Although TE studies are beneficial because they minimize animal experiments in 3D use, make many cancer mechanisms more understandable, and the 3D structure more closely resembles the microenvironment of the real structure than cell culture, 3D mimicry of complicated tumors is extremely difficult (Burdett et al., 2010; Chandra et al., 2020). Many 3D models have been generated as a result of TE, including tumoroids, spheroids, organotypic slices, cerebral organoids, and tumorospheres, which are all commonly utilized in GBM treatment (Soubéran & Tchoghandjian, 2020).

Spheroids are a low-cost and morally favorable 3D model for preclinical testing of platinum-based antineoplastic medicines. Matrix-grown spheroids better reflect the microenvironment than suspension spheroids (Soubéran & Tchoghandjian, 2020). Using three different techniques: hanging drop, liquid overlay, and suspension culture, Froehlich et al. attempted to create tumor spheroids in three different mammary cell lines. According to the research, the hanging drop spheroid creation methodology is the preferred way since pellet formation in the liquid overlay technique is dependent on the kind of well, and the suspension culture technique results in spheroid size variance (Froehlich et al., 2017). In another study, a spheroid model of HA was co-cultured with tumor and healthy pancreatic cells in another investigation, because HA is known to be increased in tumors. As a result, the rate of cancer cell migration in the spheroids increased, and the cells became more sensitive to pharmacological treatment (Wong et al., 2019). Tumorospheres, another model for neural stem cells based on the self-renewal ability of stem cells, began to be developed and gave a better knowledge of CSLCs (Weiswald et al., 2015). In the research conducted by Zhao and colleagues, an elevated CLSC rate was observed when lung CLSCs were cultured to evaluate their lung cancer tumorosphere capacity. Additionally, lung tumorospheres demonstrated increased levels of proliferation, invasion, and drug resistance. In a prior in vivo study of GBM, CD133, a marker for neural stem cells, was similarly found to be elevated in tumorospheres (Salmaggi et al., 2006; W. Zhao et al., 2016). However, the other 3D model, organotypic slices, effectively captures the heterogeneity of GBM but does not fully replicate the tumor microenvironment (Soubéran & Tchoghandjian, 2020). The study of Marques-Torrejon et al. utilized organotypic slices, a method developed because completing the GBM model with *in vivo* transplantation is time- and money-inefficient. In this study, starting from the subependymal region where CLSCs are located, it has been shown that human CLSCs can be grafted into the mouse subependymal region. CD9 was also found to

be coupled with CD133, an astrocyte marker that has been shown to be raised in earlier research. As a result, distinct tumor behaviour in different brain regions have been mentioned. Organotypic slices, on the other hand, cannot be preserved for more than 3 weeks and can activate their immunity (Angeles et al., 2018). On the one hand, the approach of Sidorcenco et al. established an ex vivo GBM tissue slice tandem co-culture to test particular inhibitors. This method avoids the use of animals by using organotypic tissue fused with a tumor in the host microenvironment and entire tumor tissue from mice xenografts. For future GBM analysis, this study is preferable to spheroids (Sidorcenco et al., 2020). Explant modeling is made by culturing selected high-quality tumor cells and is utilized to detect parameters such as microenvironment, tumor profile, and differentiation; however, it lacks healthy tissue (Soubéran & Tchoghandjian, 2020). Because of the considerable molecular alterations occurring in GBM and the recent importance of CLSC vasculature in tumor growth, it does not adapt data from cell culture to the patient. A new 3D explant system was established in a study that enhanced the explant procedure by keeping the original structure of the tumor components, and it was highlighted that this system considerably improved the cytoarchitecture of the tumor stroma (Shimizu et al., 2011). Tumoroids and GBM-derived from cerebral organoids models are very popular because they accurately depict tumor features (Soubéran & Tchoghandjian, 2020). The heterogeneity of GBM makes it challenging to treat, as current *in vitro* models struggle to sustain mutational variety. GBOs (glioblastoma organoids) can be generated by analyzing the parent tumors particular to each patient and taking an intrusive approach to transplantation. They also underline that a biobank is required for this to be more basic (Jacob et al., 2020). Tatla et al., on the other hand, created an *in vitro* vascularized tumoroid model in order to study GBM angiogenesis. The model consists of a fibrin gel filled with easily produced and cost-effective endothelial cells (HUVEC) and GBM. Despite the model's lack of vascularity and BBB, the complexities of angiogenesis were accurately summarized, and CLSCs were discovered to enhance angiogenic sprouting when cultivated (Tatla et al., 2021).

Herein, a fatal primary brain tumor GBM and the possible TE applications are summarized. Many 3D models used are still under development and have provided important information about GBM. Organotypic slices reflect heterogeneity well, explants reflect many aspects of GBM, and tumoroids imitate the milieu well. Models constructed in the matrix, such as spheroids or tumorspheres, better reflect the 3D structure, giving us information about tumor spread. The development of these 3D models and the discovery of a treatment will take time. The ability of tumoroids to imitate the microenvironment, which is one of the most attractive 3D applications, as well as newly developed advanced models (for example, Organ-on-a-Chip and Four-Dimensional Bioprinting), may lead to increased interest in this sector.

Conclusion

GBM is a lethal primary brain tumor that has a poor prognosis and no treatment. The heterogeneous nature of GBM, its tendency for mutation, and the fact that it does not manifest itself in the same way in every patient make it challenging to develop a standard treatment. There are numerous studies on GBM treatment accessible. Tumoroids, spheroids, organotypic slices, cerebral organoids, scaffolds, organ-on-a-chip, and tumorospheres are examples of TE structures that have lately been used to better comprehend complicated diseases like cancer. The use of preclinical 3D models in these 3D approaches allows researchers to learn more about the GBM microenvironment by reducing *in vivo* approaches.

Author Contributions

MK: Investigation, Methodology, Writing; POY: Supervision, writing, review and editing.

Conflict of Interest

The author(s) declare that they have no known competing financial or non-financial, professional, or personal conflicts that could have appeared to influence the work reported in this paper.

References

Aldape, K., Zadeh, G., Mansouri, S., Reifenberger, G., & von Deimling, A. (2015). Glioblastoma: pathology, molecular mechanisms and markers. *Acta Neuropathologica*, *129*(6), 829–848. https://doi.org/10.1007/S00401-015-1432-1

Ali, M. Y., Oliva, C. R., Noman, A. S. M., Allen, B. G., Goswami, P. C., Zakharia, Y., Monga, V., Spitz, D. R., Buatti, J. M., & Griguer, C. E. (2020). Radioresistance in Glioblastoma and the Development of Radiosensitizers. *Cancers*, *12*(9), 1–29. https://doi.org/10.3390/CANCERS12092511

Alifieris, C., & Trafalis, D. T. (2015a). Glioblastoma multiforme: Pathogenesis and treatment. *Pharmacology & Therapeutics*, *152*, 63–82. https://doi.org/10.1016/J.PHARMTHERA.2015.05.005

Alifieris, C., & Trafalis, D. T. (2015b). Glioblastoma multiforme: Pathogenesis and treatment. *Pharmacology & Therapeutics*, *152*, 63–82. https://doi.org/10.1016/J.PHARMTHERA.2015.05.005

Angeles, M., Torrejon, M., Gangoso, E., & Pollard, S. M. (2018). Modelling glioblastoma tumour-host cell interactions using adult brain organotypic slice co-culture. *Disease Models & Mechanisms*, *11*(2). https://doi.org/10.1242/DMM.031435

Batash, R., Asna, N., Schaffer, P., Francis, N., & Schaffer, M. (2017). Glioblastoma Multiforme, Diagnosis and

Treatment; Recent Literature Review. *Current Medicinal Chemistry*, *24*(27). https://doi.org/10.2174/0929867324666170516123206

Batchelor, T. T., Mulholland, P., Neyns, B., Nabors, L. B., Campone, M., Wick, A., Mason, W., Mikkelsen, T., Phuphanich, S., Ashby, L. S., DeGroot, J., Gattamaneni, R., Cher, L., Rosenthal, M., Payer, F., Jürgensmeier, J. M., Jain, R. K., Sorensen, A. G., Xu, J., van den Bent, M. (2013). Phase III randomized trial comparing the efficacy of cediranib as monotherapy, and in combination with lomustine, versus lomustine alone in patients with recurrent glioblastoma. *Journal of Clinical Oncology : Official Journal of the American Society of Clinical Oncology*, *31*(26), 3212–3218. https://doi.org/10.1200/JCO.2012.47.2464

Benitez, J. A., Finlay, D., Castanza, A., Parisian, A. D., Ma, J., Longobardi, C., Campos, A., Vadla, R., Izurieta, A., Scerra, G., Koga, T., Long, T., Chavez, L., Mesirov, J. P., Vuori, K., & Furnari, F. (2021). PTEN deficiency leads to proteasome addiction: A novel vulnerability in glioblastoma. *Neuro-Oncology*, *23*(7), 1072–1086. https://doi.org/10.1093/NEUONC/NOAB001

Brennan, C. W., Verhaak, R. G. W., McKenna, A., Campos, B., Noushmehr, H., Salama, S. R., Zheng, S., Chakravarty, D., Sanborn, J. Z., Berman, S. H., Beroukhim, R., Bernard, B., Wu, C. J., Genovese, G., Shmulevich, I., Barnholtz-Sloan, J., Zou, L., Vegesna, R., Shukla, S. A., McLendon, R. (2013). The somatic genomic landscape of glioblastoma. *Cell*, *155*(2), 462. https://doi.org/10.1016/J.CELL.2013.09.034

Bruns, J., Silviya, &, & Zustiak, P. (2021). Hydrogel-Based Spheroid Models of Glioblastoma for Drug Screening Applications. *Missouri Medicine*, *118*(4), 346. /pmc/articles/PMC8343644/

Burdett, E., Kasper, F. K., Mikos, A. G., & Ludwig, J. A. (2010). Engineering tumors: a tissue engineering perspective in cancer biology. *Tissue Engineering. Part B, Reviews*, *16*(3), 351–359. https://doi.org/10.1089/TEN.TEB.2009.0676

Carlsson, S. K., Brothers, S. P., & Wahlestedt, C. (2014). Emerging treatment strategies for glioblastoma multiforme. *EMBO Molecular Medicine*, *6*(11), 1359–1370. https://doi.org/10.15252/EMMM.201302627

Chandra, P. K., Soker, S., & Atala, A. (2020). Tissue engineering: current status and future perspectives. *Principles of Tissue Engineering*, 1–35. https://doi.org/10.1016/B978-0-12-818422-6.00004-6

Chi, A. S., Batchelor, T. T., Kwak, E. L., Clark, J. W., Wang, D. L., Wilner, K. D., Louis, D. N., & Iafrate, A. J. (2012). Rapid radiographic and clinical improvement after treatment of a MET-amplified recurrent glioblastoma with a mesenchymal-epithelial transition inhibitor. *Journal of Clinical Oncology : Official Journal of the American Society of Clinical Oncology*, *30*(3). https://doi.org/10.1200/JCO.2011.38.4586

Chua, J., Nafziger, E., & Leung, D. (2019). Evidence-Based Practice: Temozolomide Beyond Glioblastoma. *Current Oncology Reports*, *21*(4). https://doi.org/10.1007/S11912-019-0783-5

Denny, B. J., Tsang, L. L. H., Slack, J. A., Wheelhouse, R. T., & Stevens, M. F. G. (1994). NMR and molecular modeling investigation of the mechanism of activation of the antitumor drug temozolomide and its interaction with DNA. *Biochemistry*, *33*(31), 9045–9051. https://doi.org/10.1021/BI00197A003

Duvall, C. L., Prokop, A., Gersbach, C. A., & Davidson, J. M. (2013a). Gene Delivery into Cells and Tissues. In *Principles of Tissue Engineering: Fourth Edition*. Elsevier Inc. https://doi.org/10.1016/B978-0-12-398358-9.00035-5

Duvall, C. L., Prokop, A., Gersbach, C. A., & Davidson, J. M. (2013b). Gene Delivery into Cells and Tissues. In *Principles of Tissue Engineering: Fourth Edition*. Elsevier Inc. https://doi.org/10.1016/B978-0-12-398358-9.00035-5

Enderle, J. D., & Bronzino, J. D. (2011). Introduction to Biomedical Engineering. *Introduction to Biomedical Engineering*, 1–1253. https://doi.org/10.1016/C2009-0-19716-7

Ermoian, R. P., Furniss, C. S., Lamborn, K. R., Basila, D., Berger, M. S., Gottschalk, A. R., Nicholas, M. K., Stokoe, D., & Haas-Kogan, D. A. (2002). Dysregulation of PTEN and protein kinase B is associated with glioma histology and patient survival. *Clinical Cancer Research : An Official Journal of the American Association for Cancer Research*, *8*(5), 1100–1106.

Fisher, J. P., & Adamson, D. C. (2021). Current FDA-Approved Therapies for High-Grade Malignant Gliomas. *Biomedicines*, *9*(3). https://doi.org/10.3390/BIOMEDICINES9030324

Frei, K., Gramatzki, D., Tritschler, I., Schroeder, J. J., Espinoza, L., Rushing, E. J., & Weller, M. (2015). Transforming growth factor-β pathway activity in glioblastoma. *Oncotarget*, *6*(8), 5963. https://doi.org/10.18632/ONCOTARGET.3467

Froehlich, K., Haeger, J.-D., Heger, J., Pastuschek, J., Photini, S. M., Yan, Y., Lupp, A., Pfarrer, C., Mrowka, R., Schleußner, E., Markert, U. R., & Schmidt, A. (n.d.). Generation of Multicellular Breast Cancer Tumor Spheroids: Comparison of Different Protocols. *Journal of Mammary Gland Biology and Neoplasia*. https://doi.org/10.1007/s10911-016-9359-2

Gedeon, P. C., Schaller, T. H., Chitneni, S. K., Choi, B. D., Kuan, C. T., Suryadevara, C. M., Snyder, D. J., Schmittling, R. J., Szafranski, S. E., Cui, X., Healy, P. N., Herndon, J. E., McLendon, R. E., Keir, S. T., Archer, G. E., Reap, E. A., Sanchez-Perez, L., Bigner, D. D., & Sampson, J. H. (2018). A Rationally Designed Fully Human EGFRvIII:CD3-Targeted Bispecific Antibody Redirects Human T Cells to Treat Patient-derived Intracerebral Malignant Glioma. *Clinical Cancer Research : An Official Journal of the American Association for Cancer Research*, *24*(15), 3611–3631. https://doi.org/10.1158/1078-0432.CCR-17-0126

Gilard, V., Tebani, A., Dabaj, I., Laquerrière, A., Fontanilles, M., Derrey, S., Marret, S., & Bekri, S. (2021). Diagnosis and Management of Glioblastoma: A Comprehensive Perspective. *Journal of Personalized Medicine 2021, Vol. 11, Page 258*, *11*(4), 258. https://doi.org/10.3390/JPM11040258

Groszer, M., Erickson, R., Scripture-Adams, D. D., Dougherty, J. D., Le Belle, J., Zack, J. A., Geschwind, D. H., Liu, X., Kornblum, H. I., & Wu, H. (2006). PTEN negatively regulates neural stem cell self-renewal by modulating G0-G1 cell cycle entry. *Proceedings of the National Academy of Sciences of the United States of America*, *103*(1), 111–116. https://doi.org/10.1073/PNAS.0509939103

Horn, S., Figl, A., Rachakonda, P. S., Fischer, C., Sucker, A., Gast, A., Kadel, S., Moll, I., Nagore, E., Hemminki, K., Schadendorf, D., & Kumar, R. (2013). TERT promoter mutations in familial and sporadic melanoma. *Science*, *339*(6122), 959–961. https://doi.org/10.1126/science.1230062

Iacob, G., & Dinca, E. B. (2009). Current data and strategy in glioblastoma multiforme. *Journal of Medicine and Life*, *2*(4), 386.

Jacob, F., Salinas, R. D., Zhang, D. Y., Nguyen, P. T. T., Schnoll, J. G., Wong, S. Z. H., Thokala, R., Sheikh, S., Saxena, D., Prokop, S., Liu, D. ao, Qian, X., Petrov, D., Lucas, T., Chen, H. I., Dorsey, J. F., Christian, K. M., Binder, Z. A., Nasrallah, M., Song, H. (2020). A Patient-Derived Glioblastoma Organoid Model and Biobank Recapitulates Inter- and Intra-tumoral Heterogeneity. *Cell*, *180*(1), 188. https://doi.org/10.1016/J.CELL.2019.11.036

Jin, G., Reitman, Z. J., Duncan, C. G., Spasojevic, I., Gooden, D. M., Rasheed, B. A., Yang, R., Lopez, G. Y., He, Y., McLendon, R. E., Bigner, D. D., & Yan, H. (2013). Disruption of wild type IDH1 suppresses D-2-hydroxyglutarate production in IDH1-mutated gliomas. *Cancer Research*, *73*(2), 496. https://doi.org/10.1158/0008-5472.CAN-12-2852

Karachi, A., Dastmalchi, F., Mitchell, D. A., & Rahman, M. (2018). Temozolomide for immunomodulation in the treatment of glioblastoma. *Neuro-Oncology*, *20*(12), 1566. https://doi.org/10.1093/NEUONC/NOY072

Kardan, A., & Satter, M. (2016). Advanced Methionine Positron-Emission Tomography Imaging for Brain Tumor Diagnosis, Surgical Planning, and Treatment. *Handbook of Neuro-Oncology Neuroimaging: Second Edition*, 371–384. https://doi.org/10.1016/B978-0-12-800945-1.00034-3

Kim, J., Lee, Y., Cho, H. J., Lee, Y. E., An, J., Cho, G. H., Ko, Y. H., Joo, K. M., & Nam, D. H. (2014). NTRK1 Fusion in Glioblastoma Multiforme. *PLOS ONE*, *9*(3), e91940. https://doi.org/10.1371/JOURNAL.PONE.0091940

Kim, M. M., Umemura, Y., & Leung, D. (2018). Bevacizumab and Glioblastoma: Past, Present, and Future Directions. *Cancer Journal (Sudbury, Mass.)*, *24*(4), 180–186. https://doi.org/10.1097/PPO.0000000000000326

Kleihues, P., & Ohgaki, H. (1999). Primary and secondary glioblastomas: from concept to clinical diagnosis. *Neuro-Oncology*, *1*(1), 44–51. https://doi.org/10.1093/NEUONC/1.1.44

le Rhun, E., Preusser, M., Roth, P., Reardon, D. A., van den Bent, M., Wen, P., Reifenberger, G., & Weller, M. (2019). Molecular targeted therapy of glioblastoma. *Cancer Treatment Reviews*, *80*. https://doi.org/10.1016/J.CTRV.2019.101896

Li, Y., Li, A., Glas, M., Lal, B., Ying, M., Sang, Y., Xia, S., Trageser, D., Guerrero-Cázares, H., Eberhart, C. G., Quiñones-Hinojosa, A., Scheffler, B., & Laterra, J. (2011). c-Met signaling induces a reprogramming network and supports the glioblastoma stem-like phenotype. *Proceedings of the National Academy of Sciences of the United States of America*, *108*(24), 9951–9956. https://doi.org/10.1073/pnas.1016912108

Ma, D. J., Galanis, E., Anderson, S. K., Schiff, D., Kaufmann, T. J., Peller, P. J., Giannini, C., Brown, P. D., Uhm, J. H., McGraw, S., Jaeckle, K. A., Flynn, P. J., Ligon, K. L., Buckner, J. C., & Sarkaria, J. N. (2015). A phase II trial of everolimus, temozolomide, and radiotherapy in patients with newly diagnosed glioblastoma: NCCTG N057K. *Neuro-Oncology*, *17*(9), 1261–1269. https://doi.org/10.1093/NEUONC/NOU328

Mao, H., Lebrun, D. G., Yang, J., Zhu, V. F., & Li, M. (2012). Deregulated signaling pathways in glioblastoma multiforme: molecular mechanisms and therapeutic targets. *Cancer Investigation*, *30*(1), 48–56. https://doi.org/10.3109/07357907.2011.630050

Masui, K., Mischel, P. S., & Reifenberger, G. (2016). Molecular classification of gliomas. *Handbook of Clinical Neurology*, *134*, 97–120. https://doi.org/10.1016/B978-0-12-802997-8.00006-2

Montemurro, N. (2020). Glioblastoma Multiforme and Genetic Mutations: The Issue Is Not Over Yet. An Overview of the Current Literature. *Journal of Neurological Surgery. Part A, Central European Neurosurgery*, *81*(1), 64–70. https://doi.org/10.1055/S-0039-1688911

Nam, J. Y., & De Groot, J. F. (2017). Treatment of Glioblastoma. *Journal of Oncology Practice*, *13*(10), 629–638. https://doi.org/10.1200/JOP.2017.025536

Nejo, T., Mende, A., & Okada, H. (2020). The current state of immunotherapy for primary and secondary brain tumors: similarities and differences. *Japanese Journal of Clinical Oncology*, *50*(11), 1331–1345. https://doi.org/10.1093/JJCO/HYAA164

Norden, A. D., & Wen, P. Y. (2006). Glioma therapy in adults. *The Neurologist*, *12*(6), 279–292. https://doi.org/10.1097/01.NRL.0000250928.26044.47

Ohgaki, H., Dessen, P., Jourde, B., Horstmann, S., Nishikawa, T., Di Patre, P. L., Burkhard, C., Schüler, D., Probst-Hensch, N. M., Maiorka, P. C., Baeza, N., Pisani, P., Yonekawa, Y., Yasargil, M. G., Lütolf, U. M., & Kleihues, P. (2004). Genetic pathways to glioblastoma: a population-based study. *Cancer Research*, *64*(19), 6892–6899. https://doi.org/10.1158/0008-5472.CAN-04-1337

O'Rourke, D. M., Nasrallah, M. P., Desai, A., Melenhorst, J. J., Mansfield, K., Morrissette, J. J. D., Martinez-Lage, M., Brem, S., Maloney, E., Shen, A., Isaacs, R., Mohan, S., Plesa, G., Lacey, S. F., Navenot, J. M., Zheng, Z., Levine, B. L., Okada, H., June, C. H., … Maus, M. V. (2017). A single dose of peripherally infused EGFRvIII-directed CAR T cells mediates antigen loss and induces adaptive resistance in patients with recurrent glioblastoma. *Science Translational Medicine*, *9*(399). https://doi.org/10.1126/SCITRANSLMED.AAA0984

Ou, A., Alfred Yung, W. K., & Majd, N. (2021). Molecular Mechanisms of Treatment Resistance in Glioblastoma. *International Journal of Molecular Sciences*, *22*(1), 1–24. https://doi.org/10.3390/IJMS22010351

Parker, J. J., Lizarraga, M., Waziri, A., & Foshay, K. M. (2017). A Human Glioblastoma Organotypic Slice Culture Model for Study of Tumor Cell Migration and Patient-specific Effects of Anti-Invasive Drugs. *Journal of Visualized Experiments : JoVE*, *2017*(125), 53557. https://doi.org/10.3791/53557

Peralta-Arrieta, I., Trejo-Villegas, O. A., Armas-López, L., Ceja-Rangel, H. A., Ordóñez-Luna, M. del C., Pineda-Villegas, P., González-López, M. A., Ortiz-Quintero, B., Mendoza-Milla, C., Zatarain-Barrón, Z. L., Arrieta, O., Zúñiga, J., & Ávila-Moreno, F. (2022). Failure to EGFR-TKI-based therapy and tumoural progression are promoted by MEOX2/GLI1-mediated epigenetic regulation of EGFR in

the human lung cancer. *European Journal of Cancer (Oxford, England : 1990)*, *160*, 189–205. https://doi.org/10.1016/J.EJCA.2021.10.032

Perry, A., & Wesseling, P. (2016). Histologic classification of gliomas. *Handbook of Clinical Neurology*, *134*, 71–95. https://doi.org/10.1016/B978-0-12-802997-8.00005-0

Reardon, D. A., & Wen, P. Y. (2006). Therapeutic advances in the treatment of glioblastoma: rationale and potential role of targeted agents. *The Oncologist*, *11*(2), 152–164. https://doi.org/10.1634/THEONCOLOGIST.11-2-152

Rock, K., McArdle, O., Forde, P., Dunne, M., Fitzpatrick, D., O'Neill, B., & Faul, C. (2012). A clinical review of treatment outcomes in glioblastoma multiforme--the validation in a non-trial population of the results of a randomised Phase III clinical trial: has a more radical approach improved survival? *The British Journal of Radiology*, *85*(1017). https://doi.org/10.1259/BJR/83796755

Rybin, M. J., Ivan, M. E., Ayad, N. G., & Zeier, Z. (2021). Organoid Models of Glioblastoma and Their Role in Drug Discovery. *Frontiers in Cellular Neuroscience*, *15*, 605255. https://doi.org/10.3389/FNCEL.2021.605255

Salmaggi, A., Boiardi, A., Gelati, M., Russo, A., Calatozzolo, C., Ciusani, E., Sciacca, F. L., Ottolina, A., Parati, E. A., la Porta, C., Alessandri, G., Marras, C., Croci, D., & de Rossi, M. (2006). Glioblastoma-derived tumorospheres identify a population of tumor stem-like cells with angiogenic potential and enhanced multidrug resistance phenotype. *Glia*, *54*(8), 850–860. https://doi.org/10.1002/GLIA.20414

Sasmita, A. O., Wong, Y. P., & Ling, A. P. K. (2018). Biomarkers and therapeutic advances in glioblastoma multiforme. *Asia-Pacific Journal of Clinical Oncology*, *14*(1), 40–51. https://doi.org/10.1111/AJCO.12756

Scott, J., Tsai, Y. Y., Chinnaiyan, P., & Yu, H. H. M. (2011). Effectiveness of radiotherapy for elderly patients with glioblastoma. *International Journal of Radiation Oncology, Biology, Physics*, *81*(1), 206–210. https://doi.org/10.1016/J.IJROBP.2010.04.033

Shah, J. L., Li, G. H., & Soltys, S. G. (2021). Glioblastoma Multiforme. *CyberKnife Stereotactic Radiosurgery: Brain*, *1*, 85–98. https://doi.org/10.22290/jbnc.v24i1.1481

Shimizu, F., Hovinga, K. E., Metzner, M., Soulet, D., & Tabar, V. (2011). Organotypic explant culture of glioblastoma multiforme and subsequent single-cell suspension. *Current Protocols in Stem Cell Biology*, *Chapter 3*(SUPPL.19). https://doi.org/10.1002/9780470151808.SC0305S19

Sidorcenco, V., Krahnen, L., Schulz, M., Remy, J., Kögel, D., Temme, A., Krügel, U., Franke, H., & Aigner, A. (2020). Glioblastoma Tissue Slice Tandem-Cultures for Quantitative Evaluation of Inhibitory Effects on Invasion and Growth. *Cancers*, *12*(9), 1–15. https://doi.org/10.3390/CANCERS12092707

Smith, J. S., Tachibana, I., Passe, S. M., Huntley, B. K., Borell, T. J., Iturria, N., O'Fallon, J. R., Schaefer, P. L., Scheithauer, B. W., James, C. D., Buckner, J. C., & Jenkins, R. B. (2001). PTEN mutation, EGFR amplification, and outcome in patients with anaplastic astrocytoma and glioblastoma multiforme. *Journal of the National Cancer Institute*, *93*(16), 1246–1256. https://doi.org/10.1093/jnci/93.16.1246

Soubéran, A., & Tchoghandjian, A. (2020). Practical Review on Preclinical Human 3D Glioblastoma Models: Advances and Challenges for Clinical Translation. *Cancers*, *12*(9), 1–21. https://doi.org/10.3390/CANCERS12092347

Srividya, M. R., Thota, B., Shailaja, B. C., Arivazhagan, A., Thennarasu, K., Chandramouli, B. A., Hegde, A. S., & Santosh, V. (2011). Homozygous 10q23/PTEN deletion and its impact on outcome in glioblastoma: a prospective translational study on a uniformly treated cohort of adult patients. *Neuropathology : Official Journal of the Japanese Society of Neuropathology*, *31*(4), 376–383. https://doi.org/10.1111/J.1440-1789.2010.01178.X

Stoyanov, G. S., Dzhenkov, D., Ghenev, P., Iliev, B., Enchev, Y., & Tonchev, A. B. (2018a). Cell biology of glioblastoma multiforme: from basic science to diagnosis and treatment. *Medical Oncology (Northwood, London, England)*, *35*(3). https://doi.org/10.1007/S12032-018-1083-X

Stoyanov, G. S., Dzhenkov, D., Ghenev, P., Iliev, B., Enchev, Y., & Tonchev, A. B. (2018b). Cell biology of glioblastoma multiforme: from basic science to diagnosis and treatment. *Medical Oncology (Northwood, London, England)*, *35*(3). https://doi.org/10.1007/S12032-018-1083-X

Sun, N., Meng, X., Liu, Y., Song, D., Jiang, C., & Cai, J. (2021). Applications of brain organoids in neurodevelopment and neurological diseases. *Journal of Biomedical Science 2021 28:1*, *28*(1), 1–16. https://doi.org/10.1186/S12929-021-00728-4

Takahashi, M., Miki, S., Fujimoto, K., Fukuoka, K., Matsushita, Y., Maida, Y., Yasukawa, M., Hayashi, M., Shinkyo, R., Kikuchi, K., Mukasa, A., Nishikawa, R., Tamura, K., Narita, Y., Hamada, A., Masutomi, K., & Ichimura, K. (2019). Eribulin penetrates brain tumor tissue and prolongs survival of mice harboring intracerebral glioblastoma xenografts. *Cancer Science*, *110*(7), 2247. https://doi.org/10.1111/CAS.14067

Tan, A. C., Ashley, D. M., López, G. Y., Malinzak, M., Friedman, H. S., & Khasraw, M. (2020a). Management of glioblastoma: State of the art and future directions. *CA: A Cancer Journal for Clinicians*, *70*(4), 299–312. https://doi.org/10.3322/CAAC.21613

Tan, A. C., Ashley, D. M., López, G. Y., Malinzak, M., Friedman, H. S., & Khasraw, M. (2020b). Management of glioblastoma: State of the art and future directions. *CA: A Cancer Journal for Clinicians*, *70*(4), 299–312. https://doi.org/10.3322/CAAC.21613

Tatla, A. S., Justin, A. W., Watts, C., & Markaki, A. E. (2021). A vascularized tumoroid model for human glioblastoma angiogenesis. *Scientific Reports*, *11*(1), 19550. https://doi.org/10.1038/S41598-021-98911-Y

Tsang, L. L. H., Farmer, P. B., Gescher, A., & Slack, J. A. (1990). Characterisation of urinary metabolites of temozolomide in humans and mice and evaluation of their cytotoxicity. *Cancer Chemotherapy and Pharmacology*, *26*(6), 429–436. https://doi.org/10.1007/BF02994094

Uddin, M. S., Mamun, A. Al, Alghamdi, B. S., Tewari, D., Jeandet, P., Sarwar, M. S., & Ashraf, G. M. (2020). Epigenetics of glioblastoma multiforme: From molecular mechanisms to therapeutic approaches. *Seminars in Cancer Biology*. https://doi.org/10.1016/J.SEMCANCER.2020.12.015

Van Den Bent, M. J., Gao, Y., Kerkhof, M., Kros, J. M., Gorlia, T., Van Zwieten, K., Prince, J., Van Duinen, S., Sillevis Smitt, P. A., Taphoorn, M., & French, P. J. (2015). Changes in the EGFR amplification and EGFRvIII expression between paired primary and recurrent glioblastomas. *Neuro-Oncology*, *17*(7), 935–941. https://doi.org/10.1093/NEUONC/NOV013

Weiswald, L. B., Bellet, D., & Dangles-Marie, V. (2015). Spherical Cancer Models in Tumor Biology. *Neoplasia (New York, N.Y.)*, *17*(1), 1. https://doi.org/10.1016/J.NEO.2014.12.004

Weller, M., Butowski, N., Tran, D. D., Recht, L. D., Lim, M., Hirte, H., Ashby, L., Mechtler, L., Goldlust, S. A., Iwamoto, F., Drappatz, J., O'Rourke, D. M., Wong, M., Hamilton, M. G., Finocchiaro, G., Perry, J., Wick, W., Green, J., He, Y., Nag, S. (2017). Rindopepimut with temozolomide for patients with newly diagnosed, EGFRvIII-expressing glioblastoma (ACT IV): a randomised, double-blind, international phase 3 trial. *The Lancet. Oncology*, *18*(10), 1373–1385. https://doi.org/10.1016/S1470-2045(17)30517-X

Wen, P. Y., Schiff, D., Cloughesy, T. F., Raizer, J. J., Laterra, J., Smitt, M., Wolf, M., Oliner, K. S., Anderson, A., Zhu, M., Loh, E., & Reardon, D. A. (2011). A phase II study evaluating the efficacy and safety of AMG 102 (rilotumumab) in patients with recurrent glioblastoma. *Neuro-Oncology*, *13*(4), 437–446. https://doi.org/10.1093/NEUONC/NOQ198

Wick, W., Gorlia, T., Bady, P., Platten, M., Van Den Bent, M. J., Taphoorn, M. J. B., Steuve, J., Brandes, A. A., Hamou, M. F., Wick, A., Kosch, M., Weller, M., Stupp, R., Roth, P., Golfinopoulos, V., Frene, J. S., Campone, M., Ricard, D., Marosi, C., Hegi, M. E. (2016). Phase II Study of Radiotherapy and Temsirolimus versus Radiochemotherapy with Temozolomide in Patients with Newly Diagnosed Glioblastoma without MGMT Promoter Hypermethylation (EORTC 26082). *Clinical Cancer Research : An Official Journal of the American Association for Cancer Research*, *22*(19), 4797–4806. https://doi.org/10.1158/1078-0432.CCR-15-3153

Wong, C. W., Han, H. W., Tien, Y. W., & Hsu, S. hui. (2019). Biomaterial substrate-derived compact cellular spheroids mimicking the behavior of pancreatic cancer and microenvironment. *Biomaterials*, *213*. https://doi.org/10.1016/J.BIOMATERIALS.2019.05.013

Xu, C., Wu, X., & Zhu, J. (2013). VEGF promotes proliferation of human glioblastoma multiforme stem-like cells through VEGF receptor 2. *TheScientificWorldJournal*, *2013*. https://doi.org/10.1155/2013/417413

Yan, H., Parsons, D. W., Jin, G., McLendon, R., Rasheed, B. A., Yuan, W., Kos, I., Batinic-Haberle, I., Jones, S., Riggins, G. J., Friedman, H., Friedman, A., Reardon, D., Herndon, J., Kinzler, K. W., Velculescu, V. E., Vogelstein, B., & Bigner, D. D. (2009). IDH1 and IDH2 Mutations in Gliomas. *The New England Journal of Medicine*, *360*(8), 765. https://doi.org/10.1056/NEJMOA0808710

Zeng, A., Hu, Q., Liu, Y., Wang, Z., Cui, X., Li, R., Yan, W., & You, Y. (2015). IDH1/2 mutation status combined with Ki-67 labeling index defines distinct prognostic groups in glioma. *Oncotarget*, *6*(30), 30232. https://doi.org/10.18632/ONCOTARGET.4920

Zhang, C., Jin, M., Zhao, J., Chen, J., & Jin, W. (2020). Organoid models of glioblastoma: advances, applications and challenges. *American Journal of Cancer Research*, *10*(8), 2242. /pmc/articles/PMC7471358/

Zhao, Q., Shi, X., Xie, Y., Huang, J., BenShia, C., & Ma, S. (2015). Combining multidimensional genomic measurements for predicting cancer prognosis: observations from TCGA. *Briefings in Bioinformatics*, *16*(2), 291–303. https://doi.org/10.1093/BIB/BBU003

Zhao, W., Luo, Y., Li, B., & Zhang, T. (2016). Tumorigenic lung tumorospheres exhibit stem-like features with significantly increased expression of CD133 and ABCG2. *Molecular Medicine Reports*, *14*(3), 2598–2606. https://doi.org/10.3892/MMR.2016.5524

Zheng, H., Ying, H., Yan, H., Kimmelman, A. C., Hiller, D. J., Chen, A. J., Perry, S. R., Tonon, G., Chu, G. C., Ding, Z., Stommel, J. M., Dunn, K. L., Wiedemeyer, R., You, M. J., Brennan, C., Wang, Y. A., Ligon, K. L., Wong, W. H., Chin, L., & DePinho, R. A. (2008). p53 and Pten control neural and glioma stem/progenitor cell renewal and differentiation. *Nature*, *455*(7216), 1129–1133. https://doi.org/10.1038/NATURE07443

Zhu, H., Wang, H., Huang, Q., Liu, Q., Guo, Y., Lu, J., Li, X., Xue, C., & Han, Q. (2018). Transcriptional Repression of p53 by PAX3 Contributes to Gliomagenesis and Differentiation of Glioma Stem Cells. *Frontiers in Molecular Neuroscience*, *11*. https://doi.org/10.3389/FNMOL.2018.00187

Biotech Studies 33(1), 67-73
http://doi.org/10.38042/biotechstudies.1472022

BIOTECH STUDIES

RESEARCH PAPER

Rhein inhibits cell proliferation of glioblastoma multiforme cells by regulating the TGF-ß and apoptotic signaling pathways

Sümeyra Çetinkaya

Biotechnology Research Center, Field Crops Central Research Institute, 06170, Ankara, Türkiye

How to cite:
Çetinkaya, S. (2024). Rhein inhibits cell proliferation of glioblastoma multiforme cells by regulating the TGF-ß and apoptotic signaling pathways. *Biotech Studies*, *33*(1), 67-73. http://doi.org/10.38042/biotechstudies.1472022.

Article History
Received 10 September 2023
Accepted 26 March 2024
First Online 22 April 2024

Corresponding Author
Tel.: +09 541 575 31 96
E-mail:
sumeyracetinkaya0@gmail.com

Keywords
Apoptosis
Cell viability
Colony formation
Rhein
TGF-ß

Abstract

Rhein (4,5-dihydroxyanthraquinone-2-carboxylic acid) is a plant metabolite found in rhubarbs. It inhibits cell proliferation and stimulates apoptosis in *in vivo* and *in vitro*. However, research into the molecular mechanisms of action is insufficient for recommending it as a therapeutic agent. Therefore, this study aims to investigate the antiproliferative, apoptotic, and antimetastatic effects of rhein by targeting the TGF-β signaling pathway, and apoptotic pathway in glioblastoma cells (U87 GBM). In this study, the XTT assay was utilized to determine cell viability, the colony formation assay to measure cell survival and proliferation, RT-qPCR for the analysis of gene expressions, and ELISA for the detection of proteins. U87 GBM cells were treated with varying concentrations of rhein (5-100 µM) in a time-dependent manner (24, 48 h), after which the percentage of cell viability was calculated. The colony formation assay was performed by treating cells with the IC_{50} dose of rhein. According to the XTT assay, the IC_{50} dose of rhein was determined as 10 µM at 24 h. The ability to form colonies was significantly decreased in the cells of the treatment group. According to the gene expression analysis, rhein increased the mRNA levels of *CASP3*, *-8*, *-9*, *BAX,* and *TGF-ß1* genes, while a notable decrease was observed in the *BCL-2*, *SMAD2*, *SMAD3,* and *TIMP1* genes. In conclusion, it was determined that rhein induces apoptosis via the non-canonical TGF-β pathway.

Introduction

Rhein, scientifically known as 4,5-dihydroxyanthraquinone-2-carboxylic acid, represents a lipophilic anthraquinone compound identified as a metabolite in various plants, including the *Rheum* species (*R. tanguticum, R. officinale, R. palmatum* L.) (Polygonaceae), *Cassia tora* L. (Fabaceae), *Polygonum multiflorum* Thunb., *Aloe barbadensis* Miller (Asphodelaceae) and *P. cuspidatum* (Polygonaceae) (**Figure 1**) (Zhou et al., 2015). From an ethnobotanical perspective, these plants are traditionally used for treating inflammation, diabetes, bacterial, and helminthic infections (Henamayee et al., 2020). Pharmacologically, several studies have demonstrated its hepatoprotective (Bu et al., 2018), nephroprotective (Meng et al., 2015), anti-inflammatory (Wang et al., 2020), antioxidant (Xu et al., 2017), anticancer (Henamayee et al., 2020), and antimicrobial (Nguyen & Kim, 2020) activities. Because of these bioactivities, its use in the treatment and prevention of various diseases, such as osteoarthritis, hepatic disorders, and cancer, has been extensively researched.

Despite recent significant advances in cancer treatment, the search for therapeutic agents from plant-derived sources continues to be popular due to drug resistance and lower side effects (Atanasov et al., 2015). In this regard, chemotherapeutic drugs such as paclitaxel (taxol), vincristine, vinblastine, and docetaxel are effective drugs that are still used clinically (Habtemariam & Lentini, 2018). Rhein has been found to suppress the growth and proliferation of diverse

cancers, such as breast cancer (Chang et al., 2012), pancreatic cancer (Yang et al., 2019), hepatocellular carcinoma (Wang et al., 2020), colon cancer (Zhang et al., 2021), and lung cancer (Yang et al., 2019). These studies have determined that rhein can modulate different signaling steps in its molecular action mechanisms, thereby stimulating cell apoptosis and suppressing invasion and metastasis. Considering the current information, studies on the potential of rhein to be a therapeutic agent against cancer are intriguing. However, studies that elucidate its mechanism of action at the cellular and molecular levels are insufficient to recommend it as an effective therapeutic agent.

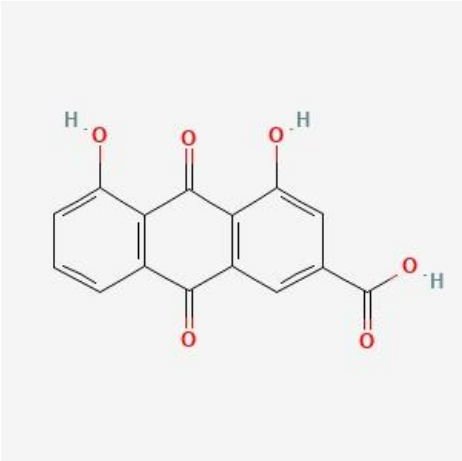

Figure 1. Chemical structure of the rhein (http://www.chemspider.com/Chemical-Structure.9762.html).

In recent times, within the context of discovering potential therapeutic agents, the transforming growth factor-β (TGF-β) signaling pathway has emerged as a major focus due to its key roles in diseases such as pancreatic cancer and its dual functionality (Tewari et al., 2022). This pathway is intricately linked to apoptotic processes, serving as a critical mediator in both promoting and inhibiting cell death, depending on the cellular context (Ramesh et al., 2009). The TGF-β pathway, through its complex interactions with downstream molecules, can trigger apoptosis by influencing the expression of genes directly involved in the cell death mechanism (Sánchez-Capelo, 2005). In light of this, the current study seeks to delve into the antiproliferative, apoptotic, and antimetastatic effects of rhein on glioblastoma cells (U87 GBM) by specifically targeting the TGF-β signaling and apoptotic pathways. Toward this goal, an extensive analysis has been conducted on the effects of rhein against U87 GBM cells, focusing on cell survival, proliferation, apoptotic, and metastatic effects regulated through the TGF-β pathway. For the gene expression changes, the expressions of *TGF-β1, SMAD1, SMAD2,* and *TIMP1*, which are associated with the TGF-β pathways, as well as apoptotic-related genes *CASP3, CASP8, CASP9, BAX,* and *BCL-2*, have been examined. This provides an understanding of how TGF-β signaling can direct cellular fate towards apoptosis. The ability of cancer cells to form colonies is considered a significant indicator of their proliferation and metastatic potential, reflecting the progression of the disease and the capacity to develop resistance to treatment. Inhibiting colony formation can prevent the spread of cancer cells and the growth of tumors, thereby enhancing the effectiveness of therapeutic strategies and aiding in the control of the disease. In this context, the colony-forming capacity of U87 GBM cells and the effect of rhein on this capacity have been investigated.

Materials and Methods

Cell culture and treatment

The U87 GBM cell line was obtained from the American Type Culture Collection (ATCC) (Virginia, USA). The cells were grown in Dulbecco's Modified Eagle Medium (DMEM-F12) (Sigma-Aldrich, USA) enriched with 10% fetal bovine serum (FBS) (Capricorn, Germany) and 100 U/ml of penicillin-streptomycin (10 mg/mL) (Capricorn Scientific, Ebsdorfergrund, Germany). The cells cultivated at a temperature of 37°C and a CO_2 level of 5%. Rhein was purchased from Sigma-Aldrich (R7269 Merck; Germany) and dissolved in 0.1% DMSO at room temperature to make a stock solution. The solution was then stored at -20°C until used.

Cell viability assay

The XTT cell proliferation assay was employed to determine the cytotoxic effect of rhein on U87 cells, according to the manufacturer's instructions (Biological Industries, 20-300-1000). U87 cells were seeded ($2x10^3$ cells/well) into 96-well plates. U87 cells were distributed into 96-well plates at a density of $2x10^3$ cells per well. After a 24 h incubation period, the cells were exposed to various concentrations of rhein, ranging from 5-10-15-20-30-40-50-75-100 µM, and incubated for additional periods of 24 and 48 h. The XTT solution was added to each of the wells and the plates were incubated for 4 h. Following incubation, the absorbance of the samples was measured using an ELISA microplate reader (BioTek, Epoch) at a wavelength of 450 nm, with 630 nm serving as the reference absorbance. To evaluate the cytotoxic efficacy of the rhein, IC_{50} values of the samples were calculated.

Colony formation assay

The method commonly known as "colony formation" is widely employed for examining the survival and proliferation capabilities of cancerous cells. In this study, the colony formation assay was carried out to evaluate the colony forming capacity of rhein on U87 GBM cells. Cells were seeded in 6-well plates at a density of $2x10^3$ cells per well and then incubated for 24 h. After the incubation period, the cells were treated with rhein and then subcultured every two days. The media were washed with PBS at the end of day 10 and fixed with 100% methanol at -20 °C. Then, the colony numbers of the control and dose groups were determined by staining with 1.0% crystal violet for 10 min and photographed with an inverted microscope. Colony

forming capacity was calculated according to colony forming numbers in each group (Güçlü et al., 2022).

Total RNA extraction, cDNA synthesis, and RT-qPCR

The expression changes of the apoptosis and TGF-β signal-related genes were evaluated using real time quantitative polymerase chain reaction (RT-qPCR) analysis. U87 GBM cells were seeded in 6-well plates at a density of $2.5x10^4$ cells per well and then incubated for 24 h at 37°C in an atmosphere containing 5% CO^2. Subsequently, cells were treated with the IC_{50} dose of rhein, and then total RNA isolation was performed with RiboEx reagent (GeneAll, 301–001). Each of the RNA sample concentrations and quality were measured using a nanodrop spectrophotometer (Thermo Scientific, USA). The DNase I enzyme (Thermo Scientific, USA) was used to avoid possible DNA contamination. Then, the purified RNAs were reversed into cDNA via the iScriptTM cDNA Synthesis Kit (Bio-Rad, 170–8891). To quantitatively assess mRNA expression levels, the BrightGreen 2x qPCR MasterMix (abm, Canada) was utilized as per the instructions provided by the manufacturer. The expression levels of *CASP3*, *CASP8*, *CASP9*, *BAX,* and *BCL-2* genes in the apoptosis pathway and *TGF-β1*, *SMAD2*, *SMAD3,* and *TIMP1* genes in the TGF-β pathway were assessed using SYBR in RT-qPCR analysis, conducted on an Applied Biosystems (Foster City, California, USA) instrument. The primer sequences for the studied genes were sourced from IDT PrimerQuest (https://eu.idtdna.com/Primerquest/Home/Index). The oligonucleotide sequences utilized in the RT-qPCR reactions are listed in **Table 1**. The conditions for the RT-qPCR were set at 95°C for 4 min, followed by 40 amplification cycles, each consisting of 95°C for 10 s, 60°C for 60 s, and 72°C for 4 min.

Table 1. Primer sequences of the selected genes used in RT-qPCR

Gene Name	Primer Sequences
GAPDH	F: 5-GTCAACGGATTTGGTCGTATTG-3
	R: 5-TGTAGTTGAGGTCAATGAAGGG-3
CASP3	F:5-GAGCCATGGTGAAGAAGGAATA-3
	R:5-TCAATGCCACAGTCCAGTTC-3
CASP8	F:5-GCCCAAACTTCACAGCATTAG-3
	R:5-GTGGTCCATGAGTTGGTAGATT-3
CASP9	F:5-CGACCTGACTGCCAAGAAA-3
	R:5-CATCCATCTGTGCCGTAGAC-3
BAX	F:5-GGAGCTGCAGAGGATGATTG-3
	R:5-GGCCTTGAGCACCAGTTT-3
BCL-2	F:5-GTGGATGACTGAGTACCTGAAC-3
	R:5-GAGACAGCCAGGAGAAATCAA-3
TIMP1	F:5-GTCAACCAGACCACCTTATACC-3
	R:5-TATCCGCAGACACTCTCCA-3
SMAD2	F: 5-GGGACTGAGTACACCAAATACG-3
	R: 5-TACCTGGAGACGACCATCAA-3
SMAD3	F: 5-CCTGAGTGAAGATGGAGAAACC-3
	R: 5-GGCTGCAGGTCCAAGTTATTA-3
TGF-β1	F: 5-CGTGGAGCTGTACCAGAAATAC-3
	R: 5-CTAAGGCGAAAGCCCTCAAT-3

Caspase-3 and caspase-9 activation analysis

Apoptosis was assessed following the manufacturer's guidelines by using a caspase-3 and caspase-9 colorimetric assay kit from BioVision, CA, USA. The assay identifies DNA fragmentation in the cytoplasm of apoptotic cells. To detect apoptosis, U87 cells were distributed into 96-well plates at a density of $5x10^5$ cells per well and incubated for 24 h. At the end of the incubation, the cells were treated with inhibitory concentrations of rhein. The cells were then collected and combined with 50 µL of lysis buffer, followed by a 10-min incubation on ice. Subsequently, 50 µL of 2X reaction buffer was added to each cytoplasmic fraction. Lastly, 5 µL of caspase-3 substrate Asp-Glu-Val-Asp (DEVD)-p-nitroaniline (pNA) and caspase-9 substrate Ac-Leu-Glu-His-Asp (LEHD)-pNA were incorporated into the protein cell lysate of each well. Incubation at 37˚C for a duration of 2 h was carried out for all samples. Following this incubation period, absorbance readings were taken at 405 nm using a microplate reader (Bio Rad Laboratories, CA, USA). The alteration in caspase-3 and caspase-9 activity was calculated by dividing the measurements from the samples treated with rhein by those from the untreated control samples.

Statistical analysis

All findings were expressed as the mean ± standard deviation (SD). The GraphPad Prism software (version 10.0.2, GraphPad Software, La Jolla, CA) was employed to conduct a comparative analysis between the control and treatment groups using Student's t-test and one-way ANOVA test.

Results

Rhein inhibits the cell viability on U87 GBM cells

The concentrations and time periods of rhein on U87 GBM cells were evaluated using the XTT assay. **Figure 2** demonstrates that administering 5-100 µM of rhein to the U87 GBM cell line for 24 and 48 h resulted in a dose- and time-dependent reduction in cell viability. The XTT assay showed that rhein treatment for 24 h (IC_{50} 10 µM) resulted in significant cell viability against the control cells. According to this result, the concentration of 10 µM was chosen as an effective dose in the subsequent analysis (**Figure 2**).

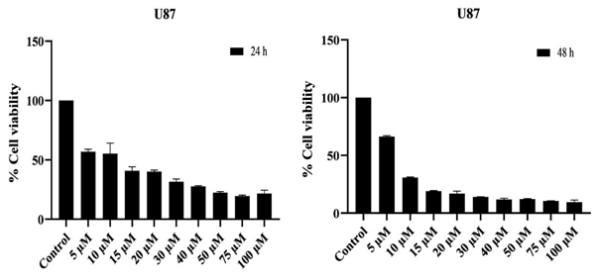

Figure 2. The cytotoxic effect of rhein on U87 GBM cell line. The cells were treated with control and rhein (5-10-15-20-30-40-50-60-75-100 µM) for 24 and 48 h. The XTT cell proliferation assay was used for the detection of IC_{50} values. The dose and control groups were subjected to least three independent experiments.

Rhein supressed the colony formation in U87 GBM cells

The colony analysis results showed that the IC_{50} dose of rhein significantly suppressed the colony formation capacities of U87 GBM cells after the treatment. The colony numbers were 582 ± 15.56 for the control group and 151±10.08 for the rhein-treated group (***p<0.001) (Figure 3).

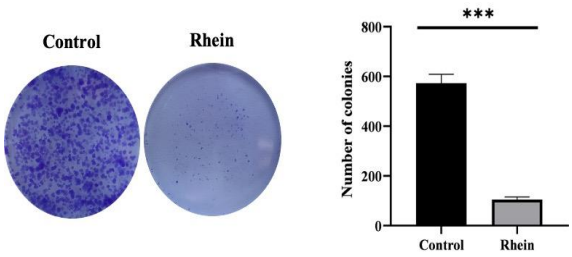

Figure 3. Rhein inhibits cell viability and colony formation of U87 GBM cells. The figure shows the colony formation of the U87 GBM cells treated with rhein for 48 h. The untreated cells were used as a control. The effect of rhein on colony formation is presented by comparing it with the control value. The results are presented as the mean ± standard deviation (std), with a sample size of 5 (n=5), and a significance level of ***p<0.001.

Rhein promoted apoptosis through TGF-β mediated pathway

The impact of rhein on cell death in U87 GBM cells was assessed using RT-qPCR analysis. After the treatment of rhein, the relative expression levels of apoptosis-related genes (*CASP3*, *CASP8*, *CASP9*, *BAX,* and *BCL-2*) were analyzed using RT-qPCR. In the gene expression results, the expression levels of *CASP3* (12.55 ± 0.8, p=0.00073), *CASP8* (2.94 ± 0.68, p=0.0016), *CASP9* (3.48 ± 0.75, p=0.00024), *BAX* (5.39 ± 0.55, p=0.00042), and *TGF-β1* (4.44 ± 0.65, p=0.00018) genes were significantly increased after the rhein treatment. In addition, *BCL-2* (-1.54 ± 0.46, 0.00031), *SMAD2* (-2.1 ± 0.7, p=0.0165), *SMAD3* (-1.04 ± 0.51, p=0.033), and *TIMP1* (-1.17 ± 0.6, p= 0.0037) genes were significantly decreased after the rhein treatment (Figure 4).

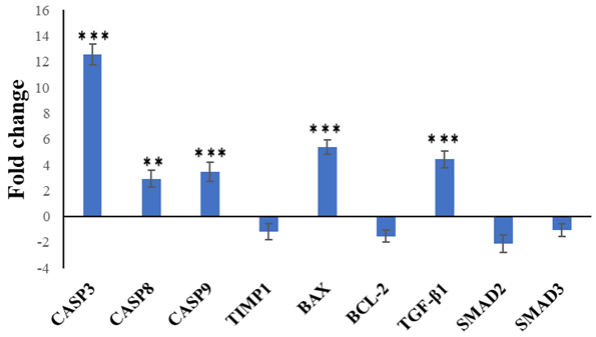

Figure 4. The bar graph presents the fold changes in the expressions of the selected genes, indicating the means of the significant fold changes compared to the control (*p <0.05, *** p <0.001).

Rhein modulates caspase-3 and caspase-9 activity in U87 GBM cells

To investigate the involvement of caspase-3 and caspase-9 in the apoptosis induced by rhein, the enzymatic activities of effector caspase (caspase-3) and initiator caspase (caspase-9) were examined. The findings revealed an increase in the activities of caspase-3 and caspase-9 following treatment with rhein. Specifically, the activities of caspase-3 and caspase-9 increased ~2 fold and ~2.5 fold, respectively, at a concentration of 10 µM compared to the control (Figure 5).

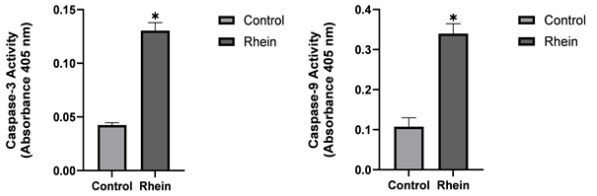

Figure 5. The activity of caspase-3 and caspase-9 after the rhein treatment. The colorimetric ELISA assay was employed to measure the activities of caspase-3 and caspase-9. These activities were then normalized to control cells and represented as a fold change. Consequently, there was an elevation in the activities of caspase-3 and caspase-9 following administration of rhein when compared to the control. Data are presented as mean ± standard deviation (std) with a sample size of 3 (n=3) and a significance level of *p <0.05.

Discussion

Rhein, an anthraquinone metabolite common in *Rheum* species, is an important metabolite used in pathological conditions such as inflammation, diabetes, osteoarthritis, and bacterial infections (Moldovan et al., 2000; Hu et al., 2019). Recent evidence has proven that rhein exerts potent antitumor effects in different cancer cell lines (Yang et al., 2019; Chen et al., 2020 ; Wei et al., 2022). The current research was investigated antiproliferative, apoptotic and antimetastatic effects of rhein in the U87 GBM cell line. First, the results of this study showed that rhein suppressed U87 cell proliferation in time- and dose-dependent manner. The IC_{50} dose that half of the maximal inhibitory concentration value was detected as 10 µM at 24 h (Figure 2). In the literature, there are limited studies about the antiproliferative effect on U87 cells of rhein. There are only two studies investigating the antiproliferative activity of rhein on U87 cell lines. One of these studies determined the IC_{50} dose of rhein as 40 µM in 72 h in glioblastoma cell lines (T98G, U87, and U251) (Chen et al., 2020). The other study detected the IC_{50} dose of rhein lysinate (the salt of rhein) by MTT assay as 160 µmol/L at 48 h. In this study, the detection of lower doses and times in higher cytotoxic activity may be due to the fact that the XTT assay is more sensitive than the MTT assay. In addition, they determined a high cytotoxic effect of rhein-piperazine-dithiocarbamate hybrids 3 synthesized from rhein against A549, PC-9 and H460 cell lines at low dose (IC_{50}= 10.81-23.78 µg/mL) (Wei et al., 2022). This finding, which is similar to the presented study, confirms the cytotoxic activity of rhein in U87 GBM cells (Figure 2).

TGF-β plays a pivotal role in a myriad of cellular processes, including cell proliferation, migration, apoptosis, embryogenesis, and tissue homeostasis, serving as a double-edged sword in the context of cancer development and progression (Hata & Chen, 2016). The complexity of the TGF-β signaling pathway, regulated by its ligands, type 1 and type 2 receptors, and Smad proteins, unfolds through both SMAD-dependent and SMAD-independent mechanisms. Upon ligand binding, SMAD 2 and 3 undergo phosphorylation, forming heteromeric complexes with SMAD 4 that translocate to the nucleus to modulate the expression of target genes (Xu et al., 2012). In pancreatic cancer, TGF-β's role oscillates between tumor suppression in the early stages to tumor promotion in the advanced stages, largely influenced by the tumor stage and microenvironment (Yang et al., 2021). This duality extends to its ability to induce apoptosis in various cell types, including prostate cells, hepatocytes, and B lymphocytes, showcasing the pathway's intricate involvement in cancer biology (Shen et al., 2017; Yang et al., 2021). In the present study, upon administering a toxic dose of rhein to U87 GBM cells, a notable upregulation of the *TGF-β1* gene expression by 4.44 fold was observed, signifying an activation or enhancement of the TGF-β signaling pathway. In the pathogenesis of glioblastoma, increased expression of TGF-β1 can modify the cellular microenvironment to support tumor progression or trigger the apoptotic pathway to promote the death of tumor cells. The increase in *TGF-β1* gene expression by rhein suggests a mechanism by which this molecule activates tumor-suppressive properties, thereby encouraging the death of glioblastoma cells. Given the lack of research specifically addressing rhein's efficacy against cancer cells in relation to the TGF-β pathway, our findings have been compared with existing studies to provide context. Zhu and colleagues' study revealed that rhein dose-dependently inhibits the mRNA expression and protein production of plasminogen activator inhibitor-1 (PAI-1) in endothelial cells induced by TGF-β1 (Zhu et al., 2003). When compared to the findings of this study, it is possible to suggest that rhein can modulate the TGF-β signaling pathway in both normal and cancerous cells, and its effects on this pathway may vary depending on the cell type. Furthermore, the research of Guo and colleagues demonstrated that rhein inhibited cell hypertrophy and extracellular matrix **(**ECM) accumulation mediated by TGF-β1, suggesting a renoprotective effect of rhein, possibly through inhibiting the overexpression of TGF-β1 (Guo et al., 2001). This evidence, alongside our findings, suggests that rhein's ability to modulate the TGF-β pathway extends beyond cancer cells to include protective effects in renal tissues, highlighting the compound's broad therapeutic potential. Our results, showing rhein's modulation of TGF-β pathway components in cancer cells, complement Guo et al.'s observations by illustrating the versatile impact of rhein across different cell types and pathological conditions. Besides, the expressions of *SMAD2*, *SMAD3*, and *TIMP1* genes were downregulated, with respective fold changes of -2.1, -1.04, and -1.17. The observed decrease in the expression of *SMAD2* and *SMAD3* under rhein treatment may indicate the promotion of cell death through non-canonical mechanisms of the TGF-β signaling pathway. The decrease in *SMAD2* and *SMAD3* expressions could be mitigating the pro-tumorigenic effects of TGF-β in the later stages of cancer. This mechanism, consistent with the cytotoxic effects of rhein observed in U87 GBM cells, could contribute to the suppression of tumor growth and metastasis via the TGF-β pathway. This situation suggests that targeting the TGF-β pathway could be a potential approach in the treatment of cancer types such as glioblastoma. Moreover, the decrease in *TIMP1* gene expression might have significant effects on the remodeling of the ECM and tumor invasion (Rojiani et al., 2015). TIMP1 functions as an inhibitor of matrix metalloproteinases (MMPs), preventing tumor cells from crossing the ECM. However, the reduced expression of TIMP1 could promote the remodeling of the ECM and potentially make tumor cells less invasive. This could contribute to the antimetastatic properties of rhein and aid in suppressing the progression of glioblastoma.

Apoptosis can be induced by mitochondria-mediated and death receptor-mediated pathways. These pathways lead to the activation of effector caspases such as caspase-3 and caspase-8. In terms of the apoptotic mechanism, TGF-β increases the expression levels of antiapoptotic protein BCL-2 and proapoptotic caspase-3 and caspase-8 (Yang et al., 2019). A study investigating the apoptotic effect of rhein in HepaRG cells showed that levels of BAX, cleaved caspase-3, -8, -9, and PARP increased while BCL-2 decreased (You et al., 2018). It has also been reported that rhein induces mitochondrial apoptosis in a caspase-dependent manner in PANC-1 and MIAPaCa-2 cell lines, characterized by the downregulation of *BCL-2*, *BCL-xL*, *survivin,* and *XIAP*, and upregulation of cleaved caspase-3, -9 and PARP (Liu et al., 2022). Moreover, Tang et al. (2017) showed that rhein triggers apoptotic and autophagic mechanisms, correlating with changes in the expression of *CASP3*, *BAX*, *Beclin-1,* and *BCL-2* genes in rat F98 glioma cells. In the present study, treatment with rhein caused an increase in the mRNA expression levels of *CASP3* (12.55 fold), *CASP8* (2.94 fold), *CASP9* (3.48), and *BAX* (5.39) in U87 cells. However, with a decrease in *BCL-2* (-1.54 fold) mRNA level, rhein triggered the induction of mitochondria-mediated apoptosis. Furthermore, a significant increase in the concentrations of caspase-3 and caspase-9 proteins compared to the control provides confirmatory evidence for gene expression analysis. In conclusion, the ability of rhein to induce apoptosis could be considered a potential therapeutic strategy in the treatment of aggressive cancer types such as glioblastoma. This highlights the development of new approaches in cancer

therapy by targeting apoptotic pathways as well as modulating the tumor microenvironment.

There are no existing findings in the literature regarding the effect of rhein on the colony-forming capacity of glioblastoma cells. However, it has been reported that rhein inhibits colony formation in colorectal (Zhuang et al., 2019; Zhang et al., 2021), and lung (Yang et al., 2019; Liu et al., 2022) cells. In a study conducted on human NSCLC cell lines, it was demonstrated that rhein inhibits the STAT3 signaling pathway and increases the expression level of the proapoptotic protein *BAX* while decreasing the expression level of the antiapoptotic protein *BCL-2*. Furthermore, a colony formation assay similarly confirmed that rhein promotes apoptosis in human NSCLC cell lines, thereby inhibiting growth and proliferation (Yang et al., 2019). In another study assessing the anticancer activity of rhein against colorectal cancer (CRC) cells, cell viability and anchorage-independent colony formation assays showed that rhein inhibits the mTOR signaling pathway, demonstrating anticancer activity against CRC (Zhang et al., 2021). Similarly, a study by Liu and colleagues (2022) showed that rhein suppresses the proliferation and migration of lung cancer cells via the Stat3/Snail/MMP2/MMP9 signaling pathway. Lastly, a study conducted by Zhang and colleagues revealed that rhein inhibits the AKT/mTOR signaling pathway in oral cancer cells, inducing the accumulation of reactive oxygen species (ROS) and cell apoptosis (Zhang et al., 2023). In the current research, the findings from the colony analysis indicated that the ability of U87 cells to form colonies was significantly reduced following treatment with rhein. The colony formation ability and cell viability assay collectively suggest the potential antiproliferative activity of rhein on U87 cells. These findings show an antimetastatic property by causing an increase in *TGF-β1* level with a decrease in rhein *TIMP1* level, stimulating mitochondria-mediated apoptosis, and supporting apoptosis mediated by SMAD-independent pathway.

In conclusion, considering all these data, the fact that rhein exhibits antiproliferative, apoptotic, and cytotoxic activities by modulating TGF-β and apoptosis pathways makes it valuable for detailed studies regarding its clinical use.

References

Atanasov, A. G., Waltenberger, B., Pferschy-Wenzig, E. M., Linder, T., Wawrosch, C., Uhrin, P., Temml, V., Wang, L., Schwaiger, S., Heiss, E. H., Rollinger, J. M., Schuster, D., Breuss, J. M., Bochkov, V., Mihovilovic, M. D., Kopp, B., Bauer, R., Dirsch, V. M., & Stuppner, H. (2015). Discovery and resupply of pharmacologically active plant-derived natural products: A review. Biotechnology advances, 33(8), 1582–1614. https://doi.org/10.1016/j.biotechadv.2015.08.001

Bu, T., Wang, C., Meng, Q., Huo, X., Sun, H., Sun, P., Zheng, S., Ma, X., Liu, Z., & Liu, K. (2018). Hepatoprotective effect of rhein against methotrexate-induced liver toxicity. *European journal of pharmacology*, *834*, 266–273. https://doi.org/10.1016/j.ejphar.2018.07.031

Chang, C. Y., Chan, H. L., Lin, H. Y., Way, T. D., Kao, M. C., Song, M. Z., Lin, Y. J., & Lin, C. W. (2012). Rhein induces apoptosis in human breast cancer cells. *Evidence-based complementary and alternative medicine: eCAM*, *2012*, 952504. https://doi.org/10.1155/2012/952504

Chen, J., Luo, B., Wen, S., & Pi, R. (2020). Discovery of a novel rhein-SAHA hybrid as a multi-targeted anti-glioblastoma drug. *Investigational new drugs*, *38*(3), 755–764. https://doi.org/10.1007/s10637-019-00821-4

Guo, X. H., Liu, Z. H., Dai, C. S., Li, H., Liu, D., & Li, L. S. (2001). Rhein inhibits renal tubular epithelial cell hypertrophy and extracellular matrix accumulation induced by transforming growth factor beta1. Acta pharmacologica Sinica, 22(10), 934–938.

Güçlü, E., Çınar Ayan, İ., Dursun, H. G., & Vural, H. (2022). Tomentosin induces apoptosis in pancreatic cancer cells through increasing reactive oxygen species and decreasing mitochondrial membrane potential. *Toxicology in vitro: an international journal published in association with BIBRA*, *84*, 105458. https://doi.org/10.1016/j.tiv.2022.105458

Habtemariam, S., & Lentini, G. (2018). Plant-Derived Anticancer Agents: Lessons from the Pharmacology of Geniposide and Its Aglycone, Genipin. *Biomedicines*, *6*(2), 39. https://doi.org/10.3390/biomedicines6020039

Hata, A., & Chen, Y. G. (2016). TGF-β Signaling from Receptors to Smads. *Cold Spring Harbor perspectives in biology*, *8*(9), a022061. https://doi.org/10.1101/cshperspect.a022061

Henamayee, S., Banik, K., Sailo, B. L., Shabnam, B., Harsha, C., Srilakshmi, S., Vgm, N., Baek, S. H., Ahn, K. S., & Kunnumakkara, A. B. (2020). Therapeutic Emergence of Rhein as a Potential Anticancer Drug: A Review of Its Molecular Targets and Anticancer Properties. *Molecules (Basel, Switzerland)*, *25*(10), 2278. https://doi.org/10.3390/molecules25102278

Hu, F., Zhu, D., Pei, W., Lee, I., Zhang, X., Pan, L., & Xu, J. (2019). Rhein inhibits ATP-triggered inflammatory responses in rheumatoid rat fibroblast-like synoviocytes. *International immunopharmacology*, *75*, 105780. https://doi.org/10.1016/j.intimp.2019.105780

Liu, J., Ding, D., Liu, F., & Chen, Y. (2022). Rhein Inhibits the Progression of Chemoresistant Lung Cancer Cell Lines via the Stat3/Snail/MMP2/MMP9 Pathway. *BioMed research international*, *2022*, 7184871. https://doi.org/10.1155/2022/7184871

Meng, Z., Yan, Y., Tang, Z., Guo, C., Li, N., Huang, W., Ding, G., Wang, Z., Xiao, W., & Yang, Z. (2015). Anti-hyperuricemic and nephroprotective effects of rhein in hyperuricemic mice. *Planta medica*, *81*(4), 279–285. https://doi.org/10.1055/s-0034-1396241

Moldovan F., Pelletier J. P., Jolicoeur F.-C., Cloutier J.-M., Martel-Pelletier J. (2000). Diacerhein and rhein reduce the ICE-induced IL-1*β* and IL-18 activation in human osteoarthritic cartilage. *Osteoarthritis and Cartilage*, *8*(3):186–196. https://doi.org/10.1053/joca.1999.0289

Nguyen, A. T., & Kim, K. Y. (2020). Rhein inhibits the growth of *Propionibacterium acnes* by blocking NADH

dehydrogenase-2 activity. *Journal of medical microbiology*, *69*(5), 689–696. https://doi.org/10.1099/jmm.0.001196

Ramesh, S., Wildey, G. M., & Howe, P. H. (2009). Transforming growth factor beta (TGFbeta)-induced apoptosis: the rise & fall of Bim. Cell cycle (Georgetown, Tex.), 8(1), 11–17. https://doi.org/10.4161/cc.8.1.7291

Rojiani, M. V., Ghoshal-Gupta, S., Kutiyanawalla, A., Mathur, S., & Rojiani, A. M. (2015). TIMP-1 overexpression in lung carcinoma enhances tumor kinetics and angiogenesis in brain metastasis. *Journal of neuropathology and experimental neurology*, *74*(4), 293–304. https://doi.org/10.1097/NEN.0000000000000175

Sánchez-Capelo, Amelia. "Dual role for TGF-beta1 in apoptosis." Cytokine & growth factor reviews vol. 16,1 (2005): 15-34. https://doi.org/10.1016/j.cytogfr.2004.11.002

Shen, W., Tao, G. Q., Zhang, Y., Cai, B., Sun, J., & Tian, Z. Q. (2017). TGF-β in pancreatic cancer initiation and progression: two sides of the same coin. *Cell & bioscience*, *7*, 39. https://doi.org/10.1186/s13578-017-0168-0

Tang, N., Chang, J., Lu, H. C., Zhuang, Z., Cheng, H. L., Shi, J. X., & Rao, J. (2017). Rhein induces apoptosis and autophagy in human and rat glioma cells and mediates cell differentiation by ERK inhibition. *Microbial pathogenesis*, *113,* 168–175. https://doi.org/10.1016/j.micpath.2017.10.031

Tewari, D., Priya, A., Bishayee, A., & Bishayee, A. (2022). Targeting transforming growth factor-β signalling for cancer prevention and intervention: Recent advances in developing small molecules of natural origin. Clinical and translational medicine, 12(4), e795. https://doi.org/10.1002/ctm2.795

Wang, A., Jiang, H., Liu, Y., Chen, J., Zhou, X., Zhao, C., Chen, X., & Lin, M. (2020). Rhein induces liver cancer cells apoptosis via activating ROS-dependent JNK/Jun/caspase-3 signaling pathway. *Journal of Cancer*, *11*(2), 500–507. https://doi.org/10.7150/jca.30381

Wang, H., Yang, D., Li, L., Yang, S., Du, G., & Lu, Y. (2020). Anti-inflammatory Effects and Mechanisms of Rhein, an Anthraquinone Compound, and Its Applications in Treating Arthritis: A Review. *Natural products and bioprospecting*, *10*(6), 445–452. https://doi.org/10.1007/s13659-020-00272-y

Wei, M. X., Zhou, Y. X., Lin, M., Zhang, J., & Sun, X. (2022). Design, synthesis and biological evaluation of rhein-piperazine-dithiocarbamate hybrids as potential anticancer agents. *European journal of medicinal chemistry*, *241*, 114651. https://doi.org/10.1016/j.ejmech.2022.114651

Xu, X., Lv, H., Xia, Z., Fan, R., Zhang, C., Wang, Y., & Wang, D. (2017). Rhein exhibits antioxidative effects similar to Rhubarb in a rat model of traumatic brain injury. *BMC complementary and alternative medicine*, *17*(1), 140. https://doi.org/10.1186/s12906-017-1655-x

Xu, P., Liu, J., & Derynck, R. (2012). Post-translational regulation of TGF-β receptor and Smad signaling. *FEBS letters*, *586*(14), 1871-1884. https://doi.org/10.1016/j.febslet.2012.05.010

Yang, L., Li, J., Xu, L., Lin, S., Xiang, Y., Dai, X., Liang, G., Huang, X., Zhu, J., & Zhao, C. (2019). Rhein shows potent efficacy against non-small-cell lung cancer through inhibiting the STAT3 pathway. *Cancer management and research*, *11*, 1167–1176. https://doi.org/10.2147/CMAR.S171517

Yang, L., Lin, S., Kang, Y., Xiang, Y., Xu, L., Li, J., Dai, X., Liang, G., Huang, X., & Zhao, C. (2019). Rhein sensitizes human pancreatic cancer cells to EGFR inhibitors by inhibiting STAT3 pathway. *Journal of experimental & clinical cancer research: CR*, *38*(1), 31. https://doi.org/10.1186/s13046-018-1015-9

Yang, Y., Ye, W. L., Zhang, R. N., He, X. S., Wang, J. R., Liu, Y. X., Wang, Y., Yang, X. M., Zhang, Y. J., & Gan, W. J. (2021). The Role of TGF-β Signaling Pathways in Cancer and Its Potential as a Therapeutic Target. *Evidence-based complementary and alternative medicine*: *eCAM*, 2021, 6675208. https://doi.org/10.1155/2021/6675208

You, L., Dong, X., Yin, X., Yang, C., Leng, X., Wang, W., & Ni, J. (2018). Rhein Induces Cell Death in HepaRG Cells through Cell Cycle Arrest and Apoptotic Pathway. *International journal of molecular sciences*, 19(4), 1060. https://doi.org/10.3390/ijms19041060

Zhang, H., Yi, J. K., Huang, H., Park, S., Park, S., Kwon, W., Kim, E., Jang, S., Kim, S. Y., Choi, S. K., Kim, S. H., Liu, K., Dong, Z., Ryoo, Z. Y., & Kim, M. O. (2021). Rhein Suppresses Colorectal Cancer Cell Growth by Inhibiting the mTOR Pathway In Vitro and In Vivo. *Cancers*, *13*(9), 2176. https://doi.org/10.3390/cancers13092176

Zhang, H., Ma, L., Kim, E., Yi, J., Huang, H., Kim, H., Raza, M. A., Park, S., Jang, S., Kim, K., Kim, S. H., Lee, Y., Kim, E., Ryoo, Z. Y., & Kim, M. O. (2023). Rhein Induces Oral Cancer Cell Apoptosis and ROS via Suppresse AKT/mTOR Signaling Pathway In Vitro and In Vivo. International journal of molecular sciences, 24(10), 8507. https://doi.org/10.3390/ijms24108507

Zhou, Y. X., Xia, W., Yue, W., Peng, C., Rahman, K., & Zhang, H. (2015). Rhein: A Review of Pharmacological Activities. *Evidence-based complementary and alternative medicine: eCAM*, *2015*, 578107. https://doi.org/10.1155/2015/578107

Zhu, J., Liu, Z., Huang, H., Chen, Z., & Li, L. (2003). Rhein inhibits transforming growth factor beta1 induced plasminogen activator inhibitor-1 in endothelial cells. Chinese medical journal, 116(3), 354–359.

Zhuang, Y., Bai, Y., Hu, Y., Guo, Y., Xu, L., Hu, W., Yang, L., Zhao, C., Li, X., & Zhao, H. (2019). Rhein sensitizes human colorectal cancer cells to EGFR inhibitors by inhibiting STAT3 pathway. *OncoTargets and therapy*, *12*, 5281–5291. https://doi.org/10.2147/OTT.S206833

BIOTECH STUDIES
VOL 33 ISSUE 1 JUNE 2024 ISSN 2687-3761 E-ISSN 2757-5233

CONTENTS

1-12 **Evaluation of anticancerogenic effect of flavonoid rich *Verbascum gypsicola* Vural & Aydoğdu methanolic extract against SH-SY5Y cell line**
Seda Şirin

13-22 **Research advances of deciphering Shalgam microbiota profile and dynamics**
Mustafa Yavuz, Halil Rıza Avcı

23-32 **Barley preferentially activates strategy-II iron uptake mechanism under iron deficiency**
Emre Aksoy

33-42 **Juglans kernel powder and jacobinia leaf powder supplementation influenced growth, meat, brain, immune system and DNA biomarker of broiler chickens fed Aflatoxin-B1 contaminated diets**
Olugbenga David Oloruntola

43-51 **Response surface methodology-based optimization studies about bioethanol production by *Candida boidinii* from pumpkin residues**
Ekin Demiray, Sevgi Ertuğrul Karatay, Gönül Dönmez

52-66 **Recent *in vitro* models and tissue engineering strategies to study glioblastoma**
Melike Karakaya, Pınar Obakan Yerlikaya

67-73 **Rhein inhibits cell proliferation of glioblastoma multiforme cells by regulating the TGF-ß and apoptotic signaling pathways**
Sümeyra Çetinkaya